Optimized Transmission and Selection Designs in Wireless Systems

Enlong Che

B.Sc. in Electrical Engineering,

Zhejiang University, Hangzhou, China

A thesis submitted in fulfilment of the requirements

for the degree of Doctor of Philosophy

Faculty of Engineering and Information Technology (FEIT),

University of Technology, Sydney (UTS)

Australia

January 2015

Abstract

Most modern wireless communication systems are hierarchical complex systems which consist of many levels of design elements and are subject to limited resources (e.g. power or bandwidth). Thanks to numerous newly-introduced devices in different forms such as sensors and relays and the integration of multiple antennas, spectral efficiency and reliability of wireless transmission could be significantly improved. Nevertheless, it also becomes much more challenging to control the devices and allocate the limited resources in an optimal fashion in order to approach capacity gains.

This dissertation is concerned with mixed-binary or combinatorial optimization problems to improve various service goals for a variety of interesting yet difficult wireless communication applications. These problems are highly prized for academic significance but remained open due to their mathematical challenges. We shall explore the hidden d.c. (difference of convex (or concave) functions) structure of the objective functions as well as the binary constraints. Further, we will prove such general d.c. programs can be equivalently converted into canonical d.c. programs with d.c. objective functions that are subject to convex and/or affine constraints only. Although global optimal algorithms are generally possible for such d.c. programs, they are normally very computation-intensive. Instead, we propose tailored path-following local-optimal d.c. algorithms with significantly reduced computational complexity. Through extensive simulation results, the designed d.c. decompositions of the problems are proven effective. The proposed algorithms are efficient and computationally affordable while locating outstanding solutions in comparison with other existing algorithms. In those more sophisticated problem scenarios, the d.c. algorithm appears to be the only suitable option thanks to the superior flexibility.

In the first part of the thesis, we will consider a sensor network for spectrum sensing in the context of cognitive radios. To improve sensing quality and prolong the battery life of sensors, the least correlated subset of sensors needs to be selected. A new Bregman matrix deviation-based framework is shown applicable to all the concerned correlation measure functions.

The second research investigates a relay-assisted multi-user wireless network. Besides the relay beamforming variables, we add into consideration a set of binary link variables which represent on/off operations of individual relays in relation to transmitter-receiver links. To achieve the maximin SNR or SINR capacity, certain relays may be optimally deactivated. This leads to reduced power consumption and complexity/ overhead of management. The relay assignment and beamforming design is a joint mixed combinatorial nonlinear program which is non-convex and non-smooth. Nonetheless, we show the it can be fit into a canonical d.c. optimization framework. Simulation results demonstrate the benefits of relay selection and beamforming.

The last research stems from the study of conventional coordinated transmission design with respect to transmit covariance and precoding matrix/vector variables. Inspired by the well-known Han-Kobayashi message splitting method in 2-user SISO interference channels, we further extend the idea of message splitting to the MIMO interference networks. An innovative non-smooth rate formula is discovered which builds the foundation of the work. The design in common and private covariance matrices or beamforming vectors, as well as the pairing variables, is formulated as a joint combinatorial nonlinear program which is non-convex and non-smooth. Due to the great difficulty, it is not imminently possible to jointly handle both variables. Therefore, we first propose an intuitive heuristic pairing algorithm to find excellent pairing choices. Then, the non-convex optimization problems in covariance matrices or beamforming vector variables are dealt with in the d.c. optimization framework. Finally, simulation results reveal the great potential of the novel message splitting scheme in approaching rate capacity.

CERTIFICATE OF ORIGINAL AUTHORSHIP

CERTIFICATE OF ORIGINAL AUTHORSHIP

I, Enlong CHE, certify that this thesis titled, 'Optimized Transmission and Selection Designs in Wireless Systems', has not previously been submitted for a degree nor has it been submitted as part of requirements for a degree except as fully acknowledged within the text.

I also certify that the thesis has been written by me. Any help that I have received in my research work and the preparation of the thesis itself has been acknowledged. In addition, I certify that all information sources and literature used are indicated in the thesis.

Signature of Student:

Date:

Signed: ____

Date: ____

Acknowledgements

I would like to express my sincere gratitude to my supervisor Prof. Tuan D. Hoang for his guidance, advice, and continued support throughout the period of this research. Prof. Tuan has provided the key technical insights and contributed tirelessly efforts in all my works. I am truly grateful for his great patience and faith in my capabilities. I feel particularly fortunate for having a supervisor who is always setting the highest standards in our research endeavours.

I am deeply appreciative of Professor Ha H. Nguyen from University of Saskatchewan, Canada. He has kindly offered help to resolve confusions, and has constantly been the most valuable contributor to all my research works. I would also like to thank Dr. Ha H. Kha for his generous and insightful advises.

I am very thankful to University of Technology, Sydney (UTS), especially to the Dean of FEIT, Professor Hung Nguyen who granted me the IRS scholarship that enabled me to fully focus on the research. I am also thankful to my supervisor Prof. Tuan D. Hoang for his kind and constant financial support under an Australian Research Council (ARC) Discovery Project.

I consider myself very fortunate to have many friends and teachers supporting and guiding me throughout my life, especially in times of difficulty. I'd like to express my sincere gratitude to Miss Yu Jianhua, Miss Xue Yan, Nicole & Chris, Zhang Tao & Brandy, Xiao Han, Qiu Shuang, Shang Tianlong, Di Jie, Ren Xujin, Li Xiaodong, Xiong Guojiang, Miss Susan Wareham, Mr. Jia Houyu and many other important people for me.

I have enjoyed the privilege to have spent my Ph.D tenure with some of the most brilliant colleagues Bao, Tam, and Zhang Tao. I am very thankful to their valuable inputs.

It is impossible to list the paramount debts that I owe to my parents, Che Jianping and Zhang Xiaojing, and to my entire family. They have always been supportive unconditionally and genuinely extended their help and hope for the very best of myself. They are the true driving force behind my life, no matter up or down.

Especially, I wish to truly thank my beloved partner, Bu Zhuoran, for her infinite love, sacrifice, support, patience and devotion. I could only and faithfully devote myself to making you the happiest lady in the world.

Contents

List of Figures

List of Tables

Abbreviations

MIMO	Multiple-Input-Multiple-Output
MISO	Multiple-Input-Single-Output
SIMO	Single-Input-Multiple-Output
SISO	Single-Input-Single-Output
(W)MMSE	(Weighted) Minimum Mean Squared Error
SDP	Semi-definite Programming
LMI	Linear Matrix Inequality
SINR	Signal to Interference plus Noise Ratio
SNR	Signal to Noise Ratio
INR	Interference to Noise Ratio
s.t.	Subject to
d.c.	Difference of Convex (Concave) Functions
DCI	D.C. Iterative Algorithm
NP-hard	Non-deterministic Polynomial-time hard
CM	Correlation Measure
DoF	Degrees of Freedom
MRC	Maximal Ratio Combining
DSP	Digital Signal Processing
BS	Base Station
MT	Mobile Terminal
CSI	Channel State Information
MIP	Mixed Integer Optimization Problem
COP	Combinatorial Optimization Problem
PSD	Power Spectral Density
TDM/ FDM	Time/Frequence Division Multiplexing

Notations

1. Matrices and vector are denoted by uppercase and lowercase characters, respectively. Variables are denoted by boldface letters.
2. $\langle \boldsymbol{X} \rangle = \mathsf{trace}(\boldsymbol{X})$ for matrix $\boldsymbol{X}$.
3. $|\boldsymbol{X}|$: the determinant of matrix $\boldsymbol{X}$.
4. $\langle \boldsymbol{X}, \boldsymbol{Y} \rangle = \mathsf{trace}(\boldsymbol{X}^H \boldsymbol{Y})$ for matrices $\boldsymbol{X}, \boldsymbol{Y}$.
5. $\langle \boldsymbol{x}, \boldsymbol{y} \rangle = \boldsymbol{x}^H \boldsymbol{y}$ for vectors $\boldsymbol{x}, \boldsymbol{y}$.
6. $\boldsymbol{X} \succ 0$ ($\boldsymbol{X} \succeq 0$, resp.): $\boldsymbol{X}$ is a (Hermitian) positive definite (semi-definite, resp.) matrix.
7. $\mathcal{S}_+^{N_t}$ denotes the cone of Hermitian symmetric positive semi-definite matrices of size $N_t \times N_t$.
8. $\vee$ is logical or operation, so $\alpha = \beta \vee \gamma$ means α is either β or γ.
9. $\log(.)$ is understood as base-2 logarithm, i.e., $\log_2(.)$.
10. $1 : N$ stands for $1, 2, \cdots, N$.
11. $\boldsymbol{x} \sim \mathcal{CN}(\bar{\boldsymbol{x}}, \boldsymbol{R}_{\boldsymbol{x}})$ means $\boldsymbol{x}$ is a vector of Gaussian random variables with. means $\bar{\boldsymbol{x}}$ and covariance $\boldsymbol{R}_{\boldsymbol{x}}$.
12. $\lambda_{max}(\boldsymbol{X})$: the maximum eigenvalue of $\boldsymbol{X}$.
13. $\boldsymbol{X} \geq 0$ and $\sqrt{\boldsymbol{X}}$ are entry-wise understood.
14. For $\boldsymbol{X} \succeq 0$, $\boldsymbol{X}^{1/2}$ is a symmetric matrix such that $\boldsymbol{X}^{1/2}\boldsymbol{X}^{1/2} = \boldsymbol{X}$.
15. $\mathbf{1}_N$: the N-dimensional vector with unity components.
16. $e_i \in R^N$ has zero components except i-th component equal 1.
17. $\odot$: the Hadamard product operator.
18. $\binom{M}{N}$: binomial coefficient.
19. $\mathsf{Re}(\boldsymbol{x})$: real-part function.
20. $[x]_b$: rounded binary value from $x \in [0, 1]$.

Dedicated to

my dearest parents, grandpas and grandmas …

Chapter 1

Introduction

This chapter introduces the motivation and scope of this dissertation for the investigation of resources selection and allocation problems encountered in wireless communications under various scenarios. A brief survey of some interesting and related research topics will be given. The structure of the dissertation and its main contributions are outlined by the end of the chapter.

1.1 Motivation and Scope

Over the past decades, the ever-faster evolution of techniques has greatly improved wireless communications with increased information throughput and reliability of transmission, while enabling unparalleled flexibility and mobility [1] as compared to wired communications. However, it still remains as one of the most challenging yet exciting research areas mainly due to two physical phenomenons. The first is the open-air electromagnetic fading channels that unpredictably attenuate the signal strength and shift its phase. As the uncertainty of the fading channels results in unreliable transmission, knowing the statistic characterization of the channels is very important but proved more difficult on most occasions. Second, interferences from various sources may significantly deteriorate the quality of signal reception which poses as a bottleneck for any attempts to improve performance. For these reasons, wireless systems are generally more complicated and challenging than wired systems, with the latter largely immune from the fading channels and interferences [2].

In the presence of fading channels, interference, power constraints, and many other factors, a wireless system is a typical complex system with many types of available and disposable resources. From an analytical perspective, these resources can be generally divided into two categories. The first group of resources may only be divided into discrete parts. In such cases, the divisibility constraints on these resources, which may be bandwidth, devices, or other logical links, may restrict the possible alternatives to a finite set [3]. The variables representing these resources are normally binary or integer variables. The second group of resources, as opposed to the first, are represented by continuous variables that are not subject to finite divisibility constraints. Depending on application requirements, all the discrete and continuous resources (variables) may be optimized collectively to reach the highest system performance in terms of certain utility function values while satisfying physical limitations and/ or design requirements. For example, to increase transfer reliability, one may rely on resource division multiplexing techniques (e.g. TDM/ FDM) to create non-interfering channels. Alternatively, various types of diversity (e.g. diversities inherent to multiple-antenna setup or fading channels) may be used to achieve the same goal. In systems where high spectral efficiency is most prized, measures to utilize multiplexing or beamforming gains are effective and commonly adopted. As such, there are many challenging problems of practical interests to wireless communications. Undeniably, one thing in common is that most of them do not have straightforward solutions and thus require delicate designs which rely on mathematical skills and optimization tools [4, 5].

In particular, given the fact that the performance of the most wireless systems is limited by interference and available power [5], it is of great academical and practical interest to consider how to handle interference subject to a limited power budget. In this context, two categories of problems have been intensively studied: maximizing data rates while not exceeding the power budget, and minimizing consumed power while satisfying rate requirements. The former problems on most occasions constitute very hard non-convex optimization tasks [10–12], while the latter problems are also non-convex for certain cases [13, 14]. To improve the degrees of freedom and diversity, multiple antennas are installed to replace the single antenna on either or both sides of a transmission link. However, multiple antennas mean increased dimensions of variables and thus higher complexity for management and design. In most cases, it also increases the level of difficulty of coordinated management of all resources. For a problem easily solvable under a single-antenna setting, its counterpart under a multiple-antenna setting could still pose serious optimization challenges. This is due to the fact that convexity of the original problem is not necessarily preserved under the new setup. Even in cases where convexity can be preserved that the new problem is still convex, further mathematical exploitation is still necessary because of increased number of variables. In general, the relatively slow introduction of multiple-antenna techniques to industries can be partly attributed to their much-increased problem sizes, complexity, and the inherent optimization challenges.

This dissertation is mainly focused on various hard non-convex optimization problems in wireless systems under various scenarios. In particular, these problems may be subject to binary or combinatorial constraints which make them (mixed) binary or combinatorial optimization problems, respectively. The concerned problems typically consist of a set of binary selection/assignment/pairing link variables and a set of continuous power, beamforming/ precoding vector, or covariance matrix design variables. On one hand, the binary link variables can refer to operations of either activation (1) or deactivation (0) of a physical device or a logical link. In a general sense, a network optimization model with this extra dimension of binary link variables is considered to have the freedom to optimally decide the size and the topology of the system. In other words, it is a *self-organizing system* which certainly enjoys many benefits such as improved flexibility and energy efficiency as compared to the traditional systems where all devices are by default regarded as activated even if some are deemed in adverse conditions [15]. On the other hand, the continuous variables refer to the designs for antenna beam patterns, power allocations, transmit codebooks or the likes. The joint design of these two sets of variables, which aims at improving different service goals, belongs to the NP-hard mixed binary or combinatorial optimization problems. In particular, enumeration in the binary constraints alone is possible but understandably unaffordable due to its exponentially increasing complexity. With the continuous variables coupled with the binary ones, even enumeration is not an option any more. As a result, most previous attempts rely on sub-optimal heuristical methods for finding a feasible binary solution first and then address the optimization in continuous variables only. Another common practice is to instead solve optimization problem with the binary constraints $\{0, 1\}$ box-relaxed to linear constraints which can be used as an upper bound. The binary constraints are then enforced to the resulted $[0, 1]$ solutions by simply rounding their numbers to either 0 or 1. It is found that performance often deteriorates dramatically after rounding. Relying on an important observation from [16], we are able to represent the binary constraints as the difference of two continuous and convex sets. In other words, the binary constraints are in fact d.c. constraints which is an important property that we will later exploit.

In the context of wireless communications, the aforementioned two commonly considered optimization problems are mostly not convex. Some are optimization problems with convex objective functions over non-convex sets (e.g. power minimization subject to rate constraints), some are with non-convex objective functions over convex sets (e.g. rate maximization subject to power constraints), and the rest are with non-convex objective functions over non-convex sets (e.g. rate maximization subject to power and rate constraints). However, as we will show later, almost all these non-convex functions, regardless of objective functions or constraint functions, can be represented as d.c. functions [16, 17]. So, the joint mixed binary optimization problem will be proven equivalent to d.c. function optimization subject to d.c., and/or convex and/or affine constraints. Subsequently, we can convert it into canonical d.c. optimization with d.c. objective functions subject to convex and/or affine constraints only. Therefore, the concerned hard mixed binary optimization problems can be universally solved in the globally optimal d.c. optimization framework. Instead of using the computationally expensive globally optimal d.c. methods as suggested in [16], we shall propose efficient path-following algorithms to find locally optimal solutions. In general, the goals of research in this dissertation are

- To study sensor selection problems and to select the least correlated group of sensors for effective and energy-efficient spectrum sensing in cognitive radio. The problems with different correlation measures are unified in a Bregman matrix deviation framework with binary variables. The integer programming problem is investigated and subsequently addressed by the proposed d.c. iterative algorithm.

- To investigate the joint relay assignment and beamforming problem in both orthogonal and non-orthogonal channels assuming a multi-user and multi-relay scenario. The binary constraints on the link variables are represented as d.c. constraints and the objective function is recast into d.c. function. The d.c. objective function minimization over d.c., convex and/or affine set is converted into the canonical d.c. optimization form with d.c. objective function over convex and/or affine set. The joint mixed binary optimization problem is then addressed by the proposed procedures based on DCIs.

- To analyze the rate capacity of SISO and MIMO interference channels. We investigate the interference mitigation with pairing and successive decoding in interference channels. The pairing problem is separately addressed first using the proposed heuristic algorithm. Then, the non-convex optimization in private and common messages is solved by the proposed d.c. algorithms. It is important to realize, that the conventional scheme which treats interference as noise is a special case of the new common messaging scheme. The former corresponds to a special situation of the latter when all common messages (or common message user pairs) are deactivated leaving private message only. Therefore, the proposed algorithms can be easily applied to the conventional beamforming vectors/covariance matrices designs by discarding all pairings and common messages.

1.2 Problems in Wireless Systems

The concept of wireless communications refers to a broad multiple-layered multi-disciplinary complex communication system. From a researcher's perspective, countless unresolved problems may be practically attractive. These problems range from communication protocol designs on a higher application/network layer, algorithm designs of transmissions on a lower algorithm/-physical layer, to DSP designs of antennas or chips. For this complex multi-disciplinary system, the research of this dissertation is particularly interested in various mixed combinatorial binary nonlinear optimization problems of coordinated transmission and resources selection/assignment which aim at either improving various QoS metrics of the system or minimizing power consumption while satisfying QoS requirements. In this section, a general review of related topics is provided.

1.2.1 Cognitive Radios

Radio spectrum is a physically limited natural resource. Currently, it is individually partitioned and licensed to *primary users (PUs)* exclusively [18]. On one hand, this system allows quality and uninterrupted transmission for important or sized institutions such as government bodies, radio stations, and media companies. On the other hand, it has been recognized that PUs often under-utilize the radio spectrum leaving *spectrum holes* [19]. Facing the booming demand for more spectrum, the inherent wastage of radio spectrum resources due to the current fixed licensing system is prohibitive and needs to be properly addressed. Consequently, *cognitive radio* has become an active interdisciplinary research topic that allows *secondary users (SUs)* to opportunistically use such licensed but unused spectrum holes only causing acceptably minimal interference to the PUs [20]. To respect the priority of PUs in using the licensed spectrum, accurate and responsive spectrum sensing is instrumental which is often carried out by a multiple-sensor network. It is thus important to reduce the correlation degree of sensors in terms of their channel fading situations. Understandably, having more than enough sensors working at the same time could only improve the sensing quality marginally [21] and may be counter-productive for distributed sensors subject to limited battery life, sensor network complexity and total coordination overhead. Therefore, an integer programming problem to select the least correlated sensors for an accurate spectrum sensing naturally arises [22, 23]. Beyond sensor selection, solving such binary optimization problems can be also inspiring for various other selection/ assignment problems encountered in other fields such as reconfigurable antenna array designs [24].

Essentially, cognitive radio can be regarded as an integrated but prioritized wireless system with cooperative PUs and SUs. Thanks to multiple antennas commonly equipped on the devices nowadays, it is ultimately possible to exploit the multiplexing gains (multiple virtual parallel channels) or spatial beamforming gains so that the interference from SU transmission to PUs is mitigated or cancelled, even without above-mentioned sharing scheme that rely on the availability of spectrum holes. Thus, it has become very attractive and useful to address the cooperative joint design of beamforming vectors or covariance matrices in the context of cognitive transmission [25, 26].

1.2.2 Wireless Relay Networks

Wireless relay network is a broad class of network topology where the source and destination nodes are interconnected by means of some nodes known as *relays*. The relays are primarily used to extend the coverage of network. Recently, a renewed interest has arisen in wireless relay networks since relays could potentially play more important roles in the exploitation of spatial multiplexing and diversities, in devising alternative power saving schemes while extending service coverage and throughput, and in the versatile roles relays play in ad-hoc or heterogeneous networks [27]. Relay networks are versatile in their many different network structures. Depending on the transmission environment and design assumptions, one or multiple source nodes may be served by one or multiple relays in transmitting messages to one or multiple destination nodes. In multi-relay networks, any signal may travel through a cloud of relays before it eventually reaches its destination. More commonly, single-hop relaying is assumed, which assumes the relay network to be single-layered [12]. The cooperation between the source and the relay node(s) is possible in three different schemes: 1) the source and destination nodes are completely separated, so connection is only possible through relay node(s) [12]; 2) the source-to-destination transmission occurs in different bandwidth or time interval from the relay-to-destination transmission;

3) the sources-to-destination transmission occurs simultaneously with the relay-to-destination transmission in the same bandwidth [28]. Any assumption of multi-hop relaying would certainly further complicate the complexity of research. On the other hand, several relaying strategies have been widely studied which include amplify-and-forward (AF), demodulate-and-forward, decode-and-forward and compress-and-forward. Among them, the AF scheme is the simplest since the relay(s) simply amplifies its received signal and forward the scaled signal to destination node(s). Due to the simplicity in implementation, the AF scheme has been commonly assumed[27] and it is studied in this thesis.

Multi-user relay-assisted wireless communications is considered as a promising architecture for future-generation multi-hop cellular networks [29–32]. The multiple-relay array, which can be essentially regarded as a scalable or reconfigurable antenna array, helps amplify-and-forward information from transmitters to their corresponding receivers. To reduce both power consumption and operational and communication overhead, it is particularly beneficial to select a well-chosen subset of relays, instead all of them, to achieve the design goals. With max-min fairness of users taken into account, it is developed as a joint program of relay assignment and beamforming which is one of the hardest mixed combinatorial binary nonlinear programs. The joint relay assignment and beamforming vectors design or outage analysis has been previously reported mainly in the context of single-user multi-relay scenarios [33–43] which constitute much easier problems. For more common multi-user multi-relay scenarios, relay beamforming designs alone are in general harder problems but they have been thoroughly studied [44–51]. Assuming orthogonal channels, the relay assignment and beamforming designs have been considered in a separated fashion under either a game theoretical framework or assuming MRC receivers. The hard $\{0, 1\}$ binary constraints were either relaxed to $[0, 1]$ then rounded, or dealt with by distance/channel strengths-based selection heuristics. For a mixed binary optimization of this complexity, these approaches obviously cannot guarantee the performance of selections. Therefore, it is really important to know how to jointly optimize the binary assignment and the continuous beamforming vector variables for both orthogonal and non-orthogonal transmissions.

1.2.3 Wireless Cellular Networks and Interference Channels/ Networks

Interference has been the core driving force behind the continuing evolution of wireless communications for decades [52]. In multi-cell multi-user SISO/MISO/MIMO downlink cellular networks, interference is conventionally treated as noise, so it is minimized in order to improve transmission rates or reliability. It has been known for long that a variety of improvements can be potentially achieved if multiple antennas are equipped on both or either side of a transmission link. Namely, diversity is much improved leading to more reliable communication [53], channel capacity is multiplied because of multiplexing gains or beamforming gains [54, 55]. However, the benefits can only be achieved when the antennas of BSs adjust their beam patterns in a coordinated fashion with the complete or partial knowledge of CSI. The most common optimization problem in downlink transmission involves the optimized coordination of all antenna beam patterns. In general, the designs can be divided into two categories: maximizing sum-rate or minimal rate of users while satisfying power budgets; and minimizing the consumed power while satisfying individual rate constraints. The difficulty of these problems depends on the structure of network but most of them render NP-hard non-convex optimization problems [10, 11, 56–58]. It is worth noting that the properties of these coordinated transmission optimization problems can be generally preserved in the context of cognitive transmissions. Therefore, most proposed algorithms can be adopted to the new problems with cognitive constraints taken into account.

From the findings of rate region studies for interference channels (ICs) [6, 59–61], simply treating interference as noise is not necessarily capacity achieving, especially in medium to strong interference channels. It is therefore ultimately important to realize the fact that interference possesses information which may be better decoded. By enabling partially decodable interferences (in the form of common messsages) [9, 59, 62, 63], the design in either beamforming vectors or covariance matrices can potentially achieve the rate capacity of interference channels or networks (cellular networks or relay networks). Admittedly, the new successive decoding scheme requires joint pairing (binary variables) and transmission coordination (continuous variables).

The resulting joint problem is a mixed combinatorial binary nonlinear optimization problem which is quite challenging.

1.3 Dissertation Outline and a List of Publications

The main contribution of this dissertation is to exploit the hidden d.c. properties of the NP-hard combinatorial nonlinear optimization problems (mixed) encountered in wireless communication systems. In particular, we are interested in three major topics:

- Selecting the least correlated subset of sensors from wireless sensor networks for spectrum sensing;
- Jointly optimizing relay assignment and beamforming vectors in multi-user multi-relay networks;
- Successive interference mitigation with pairing and common message decoding for MIMO interference channels.

The outline of the dissertation is as follows:

Chapter 1

This chapter presents the motivation and scope, the outline and the contributions of the research.

Chapter 2

A brief review of background knowledge is presented in this chapter. It includes explanations for some fundamental concepts and techniques in wireless communications. An overview of optimization theory with an emphasis on the d.c. optimization framework is also provided.

Chapter 3

A framework for the optimal sensor selection based on Bregman matrix deviation minimization is proposed for accurate spectrum sensing. Sensor selection is aimed at minimizing the measure of correlation over the selected subset of sensors. It is formulated as a binary optimization problem in $\{0, 1\}$ variables which is a hard rank-one optimization. By exploiting the hidden d.c. structure of the binary variables, we are able to equivalently convert it into a continuous d.c. optimization problem with penalty functions. This problem is further solved by an iterative sequence of d.c. optimizations which guarantee improved performance on each iteration. With the ability to handle multiple convex or non-convex correlation measures, numerical results show that the proposed framework and algorithm can handle the various binary selection problems effectively.

The results have been published in one conference paper.

- E. Che, H. D. Tuan, H. H. Kha, and H. Q. Ngo, "Bregman divergence based sensor selections for spectrum sensing", *IEEE Wireless Communications and Networking Conference (WCNC)*, 2012, France.

Chapter 4

Joint relay assignment and beamforming optimization in multi-user multi-relay wireless networks is studied. Two transmission models are considered: orthogonal and non-orthogonal transmission. In both cases, each relay is assigned with a binary variable which decides whether it is active or inactive, and a continuous beamforming weight variable for relaying signals. Fairness of services among all users is concerned by considering max-min SNR or SINR problems. Firstly, it is revealed that the $\{0, 1\}$ binary constraint is equivalent to the difference of two convex sets. Then, it is proved that strong Lagrangian duality holds for the converted canonical d.c. programs. Finally, we develop a path-following d.c. iterative procedure to jointly optimize the two variables. Numerical results demonstrate that an optimized subset of relays can almost retain the performance for the orthogonal transmission. For the non-orthogonal transmission, it is found the performance is sensitive to the number of relays deployed but minimal performance degradation is achieved by the proposed procedure. Computational complexity of the proposed algorithm is analyzed with the number of iterations and average CPU time given. These results show that the proposed algorithm can converge to optimized solutions very efficiently.

The results have been published in one journal paper and one conference paper.

- E. Che, H. D. Tuan, and H. H. Nguyen, "Joint optimization of cooperative beam forming and relay assignment in multi-user wireless relay networks", *IEEE Transactions on Wireless Communications*, Accepted, 2014.
- E. Che, H. D. Tuan, and H. H. Nguyen, "Relay selection in multi-user amplify-forward wireless relay networks", *IEEE International Conference on Acoustics, Speech and Signal Processing (ICASSP)*, 2012, Japan.

Chapter 5 and 6

These two chapters are concerned with wireless transmission designs in cellular MIMO/MISO/-SISO networks. In Chapter 5, the model of conventional transmission is introduced, which treats all intra- and inter-cell interference as noise. The considered design is to maximize the rate performance under power and/or cognitive constraints. Essentially, most relevant designs are aimed at aligning or minimizing the presence of interference so that the service goals could be achieved. An analysis of power minimization problems is also presented in which some special problems are shown to be convex. These observations are found critical for solving some of the rate maximization problems. Nonetheless, the majority of rate maximization problems in the context of MIMO networks remain NP-hard non-convex problems. Therefore, we will focus on the MIMO networks and propose optimized algorithms for locating local optimal covariance matrices and precoding matrices.

In Chapter 6, it is realized that the conventional scheme of treating interference as noise is not necessarily capacity-achieving. In a natural extension to the transmission model adopted in Chapter 5, we shall split the some user's message into two parts: a private message and a common message. The former is to be decoded by the user itself while the latter is designated to be also decodable by a pre-determined out-of-cell user. The novel scheme stems from the message-splitting idea originally proposed for interference mitigation in two-user SISO interference channels [59]. In this research, we will extend the scheme to multi-cell multi-user MIMO downlink networks. In particular, any selected transmitter may also send a common message which is decodable by its intended receiver as well as another paired receiver. The common and private messages are decoded following a successive order. It has been shown in previous works that this successive decoding scheme has a potential to improve the rate capacity for certain SISO and MISO cellular networks [7, 9, 59]. However, it has never been incorporated into MIMO transmission due to the great inherent difficulty in optimization. In this work, we formulate it into sum-rate or the worst user's rate mixed combinatorial binary nonlinear optimization problems with continuous beamforming vector or covariance matrix variables and the "binary" pairings variables. Apparently, the new optimization problems include the conventional scheme with private message only as a special case when no pairings are selected or common messages are zero. Due to the apparent difficulty of joint optimization, we propose to pre-determine the pairings of users who send and decode common messages by a heuristic procedure based on the rankings of interference to noise ratios. Then, it becomes an optimization problem in either beamforming vector or covariance matrix variables for the private and common messages. For this problem, we are able to recast it into a non-smooth d.c. optimization framework with d.c. objective functions and convex constraint sets. An tailored effective yet efficient d.c. iterative algorithm is then developed. Through deterministic studies with fixed channel gains given, we plot the sum-rate and the worst user's rate achieved by both the new scheme and the conventional scheme in the rate region. In comparison with the known inner and outer bounds of rate region developed for interference channels, we are able to see the rate capacity improvement achieved by the successive decoding scheme. Monte Carlo simulation results are also presented to show the effectiveness of the new scheme for certain cases.

Admittedly, the designs of the common and private messages in this framework can be optionally focused on transmit covariance matrices or precoding (beamforming) matrices design. Although the optimization in the former variables varies from that in the latter, d.c. framework is proven applicable to both but our current d.c. reformulation seems to work more outstanding for the covariance case. For this reason, we shall focus on the covariance matrices design for the common and private messages for the MIMO networks, and only provide a tested beamforming design for the MISO networks.

Importantly, the simplest case of ICs is the 2-user SISO IC studied by [59] which forms the foundation of all other types of interference channels. Despite the seemingly easy network setup, its rate capacity has never been fully understood until today. The common and private message splitting scheme was first developed in this case to serve as the so-called one-bit inner bound, the optimal splitting design of the messages has never been addressed. It is, therefore, very interesting to investigate how well the proposed splitting algorithm for MIMO ICs can perform in this simplest 2-user SISO case. In Appendix C, we attach a under-review paper with these concerned simulation results. It shows, for the first time, that the DCI algorithm can indeed locate rate pairs outside of the known inner bounds with a better splitting ratio between common and private messages.

Also, we note that the novel common and private message splitting scheme includes the conventional private-only messaging scheme as a special case (when common messages are zero). Even without common messages, the designs of covariance matrices or precoding (beamforming) vectors for this case are still unresolved challenging topics due to their non-convexity. For precoding vectors design, a DCI-based algorithm is proposed in [64] for private-only MIMO multi-cell multi-user downlink networks. In [58], an important observation of concavity is made to the problem which leads to an improved DCI algorithm with iterative closed-form solutions. For covariance matrices design, we present a computationally inexpensive method based on concave programming in Appendix D. The study considers a MISO multi-cell multi-user downlink system taking into consideration the additional requirements of cognitive radios. The relationship between worst user's performance and the sum-rate performance is also revealed.

In summary, The results are published in one journal paper and two conference papers while one journal paper and one conference paper have been submitted,

- E. Che and H. D. Tuan, "Sum-rate based coordinated beam forming in multi cell multi-antenna wireless networks", *IEEE Communication Letters*, vol.18, pp.1019 - 1022, Jun. 2014.

- E. Che, H. D. Tuan, H. H. M. Tam, and H. H. Nguyen "Successive interference mitigation in multiuser MIMO interference channels", submitted to *IEEE Transactions on Communication*, Jul. , 2014.

- E. Che and H. D. Tuan, "Optimized coordinated precoding in multicell MIMO wireless systems", *13th International Symposium on Communications and Information Technologies (ISCIT)*, 2013, Thailand.

- E. Che and H. D. Tuan, "Interference mitigation by jointly splitting rates and beam forming for multi-cell multi-user networks", *13th International Symposium on Communications and Information Technologies (ISCIT)*, 2013, Thailand.

- E. Che, H. D. Tuan, and H. H. M. Tam "Optimised Power Splits for Han-Kobayashi Interference Mitigation", submitted to *IEEE Global Conference on Signal and Information Processing (GlobalSIP)*, Jun., 2014.

Chaper 7

This chapter summarizes the main contributions of this dissertation and makes suggestions for future research developments.

Chapter 2

Fundamentals of Wireless Communication and Optimization

In this chapter, we will provide an overview of concepts and techniques that will be used throughout the dissertation. Firstly, we discuss several important physical phenomenons of radio wave propagation. Some of the most popular statistical wireless channel models will then be outlined and their respective features/ limitations discussed. We will present some of the most fundamental theoretical findings in the field of information theory studies which shall serve as the guideline for all wireless system designs. After that, the benefits and challenges of the state-of-the-art multiple-antenna wireless system will be briefly discussed. Finally, our focus will be shifted onto a few important aspects of optimization theory. We will frequently use this knowledge to address the mathematical challenges encountered in the various concerned wireless communication topics.

2.1 Wireless Communications

Wireless communication is the transfer of information signals between two enabled devices by electromagnetic waves through un-wired mediums such as the air. Although wireless communication dates back to 1897 with Marconi's first successful telegraphy, it has, by all means, still been one of the most exciting yet challenging areas in the communication field since the 1960s.

Wireless communication enjoys extraordinary benefits such as much-improved mobility, flexibility and the freedom from costly infrastructure investments. However, its applications are not as straightforward as that of wired communication. In fact, the challenges of wireless communication are largely due to three fundamental physical phenomenons which are otherwise not as decisive in wired communication. The first is the fading nature of wireless channels. A transmitted signal is affected by both *large-scale propagation effects* caused by path loss and shadowing over relatively large distances, and *small-scale propagation effects* which cause time variations of channel strengths mainly due to multipath fading. Due to the uncertainty of any instantaneous channel, the accurate deterministic channel sensing is very hard and sometimes not as important. Instead, statistical channel estimations over a short period of time are normally adopted. Secondly, wireless communication operates on a broadcasting basis. With multiple transmit-receive pairs operating in the same time and spectrum domain, the performance in terms of either information throughput or reliability can be adversely affected by *interference* as well as *noise*. This also significantly rises the difficulty of reliable and secret transmission because any unwanted eavesdropper device in the transmission field can always detect and potentially decode all signals emitted. Improving the safety performance for wireless communication has always been another active and interesting topic. Thirdly, the radio spectrum for wireless communication is an extremely scarce resource. To reduce the interference-induced adversaries, one has to either use techniques such as time-division duplexing (TDD), Frequency-division duplexing (FDD) and the likes, or to improve the coordination between simultaneous transmitters on different levels. Apparently, the former techniques essentially sacrifice the re-use factor of the available spectrum resources (hence, reduced spectral efficiency), while the latter often renders very hard coordination tasks from a mathematical perspective.

2.1.1 Large-scale Fading

Large-scale fading represents the average power attenuation or path loss due to motion over large areas [65]. It is mainly attributed to path loss as a function of transmission distance as well as shadowing due to large objects. We begin with the ideal line-of-sight (LOS) free space path loss model for signal propagation. Consider a fixed antenna in free space with a receive antenna d meters away in the far field [1]. Assume $u(t)$ is the complex lowpass equivalent signal of transmitted signal $s(t)$, the received signal $r(t)$ is [8]

$$r(t) = \mathsf{Re}\{\frac{\lambda\sqrt{G_l}e^{-j(2\pi d/\lambda)}}{4\pi d}u(t)e^{j2\pi f_c t}\}$$

where $\sqrt{G_l}$ is the product of the transmit and receive antenna field radiation patterns in the LOS direction and c is the speed of light. f_c is the carrier frequency and λ is the signal wavelength. Let P_t and P_r be the transmit and receive power, so it is true that

$$\frac{P_r}{P_t} = [\frac{\sqrt{G_l}\lambda}{4\pi d}]^2.$$

Due to the dissipation of power radiation, the received power P_r is inversely proportional to the square of the distance d as well as to the carrier frequency.

In more realistic models, however, multiple objects and terrains present in the physical environment which cause three typical phenomenons. Namely, they are *reflection, diffraction* and *scattering* [2, 8, 66]. These effects may lead to multiple received copies (multipath), power attenuation, time delay, phase and frequency shift. After combining all the received signals, the actual received signal may be a much distorted version of the original signal. At least, the

[1]the distance between the antennas is sufficiently greater than the wave length

actual rate of power attenuation is much faster than the ideal free-space rate of $1/d^2$. Therefore, it is impossible to obtain an accurate model which characterizes path loss across different environments. Nevertheless, a simplified model such as the following is widely adopted.

$$P_r(dBm) = P_t(dBm) + T(dB) - 10\gamma \log_{10}[d/d_0].$$

In the above model, the power decay is dependent on the parameters T (an antenna-specific constant), path loss exponent γ and distance d where d_0 is the reference distance. Based on empirical measurements, path loss exponents γ corresponding to different transmission environment types can be found in Table. 2.1 [8]. Beyond this simple model of path loss, other empirical path loss models may be available for specific transmission environments. For example, Okumura's model [67] is used for large urban macrocells which is applicable over distances of $1-100$ km and frequency range of $150-1500$ MHz. Recently, various path loss models have also been reported for indoor, tunnel or body-centric radio channels [68–71]. In addition, random variations in

Environment	γ range
Urban macrocells	$3.7-6.5$
Urban microcells	$2.7-3.5$
Office Bldg. (same floor)	$1.6-3.5$
Office Bldg. (multiple floor)	$2-6$
Store	$1.8-2.2$
Factory	$1.6-3.3$
Home	3

TABLE 2.1: Typical path loss exponents [8]

path loss are present due to signal blockage and distortion caused by large or scattering random objects as well as reflecting surfaces. As a result, path loss models are commonly accompanied by a log-normal shadowing component which reflects this addional attenuation. In particular, the path loss ϕ is assumed random with a log-normal distribution by

$$p(\phi) = \frac{\xi}{\sqrt{2\pi}\sigma_{\phi_{dB}}\phi}\exp\{-\frac{(10\log_{10}\phi - \mu_{\phi_{dB}})^2}{2\sigma^2_{\phi_{dB}}}\},\ \phi > 0,$$

where $\xi = 10/\ln 10$, $\mu_{\phi_{dB}}$ is the mean of $\phi_{dB} = 10\log_{10}\phi$ in dB and σ_{dB} is the standard deviation of ϕ_{dB} (dB).

In summary, by combining the path loss and shadowing fading, the ratio of received to transmitted power in dB is as follows [8]:

$$10 \log_{10}(\frac{P_r}{P_t}) = L_{pl} + \phi_{dB}$$

where L_{pl} is the path loss component (in dB), ϕ_{dB} is a Gaussian distributed random variable (in dB) with zero mean and variance σ_{dB}^2.

2.1.2 Small-scale Fading

Small-scale fading refers to the rapid variation of signal amplitude and phase as a result of small changes (in the wavelength scale) in the spatial separation between a receiver and transmitter [65]. In the time domain of small-scaling fading, a channel is called *fast fading* or *time-selective* if its *coherence time* T_c is much smaller than *symbol duration* T_s. Time diversity may be available for improved communication robustness. Otherwise, it is called *slow fading* or *time-flat* channel. In the frequency domain, one the other hand, a channel is classified as *Frequency-selective fading* if the *coherence bandwidth* is smaller than the bandwidth of the signal. Otherwise it is called *flat fading*. In the time-delay domain, frequency-selective channel is caused by multipath dispersion of a symbol exceeding its duration time, which yields *channel-induced inter-symbol-interference (ISI)*. By contrast, all multipath components of a symbol arrive before the transmitting of the next symbol in flat fading channel. Consequently, data transmission over flat fading channel is classified as *narrowband* transmission, and that over frequency-selective channel is called *wideband* transmission [72]. Transmitter and receiver may experience different types of channel over the period of transmission as a result of environment changes.

Nakagami fading, Rician fading and Rayleigh fading

The Nakagami fading model [2, 66, 73, 74] is a generalized fading model. The PDF of a signal envelope with Nakagami distribution is given by

$$p(r) = \frac{2m^m r^{2m-1}}{\Gamma(m)\sigma^{2m}} e^{-\frac{mr^2}{\sigma^2}}, \; r > 0,$$

where σ^2 is the average received power, $\Gamma(m)$ is the Gamma function, and m represents the degree of fading. The Nakagami fading model generalizes both the Rician fading channel where there exists a dominant stationary signal component (e.g. LOS path), and the Rayleigh fading channel where there are many independent scattered reflectors without a dominant component. Namely, the Nakagami model reduces to the Rayleigh distribution when $m = 1$, and it reduces to the Rician distribution when $m = (F+1)^2/(2F+1)$ with parameter $F = 0, 1, 2, ...$

2.1.3 MIMO Communications

In recent years, multiple antennas equipped on wireless devices have enabled the exciting development of wireless communications (e.g. 4G-LTE and 5-G networks [75]). Its potentials to greatly enhance the capabilities of wireless communications in terms of higher spectral efficiency and better transmission reliability have been recognized widely. However, to actually materialize the many benefits requires deeper and more dedicated research since the new multi-antenna communication architectures are not merely a straightforward extension from the less-sophisticated single-antenna ones. In this regard, development up-to-date is still far from capacity-achieving. In the dissertation, a significant part of research will be focused on MIMO-related (or MISO-related) topics. In hope of better understanding, we shall present here a fundamental mathematical model for MIMO wireless communications. In addition, three most noticeable features will be briefly reviewed.

Assume a simple radio transmission scenario where the transmitter is equipped with N_t antennas while the receiver with N_r antennas. Denote the channel by $H \in \mathbb{C}^{N_r \times N_t}$. The received signal vector is given by

$$\boldsymbol{y} = H\boldsymbol{x} + n,$$

where $\boldsymbol{x} \in \mathbb{C}^{N_t}$ is the Gaussian transmitted vector, $\boldsymbol{y} \in \mathbb{C}^{N_r}$ is the received signal vector and n is zero-mean complex Gaussian noise with independent, equal variance real and imaginary parts. Let R_n be the covariance of n, and $\boldsymbol{Q}$ be the covariance matrix of the input vector $\boldsymbol{x}$ which is subject to a power budget P. Assuming $\boldsymbol{x}$ and n are uncorrelated with one another, the channel capacity is given by [76]

$$C = \log_2(\frac{|R_n + H\boldsymbol{Q}H^H|}{|R_n|}).$$

In [77], it is shown that the ergodic capacity of Gaussian i.i.d. H channels is achieved with $Q = \frac{P}{N_t} I_{N_r}$. Clearly, this strategy simply distributes the available transmission power to all transmit antennas equally. For non-ergodic channels, obviously, this fixed transmission strategy generally cannot achieve the maximum channel capacity. In fact, the capacity-achieving choice of covariance matrix $\boldsymbol{Q}$ can be obtained by water-filling algorithm [77] for any instantaneous time-invariant channel H.

In general, the multi-antenna setting has enabled the wireless transmissions with the three most notable capabilities as follows.

- **Diversity** Due to the fading nature of wireless channels, *diversity* schemes are an integral part of wireless systems to improve reliability of information transmission by sending a message signal through two or more communication channels with different characteristics. Diversity helps combat fading and co-channel interference and thus improves transmission reliability. Many forms of diversity are available for these purposes, such as time diversity, frequency diversity, space/ antenna diversity, polarization diversity, cooperative diversity and so forth. In particular, the MIMO systems enjoy antenna diversity as each pair of tx-rx antennas are supposed to have an independent and uncorrelated channel. For example, for a system where (N_r) multiple antennas are equipped on the receiver where a single antenna is equipped on the transmitter (SIMO), a maximal diversity gain of N_r is possible if the receive antennas are uncorrelated. With multiple antennas (N_t) equipped on the transmitter (MIMO), the total maximal diversity gain of $N_t N_r$ for Rayleigh fading channels [53] can be achieved.

- **Spatial Multiplexing** Spatial multiplexing is a technique to transmit independent and separately coded data signals from each of the multiple antennas. Instead of sending the same symbol on all transmit antennas, *spatial multiplexing* sends multiple symbols simultaneously on parallel channels which greatly improves spectral efficiency in terms of number of bits transmitted per second and per Hz through wireless channels [55]. The maximum spatial multiplexing order is

$$N_s = \min N_t, N_r.$$

  In practise, the multiplexing gain is limited by spatial correlation since some parallel transmission streams may suffer from weak and correlated channels. In [54], it was shown that in high-SNR regime with i.i.d. Rayleigh fading channels, the number of degrees of freedom is $\min\{N_r, N_t\}$. Apparently, there is a tradeoff between the diversity gains (reliability) and the spatial multiplexing gains (throughput).

- **Precoding and Beamforming** *Precoding* is a generalization of beamfomring to provide single- or multi-data streams in MIMO or MISO transmission, known as space-division-multiple access (SDMA) in multi-user MIMO. Precoding or beamforming forces the antenna patterns into a specific angular direction by adding appropriate weights on the codes before transmitting. It takes advantage of the spatial correlation, so the intended signal can be beamformed to its intended receiver while causing minimal interference to the other unintended receivers. In general, it can lead to a maximal beamforming gain of $N_t N_r$.

2.2 Optimization Theory

Throughout this study, we will frequently use the term *optimization problem* which is denoted by the following constrained problem

$$\begin{aligned} \min_{\boldsymbol{z}} \quad & f(\boldsymbol{z}) \\ \mathsf{s.t.} \quad & \boldsymbol{z} \in \mathcal{D}. \end{aligned} \tag{2.1}$$

Problem (2.1) is called a *linear program (LP)* if both the objective function $f(*)$ and the constraint set $\mathcal{D}$ are linear. Otherwise, it is a *nonlinear program (NLP)*. It is fairly straightforward to solve LPs [78]. However, since most of the concerned problems in wireless network applications can only be formulated as NLPs, we are more interested in the latter which generally have multiple local optima and are much harder, sometimes impossible, to solve.

We start by calling a solution $z^* \in \mathcal{D}$ a *global minimizer* of f over $\mathcal{D}$ if it is true that $f(z^*) \leq f(\boldsymbol{z})\ \forall \boldsymbol{z} \in \mathcal{D}$. The corresponding value of f is called the *global minimum* of f over $\mathcal{D}$ which is denoted by $\min f(\mathcal{D})$. [2]

In a majority of wireless network applications which eventually render hard nonlinear optimization tasks, it is extremely challenging, if not impossible at all, to obtain the value of global minimum or the global minimizer. Although achieving the global optimum is possible in some cases, as found in the works [11, 79] (and references therein) where difference of monotonic increasing functions (*d.m. function*) is used to represent the objective functions while the constraint sets are approximated by the polyblocks, such tailored global optimization techniques are not easily tractable for most other applications in the field. More importantly, their computational costs are overwhelmingly expensive making them only superior to the more prohibitively expensive exhaustive grid searching algorithms. On the other hand, most local optimization methods for nonlinear programming using tools such as gradients, subgradients and derivatives

[2] the maximization problems can always be converted equivalently into the form of (2.1) since $\max f(\mathcal{D}) = -\min -f(\mathcal{D})$.

are unable to guarantee global optima. Instead, they can at most locate local minima which is defined by the following definitions.

Definition 2.1. [17] Let $\epsilon > 0$ be a real number. An ϵ-neighbourhood of a point $z^* \in \mathcal{D}$ is defined as

$$N(z^*, \epsilon) := \{\boldsymbol{z} \in \mathcal{D} : ||\boldsymbol{z} - z^*|| < \epsilon\}.$$

A point $z^* \in \mathcal{D}$ is called a *local minimizer* of f over $\mathcal{D}$ if there is an $\epsilon > 0$ such that

$$f(z^*) \leq f(\boldsymbol{z}) \;\forall\; \boldsymbol{z} \in N(z^*, \epsilon)$$

Most nonlinear programming problems are *multi-extremal optimization* problems for which there exists more than one local optima. Although local algorithms can at most find one of many local optimas whose global optimality can not be guaranteed, their comparatively low computational costs and easier applicability sometimes make them the preferred alternative to global optimization methods, especially in applications with a limited budget of computational resources.

2.2.1 Convex Optimization

Definition 2.2. A set $\mathcal{D}$ is convex if for any $\boldsymbol{z}, \boldsymbol{y} \in \mathcal{D}$ and any $0 \leq \theta \leq 1$, it is true that $\theta\boldsymbol{z} + (1-\theta)\boldsymbol{y} \in \mathcal{D}$.

Definition 2.3. A function $f(\boldsymbol{z})$ is called convex in $\boldsymbol{z}$ on a convex domain $\mathcal{D}$ if for all $\boldsymbol{z} \in \mathcal{D}$, $\boldsymbol{y} \in \mathcal{D}$ and $0 \leq \theta \leq 1$, it is true that

$$f(\theta\boldsymbol{z} + (1-\theta)\boldsymbol{y}) \leq \theta f(\boldsymbol{z}) + (1-\theta) f(\boldsymbol{y})$$

Definition 2.4. [16] Let $h: \mathbb{R}^n \rightarrow \mathbb{R}$ or $h: \mathbb{C}^n \rightarrow \mathbb{R}$ be a convex function. Then, the inequality $h(\boldsymbol{z}) \leq 0$ is called *convex* whereas the inequality $h(\boldsymbol{z}) \geq 0$ is called *reverse convex.*

Besides LPs and least-squares problems, one of the most important and exceptional class of optimization problems today is inarguably the *convex optimization problem* in which a convex/-linear objective function is minimized subject to a convex feasible set $\mathcal{D}$ (with convex inequalities and/or affine equalities)[3]. On the contrary, a problem is called non-convex optimization problem if either or both of the minimized objective function and constraint function(s) is not convex. The most fundamental property of convex optimization problems is that any local optima is also global optima. In order words, this property makes any locally optimal methods indeed capable of locating the global optimal solution for convex optimization problems. Although most convex optimization problems still do not have analytical solutions, they can be solved very efficiently by interior-point methods [80]. Therefore, it is always one's first priority to realize the possibility of reformulating a seemingly non-convex optimization problem into one or a combination of convex optimization problems, via necessary changes of variables, mathematical manipulations, and/ or solving a convex dual problem with zero duality gap.

Unfortunately, it is often hard, if not impossible, to devise a convex problem for most of non-convex problems encountered in wireless communications. In these cases, proper reformulation with relaxation (from a non-convex function to a looser but convex function) or approximation is instead needed to convexify the problem. In other words, instead of solving the non-convex optimization problem directly, one solves its approximated/ relaxed convex problem whose optimal value serves as the lower bound of the original problem. Therefore, convex optimization is still one of the most useful tools in dealing with non-convex optimization tasks in the sense that it may be useful to find a feasible initial solution for local optimization heuristics, and that it may be used to provide lower bounds for the non-convex optimization problem.

In addition, semi-definite programming (SDP) that can be efficiently solved by interior-point

[3] concave maximization problem over a convex set is equivalent to convex minimization over a convex set

methods [81] is also an important class of convex optimization problmes. A SDP is an optimization problem of the form:

$$\begin{aligned} \min_{\boldsymbol{X}} \quad & P \cdot \boldsymbol{X} \\ \text{s.t.} \quad & A_i \cdot \boldsymbol{X} = b_i, \ i = 1, 2, \cdots, m, \\ & \boldsymbol{X} \succeq 0, \end{aligned} \tag{2.2}$$

where $A_i, \ i = 1, 2, \cdots, m$ are known symmetric matrices and $\boldsymbol{X} \succeq 0$ denotes that the matrix variable $\boldsymbol{X}$ is positive semidefinite.

Furthermore, we will also encounter the so-called *second-order cone programming (SOCP)* which is a special class of SDP in convex optimization. A SOCP minimizes a linear function over the intersection of an affine linear manifold with the Cartesian product of second-order (Lorentz) cones in the following form [82]:

$$\begin{aligned} \min \quad & a^T \boldsymbol{z} \\ \text{s.t.} \quad & ||A_i \boldsymbol{z} + b_i||_2 \leq c_i^T \boldsymbol{z} + d_i, \ i = 1, \cdots, m \\ & F\boldsymbol{z} = g, \end{aligned} \tag{2.3}$$

where $a \in \mathbb{R}^n$, $A_i \in \mathbb{R}^{n_i \times n}$, $b_i \in \mathbb{R}^{n_i}$, $c_i \in \mathbb{R}^n$, $d_i \in \mathbb{R}$, $F \in \mathbb{R}^{p \times n}$ and $g \in \mathbb{R}^p$. Obviously, SOCP reduces to a LP if $A_i = 0$ for $i = 1, \cdots, m$. It is equivalent to a convex *quadratically constrained quadratic program (QCQP)* when $c_i = 0$ for $i = 1, \cdots, m$. Since the constraints can be rewritten as linear matrix inequalities using Schur complement, it is also a special case of SDP. SOCP is positioned between LP and QP and SDP. SOCP is widely applicable in such problems as logarithmic Tchebychev approximation and the problem of finding the smallest ball containing a given set of ellipsoids. In terms of computational complexity, SOCP problems can be solved by interior-point methods in polynomial time. The computation efforts per iteration required by these methods to solve SOCP problems is greater than that required to solve LP and QP problems but less than that required to solve a similar-sized SDP problem [82]. This makes SOCP a more attractive alternative to SDP on some occasions.

2.2.2 D.C. Optimization

As will be discussed in the following chapters, the research in this dissertation is concerned with various applications in the context of wireless networks. For sensor selection in spectrum sensing, we aim at selecting the least correlated group of sensors so that quality spectrum sensing can be carried out. For the various topics in multi-cell multi-user multi-antenna downlink networks, it is the ultimate goal of this research to find optimal transmission strategies (power allocation, beamforming vectors or covariances). Based on these strategies, rate capacity can be achieved subject to a limited transmit power budget and/or a cognitive interference threshold constraint to the primary users, or that the consumed power is minimized satisfying certain QoS constraints. Most of these problems come down to nonlinear programs which are non-convex or even nonsmooth and thus are extremely challenging.

To properly address such challenging optimization problems, we may exploit the explicitly-hidden d.c. structures of either the objective functions or the constraint functions, and use the following properties of d.c. programming.

Definition 2.5. [4][16] Let $\mathcal{C} \subset \mathbb{R}^n$ or $\mathcal{C} \subset \mathbb{C}^n$ be compact and convex. A function h: $\mathcal{C} \rightarrow \mathbb{R}$ is called *d.c.* on $\mathcal{C}$ if there are two convex functions $p : \mathcal{C} \rightarrow \mathbb{R}, q : \mathcal{C} \rightarrow \mathbb{C}$ such that

$$h(\boldsymbol{z}) = p(\boldsymbol{z}) - q(\boldsymbol{z}), \qquad \forall \boldsymbol{z} \in \mathcal{C}$$

A function that is d.c. on $\mathbb{R}^n$ or $\mathbb{C}^n$ will be called d.c.

Definition 2.6. A set $\mathcal{P}$ is called a *d.c. set* (difference of convex sets) if $\mathcal{P} = \mathcal{D} \setminus \mathcal{C}$, where $\mathcal{D}$ and $\mathcal{C}$ are two convex sets.

[4]Note that, conventionally, the term d.c. stands for the difference of two convex functions, which is equivalent to the difference of two concave functions. In this dissertation, we may use the term d.c. frequently which may refer to either case depending on the context.

Definition 2.7. [17] An optimization problem is called a *d.c. programming problem* if it has the form

$$\begin{aligned} \min_{\boldsymbol{z}} \quad & f(\boldsymbol{z}) \\ \text{s.t.} \quad & \boldsymbol{z} \in \mathcal{P}, \end{aligned} \tag{2.4}$$

where f is a d.c. function while $\mathcal{P}$ is a d.c. set.

Obviously, d.c. programming problems consists of a rich class of different programming problems. Namely, every concave programming problem is also a d.c. programming problem.

Denote by $\mathcal{C}^2$ the class of functions $\mathbb{R}^n \to \mathbb{R}$ or $\mathbb{C}^n \to \mathbb{R}$ whose second partial derivatives are continuous everywhere.

Theorem 2.8. *Every function $f \in \mathcal{C}^2$ is d.c.*

Proof: See proof in [17]. □

Corollary 2.9. *A real valued continuous function on a compact (convex) subset $\mathcal{D}$ of $\mathbb{R}^n$ or $\mathbb{C}^n$ is the limit of a sequence of d.c. functions on $\mathcal{D}$ which converges uniformly in $\mathcal{D}$.*

Proof: See proof in [17]. □

Theorem 2.10. *Every optimization problem with concave, convex or d.c. objective function and a combination of convex, reverse convex and d.c. constraints is a d.c. programming problem.*

Proof: See proof in [17] □

Since most of functions encountered in the field of wireless communications have continuous second partial derivatives, or they are a combination of piece-wise functions which have continuous second partial derivatives, it is possible to reformulate almost all these problems into d.c. optimization problems. Obviously, d.c. is potentially applicable to a great range of non-convex problems.

Moreover, d.c. function has the following properties which enable a great operational stability and significantly extend its applicability. We may repeatedly use these operations (especially the first three operations) in this research.

Theorem 2.11. *[17] Let p_i and q_i $(i = 1 : M)$ be convex functions, so functions $f_i = p_i - q_i$ $(i = 1 : M)$ are d.c. Then the following functions are also d.c.:*

- $\sum_{i=1}^{M} \lambda_i f_i$, *for any real numbers* λ_i*;*
- $-f_i = q_i - p_i, \quad \forall i$*;*
- $\min_{i\in[1:M]} f_i = \sum_{i\in[1:M]} p_i - \max_{i\in[1:M]} \big[q_i + \sum_{m\in[1:M]\backslash i} p_m\big]$, *with convex functions* $\sum_{i\in[1:M]} p_i$ *and* $\max_{i\in[1:M]} \big[q_i + \sum_{m\in[1:M]\backslash i} p_m\big]$*;*
- $\max_{i\in[1:M]} f_i = -\min_{i\in[1:M]} [-f_i] = -\min_{i\in[1:M]} [q_i - p_i]$*;*
- $|f(\boldsymbol{z})|$, $f^+(\boldsymbol{z}) := \max\{0, f(\boldsymbol{z})\}$ *and* $f^-(\boldsymbol{z}) := \min\{0, f(\boldsymbol{z})\}$*;*

Proof: See Proof in [17]. □

2.2.3 A Generic D.C. Optimization Framework

As defined in Theorem 2.10, a d.c. programming problem may refer to a wide range of structures, some of which are extremely hard to deal with [17]. Inspired by [14, 56, 83–89], we are particularly interested in a canonical form of d.c. program below which minimizes a d.c. function over a convex set.

$$\begin{aligned} \min_{\boldsymbol{z}} \quad & F(\boldsymbol{z}) = f(\boldsymbol{z}) - g(\boldsymbol{z}) \\ \text{s.t.} \quad & \boldsymbol{z} \in \mathcal{K}, \end{aligned} \tag{2.5}$$

where functions $f,\ g$ are convex in the continuous variable $\boldsymbol{z}$ and $\mathcal{K}$ is a convex set.

Since Theorem 2.8 suggests the wide applicability of d.c. programs, and that all d.c. programs can be essentially converted into the above canonical form [17], addressing program (2.5) properly has significant benefits for a wide range of problems. Generally, as proved in [90], the global optimal solution of certain applications in the form of (2.5) can be obtained by combining d.c. iterations (DCIs) with a customized branch-and-bound technique. However, this global optimization procedure has prohibitively high computational complexity. Therefore, we instead follow the ideas of [56, 88, 89, 91, 92] to obtain equivalent d.c. decompositions that make DCIs alone efficient.

Suppose that $z^{(\kappa)}$ is feasible to (2.5). Since g is convex, its gradient $\nabla g(z^{(\kappa)})$ at $z^{(\kappa)}$ is also a subgradient [16]. Therefore,

$$f(\boldsymbol{z}) - g(\boldsymbol{z}) \leq f(\boldsymbol{z}) - g(z^{(\kappa)}) - \langle \nabla g(z^{(\kappa)}), \boldsymbol{z} - z^{(\kappa)} \rangle \quad \forall \boldsymbol{z}.$$

It follows that for any feasible $z^{(\kappa)}$ to (2.5), the following convex program provides a global upper bound minimization for d.c. program (2.5):

$$\min_{\boldsymbol{z} \in \mathcal{K}} \left[f(\boldsymbol{z}) - g(z^{(\kappa)}) - \langle \nabla g(z^{(\kappa)}), \boldsymbol{z} - z^{(\kappa)} \rangle \right] \tag{2.6}$$

Moreover, for the optimal solution $z^{(\kappa+1)}$ of (2.6), one has

$$\begin{aligned} f(z^{(\kappa+1)}) - g(z^{(\kappa+1)}) &\leq f(z^{(\kappa+1)}) - g(z^{(\kappa)}) - \langle \nabla g(z^{(\kappa)}), z^{(\kappa+1)} - z^{(\kappa)} \rangle \\ &\leq f(z^{(\kappa)}) - g(z^{(\kappa)}) - \langle \nabla g(z^{(\kappa)}), z^{(\kappa)} - z^{(\kappa)} \rangle \\ &= f(z^{(\kappa)}) - g(z^{(\kappa)}), \end{aligned}$$

which means that $z^{(\kappa+1)}$ is better than $z^{(\kappa)}$ toward optimizing (2.5) as far as $z^{(\kappa+1)} \neq z^{(\kappa)}$, i.e. convex program (2.6) generates a proper solution $z^{(\kappa+1)}$. Thus, initialized from a feasible $z^{(0)}$, recursively generating $z^{(\kappa)}$ for $\kappa = 0, 1, \ldots$, by the optimal solution of convex program (2.6) is a path-following algorithm. In summary, a d.c. procedure for the generic d.c. program (2.5) is sketched below.

D.C. Iterations (DCIs):

- *Initialization:* Choose an initial feasible solution $z^{(0)}$ of (2.5).

- *κ-th DC iteration (DCI):* Solve convex program (2.6) to obtain the optimal solution z^* and set $\kappa \to \kappa + 1$, $z^{(\kappa)} \to z^*$. Given a tolerance level $\epsilon > 0$, stop if

$$|f(z^{(\kappa)}) - f(z^{(\kappa-1)}) - g(z^{(\kappa)}) + g(z^{(\kappa-1)})|/|f(z^{(\kappa-1)}) - g(z^{(\kappa-1)})| \le \epsilon. \tag{2.7}$$

The previous works [14, 56, 86–89, 92] demonstrated successful applications of the above DCIs to various non-convex programs, where their effective d.c. representations in the form of (2.5) can be found. Since such DCIs will be repeatedly explored in this research, let us make a new observation on its efficiency. For $z^{(0)} \neq z^{(1)} \neq .... \neq z^{(\kappa+1)}$ it is true that

$$\mathcal{F}(z^{(0)}) > \mathcal{F}(z^{(1)}) > .... > \mathcal{F}(z^{(\kappa+1)}). \tag{2.8}$$

We now show that $z^{(\kappa+1)}$ is in fact the optimal solution of the following program

$$\min_{\boldsymbol{z}\in\mathcal{K}} \mathcal{F}_\kappa(\boldsymbol{z}) := f(\boldsymbol{z}) - \max_{\nu=0,1,..,\kappa} \{g(z^{(\nu)}) + \langle \nabla g(z^{(\nu)}), \boldsymbol{z} - z^{(\nu)}\rangle\}. \tag{2.9}$$

Indeed, suppose $\bar{z}$ is the optimal solution of (2.9) and $\bar{\nu} = \arg \max_{\nu=0,1,..,\kappa} \{g(z^{(\nu)}) + \langle \nabla g(z^{(\nu)}), \bar{z} - z^{(\nu)}\rangle\}$. Then $\bar{z} = z^{(\bar{\nu}+1)}$, i.e. $\bar{z}$ is the optimal solution of

$$\min_{\boldsymbol{z}\in\mathcal{K}} \mathcal{F}(\boldsymbol{z}; z^{(\bar{\nu})}) := f(\boldsymbol{z}) - (g(z^{(\bar{\nu})}) + \langle \nabla g(z^{(\bar{\nu})}), \boldsymbol{z} - z^{(\bar{\nu})}\rangle) \tag{2.10}$$

because otherwise min of (2.10) $< \mathcal{F}(\bar{z}; z^{(\bar{\nu})}) = \mathcal{F}_\kappa(\bar{z}) =$ min of (2.9) $\le$ min of (2.10), which is a contradiction. Moreover, as $z^{(\bar{\nu}+1)}$ is the optimal solution of (2.9), it follows that

$$\mathcal{F}(z^{(\bar{\nu}+1)}) \le \text{min of (2.9)} < \min_{\nu=1,2,\ldots,\kappa} \mathcal{F}(z^{(\nu)}) = \mathcal{F}(z^{(\kappa)})$$

which together with (2.8) show that $z^{(\bar{\nu}+1)} = z^{(\kappa+1)}$.

Now, it is obvious that $\mathcal{F}(\boldsymbol{z}) \le \mathcal{F}_{\kappa+1}(\boldsymbol{z}) \le \mathcal{F}_\kappa(\boldsymbol{z}) \le ... \le \mathcal{F}_0(\boldsymbol{z}) \quad \forall\, \boldsymbol{z} \in \mathcal{K}$, so convex functions $\mathcal{F}_\kappa$ are iteratively better global approximations of non-convex function $\mathcal{F}$. Consequently, DCIs by (2.6) not only generate improved solutions but also provide successively better convexifications for d.c. program (2.5). As the set $\mathcal{K}$ is compact, the sequence $\{z^{\kappa}\}$ is bounded and thus by Cauchy theorem there is a convergent subsequence $\{z^{\kappa_\nu}\}$, so $\lim\limits_{\nu\to+\infty}[\mathcal{F}(z^{(\kappa_\nu)}) - \mathcal{F}(z^{(\kappa_{\nu+1})})] = 0$. For every κ there is ν such that $\kappa_\nu \leq \kappa$ and $\kappa+1 \leq \kappa_{\nu+1}$. By (2.8), $0 \leq \lim\limits_{\kappa\to\infty}[\mathcal{F}(z^{(\kappa)}) - \mathcal{F}(z^{(\kappa+1)})] \leq \lim\limits_{\kappa\to\infty}[\mathcal{F}(z^{(\kappa_\nu)}) - \mathcal{F}(z^{(\kappa_{\nu+1})})] = 0$, showing that $\lim\limits_{\kappa\to\infty}[\mathcal{F}(z^{(\kappa)}) - \mathcal{F}(z^{(\kappa+1)})] = 0$. Therefore, given a tolerance $\epsilon > 0$, the above DCIs will terminate after finitely many iterations under the stop criterion $\mathcal{F}(z^{(\kappa)}) - \mathcal{F}(z^{(\kappa+1)}) \leq \epsilon$, which is normalized by (2.7). Each accumulation point $\bar{z}$ of the sequence $\{z^{(\kappa)}\}$ obviously satisfies $f(z) - f(\bar{z}) - \langle \nabla g(\bar{z}), z - \bar{z}\rangle \geq 0 \; \forall z \in \mathcal{K}$, which by the convexity of f and $\mathcal{D}$ also includes the minimum principle necessary optimality condition $\langle \nabla f(\bar{z}) - \nabla g(\bar{z}), \boldsymbol{z} - \bar{z}\rangle \geq 0 \quad \forall\, \boldsymbol{z} \in \mathcal{K}$. In contrast to conditional gradient algorithms, which may be slow in the neighborhood of a local solution and prone to zigzagging [93], our simulation show that the stop criterion (2.7) is satisfied after just a finite number of iterations.

2.2.4 A Generic D.C. Optimization Framework for Mixed Binary Programming

Now, we shall analyze general (mixed) binary programming problems. We will propose a more specific d.c. optimization framework for the consideration of optimization problems with respect to either or both of continuous variables and binary link variables, i.e. (mixed) binary or combinatorial programs.

$$\min_{(\boldsymbol{z},\boldsymbol{x})\in\mathcal{K}} \quad \mathcal{F}(\boldsymbol{z}) := f(\boldsymbol{z}) - g(\boldsymbol{z}) \;:\; \boldsymbol{x} \in \{0,1\}^N, \tag{2.11}$$

where $\boldsymbol{z} \in \mathcal{Z}$ is the continuous variable with $\mathcal{Z}$ being $\mathbb{R}^q$ or $\mathbb{C}^q$, $\boldsymbol{x}$ is the binary link variable, $\mathcal{K}$ is a compact and convex set, and f and g are convex functions. The objective function $\mathcal{F}(\boldsymbol{z})$ in (2.11) depends on continuous variable $\boldsymbol{z}$ only.

Clearly, d.c. program (2.11) differs from the d.c. program (2.5) only in the additional binary constraints imposed on the variables $\boldsymbol{x}$. Since the optimization in the continuous variable $\boldsymbol{z}$ may be dependent on certain activated/deactived set membership explicitly represented by the 0/1 value of $\boldsymbol{x}$, it is important to jointly optimize both variables which is notoriously difficult [94].

Under the general framework of d.c. optimization (2.5), we further develop the following framework to handle the problem with binary constraints. The first step is to express binary constraint $\boldsymbol{x} \in \{0,1\}^N$ in (2.11) by a d.c. constraint.

Proposition 1. Under the definitions

$$D := [0,1]^N, \tag{2.12a}$$

$$C := \{\boldsymbol{x} \in R^N \ : \ \sum_{n=1}^{N} \boldsymbol{x}_n^2 - \sum_{n=1}^{N} \boldsymbol{x}_n < 0\}, \tag{2.12b}$$

the binary set $\{0,1\}^N$ is the difference of two convex sets D and C, i.e. $\{0,1\}^N = D \setminus C$.

Proof: It is obvious that $\{0,1\}^N \subset D \setminus C$. Also $\boldsymbol{x} \in \{0,1\}^N$ is equivalent to

$$\boldsymbol{x}_n - \boldsymbol{x}_n^2 = 0, \ n = 1, 2, \dots, N. \tag{2.13}$$

On the other hand, $\boldsymbol{x}_n - \boldsymbol{x}_n^2 \geq 0$ for $\boldsymbol{x} \in D$ and $\sum_{n=1}^{N} \boldsymbol{x}_n^2 - \sum_{n=1}^{N} \boldsymbol{x}_n \geq 0$ $\boldsymbol{x} \notin C$, so each $\boldsymbol{x} \in D \setminus C$ is feasible to constraint (2.13), i.e. $D \setminus C \subset \{0,1\}^N$. □

For convex sets $\mathcal{D} := \mathcal{K} \cap (\mathcal{Z}, D)$ and $\mathcal{C} := \mathcal{K} \cap (\mathcal{Z}, C)$ it is seen that (2.11) can be compactly rewritten as

$$\min_{(\boldsymbol{z},\boldsymbol{x}) \in \mathcal{D} \setminus \mathcal{C}} \ f(\boldsymbol{z}) - g(\boldsymbol{z}), \tag{2.14}$$

which is minimization of a d.c. function over a d.c. set, so (2.11)/(2.15) belongs to the class of d.c. programming [16]. Since the feasibility set of (2.14) is obviously disconnected because of the binary values of the variable $\boldsymbol{x}$, there should be no path-following procedure for its iterative solution. Inspired by recent developments [83, 84, 95] in global optimization as well as [14, 56, 86–89, 92] in local optimization, it is recommended to amend (2.14) to a canonical d.c. program, which is minimization of a d.c. function over a convex set. This makes it possible to apply the path-following DCI. For this purpose, rewrite (2.14) by

$$\min_{(\boldsymbol{z},\boldsymbol{x})\in\mathcal{D}} f(\boldsymbol{z}) - g(\boldsymbol{z}) \ : \ \sum_{n=1}^{N}\boldsymbol{x}_n - \sum_{n=1}^{N}\boldsymbol{x}_n^2 \leq 0. \tag{2.15}$$

Using the Lagrangian $\mathcal{L}(\boldsymbol{z},\boldsymbol{x},\mu) := f(\boldsymbol{z}) - g(\boldsymbol{z}) + \mu(\sum_{n=1}^{N}\boldsymbol{x}_n - \sum_{n=1}^{N}\boldsymbol{x}_n^2)$ with only one Lagrangian multiplier μ to handle the single non-convex constraint [96], (2.15) is expressed by

$$\min_{(\boldsymbol{z},\boldsymbol{x})\in\mathcal{D}} \max_{\mu\geq 0} \mathcal{L}(\boldsymbol{z},\boldsymbol{x},\mu),$$

while its Lagrangian duality is

$$\max_{\mu\geq 0} \min_{(\boldsymbol{z},\boldsymbol{x})\in\mathcal{D}} \mathcal{L}(\boldsymbol{z},\boldsymbol{x},\mu).$$

Note that in general there is a non-zero duality gap [16], i.e.

$$\min_{(\boldsymbol{z},\boldsymbol{x})\in\mathcal{D}} \max_{\mu\geq 0} \mathcal{L}(\boldsymbol{z},\boldsymbol{x},\mu) > \sup_{\mu\geq 0} \min_{(\boldsymbol{z},\boldsymbol{x})\in\mathcal{D}} \mathcal{L}(\boldsymbol{z},\boldsymbol{x},\mu).$$

However, the strong Lagrangian duality holds for (2.15) as summarized in the following proposition.

Proposition 2. The strong Lagrangian duality holds for (2.15), i.e.

$$\min_{(\boldsymbol{z},\boldsymbol{x})\in\mathcal{D}} \max_{\mu\geq 0} \mathcal{L}(\boldsymbol{z},\boldsymbol{x},\mu) = \sup_{\mu\geq 0} \min_{(\boldsymbol{z},\boldsymbol{x})\in\mathcal{D}} \mathcal{L}(\boldsymbol{z},\boldsymbol{x},\mu). \tag{2.16}$$

If the supremum of the right hand side of (2.16) attains at $0 < \mu_0 < +\infty$ then the mixed binary program (2.15) is equivalent to the following convex constrained program for $\mu \geq \mu_0$ in the sense that they share the same optimal value as well as the optimal solutions,

$$\min_{(\boldsymbol{z},\boldsymbol{x})\in\mathcal{D}} \mathcal{L}(\boldsymbol{z},\boldsymbol{x},\mu). \tag{2.17}$$

Proof: See Appendix A. □

The above Proposition 2 shows that mixed binary program (2.11)/(2.14)/(2.15) can be solved by means of program (2.17) for appropriately chosen $\mu > 0$. It can be easily seen that the objective of (2.17) is the d.c. function $(f(\boldsymbol{z}) + \mu \sum_{n=1}^{N} \boldsymbol{x}_n) - (g(\boldsymbol{z}) + \mu \sum_{n=1}^{N} \boldsymbol{x}_n^2)$, so indeed (2.17) is a canonical d.c. program, which is minimization of a d.c. function over a convex set [16].

We are now in position to outline three algorithmic steps toward the mixed binary program (2.15) by means of solutions of the canonical d.c. program (2.17).

2.2.4.1 Step 1: initialization by box relaxation

For any iterative procedure used to obtain a solution of program (2.17), one needs a good initial solution (z^*, x^*), which plays a crucial role in the computational efficiency. Obviously, an initial feasible solution to (2.17) can be easily located but it may be far away from its optimal solution and thus is not efficient. In our approach, we take (z^*, x^*) as the optimized solution of the following box-relaxed program of (2.11), which is also (2.17) for $\mu = 0$,

$$\min_{(\boldsymbol{z},\boldsymbol{x})\in\mathcal{D}} \ \mathcal{F}(\boldsymbol{z}) := f(\boldsymbol{z}) - g(\boldsymbol{z}). \tag{2.18}$$

Unlike the (2.14)/(2.11) which is a minimization of d.c. function over d.c. sets, the box-relaxed program (2.18) is a minimization of a d.c. function over convex sets with continuous variables $(\boldsymbol{z}, \boldsymbol{x})$. Therefore, program (2.18) belongs to the class of canonical program (2.5) with $\boldsymbol{z} \to (\boldsymbol{z}, \boldsymbol{x})$ subject to the convex set $\mathcal{K} \to \mathcal{D}$, convex functions $f(\boldsymbol{z}) \to f(\boldsymbol{z})$, and $g(\boldsymbol{z}) \to g(\boldsymbol{z})$.

Analogous to (2.6) for (2.5), for any feasible $z^{(\kappa)}$ to (2.18), the κ-th d.c. iteration for (2.18) is the following program

$$\min_{(\boldsymbol{z},\boldsymbol{x})\in\mathcal{D}} [f(\boldsymbol{z}) - g(z^{(\kappa)}) - \langle \nabla g(z^{(\kappa)}), \boldsymbol{z} - z^{(\kappa)} \rangle]. \tag{2.19}$$

Moreover, the DCI-based optimization procedure for (2.18) is sketched as below

DCIs:

- *Initialization:* Choose an initial feasible solution $(z^{(0)}, x^{(0)})$ of (2.18).

- *κ-th DC iteration (DCI):* Solve convex program (2.19) to obtain the optimal solution (z^*, x^*) and set $\kappa \to \kappa + 1$, $(z^{(\kappa)}, x^{(\kappa)}) \to (z^*, x^*)$. Given a tolerance level $\epsilon > 0$, stop if

$$|f(z^{(\kappa)}) - f(z^{(\kappa-1)}) - g(z^{(\kappa)}) + g(z^{(\kappa-1)})|/|f(z^{(\kappa-1)}) - g(z^{(\kappa-1)})| \leq \epsilon. \tag{2.20}$$

2.2.4.2 Step 2: mixed binary solution

Although (2.17) is already in a d.c. canonical form like (2.18) with $f(\boldsymbol{z}) \to f(\boldsymbol{z}) + \mu \sum_{n=1}^{N} \boldsymbol{x}_n$ and $g(\boldsymbol{z}) \to g(\boldsymbol{z}) + \mu \sum_{n=1}^{N} \boldsymbol{x}_n^2$, there are infinitely many d.c. representations for the same non-convex program in (2.17), which lead to quite different convex programs (2.19) for κ-th DCI, i.e. quite different sequences of feasible solutions are generated. In other words, the efficiency of the above generic DCIs is dependent on the choice of a particular d.c. representation. In our approach, we use the following equivalent d.c. representation for (2.17)

$$\min_{(\boldsymbol{z},\boldsymbol{x})\in\mathcal{D}} \Big[\underbrace{f(\boldsymbol{z}) + \mu(\sum_{n=1}^{N} \boldsymbol{x}_n + (\sum_{n=1}^{N} \boldsymbol{x}_n)^2)}_{\text{convex function: } f_1(\boldsymbol{z},\boldsymbol{x})} - \underbrace{\big(g(\boldsymbol{z}) + \mu(\sum_{n=1}^{N} \boldsymbol{x}_n^2 + (\sum_{n=1}^{n} \boldsymbol{x}_n)^2)\big)}_{\text{convex function: } f_2(\boldsymbol{z},\boldsymbol{x})} \Big]. \tag{2.21}$$

Again, the above program (2.21) is a minimization of d.c. function over convex set with respect to continuous variables $(\boldsymbol{z}, \boldsymbol{x})$. Analogously, (2.21) belongs to the class of canonical program (2.5) with $\boldsymbol{z} \to (\boldsymbol{z}, \boldsymbol{x})$ subject to the convex set $\mathcal{K} \to \mathcal{D}$, convex functions $f(\boldsymbol{z}) \to f_1(\boldsymbol{z}, \boldsymbol{x})$, and $g(\boldsymbol{z}) \to f_2(\boldsymbol{z}, \boldsymbol{x})$.

Accordingly, initialized by the optimized solution $(z^*, x^*) \to (z^{(0)}, x^{(0)})$ found by Step 1, the κ-th DCI for (2.21) is the following convex program which is analogous to (2.6) for (2.5)

$$\begin{aligned} \min_{(\boldsymbol{z},\boldsymbol{x})\in\mathcal{D}} \Big[f(\boldsymbol{z}) + \mu(\sum_{n=1}^{N} \boldsymbol{x}_n + (\sum_{n=1}^{N} \boldsymbol{x}_n)^2) - \Big(g(z^{(\kappa)}) + \mu(\sum_{n=1}^{N} (x_n^{(\kappa)})^2 + (\sum_{n=1}^{n} x_n^{(\kappa)})^2) \\ + \langle g(z^{(\kappa)}), \boldsymbol{z} - z^{(\kappa)} \rangle + 2\sum_{n=1}^{N} \big(x_n^{(\kappa)} + \sum_{n=1}^{N} x_n^{(\kappa)} \big) \big(\boldsymbol{x}_n - x_n^{(\kappa)} \big) \Big) \Big]. \end{aligned} \tag{2.22}$$

For the optimal solution $(z^{(\kappa+1)}, x^{(\kappa+1)})$ of (2.22), it is often observed that $\sum_{n=1}^{N} x_n^{(\kappa+1)} - \sum_{n=1}^{N}(x_n^{(\kappa+1)})^2 > 0$, i.e. $x^{(\kappa+1)} \notin \{0,1\}^N$ according to Proposition 2, i.e. $(z^{(\kappa+1)}, x^{(\kappa+1)})$ is infeasible to (2.15). Thus Step 2 with κ-DCI (2.22) is interpreted as an infeasible method for the mixed binary program (2.15). Of course, its performance also depends on the choice of the penalty parameter μ, which may be tricky [14]. Fortunately, we will see in the simulation that a simple choice of large enough $\mu > 0$ would make κth-DCI (2.22) generate a sequence of infeasible solutions $(z^{(\kappa)}, x^{(\kappa)})$ to (2.15), which converges to a good feasible solution for re-optimization of the next step.

2.2.4.3 Step 3: d.c. re-optimization

Suppose $(z^*, x^*) \in \mathcal{D}$ is the solution found by Step 2. It should be noted that there is still no guarantee that (z^*, x^*) is the optimal solution of either (2.17) or (2.15). Particularly, x^* may be still not binary but only nearly binary. Therefore, we make a final improvement for optimizing (2.15) by solving the following d.c. program in continuous variable $\boldsymbol{z}$ only

$$\min_{(\boldsymbol{z})\in\mathcal{K}} \mathcal{F}(\boldsymbol{z}) := f(\boldsymbol{z}) - g(\boldsymbol{z}) : \quad \boldsymbol{x} = [x^*]_b. \tag{2.23}$$

This program is similar to (2.18) but with known values of $x = [x^*]_b$. Thus the DCIs are directly applied to find the final optimized solution (z^{Ω}, x^{Ω}).

Chapter 3

Bregman Matrix Deviation Minimization for Sensor Selections in Spectrum Sensing

3.1 Introduction

Sensor networks can be found in a variety of applications including reconnaissance, surveying, target tracking and wireless networks [21, 97, 98]. In wireless networks, one of the main tasks of sensors is to perform spectrum sensing in managing the radio spectrum, which has been licensed but not efficiently utilized [99]. Indeed, the radio electro-magnetic spectrums appear to be scarce but many studies (see e.g. [100–102]) showed that most of them are at low utilization level leaving many under-utilized holes. Certainly, a great challenge in the wireless industry is to develop inexpensive yet efficient spectrum utilization. The introduction of cognitive radio with supporting policies [18, 103] offer opportunities for unlicensed secondary users to access spectrum owed by the licensed primary users. The most important task of the secondary user is to detect the spectrum holes of the primary user through spectrum sensing. In other words, reliable spectrum sensing is one of the most actual issues to identify the secondary spectrum opportunities and to guarantee that it does not cause harmful interference to the primary user. However, a single spectrum sensor may easily experience multi-path loss or be in a fading dip that prevent it from accurate measurement. Subsequent sensing of multiple sensors is indeed desirable for better sensing performance [21, 104]. On the other hand, it has been shown in [21] that the number of selected sensors is an impact factor in the sensing performance only when it is adequate. Once this number reaches a threshold, the sensing performance can only be marginally improved even if more sensors are selected. Due to the distributed nature of most sensors that are normally operating on battery, it is beneficial to select only a sufficient number of sensors. Obviously, the selected sensors should be as uncorrelated as possible for their desirable uncorrelated fading. Surprisingly, sensor selection for spectrum sensing has been only seriously raised in [105], which attempts to select a fixed number of sensors from a candidate set such that their correlation sum is minimized. Its mathematical formulation of optimization looks simple enough but still renders a hard combinatorial program with no systematic solution. Two heuristic solution procedures proposed in [105], which have been shown better than random selection, are obviously sensitive to the desired number of selected sensors. On the other hand, this combinatorial program is actual minimization of a convex function subject to binary $\{0, 1\}$ constraints and thus can be addressed by convex relaxation, where the binary constraints are relaxed to box $[0, 1]$ constraints [22]. The performance of such relaxation based method is rather unpredictable and in fact it is worse than that of the two heuristics in [105] even though its computational complexity is much higher. The reader is also referred to [106] for capacity of this convex relaxation. Unfortunately, all these procedures can not even guarantee local optimum.

The present study in this chapter is a further development of [105] in both theoretical and computational foundations. Apparently, there exist various sensible measurements of uncorrelation degree between sensors. From the perspective of sensor network, the uncorrelation measure can be represented differently depending on application purposes or targets but at least it must reflect deviation of correlation matrices from diagonality. The sum of correlations between active sensors primarily introduced in [105] is only an option for sensor uncorrelation measure. Other uncorrelation measures have been particularly and separately introduced in different contexts of the information theory (see e.g. [107] and references therein) so their topological connections have not been revealed. In this chapter we consider sensor selection for minimizing Bregman matrix deviation [108–110], which is shown to be capable of unifying various uncorrelation measure maximization over subsets. The objective functions of optimization are not necessarily convex or smooth (differentiable) so even the above-mentioned convex relaxation [22] may not be applied. Their optimizations over binary constraints have never been appropriately considered in literature. In our consideration, they are recast into continuous canonical d.c. (difference of two convex sets) program [16]. Namely, these programs are minimization of a d.c. function of structured matrix variables subject to convex quadratic constraints. The attractive advantages of this setting are:

- It gracefully and losslessly removes the intractable and discontinuous binary constraints;
- It is open for development of computationally affordable path-following procedures.

In fact, the purpose of the study in this chapter is two-fold:

- To analyze different uncorrelation degrees of sensors including simple correlation sum [105] and many other other measures such as Kullback-Leibler divergence, quantum relative entropy etc in an unified Bregman matrix deviation setting. The connections between such diversified uncorrelation degrees can be easily revealed in this new setting. Consequently, the sensor selection is effectively formulated by an generic binary program;
- To develop a systematic and efficient approach for locating the optimized solutions of the resultant binary program. A new non-smooth function optimization for handling binary constraint is combined with a local optimization search to yield optimality. The simulation results show that in all investigated uncorrelation measures, our non-smooth optimization algorithm is able to quickly locate the optimized solutions of this hard binary program in comparisons with the two above mentioned procedures of [105]. The local optimization search is used to check local optimality of the solutions found by all approaches. It reveals

that except our non-smooth optimization algorithm, which often locate an approximately optimal solutions, the solutions found by other approaches are very far from optimality.

The rest of this chapter is organized as follows. Section 3.2 is devoted to analysis of different uncorrelation measures in the unified Bregman matrix deviation, which leads to a generic optimization formulation for sensor selection. Section 3.3 deals with development of a non-smooth optimization algorithm for solution of this program. Section 3.4 introduces an efficient local search method to further improve its solutions. Section 3.5 provides several simulations of the proposed approach and its comparison with existing methods. Section 3.6 concludes the chapter.

3.2 System Model and Problem Formulation

Following [105], consider M spectrum sensors (cognitive radio) randomly localized in a relatively small circular area of radius R and the center at a base station. The sensor selection is typically based on the knowledge of sensor positions, which are typically based on full position information (i.e., complete coordinates), radius information only (i.e., only the distance from the base station) and pair-wise distance only (limited distribution information). We focus on full position information of sensors. There are three main effects of radio propagation channel: path loss, small-scale fading and shadowing (large-scale) fading. Considering primary transmitter at a distance much farther away from the sensing field than the geometrical distribution span of sensors, the path loss will be approximately same for all sensors [105]. Similarly, the effect of small-scale fading, which causes dramatic changes in signal phase and amplitude due to wavelength-level changes of spatial position between transmitter and receiver, can be also discarded in energy-based spectrum detections [111]. The shadowing fading, which is modeled as log-normal distributed random process with the path loss as its mean and with the standard deviation in the range of $4 - 10dB$ is the main contributor of correlation between sensors[112]. Moreover, the shadowing fading is spatially correlated. In fact, it has been shown in [113] that correlation degree of two sensors generally decreases exponentially in their mutual distance. Accordingly, the following deterministic matrix of pairwise correlations between these M sensors can be defined:

$$C := [c_{ij}]_{i,j=1,2,...,M} \in \mathbb{R}^{M\times M}, c_{ij} = e^{-\alpha d_{ij}}, c_{ij} = c_{ji}. \tag{3.1}$$

Here, the correlation factor α is 0.1204/meter in a typical non-line-of-sight environment [104, 113]. d_{ij} is distance between two sensors i and j. The entry c_{ij} thus represents their correlation degree. Obviously, $c_{ii} = 1$, $i = 1, 2, ..., M$ and $C \succeq 0$ as well as $C \geq 0$. There is also another way to model the correlation matrix C by considering sensor positions as stochastic parameters as well [105]. From the perspective of learning statistics (see e.g. [114]), the correlation matrix C plays the role of the kernel matrix in embedding all sensors to the so called Euclidean feature space with the dot product of two sensors i and j denoted by its entry c_{ij}. It should be emphasized the our below development is valid and effective for whatever definition of the correlation matrix C other than (3.1). For instance, in the waveform selection context (see e.g. [107]), c_{ij} is simply denoted by the dot product of waveforms i and j.

A set of active sensors in collaborative sensing is defined through the status vector $\boldsymbol{x} = (x_1, x_2, ..., x_M)^T \in \{0, 1\}^M$, where $x_i = 1$ means sensor i is picked (active) and $x_i = 0$ means sensor i is not picked (passive). For each $\boldsymbol{x} \in \{0, 1\}^M$ define the matrix

$$C_{\boldsymbol{x}} = (\boldsymbol{x}\boldsymbol{x}^T) \odot C = [x_i c_{ij} x_j]_{i,j=1,...,M},$$

and also the corresponding active sensor index set

$$J_{\boldsymbol{x}} = \{i_1 < i_2 < .... < i_N | x_{i_j} = 1,\ j = 1, 2, ..., N\}.$$

Accordingly, the correlation matrix of the active sensors is a $N \times N$ principal sub-matrix of C:

$$\mathcal{C}_{\boldsymbol{x}} = [x_i c_{ij} x_j]_{(i,j)\in J_{\boldsymbol{x}}} = [c_{ij}]_{i,j\in J_{\boldsymbol{x}}} \in R^{N\times N}.$$

The sensor selection problem can be roughly stated as to choose N sensors among these M ones so that they are as uncorrelated as possible. Equivalently, it is to seek $\boldsymbol{x} \in \{0,1\}^M$ with $\sum_{i=1}^{M} x_i = N$ such that $C_{\boldsymbol{x}}$ is as uncorrelated as possible, or the dimensionality of the feature subspace of embedded sensors $i_1, i_2, ..., i_N$ is maximized [114]. It is the same as its deviation from its diagonality matrix I_N is minimized. This problem is in contrast with compressed sampling or clustering [109, 110], which is to seek $C_{\boldsymbol{x}}$ that contains as much as possible information about the matrix C.

On the other hand, such matrices $\mathcal{C}_{\boldsymbol{x}}$ satisfy the following conditions

$$\mathcal{C}_{\boldsymbol{x}} \succeq 0,\ \mathcal{C}_{\boldsymbol{x}} \geq 0,\ \langle \mathcal{C}_{\boldsymbol{x}} \rangle = N,\ \mathcal{C}_{\boldsymbol{x}}(i,i) = 1,\ \ i = 1, 2, ..., N. \tag{3.2}$$

According to Minkowski geometry (see e.g. [115]), these conditions particularly imply that all $\mathcal{C}_{\boldsymbol{x}}$ have the same surface area $\langle \mathcal{C}_{\boldsymbol{x}} \rangle = N$, while their volume defined as $\det(\mathcal{C}_{\boldsymbol{x}})$ is bounded according to Hadamard inequality (see e.g. [116])

$$\det(\mathcal{C}_{\boldsymbol{x}}) \leq \prod_{i=1}^{N} \mathcal{C}_{\boldsymbol{x}}(i,i) = 1,$$

where the equality occurs if and only if $\mathcal{C}_{\boldsymbol{x}} = I_N$, i.e. $\mathcal{C}_{\boldsymbol{x}}$ is diagonal so all active sensors are uncorrelated. From now on we shall consider only the class of matrices that satisfy (3.2). There are $\binom{M}{N}$ possible choices of $\mathcal{C}_{\boldsymbol{x}}$, which are $N \times N$ principal sub-matrices of C. Since I_N is the diagonality matrix for all matrices $\mathcal{C}_{\boldsymbol{x}}$ satisfying (3.2), uncorrelation degree of $\mathcal{C}_{\boldsymbol{x}}$ can be expressed through its Bregman deviation [108–110] from I_N as follows. The conventional Bregman deviation of $\mathcal{C}_{\boldsymbol{x}}$ from I_N is induced by a given strictly convex and differentiable function φ in $\mathcal{C}_{\boldsymbol{x}}$ as [108–110]

$$D_{\varphi}(\mathcal{C}_{\boldsymbol{x}}, I_N) := \varphi(\mathcal{C}_{\boldsymbol{x}}) - \varphi(I_N) - \langle \nabla\varphi(I_N), \mathcal{C}_{\boldsymbol{x}} - I_N \rangle. \tag{3.3}$$

Accordingly, the Bregman deviation minimization is formulated by

$$\min_{\boldsymbol{x}} \ D_{\varphi}(\mathcal{C}_{\boldsymbol{x}}) \ : \ \sum_{i=1}^{M} x_i = N, \ \boldsymbol{x} \in \{0,1\}^M. \tag{3.4}$$

However, from (3.3) and (3.4), it is obvious that the strict convexity of φ can be relaxed by its convexity plus the condition

$$\varphi(\mathcal{C}_{\boldsymbol{x}} - I_N) = 0 \Leftrightarrow \mathcal{C}_{\boldsymbol{x}} = I_N, \tag{3.5}$$

while the differentiability of φ is not necessary with $\nabla\varphi(I_N)$ replaced by any sub-gradient of φ at I_N for definition (3.3) of $D_{\varphi}(\mathcal{C}_{\boldsymbol{x}}, I_N)$. Note that $D_{\varphi}(\mathcal{C}_{\boldsymbol{x}}, I)$ is still positive by convexity of φ [16].

Let us provide some popular used measure-induced functions ϕ with some analysis. Note that in all these below cases of ϕ, minimization of $\phi(\mathcal{C}_{\boldsymbol{x}} - I_N)$ is the same minimization of $\phi(\mathcal{C}_{\boldsymbol{x}})$ so we go directly with minimization of $\phi(\mathcal{C}_{\boldsymbol{x}})$ to save space. All of them pose very challenging combinatorial programs.

3.2.1 Correlation sum

The first principle example of Bregman matrix deviation is associated with the squared Frobenius norm for positive matrices as follows

$$\varphi(\mathcal{C}_{\boldsymbol{x}}) = \frac{1}{2}||\sqrt{\mathcal{C}_{\boldsymbol{x}}}||_F^2 := \frac{1}{2}\sum_{i,j=1}^{N} \mathcal{C}_{\boldsymbol{x}}(i,j),$$

which is the entry sum of $\mathcal{C}_{\boldsymbol{x}}$. Note that $\sqrt{I_N} = I_N$ and $\sqrt{\mathcal{C}_{\boldsymbol{x}}} - I_N \geq 0$, so it is straightforward to verify that

$$D_{\varphi}(\mathcal{C}_{\boldsymbol{x}}, I_N) = \frac{1}{2}||\sqrt{\mathcal{C}}_x - I_N||_F^2.$$

Therefore, minimization of $D_\varphi(\mathcal{C}_{\boldsymbol{x}}, I_N)$ is the same as minimization of the correlation sum function [105]

$$\phi(\mathcal{C}_{\boldsymbol{x}}) = \sum_{i,j=1}^{M} \mathcal{C}_{\boldsymbol{x}}(i,j),$$

which is the following function in vector variable $\boldsymbol{x}$

$$f_{cs}(\boldsymbol{x}) := \sum_{i,j=1}^{M} c_{ij}x_i x_j = \langle \boldsymbol{x}, C\boldsymbol{x} \rangle \tag{3.6}$$

$$= \mathbf{1}_N^T \mathcal{C}_{\boldsymbol{x}} \mathbf{1}_N \tag{3.7}$$

$$= \sum_{i=1}^{M} x_i \sum_{j=1}^{M} c_{ij} x_j. \tag{3.8}$$

This function is convex in vector variable $\boldsymbol{x}$ (because $C \succeq 0$) but is linear in the matrix variable

$$\boldsymbol{X} = [x_{ij}]_{i,j=1,2,...,M}, \; x_{ij} \leftarrow x_i x_j, \; i,j = 1,2,...,M, \tag{3.9}$$

i.e. the function $f_{cs}(\boldsymbol{X})$ defined by the right hand side (RHS) of (3.6) with variable change (3.9) is linear in matrix variable $\boldsymbol{X}$.

According to [116, p. 370]

$$\sum_{i=1}^{N} (\lambda_i(\sqrt{\mathcal{C}_{\boldsymbol{x}}}) - \lambda_i(I_N))^2 \leq ||\sqrt{\mathcal{C}_{\boldsymbol{x}}} - I_N||_F^2,$$

where $\lambda_i(\sqrt{\mathcal{C}_{\boldsymbol{x}}}), i = 1,2,...,N$ are eigenvalues of $\sqrt{\mathcal{C}_{\boldsymbol{x}}}$ and $\lambda_i(I_N) \equiv 1$ are eigenvalues of I_N. Hence, $f_{cs}(\boldsymbol{x})$ is a majorant of the squared eigenvalue function

$$f_{es}(\boldsymbol{x}) = \sum_{i=1}^{N} (\lambda_i(\sqrt{\mathcal{C}_{\boldsymbol{x}}}) - 1)^2,$$

i.e. the metric induced by f_{cs} is stronger than that induced by f_{es}. There is no tractable minimization for this function f_{es} so instead of directly minimizing it one uses minimization for its upper bound $f_{cs}(\boldsymbol{x})$.

3.2.2 Maximal individual correlation sum

The second principle example of Bregman matrix deviation is associated with another popular induced norm of positive matrices [116]

$$\varphi(\mathcal{C}_{\boldsymbol{x}}) = ||\sqrt{\mathcal{C}_{\boldsymbol{x}}}||^2_{\max} := \max_{i=1,2,\ldots,N} ||\sqrt{\mathcal{C}_{\boldsymbol{x}}}(i,:)||^2 = \max_{i=1,2,\ldots,N} \sum_{j=1}^{N} \mathcal{C}_{\boldsymbol{x}}(i,j),$$

which is convex as maximum of a family of linear functions [16]. Note that (3.5) is verified, while a subgradient of φ at I_N is any $e_i e_i^T$, $i = 1, 2, ..., N$ so,

$$||I_N||^2_{\max} = 1, \langle e_i e_i^T, \mathcal{C}_{\boldsymbol{x}} - I_N \rangle = 0$$

and minimization of $D_\varphi(\mathcal{C}_{\boldsymbol{x}}, I_N)$ is the same as minimization of the function

$$\phi(\mathcal{C}_{\boldsymbol{x}}) = \max_{i=1,2,\ldots,N} \sum_{j=1}^{N} \mathcal{C}_{\boldsymbol{x}}(i,j),$$

which is the following objective function in $\boldsymbol{x}$

$$f_{mc}(\boldsymbol{x}) := \max_{i=1,2,\ldots,M} x_i \sum_{j=1}^{M} c_{ij} x_j = \max_{i=1,2,\ldots,M} x_i (C\boldsymbol{x})_i \tag{3.10}$$

$$= \max_{i=1,2,\ldots,N} \sum_{j=1}^{N} \mathcal{C}_{\boldsymbol{x}}(i,j). \tag{3.11}$$

This function is non-convex and non-smooth in $\boldsymbol{x}$ but the function $f_{mc}(\boldsymbol{X})$ defined by RHS of (3.11) with variable change (3.9) is still convex (but non-smooth) in variable $\boldsymbol{X}$ because it is the maximization of family of M linear functions $\sum_{j=1}^{M} c_{ij} x_{ij}$, $i = 1, 2, ..., N$ [16].

3.2.3 Correlation maximal eigenvalue

Note that $\lambda_{max}(I_N) = 1$ while

$$\lambda_{\max}(\mathcal{C}_{\boldsymbol{x}}) \geq \langle \mathcal{C}_{\boldsymbol{x}} \rangle / N = N/N = 1.$$

Consider the convex function $\varphi(\mathcal{C}_{\boldsymbol{x}}) = \lambda_{\max}(\mathcal{C}_{\boldsymbol{x}})$, which verifies (3.5). A subgradient of φ at I_N is still any $e_i e_i^T$, $i = 1, 2, ..., N$ [92] so,

$$\langle e_i e_i^T, \mathcal{C}_{\boldsymbol{x}} - I_N \rangle = 0.$$

Minimization of $D_\varphi(\mathcal{C}_{\boldsymbol{x}}, I_N)$ is the same as minimization of the function

$$\phi(\mathcal{C}_{\boldsymbol{x}}) = \lambda_{\max}(\mathcal{C}_{\boldsymbol{x}}),$$

which is the following objective function in $\boldsymbol{x}$,

$$f_{eig}(\boldsymbol{x}) := \lambda_{\max}(C_{\boldsymbol{x}}) = \lambda_{\max}(\mathcal{C}_{\boldsymbol{x}}). \tag{3.12}$$

This function is non-convex and non-smooth in $\boldsymbol{x}$ but the function $f_{eig}(\boldsymbol{X})$ defined by RHS of (3.12) by the variable change (3.9) is convex in $\boldsymbol{X}$. Moreover, by Perron-Frobenius Theorem [116]

$$\begin{aligned} f_{eig}(\boldsymbol{x}) &= \min_{\tilde{\boldsymbol{x}} \in R_+^N} \max_{i=1,2,...,N} \frac{(\mathcal{C}_{\boldsymbol{x}}\tilde{\boldsymbol{x}})_i}{\tilde{x}_i} \\ &\le \max_{i=1,2,...,N} (\mathcal{C}_{\boldsymbol{x}} \mathbf{1}_N)_i \\ &= f_{mc}(\boldsymbol{x}), \end{aligned}$$

i.e. $f_{mc}(\boldsymbol{x})$ is an upper bound of $f_{eig}(\boldsymbol{x})$. The metric induced by the former is stronger than that induced by the latter.

3.2.4 Burg's entropy of the eigenvalues

Consider the LogDet function $\varphi(\mathcal{C}_{\boldsymbol{x}}) = -\log\det(\mathcal{C}_{\boldsymbol{x}})$, which is convex in $\mathcal{C}_{\boldsymbol{x}} \succeq 0, \mathcal{C}_{\boldsymbol{x}} \neq 0$. Note that $\det(\mathcal{C}_{\boldsymbol{x}})$ is understood as the product of nonzero eigenvalues of $\mathcal{C}_{\boldsymbol{x}}$ [117] so $\varphi(\mathcal{C}_{\boldsymbol{x}})$ is well defined. This function is differentiable at I_N with $\nabla\varphi(I_N) = -I_N$ so

$$D_\varphi(\mathcal{C}_{\boldsymbol{x}}) = -\log\det(\mathcal{C}_{\boldsymbol{x}}) + \log\det(I_N) + \langle I_N, \mathcal{C}_{\boldsymbol{x}} - I_N \rangle = -\log\det(\mathcal{C}_{\boldsymbol{x}})$$

which is the so called Brug's entropy of eigenvalues of $\mathcal{C}_{\boldsymbol{x}}$. Note that $1 - x_i^2 = 0$ for $x_i = 1$ and $1 - x_i^2 = 1$ for $x_i = 0$ so it can be easily checked that

$$\det(\mathcal{C}_{\boldsymbol{x}}) = \det(C_{\boldsymbol{x}} + I(\boldsymbol{x})),$$

with

$$I(\boldsymbol{x}) = \mathsf{diag}[1 - x_i^2]_{i=1,2,\dots,M}. \tag{3.13}$$

Minimization of $D_\varphi(\mathcal{C}_{\boldsymbol{x}}, I_N)$ is minimization of the following objective function in $\boldsymbol{x}$

$$f_{det}(\boldsymbol{x}) = -\log\det(\mathcal{C}_{\boldsymbol{x}}) \tag{3.14}$$

$$= -\log\det(C_{\boldsymbol{x}} + I(\boldsymbol{x})). \tag{3.15}$$

It is widely recognized (see e.g. [118]) that $-f_{det}(\boldsymbol{x})$ represents the sensor capacity of the active sensors as a set, so minimization of $f_{det}(\boldsymbol{x})$ amounts to maximize its capacity. It is also clear by (3.2) that Bregman matrix deviation minimization here is also interpreted as volume maximization of $\mathcal{C}_{\boldsymbol{x}}$ with the same surface area N. Minimization of D_φ corresponding to $\varphi(\mathcal{C}_{\boldsymbol{x}}) = -\log\det(\mathcal{C}_{\boldsymbol{x}})$ is a popular uncorrelation measure maximization in blind source separation and also other statistical signal processing problems (see e.g. [119] and references therein).
The function $f_{det}(\boldsymbol{x})$ is smooth and non-convex in $\boldsymbol{x}$ but the function

$$f_{det}(\boldsymbol{X}) := -\log\det(\boldsymbol{X} \odot C + \mathcal{L}(\boldsymbol{X})),\ \ \mathcal{L}(\boldsymbol{X}) = \mathsf{diag}[\boldsymbol{X}(i,i)]_{i=1,2,\dots,M},$$

which is defined by RHS of (3.15) with the variable change (3.9), is convex in $\boldsymbol{X}$.

3.2.5 Quantum relative entropy

Recall that [120] $\log \mathcal{C}_{\boldsymbol{x}}$ is the matrix Y satisfying

$$\mathcal{C}_{\boldsymbol{x}} = \exp(Y) := \sum_{i=0}^{\infty} \frac{Y^i}{i!}.$$

Accordingly, $\log \mathcal{C}_{\boldsymbol{x}}$ is easily calculated by the singular value decomposition $\mathcal{C}_{\boldsymbol{x}} = U\Sigma_{\boldsymbol{x}}U^H$ with diagonal $\Sigma_{\boldsymbol{x}}$ and unitary U,

$$\log \mathcal{C}_{\boldsymbol{x}} = U \log \Sigma_{\boldsymbol{x}} U^H,$$

where $\log \Sigma_{\boldsymbol{x}}$ of the diagonal matrix $\Sigma_{\boldsymbol{x}}$ is diagonal entry-wise understood

$$\log \Sigma_{\boldsymbol{x}} = \mathsf{diag}[\Sigma_{\boldsymbol{x}}(i,i)]_{i=1,2,\dots,N}$$

under the agreement $\log 0 = 0$.

Consider the von Neuman entropy function [120]

$$\varphi(\mathcal{C}_{\boldsymbol{x}}) = \langle \mathcal{C}_{\boldsymbol{x}} \log \mathcal{C}_{\boldsymbol{x}} - \mathcal{C}_{\boldsymbol{x}} \rangle = \langle \mathcal{C}_{\boldsymbol{x}} \log \mathcal{C}_{\boldsymbol{x}} \rangle - N.$$

Accordingly, $D_\varphi(\mathcal{C}_{\boldsymbol{x}}, I_N)$ is the quantum relative entropy of $\mathcal{C}_{\boldsymbol{x}}$ [120]

$$D_\varphi(\mathcal{C}_{\boldsymbol{x}}, I_N) = \langle \mathcal{C}_{\boldsymbol{x}}(\log \mathcal{C}_{\boldsymbol{x}} - \log I_N) - \mathcal{C}_{\boldsymbol{x}} + I_N \rangle = \langle \mathcal{C}_{\boldsymbol{x}} \log \mathcal{C}_{\boldsymbol{x}} \rangle. \tag{3.16}$$

Minimization of this convex function in $\mathcal{C}_{\boldsymbol{x}}$ is the minimization of the following objective function which is non-convex in $\boldsymbol{x}$

$$f_{vN}(\boldsymbol{x}) = \langle \mathcal{C}_{\boldsymbol{x}} \log \mathcal{C}_{\boldsymbol{x}} \rangle. \tag{3.17}$$

On the other hand, by writing

$$\begin{aligned}\langle \mathcal{C}_{\boldsymbol{x}} \log \mathcal{C}_{\boldsymbol{x}} \rangle &= \sum_{i=1}^{N} \lambda_i(\mathcal{C}_{\boldsymbol{x}}) \log \lambda_i(\mathcal{C}_{\boldsymbol{x}}) \\ &= \sum_{i=1}^{N} \lambda_i(\mathcal{C}_{\boldsymbol{x}}) \log \frac{\lambda_i(\mathcal{C}_{\boldsymbol{x}})}{\lambda_i(I_N)} - \langle \mathcal{C}_{\boldsymbol{x}} \rangle + \langle I_N \rangle, \end{aligned} \tag{3.18}$$

where $\lambda_i(\mathcal{C}_{\boldsymbol{x}}), i = 1, 2, ..., N$ are eigenvalues of $\mathcal{C}_{\boldsymbol{x}}$ arranged in decreasing order, $f_{vN}(\boldsymbol{x})$ is also interpreted as generalized Kullback-Leibler deviation of $\mathcal{C}_{\boldsymbol{x}}$ from I_N as well [116]. Minimizing $f_{vN}(\boldsymbol{x})$ amounts to smoothing out the eigenvalue of $\mathcal{C}_{\boldsymbol{x}}$, i.e. to making them as evenly as possible [120, 121]. By doing so, the feature subspace of embedded sensors $i_1, i_2, .., i_N$ is as highly dimensional as possible. In other words, minimizing $f_{vn}(\boldsymbol{x})$ is actually to maximize the dimensionality of the feature subspace of embedded sensors $i_1, i_2, ..., i_N$.

With definition (3.13), it can be shown that

$$f_{vN}(\boldsymbol{x}) = \langle (C_{\boldsymbol{x}} + I(\boldsymbol{x})) \log(C_{\boldsymbol{x}} + I(\boldsymbol{x})) \rangle \tag{3.19}$$

which is still non-convex in $\boldsymbol{x}$ but nevertheless the function $f_{vN}(\boldsymbol{X})$ defined by the RHS of (3.19) with the variable change (3.9) is convex in $\boldsymbol{X}$. The differential $\frac{df_{vN}(\boldsymbol{X})}{d\boldsymbol{X}}$ can be easily identified from

$$f_{vn}(\boldsymbol{X} + \Delta X) = f_{vn}(\boldsymbol{X}) + \langle \log(\boldsymbol{X} \odot C + \mathcal{L}(\boldsymbol{X})) + I_M, C \odot \Delta X + \mathcal{L}(\Delta X) \rangle + o(\Delta X) \tag{3.20}$$

or

$$f_{vn}(\boldsymbol{X} + \Delta X) \geq f_{vn}(\boldsymbol{X}) + \langle \log(\boldsymbol{X} \odot C + \mathcal{L}(\boldsymbol{X})) + I_M, C \odot \Delta X + \mathcal{L}(\Delta X) \rangle \tag{3.21}$$

3.2.6 Combinatorial optimization formulation

The combinatorial optimization problem is as follows:

$$\min_{\boldsymbol{x}} \ F(\boldsymbol{x}) \ : \ \sum_{i=1}^{M} x_i = N, \ \boldsymbol{x} \in \{0, 1\}^M, \tag{3.22}$$

with $F(\boldsymbol{x}) \in \{f_{cs}(\boldsymbol{x}), f_{mc}(\boldsymbol{x}), f_{eig}(\boldsymbol{x}), f_{det}(\boldsymbol{x}), f_{vN}(\boldsymbol{x})\}$ neither convex nor smooth in binary vector variable $\boldsymbol{x}$ but the corresponding $F(\boldsymbol{X}) \in \{f_{cs}(\boldsymbol{X}), f_{mc}(\boldsymbol{X}), f_{eig}(\boldsymbol{X}), f_{det}(\boldsymbol{X}), f_{vN}(\boldsymbol{X})\}$ defined by x_{ij} substituting $x_i x_j$ in the definitions of $F(\boldsymbol{x})$ is still convex in the binary matrix variable $\boldsymbol{X}$ defined by (3.9).

This formulation of sensor selection problem is recognized as an *integer program.* As mentioned above, there are two developed algorithms, which are based on the knowledge of full sensor positions and correlation information for the particular correlation sum function $F(\boldsymbol{x}) = f_{cs}(\boldsymbol{x})$ [105]. The first one is the so called correlation measurement algorithm (CM), which initially selects a large enough candidate sensor set randomly from the full set, and then iteratively removes one-by-one sensors with the largest sum of its correlations with all other member of the current active set. The iterations continue till the targeted number of active sensors reaches. The second one is the so called reverse CM (RCM), which works in a reverse manner in comparison to CM. The active set starts from one or two randomly selected sensors and then sensors are one-by-one added to the active set based on the minimal sum of its correlations with the current active set. Both CM and RCM have been shown better than the random selection and other previously developed approaches including the mentioned convex relaxation [22]. Interestingly enough, both CM and RCM are even more suitable for minimizing maximal individual correlation sum function f_{mc} and correlation maximal eigenvalue function f_{eig} as they successively remove the largest sum or add the smallest sum. By these lines, CM (RCM, resp.) for minimization of Burg's entropy function f_{det} or von Neuman entropy function f_{vN} is to iteratively remove (add, resp.) one-by-one sensor such that the incumbent correlation matrix C_{inc} has the maximal determinant or minimal $\langle C_{inc} \log C_{inc} \rangle$. Surprisingly, CM is able the output the optimal solution for minimizing von Neuman entropy function f_{vN} as our simulation will show.

Also, as correlation sum function $f_{cs}(\boldsymbol{x})$ is convex in binary vector variable $\boldsymbol{x}$, a simple relaxation (see e.g. [22]) is to relax the integer constraints in (3.22) by the bounded (convex) constraint

$$\boldsymbol{x} \in [0, 1]^M \tag{3.23}$$

and then a solution of (3.22) is taken by rounding the N largest x_i by 1 and others by 0. Obviously, when the objective function is non-convex such as $f_{mc}(\boldsymbol{x}), f_{eig}(\boldsymbol{x})$, and $f_{det}(\boldsymbol{x})$, just relaxing the integer constraint does not make (3.22) convex yet and so convex relaxation is not readily applied. Moreover, CM still outputs a better solution for minimizing $f_{cs}(\boldsymbol{x})$ than this relaxation.

It is fair to state that there is no existing deterministic approach to find a computational solution of combinatorial program (3.22). The next two sections are our attempts to solve it systematically and efficiently. They are further developments of [106], which in essential addressed the simplest case of (3.22) when F linear in $\boldsymbol{X}$ and also there is no constraint for binary variables $\boldsymbol{x}$.

3.3 A Non-smooth Optimization Approach

In this section, we present an efficient algorithm to solve (3.22) by an exact penalty function approach of d.c. (difference of two convex functions) programming [16]. Note that the discrete constraint $x_i \in \{1, 0\}$ in (3.22) is equivalent to the continuous constraint

$$x_i^2 = x_i, \; i = 1, 2, ..., M. \tag{3.24}$$

On the other hand, as mentioned above the objective function $F(\boldsymbol{X})$ is convex in matrix variables $\boldsymbol{X}$ defined by (3.9). The following Lemma establishes the equivalence between the discrete program (3.22) and a continuous minimization of a convex function over a d.c. set.

Lemma 1. Suppose $\boldsymbol{X} \in \mathbb{R}^{M \times M}$ is a symmetric matrix variable

$$\boldsymbol{X} = \begin{bmatrix} x_{11} & x_{12} & \dots & x_{1M} \\ x_{12} & x_{22} & \dots & x_{2M} \\ \dots & \dots & \dots & \dots \\ x_{1M} & x_{2M} & \dots & x_{MM} \end{bmatrix}, \tag{3.25}$$

and $\mathcal{A} : \mathbb{R}^{M\times M} \rightarrow \mathbb{R}^{(M+1)\times(M+1)}$ is an affine operator to define the following structured matrix

$$\mathcal{A}(\boldsymbol{X}) = \begin{bmatrix} x_{11} & x_{12} & \dots & x_{1M} & x_{11} \\ x_{12} & x_{22} & \dots & x_{2M} & x_{22} \\ \dots & \dots & \dots & \dots & \dots \\ x_{1M} & x_{2M} & \dots & x_{MM} & x_{MM} \\ x_{11} & x_{22} & \dots & x_{MM} & 1 \end{bmatrix}. \tag{3.26}$$

The discrete program (3.22) is equivalent to the following continuous program

$$\min_{\boldsymbol{X}} \; F(\boldsymbol{X}) \tag{3.27a}$$

$$\text{s.t.} \quad 0 \preceq \mathcal{A}(\boldsymbol{X}), \sum_{i=1}^{M} x_{ii} = N, \; 0 \leq x_{ii} \leq 1, i = 1, \, 2, \, \cdots, \, M, \tag{3.27b}$$

$$\langle \mathcal{A}(\boldsymbol{X}) \rangle - \lambda_{\max}(\mathcal{A}(\boldsymbol{X})) \leq 0. \tag{3.27c}$$

Proof: Note that the constraints (3.27b) and (3.27c) force $N + 1 = \langle \mathcal{A}(\boldsymbol{X}) \rangle = \lambda_{\max}(\mathcal{A}(\boldsymbol{X}))$, which means $\mathcal{A}(\boldsymbol{X})$ has only one nonzero eigenvalue $N + 1$, so

$$\mathcal{A}(\boldsymbol{X}) = \begin{bmatrix} \boldsymbol{x} \\ 1 \end{bmatrix} \begin{bmatrix} \boldsymbol{x} & 1 \end{bmatrix}$$

for some $\boldsymbol{x} = (x_1, x_2, ..., x_M)^T \in R^M$. Furthermore, the structure (3.26) of $\mathcal{A}(\boldsymbol{X})$ forces x_i to satisfy (3.24), so $x_i \in \{0, 1\}$ and thus $\boldsymbol{x} \in \{0, 1\}^M$ with $\sum_{i=1}^{M} x_i = N$. Also, it is clearly contradictive to constraint (3.27c) to assume the existence of more than 1 maximal eigenvalues due to the fact that any solution must satisfy $\lambda_{\max}(\mathcal{A}(\boldsymbol{X})) \leq \langle \mathcal{A}(\boldsymbol{X}) \rangle \leq \lambda_{\max}(\mathcal{A}(\boldsymbol{X}))$. □

For program (3.27), only constraint (3.27c) is non-convex. Actually, as $\lambda_{\max}(\mathcal{A}(\boldsymbol{X}))$ is a convex function in $\boldsymbol{X}$, (3.27c) is a reverse convex constraint and (3.27) is a convex program with reversed convex constraint [16]. The feasibility set of (3.27b)-(3.27c) is a d.c.

It is known theoretically that there is non-convex duality with zero duality gap [16] that transfers the convex program with reverse convex constraint (3.27) to a d.c. program over convex constraint, which is more computationally efficient in term of global optimization. This is also true for local optimization as well because d.c. program over convex constraints admits a few path-following to locate its optimal solution [89], while all local optimization procedures for a convex program over non-convex constraints suffer from the so called zero-progressive steps [122–126].

Nevertheless, following [106], the following Lemma shows a direct equivalence between the convex program with reverse convex constraint (3.27) and a d.c. program over convex sets bypassing the complicated non-convex duality.

Lemma 2. There is $0 < \mu_0 < +\infty$ such that (3.27) is equivalent to the following d.c. program over convex constraint

$$\min_{\boldsymbol{X}} \; F(\boldsymbol{X}) + \mu(\langle \mathcal{A}(\boldsymbol{X})\rangle - \lambda_{max}(\mathcal{A}(\boldsymbol{X}))) \quad \text{s.t.} \quad (3.27b), \tag{3.28}$$

whenever $\mu \geq \mu_0$.

Proof: Obviously, each feasible solution X of (3.27) is also feasible to (3.28) so the optimal value of (3.27) is not less than the optimal value of (3.28) for all $\mu > 0$. It also means the optimal value of (3.28) is upper bounded by the optimal value of (3.27) for all $\mu > 0$. Thus, it suffices to show the existence of $\mu_0 > 0$ such that for $\mu > \mu_0$, all optimal solution $X^{(\mu)}$ of (3.28) must satisfy $\langle X^{(\mu)}\rangle - \lambda_{\max}(X^{(\mu)}) = 0$ so they are feasible to (3.27), implying that the optimal value of (3.28) is not less than the optimal value of (3.27) too.

Note that the feasible set of (3.28) is compact. Assume to the contrary that there is no such μ_0. By taking a subsequence $X^{(\mu)}$ if necessary, it follows that $X^{(\mu)} \to X^{\infty}$ as $\mu \to +\infty$ with $\langle X^{(\infty)}\rangle - \lambda_{\max}(X^{\infty}) > 0$. This mean the optimal value of (3.28) is infinity as $\mu \to +\infty$, a contradiction with their upper boundedness by the finite optimal value of (3.27). □

Apparently, (3.28) belongs to the class of general canonical d.c. program (2.5) defined in Chapter 2. More specifically, (3.28) is (2.5) with variables $\boldsymbol{z} \to \boldsymbol{X}$, convex functions $f(\boldsymbol{z}) \to F(\boldsymbol{X}) + \mu\langle \mathcal{A}(\boldsymbol{X})\rangle$ and $g(\boldsymbol{z}) \to \mu\lambda_{max}(\mathcal{A}(\boldsymbol{X}))$. The convex set $\mathcal{K}$ is defined by (3.27b). Remarkably, (3.28) is a modified version of (2.5) since the second convex function $\mu\lambda_{max}(\mathcal{A}(\boldsymbol{X}))$ in (3.28) is non-smooth.

Recall that a matrix $\partial\varphi(X) \in R^{M\times M}$ is called a subgradient of a convex function $\varphi(\boldsymbol{X})$ at X if

$$\varphi(Y) \geq \varphi(X) + \langle \partial\varphi(X), Y - X\rangle \quad \forall\ Y.$$

Lemma 3. [92] A subgradient of function $\lambda_{\max}(\mathcal{A}(\boldsymbol{X}))$ at X is identified from the following equation

$$\lambda_{\max}(\mathcal{A}(Y)) \geq \lambda_{\max}(\mathcal{A}(X)) + \langle \bar{x}_{\max}\bar{x}_{\max}^T, \mathcal{A}(Y) - \mathcal{A}(X)\rangle, \tag{3.29}$$

where $\bar{x}_{\max}$ is the eigenvector of $\mathcal{A}(X)$ corresponding to $\lambda_{\max}(\mathcal{A}(X))$.

From Lemma 3, the following Theorem is a foundation for path-following procedure to locate the optimal solution of d.c. program (3.28).

Theorem 1. For a feasible solution $X^{(\kappa)}$ to d.c. program (3.28), the following convex program outputs its optimal solution $X^{(\kappa+1)}$, which is not only feasible to d.c. program (3.28) too but also better than $X^{(\kappa)}$:

$$\min_{\boldsymbol{X}}\ F(\boldsymbol{X}) + \mu(\langle\mathcal{A}(\boldsymbol{X})\rangle - \lambda_{max}(\mathcal{A}(X^{(\kappa)})) - \langle \bar{x}^{(\kappa)}\bar{x}^{(\kappa)H}, \mathcal{A}(\boldsymbol{X}) - \mathcal{A}(X^{(\kappa)})\rangle) \quad \text{s.t.} \quad (3.27b), \tag{3.30}$$

where $\bar{x}^{(\kappa)}$ is the eigenvector corresponding to the eigenvalue $\lambda_{\max}(\mathcal{A}(X^{(\kappa)}))$.

Consequently, initialized from feasible $X^{(0)}$ to (3.28), the recursive programs (3.30) are derived from (2.6) for $\kappa = 0, 1, 2, ...$ generate a sequence $\{X^{\kappa}\}$ of improved solutions, which converges to a local optimal solution of (3.28).

The above theorem is originated from the canonical d.c. optimization framework (2.5) which is proposed in Chapter 2. The program (3.30) is the κ-th DCI for (3.28) which is analogous to (2.6) for (2.5). Therefore, the DCI procedure developed for (2.5) in Chapter 2 can be directly applied.

One can use any existing SDP solvers such as SeDuMi [127] for solution of SDP (3.30). The Algorithm 1 sketches computational implementation of Theorem 1.

Algorithm 1 Penalty function iterative algorithm (PENF)

The Initial Stage:

-*Initial Step.* Initialize moderately large μ and a feasible solution $X^{(0)}$ to convex constraint (3.27b). Set $\kappa = 0$.

-*Step* κ. Solve (3.30). If the optimal solution $X^{(\kappa+1)}$ satisfies $\langle \mathcal{A}(X^{(\kappa+1)}) \rangle \approx \lambda_{max}(\mathcal{A}(X^{(\kappa+1)}))$, reset $X^{(\kappa+1)} \to X^{(0)}$ and terminate the whole stage to output μ and $X^{(0)}$. Otherwise, if $X^{(\kappa+1)} \approx X^{(\kappa)}$, reset $2\mu \to \mu$ and return to the Initial step. Otherwise reset $\kappa + 1 \to \kappa, X^{(\kappa+1)} \to X^{(\kappa)}$ for the next iteration.

The Optimization Stage:

- Set $\kappa = 0$. Solve (3.30) to obtain the optimal solution $X^{(\kappa+1)}$, unless $X^{(\kappa+1)} = X^{(\kappa)}$, continue iterations by setting $\kappa + 1 \to \kappa$ and $X^{(\kappa+1)} \to X^{(\kappa)}$.

3.4 Optimization Capacity by Local Optimality Test

The optimality of any solution by program (3.22) can be revealed by checking whether it is at least local optimal or not. This motivates to employ a local optimality search for the solution of (3.22). Recall that a feasible solution $\bar{x}$ of (3.22) is said to be locally optimal if there is a neighborhood $\mathcal{U}(\bar{x}) \subset R^M$ such that $\mathcal{O}(\bar{x}) := \mathcal{U}(\bar{x}) \cap \{0,1\}^M \cap \{x \in \mathbb{R}^M : \sum_{i=1}^{M} x_i = N\} \neq \emptyset$ and $\mathcal{O}(\bar{x}) \neq \{\bar{x}\}$ and

$$F(x) \geq F(\bar{x}) \quad \forall \quad x \in \mathcal{O}(\bar{x}).$$

Now, take

$$\mathcal{U}(\bar{x}) := \{x \in \mathbb{R}^M \ : \ ||x - \bar{x}||^2 \leq 2\}$$

then

$$\mathcal{O}(\bar{x}) = \{x \in \{0,1\}^M \ : \ \sum_{i=1}^{M} x_i = N, \ ||x - \bar{x}||^2 = 2\},$$

i.e. $\mathcal{O}(\bar{x})$ consists from $N(N - M)$ feasible solutions of (3.22) that are nearest to $\bar{x}$ as they are different from $\bar{x}$ by two components only. Such $\mathcal{O}(\bar{x})$ is analytically defined by one-by-one swap 1-components of $\bar{x}$ with its zero components. Accordingly, the local optimality search starting from $\bar{x}$ in $\mathcal{O}(\bar{x})$ can be easily implemented as follows. For each $x \in \mathcal{O}(\bar{x})$ check if $F(x) < F(\bar{x})$

and define

$$\mathcal{O}_i(\bar{x}) = \{x \in \mathcal{O}(\bar{x}) \ : \ F(x) < F(\bar{x})\}.$$

If $\mathcal{O}_i(\bar{x}) = \emptyset$ then $\bar{x}$ is a local optimal solution of (3.22) because there is no better solution of (3.22) in a neighborhood of $\bar{x}$. Otherwise, $\mathcal{O}_i(\bar{x}) \neq \emptyset$ then $\bar{x}$ is not local optimal solution then reset

$$\bar{x} \leftarrow \arg \min_{x \in \mathcal{O}_i(\bar{x})} F(x) \tag{3.31}$$

for restarting the local optimality search, which terminates till $\mathcal{O}_i(\bar{x}) = \emptyset$, i.e. till a local optimal solution $\bar{x}$ of (3.22) is found. The simulation results in the next section demonstrate its efficiency in locating optimal solutions of (3.22). Note that the update (3.31) is regarded as the conventional steepest descent or Fedorov exchange [128, 129].

3.5 Simulation and Numerical Results

In this section, simulations are implemented in well-designed scenarios to demonstrate the performances of different algorithms for the five uncorrelation measure maximization problems.

Like [105], M sensors are randomly and uniformly distributed in a 2-D circular cell of radius R(m). The distance between primary transmitter and sensor network is well beyond R and accurate information of sensors' position is known. For any distribution of sensors network, a correlation matrix C is calculated based on their information of position according to (3.1), which is commonly used in the literature (see e.g. [21],[105]).

Obviously, the computational complexity and performance in term of the convergence speed and optimization accuracy of each implemented algorithms for solution of the combinatorial program (3.22) depends on major factors such as

- The objective function of optimization. The considered five objective functions f_{cs}, f_{mc}, f_{eig}, f_{det} and f_{vN} are non-convex but their non-convex degrees for definition of their hardness status are not the same. Moreover, their partial convex structures that are useful for optimization, are yet to be recognized.

- The total sensor number M, which determines the size of optimization problem and thus the computational complexity of each iteration.

- The number N of selected sensors, which together with the total number M determine the combinatoric degree $\binom{M}{N}$ of the problem. Under fixed M, the impact of N in materializing $\binom{M}{N}$ is not always monotonic.

Furthermore, considering the negatively exponential relationship (3.1) between correlation degree of two sensors and their mutual distance, the field radius R should not be considerably greater than M so to avoid the impractically low average mutual correlation.

All results are averaged over 200 Monte-Carlo simulation runs.

The computational performances of the concerned procedures with $(M, N) = (35, 20)$ and R ranging from 50 to 150 at increment 20 are given by Figures 3.1-3.4. The efficiency of the newly developed procedure of *PENF* plus local search test *LOC* is evident from these figures as it always outperforms the other existing procedure in any problem setting.

To see more about the capacity of each concerned algorithm for locating local optimal solution of (3.22), we provide Table 3.1 detailing the best value found by them and also their improvements by employing LOC, for the particular case $(M, N, R) = (35, 20, 100m)$. Table 3.1 reveals the following facts

- All problems (3.22) by different objective functions admit many local optimal solutions.

- CM and Random do not locate locally optimal solution and their improvements by LOC result in local optimal solutions, which are still far from the global optimal solution.

- PENF always locate approximately local optimal solutions, which are much better than other found local optimal solutions.

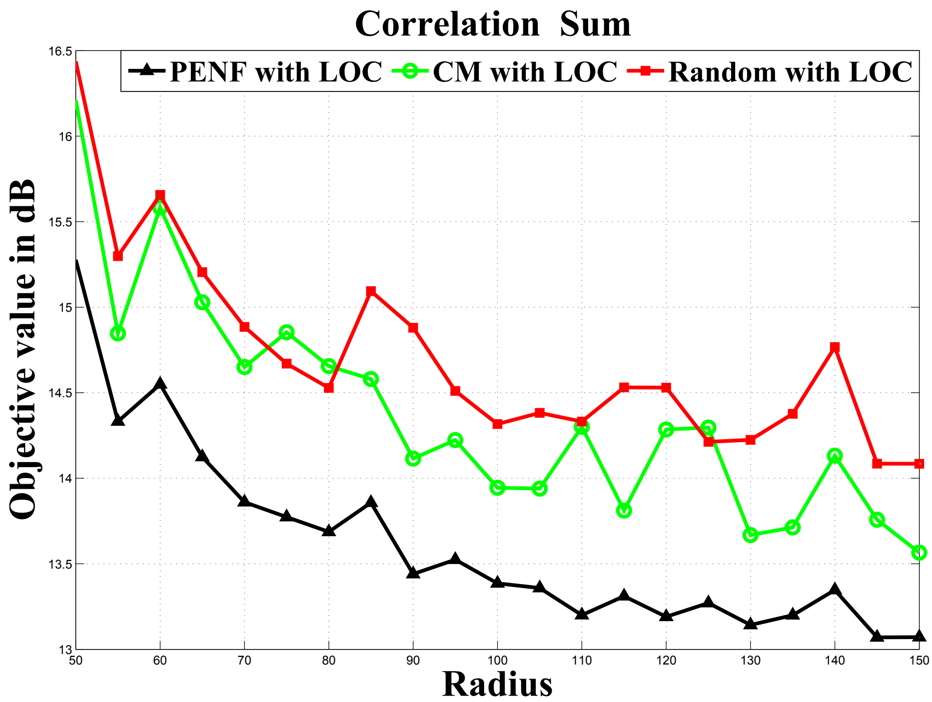

FIGURE 3.1: The correlation sum performance

Furthermore, Table 3.2 provides the averaged number of iterations needed for *PENF* implementations, which is also the number of convex program (3.30) called for its implementation. Although different as expected with different objective functions, they are low that make PENF computationally practically and efficient.

	f_{det}	f_{cs}	f_{mc}	f_{eig}
PENF	-14.34	13.58	0.42	0.32
PENF+LOC	-15.15	13.02	0.41	0.24
CM	-8.55	16.51	2.04	1.34
CM+LOC	-10.27	13.98	0.98	0.96
Random	-4.52	17.45	3.04	2.14
Random+LOC	-9.75	14.64	1.38	1.07

TABLE 3.1: Averaged objective values

	# of iterations			
(M, N)	f_{det}	f_{cs}	f_{mc}	f_{eig}
$(35, 20)$	8.5	4.2	4.6	9.1
$(35, 10)$	7.7	3.7	3.5	8.8
$(25, 20)$	5.9	2.7	3.5	6.0

TABLE 3.2: Averaged iterations by *PENF* for each problem, $R = 100m$

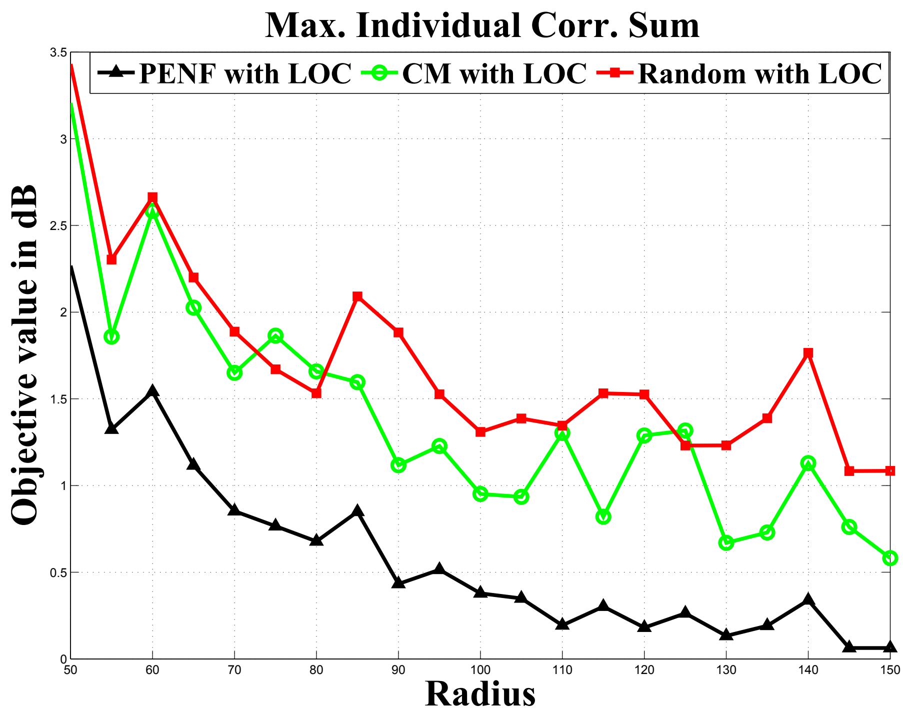

FIGURE 3.2: The maximal individual correlation sum performance

The computation time (complexity) of each algorithm versus problem size (M) is analyzed for Burg's entropy case as a general example.

With $R = 100m, N = 6$, increase M from 6 to 50 by unit steps. At each step, 10 random models are tested and their computation time is averaged. Fig. 3.7 shows the mean time needed by algorithms with problem size increasing.

With its solution space exponentially expanding as M increases, the selection problem soon becomes a trade-off decision. At a moderate cost of complexity, *PENF* offers a solution with the best performance in comparing with other existing approaches.

Finally, Fig. 3.5 and Fig. 3.6 provide the von Neuman entropy performance by CM only for the cases $(M, N) = \{(35, 20), (101, 30)\}$, respectively. Although CM is a heuristic procedure with cheap computational complexity, it nevertheless is able to provide at least the local optimal solution of (3.22) with f_{vN} so LOC could not improve its solution at all.

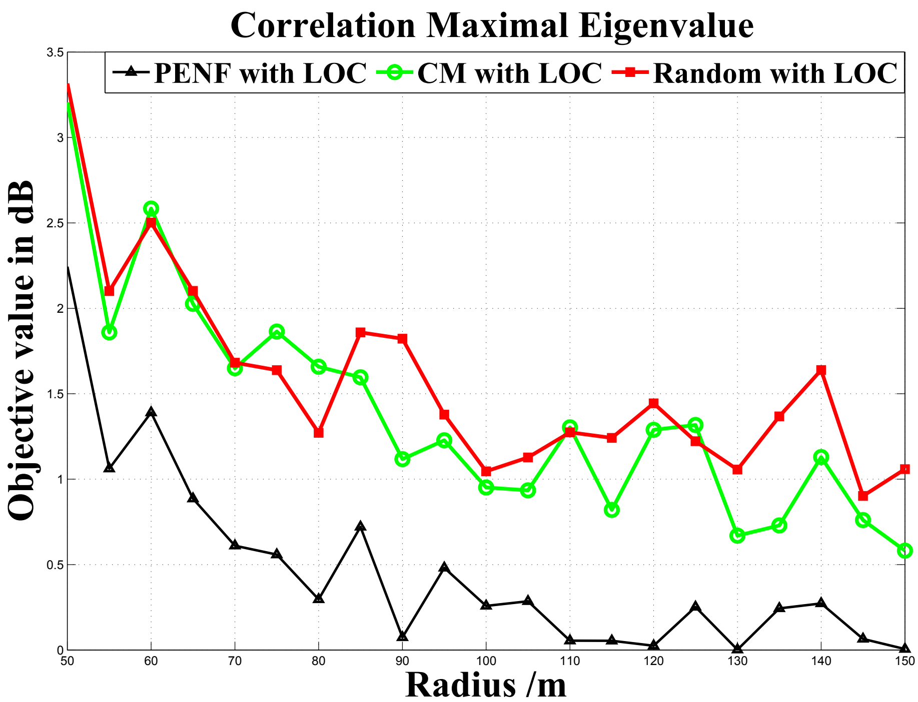

Figure 3.3: The correlation maximal eigenvalue performances

3.6 Conclusion

This chapter studied on the optimal sensor selection problem. We unified various uncorrelation measures in the context of Bregman matrix deviation, and then transformed the resultant integer program into a minimization of a d.c. function subject to convex constraints. Accordingly, a computationally affordable path-following algorithm was proposed for its solutions. An efficient local search was also implemented to effectively enhance the computational performances. The efficiency and robustness of the proposed algorithm has been validated through comparison with other existing methods.

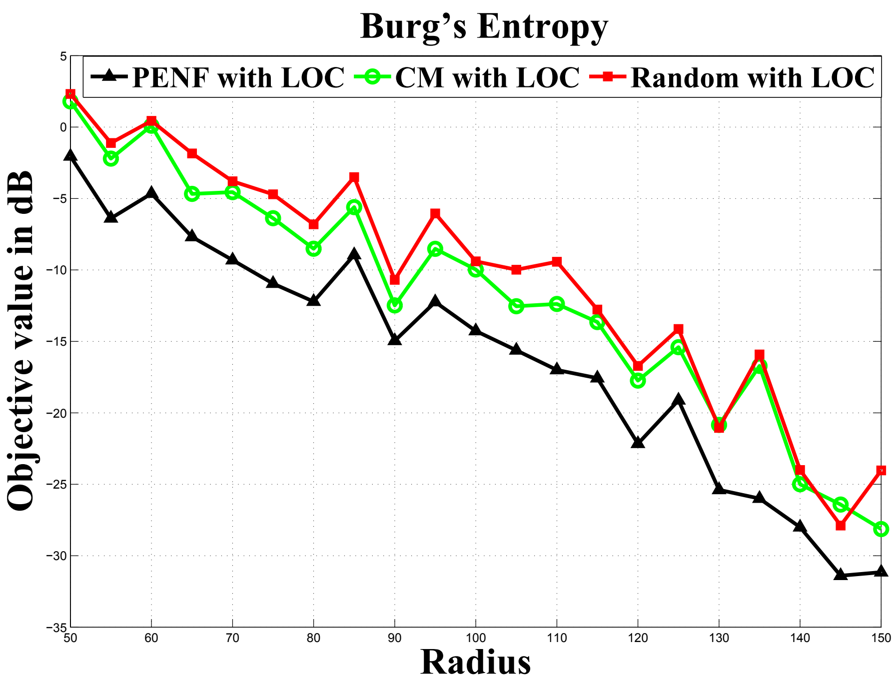

FIGURE 3.4: Burg's entropy performances

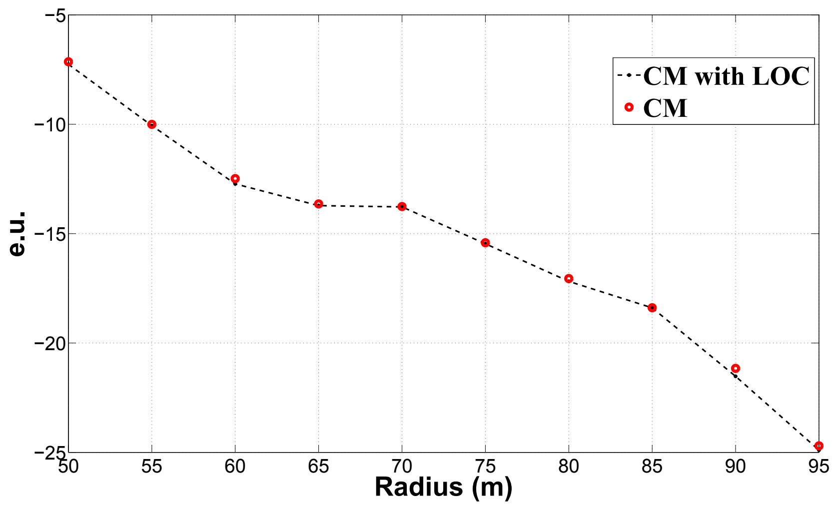

FIGURE 3.5: Von Neuman entropy performance by CM $(M, N) = (35, 20)$

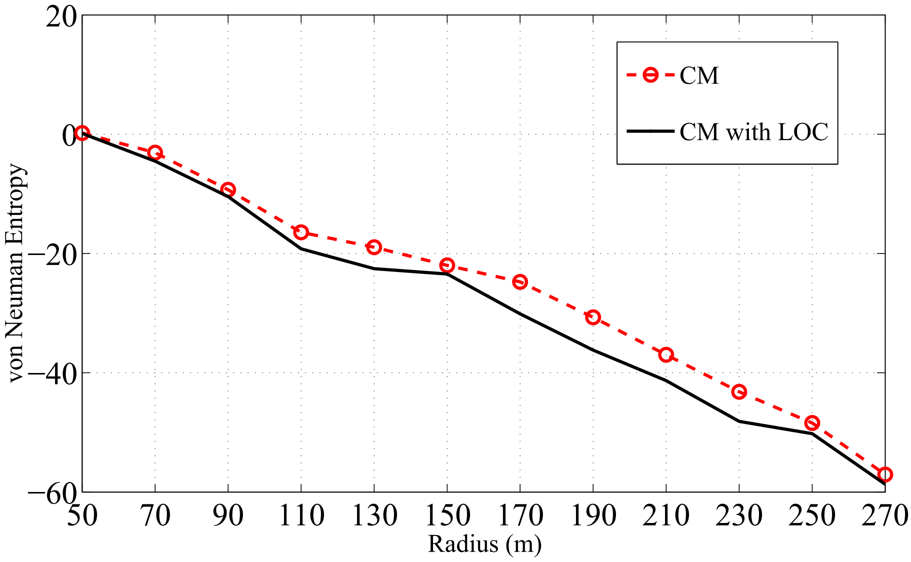

FIGURE 3.6: Von Neuman entropy performance by CM $(M, N) = (101, 30)$

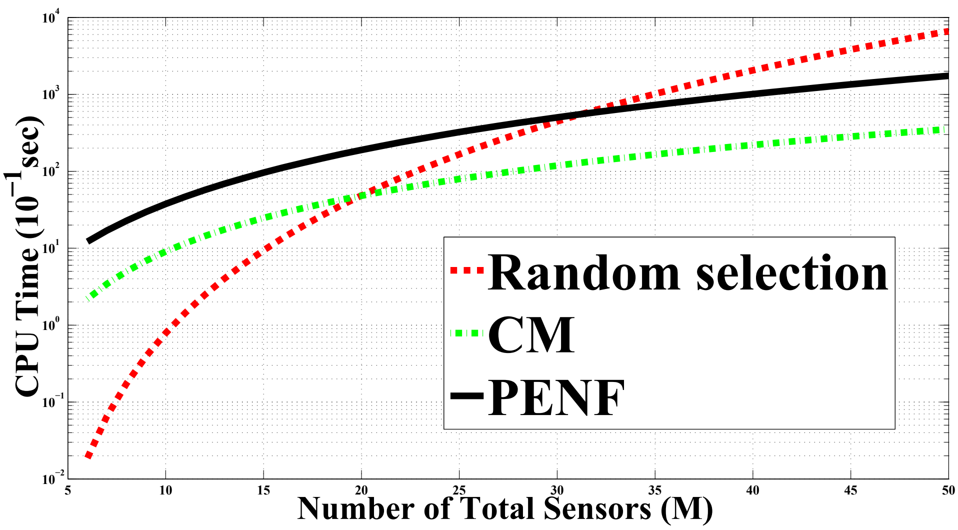

FIGURE 3.7: Computational analysis (CPU Time) $N = 6$

Chapter 4

Joint Optimization of Cooperative Beamforming and Relay Assignment in Multi-User Wireless Relay Networks

4.1 Introduction

Multi-user relay-assisted wireless communication is considered as a promising architecture for future-generation multi-hop cellular networks [29–32]. Recent research efforts have focused on distributed relay processing methods and techniques in order to enhance communication coverage, data rates and diversified QoS of multi-user communication networks. Among these research efforts, it has been recognized that relay assignment and beamforming are very effective techniques, especially in the context of amplify-and-forward (AF) protocol, in which the role of relays is to amplify the signals received from the sources and then forward the results to destinations.

To date, the design problems concerning relay assignment have been examined mainly for single-user scenarios and with a focus on the outage probability analysis of the best relay selection (see e.g. [33–38] and references therein). On the other hand, for a multi-relay network supporting a single user, the phase of the optimal beamforming at each relay can be predetermined and the relay beamforming thus reduces to merely power allocation problems (see e.g. [39–43]). There appears no efficient procedure for determining jointly-optimized relay assignment and power allocation. For example, Reference [130] considered power optimization for each possible subset of relays while Reference [32] considered power optimization on a subset of relays, which is heuristically chosen by relaxation-based rounding.

Multi-user beamforming in a multi-relay network is a much harder problem and it has already been thoroughly studied in recent years [44–51]. In particular, joint power allocation and relay assignment problems in *orthogonal* multi-user scenarios have recently been considered in [131–135], either under a game-theoretical framework or by adopting a maximum-ratio-combining receiver. By relaxing the binary constraints $\{0, 1\}$ of relay assignment to a box constraint on $[0, 1]$, the optimization problems in these papers become convex programs. So again, the optimization approach in these papers is to first conduct relay assignment by relaxation-based rounding and then re-optimize power for the assigned relays.

From the above discussion and to the authors' best knowledge, the jointly-optimal designs of the beamforming and relay selection have not been adequately addressed. Apparently, the main reason is the hardness of the joint optimization. In fact, finding separately-optimized beamforming and relay selection in multi-user multi-relay networks is already challenging. Specifically, the binary program of relay assignment is a very hard combinatorial one. The only known approach is to relax the binary constraints to box constraints, which would still lead to a highly non-convex program. The relay beamforming design problems that consider the practical individual power constraints at the relays are also highly non-convex optimization and they were recently solved in [48–50, 136]. Certainly, the joint optimization of beamforming and relay selection to maximize the minimum of the received SINRs constitutes the hardest nonlinear mixed binary program. This is because such a program involves non-convex objective and coupled non-convex constraints in continuous variables of beamforming and binary variables of assignment.

The present research appears to be the first attempt to address this joint SINR optimization in a systematic way, which is also practical and efficient. Similar to our past [88, 89, 92] and recent [48–50, 56, 137] developments we use d.c. (difference of two convex functions/sets) programming [16] as the tool for finding the solutions. The main reason for using this tool comes from its universality [16, Chapter 3]: almost all NP-hard optimization programs can be theoretically represented by d.c programs, which are to minimize d.c. functions over d.c. constraints. Although these d.c. programs are still very hard, they motivate exploring hidden convex structures of the problem at hand in order to obtain the constructive solutions [16, 91]. It has been recognized for a long time [16] that d.c. structure of binary constraints has yet to be explored as the binary constraints seem to be more suitable in a d.m. (difference of two monotonic functions/sets) setting [138, 139]. Moreover, different from the binary quadratic problem [106], which has been successfully solved by d.c. optimization, the constructive d.c. representations of the mixed-binary programs considered in the present research are not readily available. Through elegant variable changes and effective approximations, our contribution is to reformulate these problems as tractable d.c. programs, which become solvable by d.c. iterations of polynomial complexity and also re-optimization processes. Simulation results show that the proposed computational procedures are capable of locating approximation solutions that are very close to the global optimal solutions. This is evidenced by the fact that the approximation solutions achieve SINR performances that are very close to their upper bounds.

Needless to say, similar to the majority of previous works on cooperative beamforming and/or precoding (see e.g. [44–51, 131–135, 140]) the perfect channel state information of both communication links connected to a relay is assumed to be available at the relay. The reader is also referred to [141] and references therein for channel estimation techniques in relay networks, [136] for the robustness of cooperative beamforming against channel estimation error, and [142–144] for strategies to reduce the overall delay incurred in relaying signals to multiple receivers.

The chapter is structured as follows. The joint program of beamforming and relay assignment for the case of orthogonal transmission of the users is presented in Section 4.2. Section 4.3 presents the simulations results for orthogonal transmission. Section 4.4 is devoted to the problem of jointly optimized beamforming and relay assignment in non-orthogonal transmission of the relays. The simulation results of non-orthogonal transmission are presented in Section 4.5. Section 4.6 concludes the chapter.

4.2 Joint Beamforming and Relay Selection with Orthogonal Transmission

Studied in this section is a wireless relay network in which M source nodes communicate in pair with M destinations nodes with the help of N relays (see Fig. 4.1). All relays, source and destination nodes are each equipped with a single antenna and operate in a half-duplex mode. Information transmission from a source to a destination occurs in two time slots. In the first time-slot, the sources send their signal to the relays. The relays amplify their received signals by multiplying with complex weights and then simply forward these processed signals to all the destinations.

Let $s = (s_1, s_2, \ldots, s_M)^T \in \mathbb{C}^M$ be the vector of data symbols sent by M sources, which is normalized to zero mean and component-wise independent with variance $\mathbb{E}[|s_i|^2] = 1$. Let $h_n = (h_{n1}, h_{n2}, \ldots, h_{nM})^T \in \mathbb{C}^M,\ n = 1, 2, \ldots, N$ be the vector of uplink channel coefficients between relay n and all users and let $\ell_n = (\ell_{n1}, \ell_{n2}, \ldots, \ell_{nM})^T \in \mathcal{C}^M,\ n = 1, 2, \ldots, N$ be the vector of downlink channel coefficients between relay n and all the destinations. As mentioned before, these channel coefficients are assumed to be available at N relays. Communications in source-to-destination links are not taken into account due to severer path loss. Furthermore, let

$$\boldsymbol{x}_m = (\boldsymbol{x}_{1m}, \boldsymbol{x}_{2m}, \ldots, \boldsymbol{x}_{Nm})^T \in \{0,1\}^N \subset R^N,\ m = 1, 2, \ldots, M \tag{4.1}$$

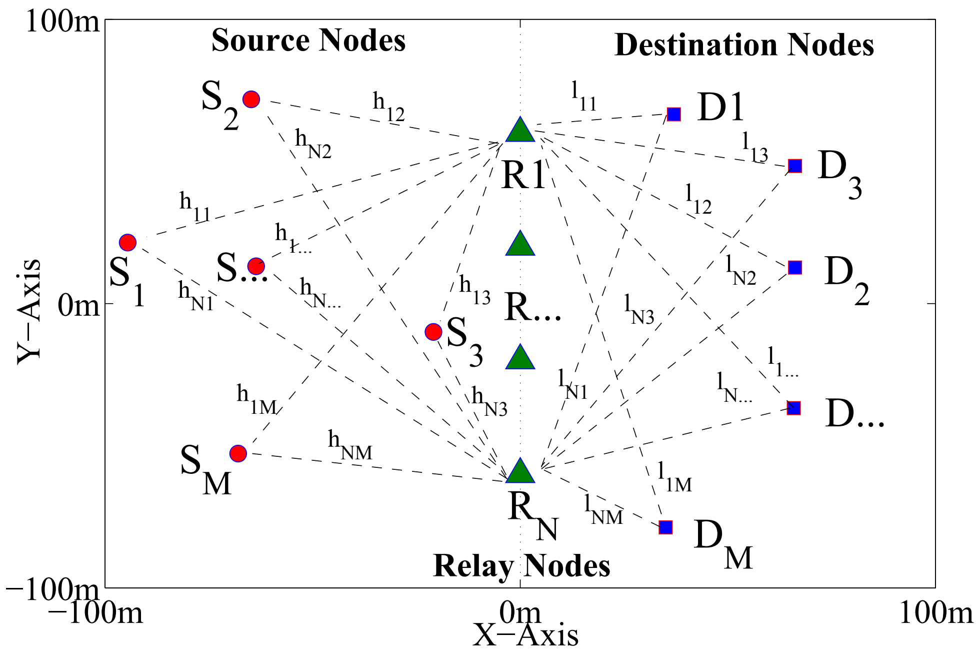

Figure 4.1: System model: multi-user multi-relay wireless relay networks.

be the vector representing the link connectivity between the user-destination pair m and all the relays. Specifically, $\boldsymbol{x}_{nm} = 1$ means that user m sends its signal s_m to the relay n through channel h_{nm} and this relay is also connected to destination m to forward the processed signal through channel ℓ_{nm}. On the other hand, $\boldsymbol{x}_{nm} = 0$ means that relay n is disconnected from the both user m and destination m. To control how the N relays are used to help M source-destination pairs, the number of relays assigned to each user shall be limited to at most N_R [132, 135]:

$$\sum_{n=1}^{N} \boldsymbol{x}_{nm} \leq N_R, \; m = 1, 2, \dots, M. \tag{4.2}$$

This section focuses on a scenario when user-destination pairs operate in orthogonal channels, i.e. the transmissions from the sources to the relays and from the relays to the destinations are orthogonal. For simplicity, time-division multiplexing shall be assumed, but other forms of orthogonal transmission such as frequency-division multiplexing and orthogonal code-division multiplexing can also be applied. Under orthogonal transmission, the received signal at relay n from user m is

$$y_{nm} = \boldsymbol{x}_{nm} h_{nm} s_m + n_n, \tag{4.3}$$

where n_n represents AWGN at the relay, which is modeled as a zero-mean circularly complex Gaussian random variable with variance σ_R^2. The received signal y_{nm} is then multiplied by a complex beamforming weight $\boldsymbol{\alpha}_{nm}$ before being forwarded to the destination m. Since relay n can help multiple sources, the constraint on its transmitted power is expressed as

$$\sum_{m=1}^{M} (\boldsymbol{x}_{nm}|\boldsymbol{\alpha}_{nm}|)^2(|h_{nm}|^2 + \sigma_R^2) \leq P_n, \quad n = 1, 2, \ldots, N, \tag{4.4}$$

while the total relaying constraint is

$$\sum_{n=1}^{N}\sum_{m=1}^{M} (\boldsymbol{x}_{nm}|\boldsymbol{\alpha}_{nm}|)^2(|h_{nm}|^2 + \sigma_R^2) \leq P_T. \tag{4.5}$$

It should be noted that constraint (4.4) is related to the hardware power limitation of each relay's transmitter, while constraint (4.5) expresses the allowable total power that all relays consume in amplifying all of their received signals. Since all the relays transmit to the destination simultaneously, the received signal at destination m is

$$y_{D,m} = \sum_{n=1}^{N} \boldsymbol{x}_{nm}\boldsymbol{\alpha}_{nm}\ell_{nm}(h_{nm}s_m + n_n) + n_{D,m}. \tag{4.6}$$

Using the polar representation $\boldsymbol{\alpha}_{nm} = |\boldsymbol{\alpha}_{nm}|\mathrm{e}^{\jmath \mathsf{arg}(\boldsymbol{\alpha}_{nm})}$ it can be easily shown that, in order to maximize the SNR at destination m, the optimal phase of $\boldsymbol{\alpha}_{nm}$ is $-\mathsf{arg}(\ell_{nm}h_{nm})$. That is,

$$\boldsymbol{\alpha}_{nm} = |\boldsymbol{\alpha}_{nm}|\mathrm{e}^{-\jmath \mathsf{arg}(\ell_{nm}h_{nm})}. \tag{4.7}$$

It then follows that equation (4.6) reduces to the following form, which involves only the magnitudes $|\boldsymbol{\alpha}_{nm}|$:

$$y_{D,m} = \sum_{n=1}^{N} \boldsymbol{x}_{nm}|\boldsymbol{\alpha}_{nm}|(|\ell_{nm}h_{nm}|s_m + \mathrm{e}^{-\jmath \mathsf{arg}(\ell_{nm}h_{nm})}n_n) + n_{D,m}, \quad n = 1, 2, \ldots, N. \tag{4.8}$$

Define the variables

$$\boldsymbol{\alpha}_m = (\boldsymbol{\alpha}_{1m}, \ldots, \boldsymbol{\alpha}_{Nm})^T \in \mathbb{C}^N,\ m = 1, 2, \ldots, M,$$

$$\boldsymbol{\alpha} = (\boldsymbol{\alpha}_1, \ldots, \boldsymbol{\alpha}_M) \in \mathbb{C}^{N\times M},$$

and

$$\boldsymbol{x} = (\boldsymbol{x}_1, \ldots, \boldsymbol{x}_M) \in \mathbb{R}^{N\times M}.$$

Then the SNR at destination m can be written as

$$\mathbf{SNR}_m(\boldsymbol{x}_m, \boldsymbol{\alpha}_m) = \frac{(\sum_{n=1}^{N} \boldsymbol{x}_{nm}|\boldsymbol{\alpha}_{nm}||\ell_{nm}h_{nm}|)^2}{\sigma_R^2 \sum_{n=1}^{N} (\boldsymbol{x}_{nm}|\boldsymbol{\alpha}_{nm}|)^2 |\ell_{nm}|^2 + \sigma_D^2}, \tag{4.9}$$

where σ_D^2 is the variance of AWGN at the destination. In order to improve the overall throughput of the relay network as well as to offer fairness among the users, we consider the following SNR maximin program:

$$\max_{\boldsymbol{x},\boldsymbol{\alpha}} \min_{m=1,2,\ldots,M} \mathbf{SNR}_m(\boldsymbol{x}_m, \boldsymbol{\alpha}_m) \quad \text{s.t.} \quad (4.1), (4.2), (4.4), (4.5). \tag{4.10}$$

With the following variable change

$$\boldsymbol{x}_{nm}|\boldsymbol{\alpha}_{nm}| \to \bar{\boldsymbol{\alpha}}_{nm},\ \bar{\boldsymbol{\alpha}}_m = (\bar{\boldsymbol{\alpha}}_{1m}, \ldots, \bar{\boldsymbol{\alpha}}_{Nm})^T \in \mathbb{C}^N,\ \bar{\boldsymbol{\alpha}} = (\bar{\boldsymbol{\alpha}}_1, \ldots, \bar{\boldsymbol{\alpha}}_M) \in \mathbb{R}^{N\times M}, \tag{4.11}$$

and additional variable $\boldsymbol{y} = (y_1, y_2, ..., y_M)^T \in \mathbb{R}^M$ for the additional constraints

$$\sigma_R^2 \sum_{n=1}^{N} \bar{\boldsymbol{\alpha}}_{nm}^2 |\ell_{nm}|^2 \leq \boldsymbol{y}_m, m = 1, 2, ..., M, \tag{4.12}$$

and using the fact that $\boldsymbol{x}_{nm}^2 = \boldsymbol{x}_{nm}$ for $\boldsymbol{x}_{nm} \in \{0, 1\}$, the SNR maximin program in (4.10) is

$$\max_{\boldsymbol{x},\bar{\boldsymbol{\alpha}},\boldsymbol{y}} \min_{m=1,2,\ldots,M} \mathbf{SNR}_m(\bar{\boldsymbol{\alpha}}_m, \boldsymbol{y}_m) := \frac{(\sum_{n=1}^{N} \bar{\boldsymbol{\alpha}}_{nm}|\ell_{nm}h_{nm}|)^2}{\boldsymbol{y}_m + \sigma_D^2} \quad : \quad (4.1), (4.2), (4.12), \tag{4.13a}$$

$$\sum_{m=1}^{M} \bar{\boldsymbol{\alpha}}_{nm}^2(|h_{nm}|^2 + \sigma_R^2) \leq P_n, \ n = 1, 2, ..., N, \tag{4.13b}$$

$$\sum_{m=1}^{M} \sum_{m=1}^{M} \bar{\boldsymbol{\alpha}}_{nm}^2(|h_{nm}|^2 + \sigma_R^2) \leq P_T, \tag{4.13c}$$

$$\bar{\boldsymbol{\alpha}}_{nm}^2(|h_{nm}|^2 + \sigma_R^2) \leq \boldsymbol{x}_{nm}P_n, \quad n = 1, 2, \ldots, N\, ; m = 1, 2, \ldots, M. \tag{4.13d}$$

Now, (4.13) is equivalent to

$$\max_{\boldsymbol{x},\bar{\boldsymbol{\alpha}},\boldsymbol{y}} \min_{m=1,2,\ldots,M} \left[2\ln\left(\sum_{n=1}^{N} \bar{\boldsymbol{\alpha}}_{nm}|\ell_{nm}h_{nm}|\right) - \ln\left(\boldsymbol{y}_m + \sigma_D^2\right)\right] \tag{4.14a}$$

$$\text{s.t.} \qquad (4.1), (4.2), (4.12), (4.13b) - (4.13d) \tag{4.14b}$$

One can see that the maximin program (4.14) is more favorable than the maximin program (4.13) because the coupled nonlinear terms $\boldsymbol{x}_{nm}|\boldsymbol{\alpha}_{nm}|^2$ in (4.10) have been decoupled by the variable change in (4.11). The difficulty of the maximin program (4.14) now lies on its non-convex objective function (with respect to only the beamforming power variable $\bar{\boldsymbol{\alpha}}$) and the binary constraint in (4.1) (with respect to only assignment variable $\boldsymbol{x}$). More importantly, using [16, Prop. 3.1] program (4.14) can be represented by

$$-\min_{\boldsymbol{x},\bar{\boldsymbol{\alpha}},\boldsymbol{y}} [f_1(\bar{\boldsymbol{\alpha}}, \boldsymbol{y}) - f_2(\boldsymbol{y})] \ : \ (4.1), (4.2), (4.12)(4.13b) - (4.13d), \tag{4.15}$$

where $f_1(\bar{\boldsymbol{\alpha}})$ and $f_2(\bar{\boldsymbol{\alpha}})$ are defined as

$$\begin{aligned} f_1(\bar{\boldsymbol{\alpha}}, \boldsymbol{y}) &= \max_{m=1,2,\ldots,M} \left[-2\ln\left(\sum_{n=1}^{N} \bar{\boldsymbol{\alpha}}_{nm}|\ell_{nm}h_{nm}|\right) - \sum_{i\neq m} \ln\left(\boldsymbol{y}_i + \sigma_D^2\right)\right] \\ f_2(\boldsymbol{y}) &= -\sum_{m=1}^{M} \ln\left(\boldsymbol{y}_m + \sigma_D^2\right), \end{aligned} \tag{4.16}$$

which are convex functions as the maximum and summation of convex functions [16]. Therefore (4.15) is already in the form of (2.11) with

$$\begin{aligned}
(\boldsymbol{z},\boldsymbol{x}) &\to ((\bar{\boldsymbol{\alpha}},\boldsymbol{x}),\boldsymbol{x}),\\
\mathcal{K} &\to \Big\{((\bar{\boldsymbol{\alpha}},\boldsymbol{y}),\boldsymbol{x}) \;:\; (4.2),(4.12),(4.13b)-(4.13d)\Big\},\\
f(\boldsymbol{z}) &\to f(\bar{\boldsymbol{\alpha}},\boldsymbol{y}),\\
g(\boldsymbol{z}) &\to g(\boldsymbol{y}).
\end{aligned}$$

Clearly, the corresponding d.c. expression (2.17) is

$$-\min_{\bar{\boldsymbol{\alpha}},\boldsymbol{y},\boldsymbol{x}} \;[f_1(\bar{\boldsymbol{\alpha}},\boldsymbol{y})-f_2(\boldsymbol{y})+\mu(\sum_{m=1}^{M}\sum_{n=1}^{N}\boldsymbol{x}_{nm}-\sum_{m=1}^{M}\sum_{n=1}^{N}\boldsymbol{x}_{nm}^2)] \tag{4.17a}$$

$$\text{s.t.:} \quad (4.2),(4.12)(4.13b)-(4.13d), \tag{4.17b}$$

$$\boldsymbol{x}_{nm}\in[0,1], n=1,2,\dots,N;\; m=1,2,\dots,M. \tag{4.17c}$$

Therefore, we shall apply the generic procedure (Step 1 to Step 3) described in Chapter 2 to address the problem (4.17)/(4.15)/(4.10). In what follows, we shall discuss in details for finding optimized solutions of program (4.17).

4.2.1 Step 1: initialization by all relay beamforming optimization

The box-relaxed program (2.18) corresponding to (4.15) is

$$-\min_{\boldsymbol{x},\bar{\boldsymbol{\alpha}},\boldsymbol{y}} [f_1(\bar{\boldsymbol{\alpha}},\boldsymbol{y})-f_2(\boldsymbol{y})] \;:\; (4.2),(4.12),(4.13b)-(4.13d),(4.17c), \tag{4.18}$$

which is just the corresponding beamforming design for all relays.

According to our computational experience, the following initialization is good with respect to the convergence of its DCIs:

$$\bar{\alpha}_{nm}^{(0)} = [\min\left\{\frac{P_n}{M(|h_{nm}|^2+\sigma_R^2)}, P_n\right\}]^{1/2},\ n=1,2,\ldots,N;\ m=1,2,\ldots,M,$$
$$y_m^{(0)} = \sigma_R^2\sum_{n=1}^{N}(\bar{\alpha}_{nm}^{(0)})^2|\ell_{nm}|^2, m=1,2,...,M.$$

For $\kappa = 0,1,\ldots,$ the κ-th iteration (2.19) for program (4.18) that yields an iterative solution $\bar{\alpha}_{nm}^{(\kappa+1)}$ and $y_m^{(\kappa+1)}$ is

$$\min_{\boldsymbol{x},\bar{\boldsymbol{\alpha}},\boldsymbol{y}} \{[f_1(\bar{\boldsymbol{\alpha}},\boldsymbol{y}) - f_2(y^{(\kappa)}) + \langle\nabla f_2(y^{(\kappa)}), \boldsymbol{y}-y^{(\kappa)}\rangle]\ :\ (4.13b)-(4.13d), (4.17b), \tag{4.19}$$

where

$$\langle\nabla f_2(y^{(\kappa)}), \boldsymbol{y}-y^{(\kappa)}\rangle = \sum_{m=1}^{M}\frac{1}{y_m^{(\kappa)}+\sigma_D^2}(\boldsymbol{y}_m - y_m^{(\kappa)}). \tag{4.20}$$

There are totally $2NM+M$ decision variables and $3NM+N+1$ convex and linear constraints in the the convex program (4.19) so its computational complexity is $O((2NM+M)^3(3NM+N+1))$ (see e.g. [145]).

Alternatively, the optimal solution of d.c. program (4.18) can be found through bisection in parameter $\boldsymbol{t}$ for the following parametric second-order cone program:

$$\begin{aligned} &\max_{\boldsymbol{x},\bar{\boldsymbol{\alpha}},\boldsymbol{t}}\ \boldsymbol{t} \\ \text{s.t.:}\quad &(4.2), (4.13b)-(4.13d), \\ &\sum_{n=1}^{N}\bar{\boldsymbol{\alpha}}_{nm}|\ell_{nm}h_{nm}| \geq \boldsymbol{t}[\sigma_R^2\sum_{n=1}^{N}\bar{\boldsymbol{\alpha}}_{nm}^2|\ell_{nm}|^2+\sigma_D^2]^{1/2},\ m=1,2,\ldots,M, \end{aligned} \tag{4.21}$$

which requires a second-order cone program (SOCP) solver to check for the feasibility of the linear constraints (4.21) when $\boldsymbol{t}$ is held fixed.

It should be noted that theoretically the parametric SOCP (4.21) yields its global optimal solution, while DCIs (4.19) of local search yield not necessarily optimal solution of d.c. program (4.18). Our simulation will suggest that the optimized solution located by these two different procedures are the same and thus indeed DCIs (4.19) are capable of locating the near-global optimal solution of (4.18).

In summary, as an initial solution $(\bar{\alpha}^*, x^*)$ used in the next step 2 of the solution algorithm for mixed binary program (4.15), we take $\bar{\alpha}^*$ found through either the above DCIs (4.19) for d.c program (4.18) or the parametric linear program (4.21), while

$$x^*_{nm} = (\bar{\alpha}^*_{nm})^2(|h_{nm}|^2 + \sigma_R^2)/P_n, \; n = 1, 2, \ldots, N; \; m = 1, 2, \ldots, M. \tag{4.22}$$

4.2.2 Step 2: mixed beamforming and assignment optimization

Using the solution $(\bar{\alpha}^*, y^*, x^*)$ found from Step 1 as the initial solution $(\bar{\alpha}^{(0)}, y^{(0)}, x^{(0)})$, for $\kappa = 0, 1, \ldots$, the corresponding κ-th DCI (2.22) that gives the iterative solution $(\bar{\alpha}^{(\kappa+1)}, y^{(\kappa+1)}, x^{(\kappa+1)})$ of (4.17) is the following convex program:

$$\begin{aligned} \min_{\boldsymbol{x},\bar{\boldsymbol{\alpha}},\boldsymbol{y}} \quad & [f_1(\bar{\boldsymbol{\alpha}}, \boldsymbol{y}) + \mu h_1(\boldsymbol{x}) - f_2(y^{(\kappa)}) - \mu h_2(x^{(\kappa)}) - \langle \nabla f_2(y^{(\kappa)}), \boldsymbol{y} - y^{(\kappa)} \rangle] - \mu \langle \nabla h_2(x^{(\kappa)}), \boldsymbol{x} - x^{(\kappa)} \rangle] \\ \text{s.t.:} \quad & (4.2), (4.12), (4.13b) - (4.13d), (4.17b), \end{aligned} \tag{4.23}$$

where $\langle \nabla f_2(y^{(\kappa)}), \boldsymbol{y} - y^{(\kappa)} \rangle$ is defined by (4.20), while

$$h_1(\boldsymbol{x}) = \sum_{m=1}^{M} (\sum_{n=1}^{N} \boldsymbol{x}_{nm} + (\sum_{n=1}^{N} \boldsymbol{x}_{nm})^2),$$

$$h_2(\boldsymbol{x}) = \sum_{m=1}^{M} (\sum_{n=1}^{N} \boldsymbol{x}^2_{nm} + (\sum_{n=1}^{N} \boldsymbol{x}_{nm})^2),$$

and

$$\langle \nabla h_2(x^{(\kappa)}), \boldsymbol{x} - x^{(\kappa)} \rangle = 2 \sum_{m=1}^{M} \left(\sum_{n=1}^{N} \left(x^{(\kappa)}_{nm} + \sum_{n=1}^{N} x^{(\kappa)}_{nm} \right) \left(\boldsymbol{x}_{nm} - x^{(\kappa)}_{nm} \right) \right).$$

The computational complexity of (4.23) is $O((2NM + M)^3(2NM + 2M + N + 1))$.

4.2.3 Step 3: assigned relay beamforming re-optimization

Suppose that $(\bar{\alpha}^*, x^*)$ is a solution found by Step 2 as above. The corresponding d.c. program (2.23) to improve the solution further by substituting the binary solution x^* in constraints (4.13b)-(4.13c) is the following program in only continuous variable $\bar{\boldsymbol{\alpha}}$ of power allocation:

$$-\min_{\bar{\boldsymbol{\alpha}},\boldsymbol{y}} \quad [f_1(\bar{\boldsymbol{\alpha}},\boldsymbol{y}) - f_2(\boldsymbol{y})] \tag{4.24a}$$

$$\text{s.t.} \quad (4.12), (4.13b) - (4.13c), \tag{4.24b}$$

$$\bar{\boldsymbol{\alpha}}^2_{nm}(|h_{nm}|^2 + \sigma_R^2) \le [x^*_{nm}]_b P_n, \; n = 1,2,\ldots,N; \; m = 1,2,\ldots,M. \tag{4.24c}$$

Constraint (4.24b) given $[x^*]_b$ implies that program (4.24) involves only $N_R M$ variables $\bar{\boldsymbol{\alpha}}_{nm}$, which correspond to $[x^*_{nm}]_b = 1$ in (4.24b), i.e. program (4.24) is assigned relay beamforming re-optimization. Therefore the DCIs adapted to the d.c. program (4.24) is to initialize from $\bar{\alpha}^{(0)} = \alpha^*$ and for $\kappa = 0, 1, \ldots$, κ-th DCI to output the iterative solution $\bar{\alpha}^{(\kappa+1)}$ is the following convex program:

$$\min_{\bar{\boldsymbol{\alpha}},\boldsymbol{y}} \left[f_1(\bar{\boldsymbol{\alpha}},\boldsymbol{y}) - f_2(y^{(\kappa)}) - \langle \nabla f_2(y^{(\kappa)}), \boldsymbol{y} - y^{(\kappa)} \rangle \right] \; : \; (4.12), (4.13b) - (4.13c), (4.24b), \tag{4.25}$$

with $\langle \nabla f_2(\bar{\alpha}^{(\kappa)}), \bar{\boldsymbol{\alpha}} - \bar{\alpha}^{(\kappa)} \rangle$ defined by (4.20). Its computational complexity is $O((N_R+M)^3(2NM+N+M+1)$. The stopping criterion in (2.20) can also be used to output the final solution.

Alternatively, relay beamforming based on $[\boldsymbol{x}^*]_b \in \{0,1\}^{N\times M}$ can also be done by the a similar parametric second-order cone program:

$$\max_{\bar{\boldsymbol{\alpha}},\boldsymbol{t}} \boldsymbol{t} \; : \; (4.13b) - (4.13c), (4.24b), \sum_{n=1}^{N} \bar{\boldsymbol{\alpha}}_{nm} |\ell_{nm} h_{nm}| \ge \boldsymbol{t}[\sigma_R^2 \sum_{n=1}^{N} \bar{\boldsymbol{\alpha}}^2_{nm} |\ell_{nm}|^2 + \sigma_D^2]^{1/2}, \; m = 1,2,\ldots,M. \tag{4.26}$$

In summary, the proposed procedure for finding the solutions of the mixed binary program in (4.15) consists of the above three sequential steps: the initial Step 1 for locating a good initial solution for Step 2, Step 2 for locating the optimized mixed beamforming and assignment solutions, and Step 3 for re-optimizing the assigned relay beamforming.

4.2.4 A case study with MRC

It is worthwhile to point out that the above procedure is also applicable to the following optimization problem concerning the maximal-ratio-combining (MRC) receiver as studied in [132]:

$$\max_{\boldsymbol{x},\bar{\boldsymbol{\alpha}}} \min_{m=1,2,\ldots,M} \varphi_m^{\text{MRC}}(\bar{\boldsymbol{\alpha}}) \; : \; (4.1), (4.2), (4.13b) - (4.13d), \tag{4.27}$$

where

$$\varphi_m^{\text{MRC}}(\bar{\boldsymbol{\alpha}}) := \sum_{n=1}^{N} \frac{\bar{\boldsymbol{\alpha}}_{nm}|\ell_{nm}h_{nm}|^2}{\sigma_R^2\bar{\boldsymbol{\alpha}}_{nm}|\ell_{nm}|^2 + \sigma_D^2} = \sum_{n=1}^{N} \frac{|\ell_{nm}h_{nm}|^2}{\sigma_R^2|\ell_{nm}|^2} - \sum_{n=1}^{N} \frac{\sigma_D^2|\ell_{nm}h_{nm}|^2}{\sigma_R^2|\ell_{nm}|^2(\sigma_R^2|\ell_{nm}|^2\bar{\boldsymbol{\alpha}}_{nm} + \sigma_D^2)}. \tag{4.28}$$

In contrast to the objective functions in (4.13a), which are not concave, the objective functions in (4.28) are clearly seen concave in $\bar{\boldsymbol{\alpha}}_{nm} = |\boldsymbol{\alpha}_{nm}|^2$. It can be also seen that (4.28) is an upper bound of the objective function in (4.14a) as well. The sum-rate maximization considered in [133] is actually

$$\max_{\boldsymbol{x},\bar{\boldsymbol{\alpha}}} \sum_{m=1}^{M} \varphi_m^{\text{MRC}}(\bar{\boldsymbol{\alpha}}) \; : \; (4.1), (4.2), (4.13b) - (4.13d),$$

which is quite similar to (4.27) but looks less meaningful.

Obviously, mixed binary program in (4.27) is a special case of mixed binary program in (4.15) with

$$f_1(\bar{\boldsymbol{\alpha}}) := \max_{m=1,2,\ldots,M} \left[-\varphi_m^{\text{MRC}}(\bar{\boldsymbol{\alpha}})\right], \quad f_2(\bar{\boldsymbol{\alpha}}) \equiv 0. \tag{4.29}$$

Accordingly, the realizations of Step 1 to Step 3 to obtain the solution of (4.27) are simplified as follows.

- Step 1: With $f_2(\bar{\boldsymbol{\alpha}}) \equiv 0$, program (4.18) becomes the following convex program:

$$-\min_{\bar{\boldsymbol{\alpha}}} \max_{m=1,2,\ldots,M} \left[-\varphi_m^{\text{MRC}}(\bar{\boldsymbol{\alpha}})\right] \quad : \quad (4.2), (4.13b) - (4.13c), \\ 0 \leq \bar{\boldsymbol{\alpha}}_{nm} \leq P_n, \; n = 1, 2, \ldots, N; \; m = 1, 2, \ldots, M, \tag{4.30}$$

  which can be easily solved by convex programming solvers instead of DCIs.

- Step 2: Initialized from $\bar{\alpha}^{(0)} = \bar{\alpha}^*$ and $x_{nm}^{(0)} = P_n/\bar{\alpha}_{nm}^{(0)}$, where $\bar{\alpha}^*$ is the optimal solution of (4.30), for $\kappa = 0, 1, 2, \ldots$ use DCIs to solve program (4.23) with $f_1(\cdot)$ and $f_2(\cdot)$ defined by (4.29) to generate a sequence of improved solutions $\{(\bar{\alpha}^{(\kappa)}, x^{(\kappa)})\}$ for the mixed binary program (4.27).

- Step 3: With the binary solution x^* found from Step 2, substituting $\boldsymbol{x} = [x^*]_b$ in constraint (4.14c) of program (4.27) to result in the following convex program in only continuous variables $\boldsymbol{\alpha}_{nm}$ (with $[x_{nm}^*]_b = 1$):

$$\max_{\bar{\boldsymbol{\alpha}}} \min_{m=1,2,\ldots,M} \varphi_m^{\text{MRC}}(\bar{\boldsymbol{\alpha}}) \; : \; (4.13b) - (4.13c), (4.24b). \tag{4.31}$$

The above procedure is different from that presented in [132] in the crucial Step 2. A joint optimization in mixed binary optimization $(\boldsymbol{\alpha}, \boldsymbol{x})$ is treated in [132]. From the optimal solution $\bar{\alpha}^*$ of Step 1, Step 2 in [132] is to take N_U largest $\bar{\boldsymbol{\alpha}}_{nm}^*$ for each m and then assign $x_{nm} = 1$ for these relays to solve (4.31) in $\bar{\boldsymbol{\alpha}}$. The simulation results presented in Section 4.3 will show the superior performance of our solutions compared to that obtained in [132].

4.3 Numerical Results for Orthogonal Transmission

For simulation, consider a 200m × 200m square region as illustrated in Figure 4.1, where N relays are fixed at coordinates $(0, \frac{200}{N+1})$, $(0, 2 \times \frac{200}{N+1})$,..., $(0, N \times \frac{200}{N+1})$ and M source nodes (destination nodes, resp.) are randomly allocated on the left hand side (right hand side, resp.) of the relay array. Following [39, 146], fading channels with path loss and a Rayleigh component are generated by $h_{nm} \sim \mathcal{N}(0, \sigma^2_{hnm})$ and $\ell_{nm} \sim \mathcal{N}(0, \sigma^2_{\ell nm})$, where their variances are proportional to the physical link distance [66]: $\sigma^2_{hnm} = C/d^{\beta}_{hnm}$ and $\sigma^2_{\ell nm} = C/d^{\beta}_{\ell nm}$. Here, d_{hnm} ($d_{\ell nm}$, resp.) denotes the distance between the mth source node and the nth relay node in meters (the nth relay node and the mth destination node, resp.). The constant C is given as $C = G_t G_r \lambda^2/(4\pi)^2 L$, where G_t is the transmitter antenna gain, G_r is the receiver antenna gain, λ is the wavelength in meters, $L \leq 1$ is the system loss factor not related to propagation and β is the path loss exponent. An urban environment with $\beta = 3, G_t = G_r = 1, \lambda = 1/3m, L = 1$ is used in all simulations. In addition, the variances of AWGN noise samples at relays and destination nodes are assumed to be 10^{-10}. The value of penalty parameter μ in program (4.17) of orthogonal source transmission and program (4.43) for non-orthogonal source transmission is set to be 50 and 10, respectively. In all simulations, the proposed algorithm are indeed capable of locating the approximately global optimal solutions of the mixed binary programs (4.10) and (4.38) as they output the optimized values that basically match their upper bounds provided by the optimal values of the relaxed programs (4.18) and (4.44), respectively.

For ease of presentation and discussion, we refer to our proposed solution procedure (Step 1 to Step 3 in Section 4.2) as Procedure I. To show the effectiveness of its jointly optimized beamforming and relay assignment capability we also compare its minimum SNR performance with that obtained by the following existing heuristic procedures for the relay assignment:

- Procedure II: based on the solution $\bar{\alpha}^*$ of the box-relaxed program (4.18) (found by Step 1), for each user m it assigns $x^*_{nm} = 1$ to N_R relays corresponding to the N_R highest beamforming gains $\bar{\alpha}^*_{nm}$.

- Separated best link choices for each user: (i) "Best S-D channels" selects N_R relays corresponding to N_R strongest uplink and down link products $|h_{nm}\ell_{nm}|$; (ii) "Best S-R channels" selects N_R relays corresponding to N_R strongest uplinks $|h_{nm}|$; (iii) "Best R-D channels" selects N_R relays corresponding to N_R strongest downlinks $|\ell_{nm}|$.

With these relay assignments, program (4.24) is then implemented for re-optimization to output the corresponding minimum SNR performances.

We start from the single-user case ($M = 1$) with $N_R = 3$ relays assigned from $N = 5$ and $N = 10$ relays. Figure 4.2 plots the minimum SNR versus the relay power limit P_n. The total power $P_T = 0.7N_RP_n$ is set so it is independent from the total relay number N. The proposed Procedure I yields the performance curves that almost match the All-relay BF curves of the upper bounds provided by the relaxed program (4.18). It is clearly observed that the performance of Procedure II is inferior to that of Procedure I by up to 2 dB, although it is still better than performances by the above three mentioned best link selections. The communication coverage is better provided with a larger number of relays, which explains the improvement of all performance curves when increasing N from 5 to 10.

Next, for the multi-user case, $(M, N, N_R) = (5, 10, 3)$, Figure 4.3 plots the minimum SNR versus the relay power limit P_n, where, as before, the total power is $P_T = 0.7N_RP_n$. Similarly, the proposed Procedure I outputs the minimum SNRs that match their upper bound provided by the relaxed program (4.18). Procedure II performs poorer than Procedure I but it still outperforms all the channel strength-based selection algorithms. It is important to realize that under the same relaying power constraints, a properly selected relay subset for each user is able to retain the minimum SINR performance of the conventional nonselective scheme and thus actually improves the bandwidth efficiency and the life time of the network. Next, with the number of user pairs $M = 5$ and the individual relay power limit $P_n = 0$dB, Figure 4.4 plots the minimum SNR versus the total relay numbers N with $N_R = \lceil \frac{N}{M} \rceil + 2$ ($\lceil \cdot \rceil$ is the ceiling function). Again, it shows that only Procedure I is able to perform closely with the upper bound provided by the optimal value of (4.18). Such choice of selected relays N_R seems to be reasonable. On the contrary, with $N_R = 3$ fixed, the SNR performance becomes saturated although the total number of relays is increased to improve the communication coverage.

The computational complexity of Procedure I is provided in Table 4.1. The iteration numbers for different versions of Step 1 correspond to the number of required SOCP programs for solutions of

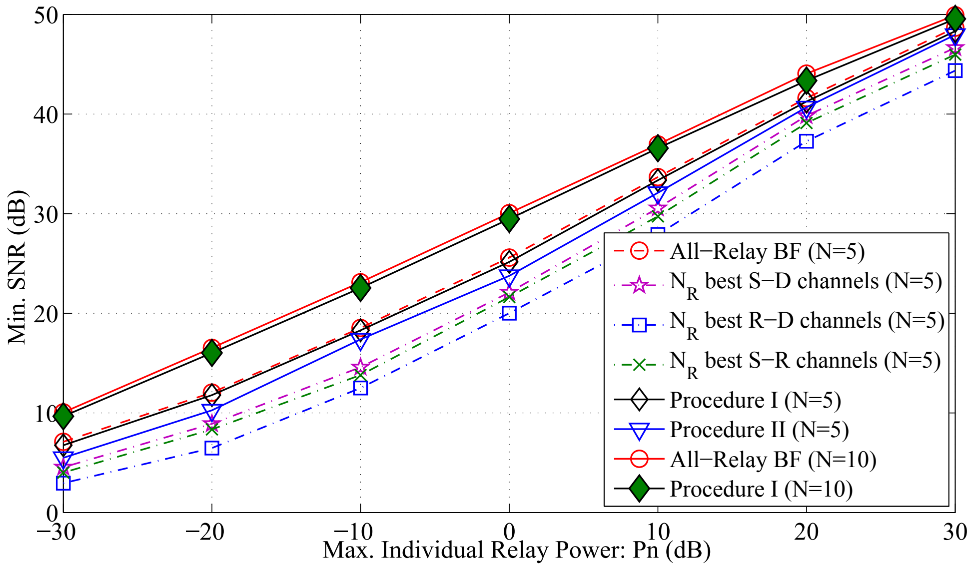

FIGURE 4.2: Min. SNR vs. individual relay power for $M = 1$, $N_R = 3$ and $N \in \{5, 10\}$.

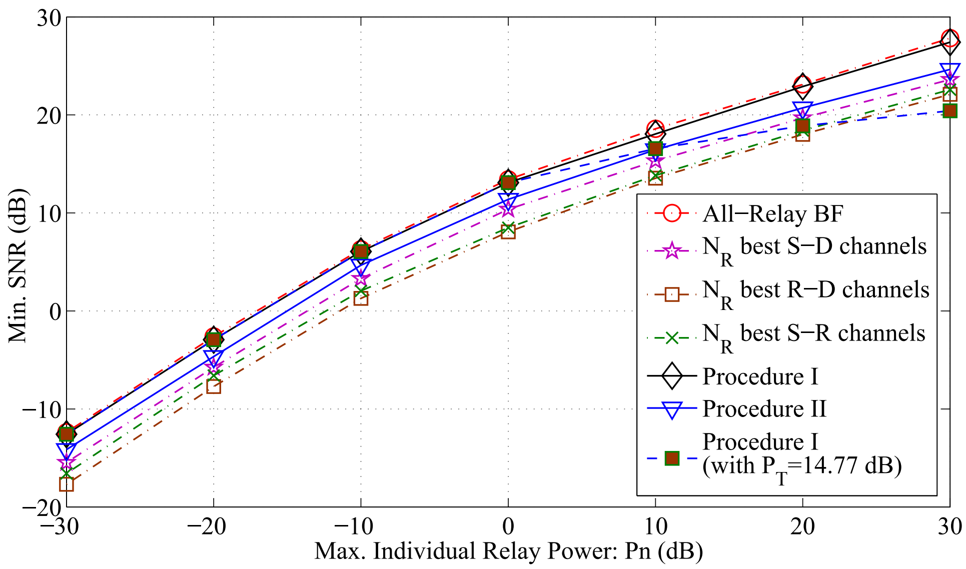

FIGURE 4.3: Min. SNR vs. individual relay power for $(M, N, N_R) = (5, 10, 3)$.

the parametric program (4.21) and the number of required convex programs (4.19) for solutions of the d.c. program (4.18), respectively. It is found that both can yield similar optimized solutions, while the former has a guaranteed optimality given some accuracy tolerance (set as 10^{-6}). However, the latter (4.19) converges even faster to those well optimized solutions. Similarly, the iteration numbers for Step 2 (Step 3, resp.) correspond to the number of required convex programs (4.23) ((4.25) or (4.26), resp.) for the solution of program (4.17) ((4.24), resp.).

Figure 4.5 shows the corresponding simulation results for MRC program (4.27). Again, the

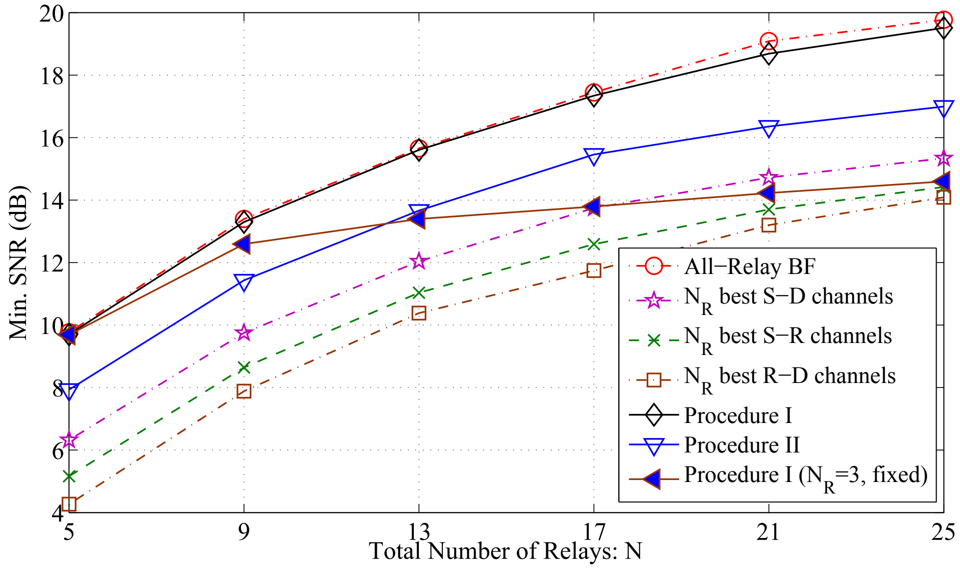

FIGURE 4.4: Min. SNR vs. the number of relays for $M = 5$, $N_R = \lceil \frac{N}{M} \rceil + 2$

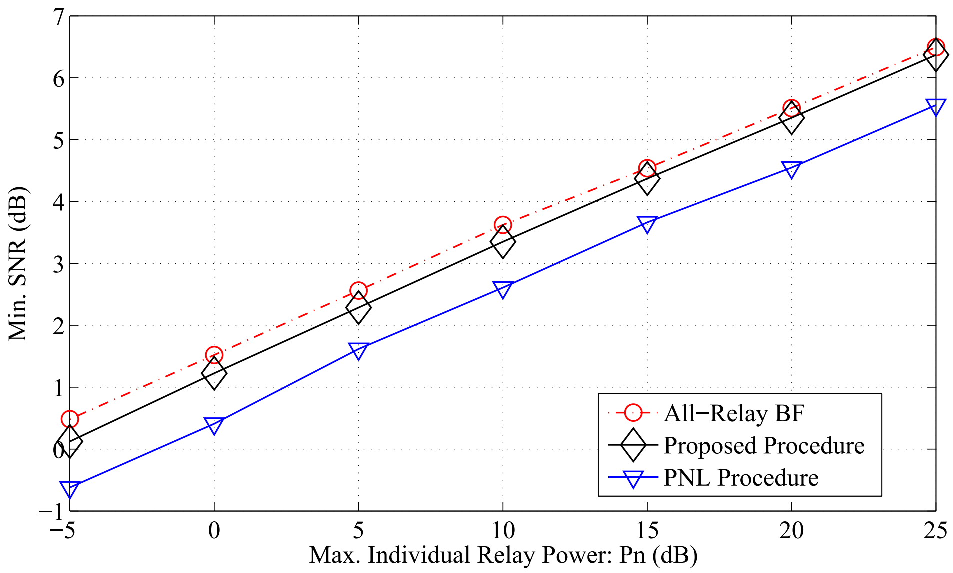

FIGURE 4.5: Min. SNR vs. the individual relay power for MRC receiver: $(M, N, N_R) = (5, 10, 3)$.

corresponding Procedure I could locate the best optimized solution for (4.27) as its performance curve is very close to the upper bound. However, the procedure proposed in [132], referred to as “PNL Procedure” (discussed at the end of Section 4.2) has a poorer performance.

4.4 Joint Beamforming and Relay Selection with Non-orthogonal Transmission

In a multi-user wireless relay network, the bandwidth resource is most efficiently utilized if all the users' signals are allowed to be transmitted over the same channel to and from each relay. The price to be paid for such a higher spectral efficiency is the existence of inter-user interference at each relay and each destination node.

Specifically, the received signal at relay n is now given by

$$y_{R,n} = \boldsymbol{x}_n(\sum_{m=1}^{M} h_{nm}s_m + n_n),$$

where, as before, n_n represents AWGN at each relay whose variance is σ_R^2 and $\boldsymbol{x}_n$ is the link connectivity between relay n and the users and destinations. $x_n = 1$ means that relay n is selected for the connection and $x_n = 0$ means that relay n is not selected. The relay selection is restricted by

$$\sum_{n=1}^{N} \boldsymbol{x}_n \leq N_R,\ \boldsymbol{x} = (\boldsymbol{x}_1, \ldots, \boldsymbol{x}_N)^T \in \{0,1\}^N. \tag{4.32}$$

Relay n then amplifies its received signal by a complex gain $\boldsymbol{\alpha}_n$, $n = 1, 2, \ldots, N$. Thus, relay n sends the following signal to destination m:

$$y_n = \boldsymbol{x}_n\boldsymbol{\alpha}_n(\sum_{m=1}^{M} h_{nm}s_m + n_n) \tag{4.33}$$

The complex gain $\boldsymbol{\alpha}_n$ is constrained by the following individual relaying power

$$\boldsymbol{x}_n|\boldsymbol{\alpha}_n|^2(\sum_{m=1}^{M} |h_{nm}|^2 + \sigma_R^2) \leq P_n,\ n = 1, 2, \ldots, N, \tag{4.34}$$

as well as the total relaying power

$$\sum_{n=1}^{N} \boldsymbol{x}_n|\boldsymbol{\alpha}_n|^2(\sum_{m=1}^{M} |h_{nm}|^2 + \sigma_R^2) \leq P_T. \tag{4.35}$$

Accordingly the received signal at the destination m is

$$y_{D,m} = \sum_{n=1}^{N} \boldsymbol{x}_n \boldsymbol{\alpha}_n \ell_{nm} (\sum_{m=1}^{M} h_{nm} s_m + n_n) + n_{D,m} \tag{4.36}$$

where $n_{D,m}$ is AWGN at destination m, whose variance is σ_D^2.

As only signal $\sum_{n=1}^{N} \boldsymbol{\alpha}_n \boldsymbol{x}_n^2 \ell_{nm} h_{nm} s_m = \sum_{n=1}^{N} \boldsymbol{\alpha}_n \boldsymbol{x}_n \ell_{nm} h_{nm} s_m$ is of interest in (4.36), the SINR at destination m is given by

$$\mathbf{SINR}_m(\boldsymbol{\alpha}, \boldsymbol{x}) = \frac{\left| \sum_{n=1}^{N} \boldsymbol{x}_n \boldsymbol{\alpha}_n \ell_{nm} h_{nm} \right|^2}{\sum_{j \neq m}^{M} \left| \sum_{n=1}^{N} \boldsymbol{x}_n \boldsymbol{\alpha}_n \ell_{nm} h_{nj} \right|^2 + \sigma_R^2 \sum_{n=1}^{N} \boldsymbol{x}_n |\boldsymbol{\alpha}_n|^2 |\ell_{nm}|^2 + \sigma_D^2}. \tag{4.37}$$

The joint optimization in beamforming weight $\boldsymbol{\alpha}_n$ and relay assignment $\boldsymbol{x}$ is formulated as follows

$$\max_{\boldsymbol{\alpha}, \boldsymbol{x}} \min_{m=1,2,\ldots,M} \mathbf{SINR}_m(\boldsymbol{\alpha}, \boldsymbol{x}) \ : \ (4.32), (4.34), (4.35). \tag{4.38}$$

For each fixed binary x^* that is feasible to (4.32), (4.38) is still a (non-convex) maximin program, which has been successfully addressed in [136]. However, it is not practical to address (4.38) by solving $C(N, N_R)$ such maximin programs.

The objective functions in program (4.38), which are fractions of multivariate polynomials, are highly complex. The next Theorem is the first step to recognize its partial convexities that will be useful for the later development.

Theorem 2. With the following variable change

$$\boldsymbol{x}_n \boldsymbol{\alpha}_n \to \tilde{\boldsymbol{\alpha}}_n, \ \tilde{\boldsymbol{\alpha}} := (\tilde{\boldsymbol{\alpha}}_1, ..., \tilde{\boldsymbol{\alpha}}_N)^T \tag{4.39}$$

the mixed binary program (4.38) is equivalent to the following mixed binary program

$$\max_{\boldsymbol{x},\tilde{\boldsymbol{\alpha}},\boldsymbol{y}} \min_{m=1,2,\dots,M} \varphi_m(\tilde{\boldsymbol{\alpha}},\boldsymbol{y}) := \frac{|\sum_{n=1}^{N}\tilde{\boldsymbol{\alpha}}_n\ell_{nm}h_{nm}|^2}{\boldsymbol{y}_m+\sigma_D^2} \ : \ (4.32), \tag{4.40a}$$

$$\sum_{j\neq m}^{M}|\sum_{n=1}^{N}\tilde{\boldsymbol{\alpha}}_n\ell_{nm}h_{nj}|^2+\sigma_R^2\sum_{n=1}^{N}|\tilde{\boldsymbol{\alpha}}_n|^2|\ell_{nm}|^2 \le \boldsymbol{y}_m,\ m=1,2,\dots,M, \tag{4.40b}$$

$$|\tilde{\boldsymbol{\alpha}}_n|^2(\sum_{m=1}^{M}|h_{nm}|^2+\sigma_R^2) \le P_n,\ n=1,2,\dots,N, \tag{4.40c}$$

$$\sum_{n=1}^{N}|\tilde{\boldsymbol{\alpha}}_n|^2(\sum_{m=1}^{M}|h_{nm}|^2+\sigma_R^2|) \le P_T, \tag{4.40d}$$

$$|\tilde{\boldsymbol{\alpha}}_n|^2(\sum_{m=1}^{M}|h_{nm}|^2+\sigma_R^2|) \le \boldsymbol{x}_nP_T,\ n=1,...,N, \tag{4.40e}$$

where each function φ_m is convex in $(\tilde{\boldsymbol{\alpha}},\boldsymbol{y})$.

Proof: Any feasible solution (α,x) to (4.38) leads to the obviously feasible solution $(\tilde{\alpha},y,x)$ to (4.40) with $\tilde{\alpha}$ defined by (4.39) and y_m accordingly defined by the left hand side of (4.40b). Therefore max (4.38) $\le$ max (4.40). On the other hand, for the optimal solution $(\tilde{\alpha}^{opt},y^{opt},x^{opt})$ of (4.40) and then $\alpha_n^{opt}=x_n\tilde{\alpha}_n$, $n=1,2,\dots,N$, it is clear that (α^{opt},x^{opt}) is feasible to (4.38) and then by (4.40b) it is $\mathbf{SINR}_m(\alpha^{opt},x^{opt}) \ge \varphi_m(\tilde{\alpha}^{opt},y^{opt})$, $m=1,2,\dots,M$. The last inequalities imply max (4.40) $\le$ max (4.38), which together with max (4.38) $\le$ max (4.40) show that max (4.40) $=$ max (4.38).

Finally, each function $\varphi_m(\tilde{\boldsymbol{\alpha}},\boldsymbol{y})$ is convex as a composite of the convex function $\phi(\boldsymbol{s},\boldsymbol{y}_m) = |\boldsymbol{s}|^2/(\boldsymbol{y}_m+\sigma_D^2)$ and linear function $s(\tilde{\boldsymbol{\alpha}}_n)=|\sum_{n=1}^{N}\tilde{\boldsymbol{\alpha}}_n\ell_{nm}h_{nm}|^2$ [16]. The convexity of $\phi(\boldsymbol{s},\boldsymbol{y}_m)$ on $\mathcal{C}\times R_+$ immediately follows from positive definiteness of its Hessian. □

Using [16, Prop. 3.1] again to rewrite program (4.40) as

$$-\min_{\boldsymbol{x},\tilde{\boldsymbol{\alpha}},\boldsymbol{y}} [f_1(\tilde{\boldsymbol{\alpha}},\boldsymbol{y})-f_2(\tilde{\boldsymbol{\alpha}},\boldsymbol{y})] \ : \ (4.40b)-(4.40e),(4.32) \tag{4.41}$$

with $f_1(\boldsymbol{\alpha},\boldsymbol{y}) := \max_{m=1,2,\dots,M}\sum_{i\neq m}\phi_i(\boldsymbol{\alpha},\boldsymbol{y})$ and $f_2(\boldsymbol{\alpha},\boldsymbol{y}) := \sum_{m=1}^{M}\phi_m(\boldsymbol{\alpha},\boldsymbol{y})$. Each $\phi_m(\boldsymbol{\alpha},\boldsymbol{y})$ is convex by Theorem 2, so indeed f_1 and f_2 are convex as maximum and sum of convex functions [16].

Therefore, program (4.41) is in form (2.11) with

$$\begin{aligned}
\boldsymbol{z} &\to (\tilde{\boldsymbol{\alpha}}, \boldsymbol{y}),\\
\boldsymbol{x} &\to \boldsymbol{x},\\
f(\boldsymbol{z}) &\to f_1(\tilde{\boldsymbol{\alpha}}, \boldsymbol{y}),\\
g(\boldsymbol{z}) &\to f_2(\tilde{\boldsymbol{\alpha}}, \boldsymbol{y}),\\
\mathcal{K} &\to \left\{(\tilde{\boldsymbol{\alpha}}, \boldsymbol{y}, \boldsymbol{x}) \;:\; (4.40b) - (4.40e), \boldsymbol{x} \in [0,1]^N,\; \sum_{n=1}^{N} \boldsymbol{x}_n \le N_R\right\},
\end{aligned} \tag{4.42}$$

and its exact canonical d.c. expression (2.17) accordingly is

$$\begin{aligned}
&\min_{\boldsymbol{x}, \tilde{\boldsymbol{\alpha}}, \boldsymbol{y}} \left[f_1(\tilde{\boldsymbol{\alpha}}, \boldsymbol{y}) - f_2(\tilde{\boldsymbol{\alpha}}, \boldsymbol{y}) + \mu(\sum_{n=1}^{N} \boldsymbol{x}_n - \sum_{n=1}^{N} \boldsymbol{x}_n^2)\right]\\
&\text{s.t.} : (4.40b) - (4.40e), \sum_{n=1}^{N} \boldsymbol{x}_n \le N_R,\; \boldsymbol{x} \in [0,1]^N.
\end{aligned} \tag{4.43}$$

4.4.1 Step 1: initialization by all relay beamforming optimization

By (4.42), the corresponding box relaxed program (2.18) corresponding to (4.41)/(4.43) is

$$-\min_{\tilde{\boldsymbol{\alpha}}, \boldsymbol{y}} \left[f_1(\tilde{\boldsymbol{\alpha}}, \boldsymbol{y}) - f_2(\tilde{\boldsymbol{\alpha}}, \boldsymbol{y})\right] \;:\; (4.42), \tag{4.44}$$

which is simply an all-relay beamforming SINR maximin optimization. Therefore, initializing from $(\tilde{\alpha}^{(0)}, y^{(0)})$, for $\kappa = 0, 1, \ldots$, the corresponding κ-th DCI (2.18) to output iterative $(\tilde{\alpha}^{(\kappa+1)}, y^{(\kappa+1)})$ in DCIs is the following convex program

$$\min_{\tilde{\boldsymbol{\alpha}}, \boldsymbol{y}} \left[f_1(\tilde{\boldsymbol{\alpha}}) - f_2(\tilde{\alpha}^{(\kappa)}, y^{(\kappa)}) - \langle \nabla f_2(\tilde{\alpha}^{(\kappa)}, y^{(\kappa)}), (\tilde{\boldsymbol{\alpha}} - \alpha^{(\kappa)}, \boldsymbol{y} - y^{(\kappa)})\rangle\right] \;:\; (4.42), \tag{4.45}$$

where

$$\langle \nabla f_2(\tilde{\alpha}^{(\kappa)}, y^{(\kappa)}), (\tilde{\boldsymbol{\alpha}} - \tilde{\alpha}^{(\kappa)}, \boldsymbol{y} - y^{(\kappa)}) \rangle =$$
$$\sum_{m=1}^{M} \left[\frac{2\text{Re}\{(\overline{\sum_{n=1}^{N} \tilde{\alpha}_n^{(\kappa)} \ell_{nm} h_{nm}}) \sum_{n=1}^{N} \ell_{nm} h_{nm} (\tilde{\boldsymbol{\alpha}}_n - \tilde{\alpha}_n^{(\kappa)})\}}{y_m^{(\kappa)} + \sigma_D^2} - \frac{|\sum_{n=1}^{N} \tilde{\alpha}_n^{(\kappa)} \ell_{nm} h_{nm}|^2 (\boldsymbol{y}_m - y_m^{(\kappa)})}{(y_m^{(\kappa)} + \sigma_D^2)^2} \right] \tag{4.46}$$

The computational complexity of convex program (4.45) is $O((N+M)^3(4N+M+2)$. Note that the effective capacity of κ-th DCI (4.45) for locating the approximately global optimal solutions of (4.44) has been shown in [136].

4.4.2 Step 2: mixed beamforming and assignment optimization

Suppose $\tilde{\alpha}^*$ is found from the above Step 1 and then $x_n^* = |\tilde{\alpha}_n^*|^2(\sum_{m=1}^{M} |h_{nm}|^2 + \sigma_R^2)/P_T$, $n = 1, 2, \ldots, N$, while y_n^* is defined by the left hand side of (4.40b) at $\tilde{\alpha}^*$. Such $(x^*, \tilde{\alpha}^*, y^*)$ is obviously feasible to (4.41). Initialized by $(x^{(0)}, \tilde{\alpha}^{(0)}, y^{(0)}) = (x^*, \tilde{\alpha}^*, y^*)$, the corresponding κ-th DCI (2.22) for program (4.43) to output iterative solution $(x^{(\kappa+1)}, y^{(\kappa+1)})$ for $\kappa = 0, 1, \ldots,$ is

$$\min_{\boldsymbol{x}, \tilde{\boldsymbol{\alpha}}, \boldsymbol{y}} \Big[f_1(\tilde{\boldsymbol{\alpha}}, \boldsymbol{y}) + \mu h_1(\boldsymbol{x}) - f_2(\tilde{\alpha}^{(\kappa)}, y^{(\kappa)}) - \mu h_2(x^{(\kappa)}) - \langle \nabla f_2(\tilde{\alpha}^{(\kappa)}, y^{(\kappa)}), (\tilde{\boldsymbol{\alpha}}, \boldsymbol{y}) - (\tilde{\alpha}^{(\kappa)}, y^{(\kappa)}) \rangle$$
$$- \mu \langle \nabla h_2(x^{(\kappa)}), \boldsymbol{x} - x^{(\kappa)} \rangle \Big] \ : \ (4.42), \tag{4.47}$$

where $\langle \nabla f_2(\tilde{\alpha}^{(\kappa)}, y^{(\kappa)}), (\tilde{\boldsymbol{\alpha}}, \boldsymbol{y}) - (\tilde{\alpha}^{(\kappa)}, y^{(\kappa)}) \rangle$ is defined by (4.46), while

$$\langle \nabla h_2(x^{(\kappa)}), \boldsymbol{x} - x^{(\kappa)} \rangle = 2 \sum_{n=1}^{N} (x_n^{(\kappa)} + \sum_{n=1}^{N} x_n^{(\kappa)})(\boldsymbol{x}_n - x_n^{(\kappa)}).$$

Its computational complexity is $O((NM+M)^3(N+NM+2M))$.

4.4.3 Step 3: assigned relay re-optimization

Suppose $x^* \in \{0,1\}^N$ is the optimized binary solution found from Step 2. The corresponding program (2.23) for assigned beamforming re-optimization is

$$\max_{\boldsymbol{\alpha},\boldsymbol{y}} \min_{m=1,2,\dots,M} \varphi_m(\boldsymbol{\alpha},\boldsymbol{y}) \;:\; ([x_1^*]_b\boldsymbol{\alpha}_1,\dots,[x_N^*]_b\boldsymbol{\alpha}_N,\boldsymbol{y},[x^*]_b) \in \mathcal{K}, \tag{4.48}$$

with $\mathcal{K}$ defined by (4.42), which is similar to program (4.44) and thus can be solved by the same DCIs for program (4.44). In fact, program (4.48) involves only N_R variables $\boldsymbol{\alpha}_n$ corresponding to $[x_n^*]_b = 1$.

In summary, our proposed solution procedure for the mixed binary program (4.40)/(4.43) for joint optimization in beamforming weights $\boldsymbol{\alpha}$ and relay assignment binary variable $\boldsymbol{x}$ consists of three steps: based on the initial solution founded by Step 1, Step 2 aims at jointly optimizing continuous variables $\boldsymbol{\alpha}$ and binary variables $\boldsymbol{x}$ through d.c. approximation and optimization, while Step 3 re-optimizes the beamforming weight $\boldsymbol{\alpha}$.

Before closing this section, it is pointed out again that the formulations (4.10) and (4.38) for orthogonal and non-orthogonal transmissions are based on the availability of perfect channel state information of both communication links connected to the relays. Similar to [136], formulations similar to (4.10) and (4.38) but taking into account channel uncertainties are possible. Such design problems and solutions would likely require much more computational effort and deserve a separate study.

4.5 Numerical Results for Non-orthogonal Transmission

By Procedure I we refer to the solution procedure proposed in Section 4.4. For comparison, another procedure is included with the proposed Procedure I, still called by Procedure II. Specifically, based on the optimized beamforming α^* of the box relaxed program (4.44) (founded by the above Step 1 in Section 4.4) Procedure II solves the following binary program for the relay assignment by enumeration for all feasible relay assignments $\boldsymbol{x}$

$$\max_{\boldsymbol{x}\in\{0,1\}^N} |\sum_{n=1}^{N} \boldsymbol{x}_n \alpha_n^* \ell_{nm} h_{nm}|^2 \; : \; \sum_{n=1}^{N} \boldsymbol{x}_n = N_R. \tag{4.49}$$

Figure 4.6 shows the minimum SINR performance versus individual relaying power limit P_n, where the total relaying power $P_T = 0.7 N_R P_n$ is set. For two network settings of $(N, M, N_R) = (25, 5, 20)$ and $(N, M, N_R) = (30, 5, 20)$, the performance of the proposed procedure I well approximates the upper bound found by the relaxed program (4.44). It is clear from Figure 4.6 that the optimized values of both (4.38) and (4.44) increase with the individual relaying power P_n.

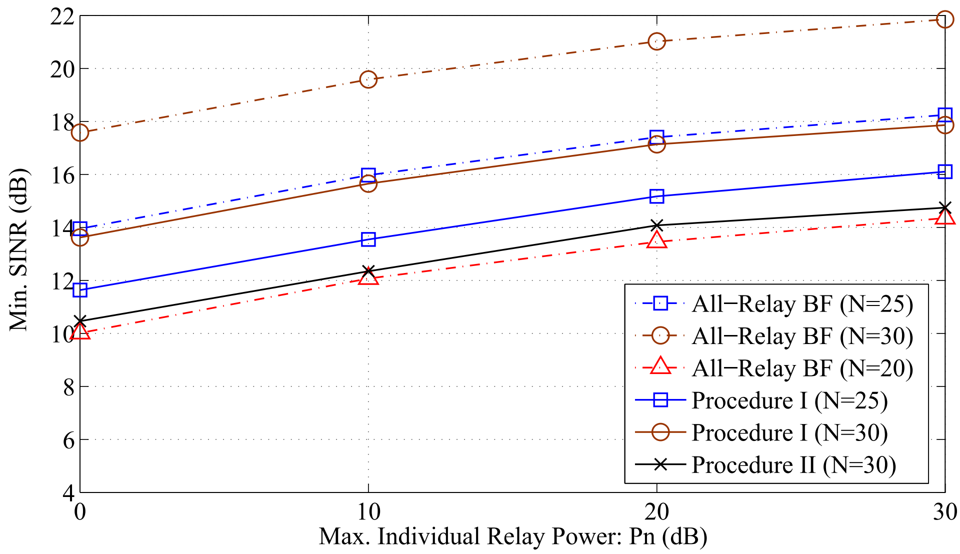

FIGURE 4.6: Min. SINR vs. individual relay power: $M = 5$, $N_R = 20$.

Unlike the orthogonal source transmission, for which relays can be individually deactivated user-wise in its up/down links and thus the size of the relay network is not necessarily reduced, it is important to realize that the performance for the non-orthogonal source transmission is indeed more sensitive on the number NR of active relays. This contributes to the gap between the performance plots for (4.38) and (4.44). Nevertheless, it is seen that the SINR performance can be significantly improved by choosing a fixed number of relays from a larger set of relays, which

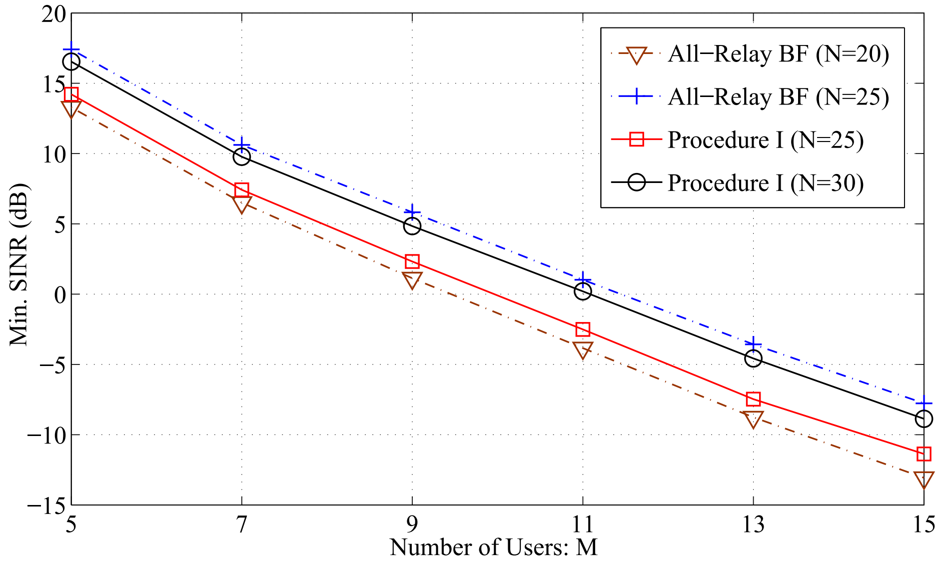

FIGURE 4.7: Min. SINR vs. num. of users: $N_R = 20$, $P_n = 20$dB, $P_T = 31.46$dB

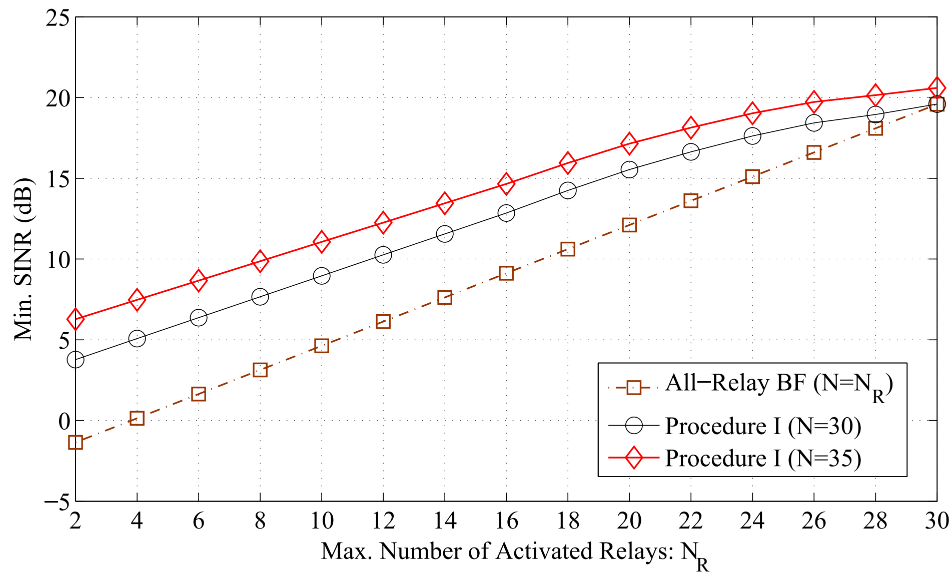

FIGURE 4.8: Min. SINR vs. max. num. of activated relays: $M = 5$, $P_n = 10$dB, $P_T = 0.7P_nN_R$

clearly justifies the advantage of relay assignment. The figure also shows that the performance of Procedure II (separated relay assignment) is much less favorable.

Furthermore, we analyze the SINR performances versus the user number M under fixed relay number $(N, NR) = (25, 20)$ or $(N, NR) = (30, 20)$ and power constraints of $P_n = 20$ dB and $P_T = 31.46dB$. It can be seen in Figure 4.7 that the minimum SINR performance is degraded as more users share the same relay resource. However, Procedure I is still able to improve the performance by as much as 5 dB against the bottom dash-line, which represents the performance of the non-selective scheme.

The computational experience is provided in Table 4.2. Like Table 4.1, the most computational loads are due to Step 1 (for locating a good enough initial solution) and Step 3 (for beamforming re-optimization).

Finally, the performance difference between selective and non-selective beamforming is further analyzed by Figure 4.8. With the same number N_R of activated relays, the performance advantage of selective beamforming over non-selective beamforming is clearly observed. It is again found that the performance of selective beamforming is improved by choosing N_R relays from a larger set of N candidate relays. This not only reiterates the above-mentioned findings, but also clearly shows the superior performance of Procedure I over other procedures in the most crucial step of relay assignment.

TABLE 4.1: The averaged iteration numbers for orthogonal transmissions: $M = 5, P_n = 0$ dB

N	5	9	13	17	21	25
Step 1 by SOCP	12.03	12.38	13.27	13.94	14.14	14.37
Step 1 by d.c.	4.52	5.92	7.61	7.97	10.23	11.06
Step 2 by d.c.	2.11	2.91	4.02	4.81	6.77	8.05
Step 3 by SOCP	12.00	12.10	12.46	13.28	13.74	13.66
Step 3 by d.c.	6.78	6.94	8.06	9.12	10.83	11.98

TABLE 4.2: The averaged iteration numbers for non-orthogonal transmissions: $P_n = 20$ dB, $P_T = 31.46$ dB, $N_R = 20$

M		5	7	9	11	13	15
Step 1	$(N = 25)$	15.10	16.32	19.67	23.09	24.14	27.92
	$(N = 30)$	18.54	20.77	21.94	25.01	27.35	29.01
Step 2	$(N = 25)$	3.82	4.02	4.92	5.91	7.88	9.45
	$(N = 30)$	5.04	6.23	7.51	8.44	10.09	12.61
Step 3	$(N = 25)$	18.25	20.40	22.99	24.12	25.81	27.27
	$(N = 30)$	19.41	22.35	26.02	29.40	31.31	34.87

4.6 Conclusions

The joint optimization in beamforming and relay assignment is a hard mixed combinatoric program. It has been shown in this research that such a problem can be solved very efficiently by d.c iterations (DCIs) of d.c. programming, which are of local search in nature and thus can converge quickly, but nevertheless yield globally optimized solutions. Extensive numerical results have demonstrated the viability of our DCIs as well as their superiority performance over other iterative procedures.

Chapter 5

Coordinated Transmission Designs in Cognitive Multi-cell MIMO Wireless Systems

5.1 Introduction

In multi-cell multi-user downlink networks, interference poses the key challenge to system designs, as users are exposed to not only intra-cell interference, but also inter-cell interference [147]. In particular, inter-cell interference is the dominating factor for system performance as cell-edge users may be deeply impacted [52]. To address this problem, conventional non-cooperative approaches adopt resource partitioning (in the space/frequency/time domain) to remove inter-cell interference effectively but are limited by the limited divisible dimensions of resource [148]. Moreover, these non-cooperative methods generally suffer from degraded spectral efficiency which is prohibitive considering the scarcity of bandwidth. Alternatively, coordinated transmission of base stations (BSs) is more capable of interference management and the full utilization of spectral resources [5]. So far, it has been considered as necessary for effectively alleviating inter-cell interference and thus approaching the capacity of multi-user cellular networks [5, 57, 148–152].

Two classes of coordinated downlink transmission have been mostly considered in the literature due to their practical importance. One is the minimization of transmitted power subject to rate (or BER) and/or cognitive constraints (i.e. the interference caused by SUs to PUs is below certain level) . This is mostly encountered in energy-limited applications with QoS requirements [9]. The other is the maximization of information throughput in terms of various rate or SINR functions subject to power and/or cognitive constraints. These problems arise under various scenarios but they generally involve the optimization of either transmit covariance matrices (including power allocation) [11, 56, 153] or precoding matrices (including beamforming vectors) [57, 149]. Understandably, the solvability of these problems varies significantly as different rate functions, power constraints, network structures (MIMO? MISO? SISO? SIMO?), or design variables may be considered. The evolvement of networks can be categorically depicted as a development from the simplest single-antenna networks (SISO) to mixed-antenna networks (SIMO or MISO), and finally to the complicated multi-antenna networks (MIMO). Despite its obvious benefits (DoF, multiplexing, diversity and etc.), the introduction of multi-antenna devices into the networks has been relatively reluctant due to the much-increased complexity of electronic design and more importantly, to the incompatibility of techniques designed for single-antenna/mixed-antenna networks. From an optimization standpoint, the optimization tasks of the multi-antenna networks are generally much more challenging than their single-antenna/mixed-antenna versions which resulted in such incompatibility. Fortunately, it is safe to assume that optimization methods designed for MIMO networks are well compatible to single-antenna or mixed-antenna (i.e. any transmitter or receiver may have an arbitrary number of antennas) networks since the latter can be treated as special cases of the former. Therefore, solving challenges encountered in MIMO networks could not only materialize the theoretical benefits of the multi-antenna structure, but also extend to simpler-structured networks easily.

In MIMO networks, as far as the aggregate rate of user's multiple data streams is concerned (normally expressed by $\log\det(*)$ function), both classes of problems are recognized as NP-hard non-convex problems for which no global optimal solutions can be found in polynomial time [57, 153, 154]. Nonetheless, there exist some exceptions where MIMO optimization problems under certain scenarios can be converted into convex programs. Namely, when rates of sub-channels are individually considered, the power minimization in precoding matrices with rate (i.e. SINR) constraints can be equivalently expressed by a SOCP program that is easily tractable [82, 149]. Therefore, it means the corresponding maximin rate (i.e. maximin SINR) problems can be solved by a sequence of such SOCPs. For MISO or SISO networks, it was realized that the optimal covariance matrices for power minimization subject to rate (i.e. SINR) constraints are always rank-one. This means the power minimization in beamforming variables and that in covariance matrix variables can be equivalently solved either by SOCP in beamforming variables [149] or SDP in covariance matrix variables [13, 155]. Consequently, the maximin rate (i.e. SINR) problem can be addressed by a bisection procedure involving such SDPs/SOCPs with increasing SINR constraints.

Despite the above-mentioned cases, the sum rate maximization problem has always remained a NP-hard non-convex problem for all network structures (see [11, 57] and references therein). In [11, 156], monotonic optimization algorithms [157] are applied to a range of problems including sum rate and minimal rate maximization for MISO networks with respect to covariance matrices. These algorithms could locate global optimal solutions but obviously suffer from unaffordable computational complexity, with 10^4 to 10^8 SDP/SOCP solver calls required just for a mini-sized network. Reference [158] studies ergodic capacity of MIMO channels. It shows that either allocating all the power to one transmit antenna or distributing the power equally to all antennas can the optimal strategy for achieving ergodic mutual capacity in the studied simple cases. However, these fixed solutions are far from optimal for non-ergodic channels studied in this research. Further, [153] provides a survey of covariance matrix designs for sum rate optimization problems in MIMO channels. Some useful algorithms are reviewed ranging from the non-cooperative water-filling algorithms, the Nash equilibrium-based algorithms to the cooperative gradient projection-based (GP) algorithms . In particular, the GP algorithms are shown to outperform the non-cooperative algorithms with relatively affordable computational complexity. However, the GP algorithms tend to encounter convergence difficulties which limit their overall performance. In [57], the multicell MIMO downlink network is categorized as a MIMO interfering broadcast channel (MIMO-IBC). To maximize the weighted sum-rate of the overall system, the problem is converted into an equivalent weighted sum MSE minimization problem (WMMSE) and then treated in an iterative variable-alternating manner. An array of other works [46, 159–161] have been reported which are essentially based on the observation of the equivalence. In general, these algorithms hold the potential for distributed implementation and their performance is better than the predecessors. However, the converted problems based on this approach are still non-convex but with even more variables. More recently, in [162], we have shown that the WMMSE algorithm [57] is in fact a special case of the broader d.c. program. In [148], two sum-rate maximization problems are considered for the downlink MIMO precoding systems by solving the Karush-Kuhn-Tucker (KKT) conditions or implementing the Blahut-Arimoto algorithm. In the context, base station coordination is essentially coordinated scheduling/beamforming (CS/CB) as orthogonal frequency-division multiple access (OFDMA) transmission is assumed. Similarly, [150] considers coordinated beamforming in a multi-cell MISO network with orthogonal co-channels via space-division multiple-access (SDMA). Although frequency re-use factor is still unit, such orthogonal transmission systems are normally affected by co-channel leakage and availability, considering the emerging tendency of deploying many more smaller-sized cells to serve the same number of users.

The research in this chapter is concerned with the sum rate and minimal rate maximization problems with respect to both precoding and covariance matrix variables for MIMO networks in cognitive radios. Due to the discriminated resource distribution under the sum rate maximization scheme (see Appendix D where some poorly-conditioned users are not serviced entirely), the maximin rate optimization is considered for addressing fairness issues among the users. Unfortunately, the latter poses an even more challenging non-convex optimization task than the former for the involvement of non-smooth rate functions. For this particular reason, the maximin rate optimization problem has been inadequately studied and the various algorithms (e.g. the WMMSE [57], the GP [153] and the cyclic descending algoirithm [163]) are obviously not applicable. In Appendix D, we show that sum rate can be maximized in the presence of rate and power/cognitive constraints for MISO networks with respect to covariance matrix variables.

As we move to MIMO networks, the rate constraints are no longer convex so such integration is not applicable.

Similar to the research in the previous chapters, we shall rely on the explicit d.c. structure of the rate functions to develop effective and efficient algorithms to address the covariance and precoding matrices design for both sum rate and minimal rate maximization problems. From simulation results, we shall investigate the relevance between the covariance matrix problems and the precoding matrix problems. Moreover, we will show how the addition of cognitive constraints would affect the system performance.

The chapter is organized as follows. Section 5.2 is devoted to the problem formulation. Section 5.3 is dedicated to the covariance matrix designs. In Section 5.4, the optimization procedures for precoding matrices are developed. Section 5.5 presents the simulation results, and Section 5.6 concludes the paper.

5.2 Problem Formulation

Consider the downlink transmission in a multi-cell multiuser cellular MIMO network consisting of N cells. Each cell has one base-station (BS) equipped with $N_t \geq 1$ antennas to serve its K mobile terminals (MTs or users), each of which is equipped with $N_r \geq 1$ antennas. Define $\mathcal{I} := \{1, 2, \ldots, N\}$ and $\mathcal{J} := \{1, 2, \ldots, K\}$. Let $s_{i,j} \in \mathbb{C}^d$ denote the intended signal vector for the jth MT in the ith cell (denoted by user (i, j)) which satisfies $E(ss^H) = I_d$, and $x_{i,j} \in \mathbb{C}^{N_t}$ denote the corresponding transmit signal vector. Let $\boldsymbol{Q}_{i,j} \in \mathcal{S}_+^{N_t}$ be the covariance matrix of $x_{i,j}$ and $\boldsymbol{V}_{i,j}^{N_t \times d}$ be the precoding matrix associated to $s_{i,j}$. Accordingly, $\boldsymbol{Q} := [\boldsymbol{Q}_{i,j}]_{(i,j)\in\mathcal{I}\times\mathcal{J}} \in \mathbb{C}^{(N_t N)\times(KN_t)}$ is the collection of all covariance matrices, while $\boldsymbol{V} := [\boldsymbol{V}_{i,j}]_{(i,j)\in\mathcal{I}\times\mathcal{J}} \in \mathbb{C}^{(N_t N)\times(dK)}$ is the collection of all precoding matrices. The multiple output $y_{i,j} \in \mathbb{C}^{N_r}$ at user (i, j) is the following combination of intra-cell and inter-cell signals and noise:

$$y_{i,j} = \sum_{k\in\mathcal{J}} \sqrt{\delta_{i,j}} h_{i,i,j} x_{i,k} + \sum_{m\in\mathcal{I}\setminus\{i\}} \sum_{k\in\mathcal{J}} \sqrt{\eta_{m,i,j}} h_{m,i,j} x_{m,k} + n_{i,j}. \tag{5.1}$$

Alternatively, each intended signal vectors $s_{i,j}$ can be linearly processed by its associated precoding matrix $\boldsymbol{V}_{i,j}$ before transmission, i.e. $x_{i,j} = \boldsymbol{V}_{i,j} s_{i,j}, \forall (i,j) \in \mathcal{I} \times \mathcal{J}$, so the output vector $y_{i,j}$ is also given as,

$$y_{i,j} = \sum_{k \in \mathcal{J}} \sqrt{\delta_{i,j}} h_{i,i,j} \boldsymbol{V}_{i,k} s_{i,k} + \sum_{m \in \mathcal{I} \setminus \{i\}} \sum_{k \in \mathcal{J}} \sqrt{\eta_{m,i,j}} h_{m,i,j} \boldsymbol{V}_{m,k} s_{m,k} + n_{i,j}. \tag{5.2}$$

In (5.1) and (5.2), $n_{i,j} \in \mathbb{C}^{N_r}$ and its entries are independent and identically distributed (i.i.d.) noise samples with zero-mean and variance σ^2. Each matrix $h_{m,i,j} \in \mathbb{C}^{N_r \times N_t}$ represents the normalized MIMO channel from BS m to user (i,j). Each scalar value $\delta_{i,j}$ represents the strength of the direct channel between BS i and its j-th user, whereas each $\eta_{m,i,j}$ $(m \neq i)$ indicates the strength of the interfering channel between BS m and the out-of-cell user (i,j) (i.e. $i \neq m$). Therefore, we can define the actual direct channels as $H_{i,i,j} := \sqrt{\delta_{i,i,j}} h_{i,i,j}$ $\forall (i,j) \in \mathcal{I} \times \mathcal{J}$, and the interfering channels as $H_{m,i,j} = \sqrt{\eta_{m,i,j}} h_{m,i,j}$ for $m \neq i$.

In (5.2), linear precoding matrices $\boldsymbol{V}$ are applied to the information signal vectors before transmission in order to maximize certain system performance measure. Whereas in (5.1), the same goal is realized by controlling the emitted signal vectors $x_{i,j}$ from the transmit antenna arrays.

It is particularly noted that the intended signal vector $s_{i,j}$ for user (i,j) is of dimension d, which represents the number of data symbols to be multiplexed. To avoid inter-symbol interference for reliable transmission, d must be no greater than $\min\{N_r, N_t\}$. More precisely, d is restrained by the number of non-zero singular values of each channel H [2, p.292]. Therefore, if $d = 1$ and $N_t > 1$, all the transmit antennas are used to beamform a single data symbol so the precoding matrices $\boldsymbol{V}$ are equivalently known as *beamforming vectors*. Further, in a MISO network with $1 \leq d \leq \min\{N_r, N_t\} = 1$, all precoding matrices are equivalently known as beamforming vectors. Finally, the precoding and covariance matrices are effectively reduced to the same scalar *power allocation* variables for SISO or SIMO networks with $N_t = 1$ [56].

The design of the covariance matrices for (5.1) [11, 153] and that of the precoding matrices for (5.2) [57, 149] have been the centre of research in recent years. They have be recognized as the most efficient ways to materialize the greatly enhanced capacity of MIMO interference channels. However, the encountered rate-oriented or power-critical problems [149] are normally very challenging so there is a significant shortage of effective yet efficient algorithms. In particular, we are interested in the sum rate and minimal rate maximization problems with power and/or cognitive constraints which aim at improving the overall rate performance or rate fairness, respectively. We shall address the optimization problems in both covariance and precoding matrix variables in the following sections.

5.3 A New Efficient Covariance Solution

Based on the signal model (5.1), let $\mathcal{M}_{i,j} \in \mathbb{C}^{N_r \times N_r}, \forall (i,j) \in \mathcal{I} \times \mathcal{J}$ denote the matrix of the received intra-cell and inter-cell interference at user (i,j) which is defined by

$$\mathcal{M}_{i,j}(\boldsymbol{Q}) := \sum_{(n,k)\in\mathcal{I}\times\mathcal{J}\setminus(i,j)} H_{n,i,j}\boldsymbol{Q}_{n,k}H_{n,i,j}^H.$$

Let $H_{0,i,r}$ denote the channel matrix from BS i to PU r and P_O the maximal acceptable interference allowed from SU to PU. The design covariance matrices are subject to a convex set defined by function constraints such as

$$\mathcal{W}_B = \{\boldsymbol{Q} : \sum_{j\in\mathcal{J}} \mathsf{trace}(\boldsymbol{Q}_{i,j}) \le P_B, i \in \mathcal{I}\}, \tag{5.3a}$$

$$\mathcal{W}_C = \{\boldsymbol{Q} : \sum_{(i,j)\in\mathcal{I}\times\mathcal{J}} \mathsf{trace}(H_{0,i,r}\boldsymbol{Q}_{i,j}H_{0,i,r}^H) \le P_O\}, \forall r \tag{5.3b}$$

which are called the BS transmit power limit and cognitive constraints, respectively.

For user (i,j), the achievable information rate (in nats) with respect to covariance matrices is

$$\boldsymbol{\nu}_{i,j}(\boldsymbol{Q}) = \log\det(\boldsymbol{I}_{N_r} + H_{i,i,j}\boldsymbol{Q}_{i,j}H_{i,i,j}^H(\mathcal{M}_{i,j}(\boldsymbol{Q}) + \sigma^2\boldsymbol{I}_{N_r})^{-1}).$$

We are concerned with the following sum rate or minimal rate maximization problem

$$\max_{\boldsymbol{Q}\in\mathcal{W}_B\cap\mathcal{W}_C\cap\mathcal{S}_+^{N_t}} \varphi(\boldsymbol{Q}), \tag{5.4}$$

where $\varphi(\boldsymbol{Q}) := \varphi^{\mathsf{S}}(\boldsymbol{Q}) \vee \varphi^{\mathsf{M}}(\boldsymbol{Q})$ represents either the sum rate function $\varphi^{\mathsf{S}}(\boldsymbol{Q})$ or the minimal rate function $\varphi^{\mathsf{M}}(\boldsymbol{Q})$ which is given respectively as

$$\begin{aligned} \varphi^{\mathsf{S}}(\boldsymbol{Q}) &= \sum_{(i,j)\in\mathcal{I}\times\mathcal{J}} \boldsymbol{\nu}_{i,j}(\boldsymbol{Q}), \\ \varphi^{\mathsf{M}}(\boldsymbol{Q}) &= \min_{(i,j)\in\mathcal{I}\times\mathcal{J}} \boldsymbol{\nu}_{i,j}(\boldsymbol{Q}). \end{aligned} \tag{5.5}$$

For sum rate and minimal rate maximization problems with respect to transmit covariance matrices (5.4), we now explore the partial concavities of the objective functions $\varphi(\boldsymbol{Q})$ which are very useful for the purpose of maximization. First, each rate function $\boldsymbol{\nu}_{i,j}(\boldsymbol{Q})$ in (5.4)/(5.5) is a difference of two concave functions (d.c.):

$$\boldsymbol{\nu}_{i,j}(\boldsymbol{Q}) = g_{i,j}(\boldsymbol{Q}) - f_{i,j}(\boldsymbol{Q})$$

with concave functions [116, p. 405]

$$\begin{aligned} g_{i,j}(\boldsymbol{Q}) &:= \log\det(\mathcal{M}_{i,j}(\boldsymbol{Q}) + H_{i,i,j}\boldsymbol{Q}_{i,j}H_{i,i,j}^H + \sigma^2\boldsymbol{I}_{N_r}), \\ f_{i,j}(\boldsymbol{Q}) &:= \log\det(\mathcal{M}_{i,j}(\boldsymbol{Q}) + \sigma^2\boldsymbol{I}_{N_r}). \end{aligned}$$

Using the properties of d.c. functions outlined in Theorem. 2.11 which is originated from [16, 17], one has the following d.c. representations:

- For the sum rate problem, $\varphi^{\mathsf{S}}(\boldsymbol{Q}) = \sum_{(i,j)\in\mathcal{I}\times\mathcal{J}} \boldsymbol{\nu}_{i,j}(\boldsymbol{Q}) = G^s(\boldsymbol{Q}) - F(\boldsymbol{Q})$, with concave functions

$$\begin{aligned} G^{\mathsf{S}}(\boldsymbol{Q}) &:= \sum_{(i,j)\in\mathcal{I}\times\mathcal{J}} g_{i,j}(\boldsymbol{Q}), \\ F(\boldsymbol{Q}) &:= \sum_{(i,j)\in\mathcal{I}\times\mathcal{J}} f_{i,j}(\boldsymbol{Q}). \end{aligned}$$

- For the minimal rate problem, $\varphi^{\mathsf{M}}(\boldsymbol{Q}) = \min_{(i,j)\in\mathcal{I}\times\mathcal{J}} \boldsymbol{\nu}_{i,j}(\boldsymbol{Q}) = G^{\mathsf{M}}(\boldsymbol{Q}) - F(\boldsymbol{Q})$, where $F(\boldsymbol{Q})$ is defined as above, and $G^{\mathsf{M}}(\boldsymbol{Q})$ is the following concave function

$$G^{\mathsf{M}}(\boldsymbol{Q}) := \min_{(i,j)\in\mathcal{I}\times\mathcal{J}} \big[g_{i,j}(\boldsymbol{Q}) + \sum_{(n,k)\in\mathcal{I}\times\mathcal{J}\setminus(i,j)} f_{n,k}(\boldsymbol{Q})\big].$$

Based on the above decompositions, we obtain the following results:

Theorem 3. *For* $G(\boldsymbol{Q}) = G^{\mathsf{S}}(\boldsymbol{Q}) \vee G^{\mathsf{M}}(\boldsymbol{Q})$, *problem* (5.4) *is the following convex constrained d.c. function maximisation:*

$$\max_{\boldsymbol{Q}} \; [G(\boldsymbol{Q}) - F(\boldsymbol{Q})] : \; \boldsymbol{Q} \in \mathcal{W}_B \cap \mathcal{W}_C \cap \mathcal{S}_+^{N_t}. \tag{5.6}$$

Essentially, the above maximization of the difference of concave functions in (5.6) can be converted to minimization of the difference of convex functions as in (2.5)/(2.11). Therefore, the d.c.-based (difference of convex functions) iterative algorithms developed in Chapter 2 can be applied to (5.6). Nevertheless, we now derive a generic algorithm based on maximization of a d.c. function (difference of concave functions) over convex sets. This may pave ways for developing Frank-and-Wolf type of algorithms which are generally less computationally demanding [10, 162].

It is clear that (5.6) belongs to the following canonical d.c. programming (difference of concave functions) [16]

$$\max_{\boldsymbol{z}\in\mathcal{D}} \mathcal{G}(\boldsymbol{z}) := G(\boldsymbol{z}) - F(\boldsymbol{z}), \tag{5.7}$$

where $\mathcal{D}$ is a compact convex set in a finite dimensional space, while G and F are concave functions with F smooth. Suppose that $z^{(\kappa)}$ is feasible to (5.7). Since F is concave, its gradient $\nabla F(z^{(\kappa)})$ at $z^{(\kappa)}$ is also a super-gradient [16]. Therefore,

$$G(\boldsymbol{z}) - F(\boldsymbol{z}) \geq G(\boldsymbol{z}) - F(z^{(\kappa)}) - \langle \nabla F(z^{(\kappa)}), \boldsymbol{z} - z^{(\kappa)} \rangle \quad \forall \boldsymbol{z}.$$

It follows that for any feasible $z^{(\kappa)}$ to (5.7), the following convex program provides a global lower bound maximisation for d.c. program (5.7):

$$\max_{\boldsymbol{z}\in\mathcal{D}} [G(\boldsymbol{z}) - F(z^{(\kappa)}) - \langle \nabla F(z^{(\kappa)}), \boldsymbol{z} - z^{(\kappa)}\rangle]. \tag{5.8}$$

Moreover, for the optimal solution $z^{(\kappa+1)}$ of (5.8), one has

$$\begin{aligned} G(z^{(\kappa+1)}) - F(z^{(\kappa+1)}) &\geq G(z^{(\kappa+1)}) - F(z^{(\kappa)}) - \langle \nabla F(z^{(\kappa)}), z^{(\kappa+1)} - z^{(\kappa)}\rangle \\ &\geq G(z^{(\kappa)}) - F(z^{(\kappa)}) - \langle \nabla F(z^{(\kappa)}), z^{(\kappa)} - z^{(\kappa)}\rangle \\ &= G(z^{(\kappa)}) - F(z^{(\kappa)}), \end{aligned}$$

which means that $\mathcal{G}(z^{(\kappa+1)}) > \mathcal{G}(z^{(\kappa)})$, i.e., $z^{(\kappa+1)}$ is better than $z^{(\kappa)}$ toward optimizing (5.7) as long as $z^{(\kappa+1)} \neq z^{(\kappa)}$. Thus, initialized from a feasible $z^{(0)} \in \mathcal{D}$, recursively generating $z^{(\kappa+1)}$ for $\kappa = 0, 1, \ldots$, by the optimal solution of convex program (5.8) is a path-following procedure, which converges to at least a local optimal solution of (5.7) satisfying the first optimality principle.

To summarize, a d.c. procedure for the generic d.c. program (5.7) is sketched below.

D.C. Iterations (DCIs):

- *Initialisation:* Choose an initial feasible solution $z^{(0)} \in \mathcal{D}$ of (5.7).
- *κ-th DC iteration (κ-DCI):* Solve convex program (5.8) to obtain the optimal solution z^* and set $\kappa \to \kappa + 1$, $z^{(\kappa)} \to z^*$. Given a tolerance level $\epsilon > 0$, stop if

$$|\mathcal{G}(z^{(\kappa)}) - \mathcal{G}(z^{(\kappa-1)})|/|\mathcal{G}(z^{(\kappa-1)})| \leq \epsilon. \tag{5.9}$$

Our previous works [56, 92, 137, 164, 165] demonstrated successful applications of the above DCIs to various non-convex optimization problems. The reader is also referred to [12] for a new observation on its efficiency. In particular, the incumbent $z^{(\kappa+1)}$ is in fact the optimal solution of the following program:

$$\max_{(\boldsymbol{z},\boldsymbol{x})\in\mathcal{D}} \mathcal{G}_\kappa(\boldsymbol{z}) := G(\boldsymbol{z}) - \min_{\nu=0,1,\ldots,\kappa} \{F(z^{(\nu)}) + \langle\nabla F(z^{(\nu)}), \boldsymbol{z} - z^{(\nu)}\rangle\}. \tag{5.10}$$

It is obvious that $\mathcal{G}(\boldsymbol{z}) \geq \mathcal{G}_{\kappa+1}(\boldsymbol{z}) \geq \mathcal{G}_\kappa(\boldsymbol{z}) \geq \ldots \geq \mathcal{G}_0(\boldsymbol{z}),\ \forall\ \boldsymbol{z} \in \mathcal{D}$, so concave functions $\mathcal{G}_\kappa$ are iteratively better global approximations of d.c function $\mathcal{G}$. Consequently, DCIs by (5.8) not only generate improved solutions but also provide successively better convexifications for d.c. program (5.7).

Now, it is pointed out that (5.6) belongs to the canonical d.c. programming (5.7). In particular, (5.6) is (5.7) with $\boldsymbol{z} \rightarrow \boldsymbol{Q}$, $G(\boldsymbol{z}) \rightarrow G(\boldsymbol{Q})$, $F(\boldsymbol{z}) \rightarrow F(\boldsymbol{Q})$ which is a smooth function and the convex set $\mathcal{D} \rightarrow \mathcal{W}_B \cap \mathcal{W}_C \cap \mathcal{S}_+^{N_t}$. Therefore, (5.6) can be solved by the DCIs described above. The gradients $\langle\nabla F(Q^{(\kappa)}), \boldsymbol{Q} - Q^{(\kappa)}\rangle$ or $\langle\nabla f^{\mathsf{p}}(Q^{\mathsf{p}(\kappa)}), \boldsymbol{Q}^{\mathsf{p}} - Q^{\mathsf{p}(\kappa)}\rangle$ in implementing $(\kappa+1)$th-DCI (5.8) can be easily calculated based on Equation (B.1) given in Appendix B.

Finally, our approach toward finding the solutions of sum rate and minimal rate optimization problems (5.4)/(5.6) is as follows.

- Choose an initial feasible solution $Q^{(0)}$ of the coordinated covariance matrix problems (5.4);
- Use DCIs to find optimized solution Q of (5.4)/(5.6).

Remarkably, we have also particularly studied the covariance matrix design for a simpler MISO case where the MTs are each equipped with a single antenna. In Appendix D, we shall propose the Frank-and-Wolf type of algorithm for sum rate optimization with BS power, cognitive, and individual QoS constraints. The presented research in Appendix D is currently under submission.

5.4 A New Efficient Precoding Solution

Now, we shift our focus onto the design of precoding/beamforming matrices for optimization problems.

Denote the received interference matrix with respect to precoding matrices at user (i,j) as

$$\mathcal{M}_{i,j}(\boldsymbol{V}) := \sum_{(n,k)\in\mathcal{I}\times\mathcal{J}\setminus(i,j)} H_{n,i,j}\boldsymbol{V}_{n,k}\boldsymbol{V}_{n,k}^H H_{n,i,,j}^H.$$

Similar to the above section, the design precoding matrix variables are also subject to realistic BS power, and cognitive constraints which are defined by

$$\mathcal{V}_B = \{\boldsymbol{V} : \sum_{j\in\mathcal{J}} \mathsf{trace}(\boldsymbol{V}_{i,j}\boldsymbol{V}_{i,j}^H) \le P_B, i\in\mathcal{I}\}, \tag{5.11a}$$

$$\mathcal{V}_C = \{\boldsymbol{V} : \sum_{(i,j)\in\mathcal{I}\times\mathcal{J}} \mathsf{trace}(H_{0,i,r}\boldsymbol{V}_{i,j}\boldsymbol{V}_{i,j}^H H_{0,i,r}^H) \le P_O\}, \forall r. \tag{5.11b}$$

It is noted that the above constraints are convex.

The achievable information rate (in nats) at user (i,j) can be expressed by

$$\boldsymbol{\nu}_{i,j}(\boldsymbol{V}) = \log\det(\boldsymbol{I}_d + \boldsymbol{V}_{i,j}^H H_{i,i,j}^H(\mathcal{M}_{i,j}(\boldsymbol{V}) + \sigma^2\boldsymbol{I}_{N_r})^{-1}H_{i,i,j}\boldsymbol{V}_{i,j}).$$

Therefore, the concerned sum rate and minimal rate maximization problems can be universally formulated as

$$\max_{\boldsymbol{V}\in\mathcal{V}_B\cap\mathcal{V}_C} \varphi(\boldsymbol{V}), \tag{5.12}$$

where $\varphi(\boldsymbol{V}) := \varphi^{\mathsf{S}}(\boldsymbol{V}) \vee \varphi^{\mathsf{M}}(\boldsymbol{V})$ with the respective sum rate and minimal rate functions in precoding matrix variables defined by

$$\begin{aligned} \varphi^{\mathsf{S}}(\boldsymbol{V}) &= \sum_{(i,j)\in\mathcal{I}\times\mathcal{J}} \boldsymbol{\nu}_{i,j}(\boldsymbol{V}), \\ \varphi^{\mathsf{M}}(\boldsymbol{V}) &= \min_{(i,j)\in\mathcal{I}\times\mathcal{J}} \boldsymbol{\nu}_{i,j}(\boldsymbol{V}). \end{aligned} \tag{5.13}$$

In what follows, we shall exploit explicit d.c. structure of the objective rate functions and develop accordingly efficient algorithms.

First, introduce matrix variables $\boldsymbol{Y} := [\boldsymbol{Y}_{i,j}]_{(i,j)\in\mathcal{I}\times\mathcal{J}} \in \mathbb{C}^{N_rN\times N_rK}$ which satisfy the following matrix inequality constraints

$$\mathcal{M}_{i,j}(\boldsymbol{V}) \leq \boldsymbol{Y}_{i,j},\ \forall(i,j)\in\mathcal{I}\times\mathcal{J}. \tag{5.14}$$

Theorem 5.1. *The sum rate or minimal rate maximization program (5.12) is equivalent to the following program in the sense that they share the same values at optimal solution V^* and (V^*, Y^*) with $Y^*_{i,j} = \mathcal{M}_{i,j}(V)$, respectively .*

$$\max_{\boldsymbol{Y},\boldsymbol{V}\in\mathcal{V}_B\cap\mathcal{V}_C} \phi(\boldsymbol{V},\boldsymbol{Y}) \ :\ (5.14), \tag{5.15}$$

where

$$\begin{aligned} \phi(\boldsymbol{V},\boldsymbol{Y}) &:= \phi^{\mathsf{S}}(\boldsymbol{V},\boldsymbol{Y}) \vee \phi^{\mathsf{M}}(\boldsymbol{V},\boldsymbol{Y}), \\ \phi^{\mathsf{S}}(\boldsymbol{V},\boldsymbol{Y}) &:= \sum_{(i,j)\in\mathcal{I}\times\mathcal{J}} \psi_{i,j}(\boldsymbol{V},\boldsymbol{Y}), \\ \phi^{\mathsf{M}}(\boldsymbol{V},\boldsymbol{Y}) &:= \min_{(i,j)\in\mathcal{I}\times\mathcal{J}} \psi_{i,j}(\boldsymbol{V},\boldsymbol{Y}), \end{aligned} \tag{5.16}$$

with

$$\psi_{i,j}(\boldsymbol{V},\boldsymbol{Y}) := \log\det(\boldsymbol{I}_d + \boldsymbol{V}^H_{i,j}H^H_{i,i,j}(\boldsymbol{Y}_{i,j}+\sigma^2\boldsymbol{I}_{N_r})^{-1}H_{i,i,j}\boldsymbol{V}_{i,j}) \tag{5.17}$$

Proof: Each feasible $(\bar{V},\bar{Y})$ to (5.15) makes $\bar{V}$ feasible to (5.12) with $\psi_{i,j}(\bar{V},\bar{Y}) \leq \boldsymbol{\nu}_{i,j}(\bar{V})$, $\forall(i,j)\in\mathcal{I}\times\mathcal{J}$ and thus $\phi(\bar{V},\bar{Y}) \leq \varphi(\bar{V})$ so max (5.15) $\leq$ max (5.12). On the other hand, each feasible $\bar{V}$ to (5.12) makes $(\bar{V},\bar{Y})$ feasible to (5.15) with $\bar{Y}_{i,j} = \mathcal{M}_{i,j}(\bar{V})$, $\forall(i,j)\in\mathcal{I}\times\mathcal{J}$, $\psi_{i,j}(\bar{V},\bar{Y}) = \boldsymbol{\nu}_{i,j}(\bar{V})$, $\forall(i,j)\in\mathcal{I}\times\mathcal{J}$ and thus $\varphi(\bar{V}) = \phi(\bar{V},\bar{Y})$. Therefore, max (5.12) $\leq$ max (5.15). □

Next, Lemma 4 shows that each atomic function $\psi_{i,j}(\boldsymbol{V},\boldsymbol{Y}), \forall(i,j)\in\mathcal{I}\times\mathcal{J}$ is in fact a d.c. (difference of convex functions) function.

Lemma 4. The functions

$$\begin{aligned} g_{i,j}(\boldsymbol{V},\boldsymbol{Y}) &= \mathsf{trace}(\boldsymbol{V}_{i,j}^H H_{i,i,j}^H(\boldsymbol{Y}_{i,j}+\sigma^2\boldsymbol{I}_{N_r})^{-1}H_{i,i,j}\boldsymbol{V}_{i,j}) \\ f_{i,j}(\boldsymbol{V},\boldsymbol{Y}) &= \mathsf{trace}(\boldsymbol{V}_{i,j}^H H_{i,i,j}^H(\boldsymbol{Y}_{i,j}+\sigma^2\boldsymbol{I}_{N_r})^{-1}H_{i,i,j}\boldsymbol{V}_{i,j}) \\ &\quad -\log\det(\boldsymbol{I}_d+\boldsymbol{V}_{i,j}^H H_{i,i,j}^H(\boldsymbol{Y}_{i,j}+\sigma^2\boldsymbol{I}_{N_r})^{-1}H_{i,i,j}\boldsymbol{V}_{i,j}). \end{aligned}$$

are convex in $(\boldsymbol{V},\boldsymbol{Y})$ and each function $\psi_{i,j}(\boldsymbol{V},\boldsymbol{Y})$, $\forall(i,j)\in\mathcal{I}\times\mathcal{J}$ admits the following d.c. decomposition

$$\psi_{i,j}(\boldsymbol{V},\boldsymbol{Y}) = g_{i,j}(\boldsymbol{V},\boldsymbol{Y}) - f_{i,j}(\boldsymbol{V},\boldsymbol{Y})$$

Proof: The convexity proof for functions $g_{i,j}(\boldsymbol{V},\boldsymbol{Y})$, $\forall(i,j)\in\mathcal{I}\times\mathcal{J}$ can be found in [28, Appendix C]. Since $\boldsymbol{V}_{i,j}^H H_{i,i,j}^H(\boldsymbol{Y}_{i,j}+\sigma^2\boldsymbol{I}_{N_r})^{-1}H_{i,i,j}\boldsymbol{V}_{i,j}$ is positive definite, from [116, Th.7.6.6], function $\log\det(\boldsymbol{I}_d+\boldsymbol{V}_{i,j}^H H_{i,i,j}^H(\boldsymbol{Y}_{i,j}+\sigma^2\boldsymbol{I}_{N_r})^{-1}H_{i,i,j}\boldsymbol{V}_{i,j})$ is concave. So, function $f_{i,j}(\boldsymbol{V},\boldsymbol{Y})$ is convex. □

Lemma 5. (Convex and monotonic function) Define function

$$\chi(\boldsymbol{S}) := \langle \boldsymbol{S}\rangle - \ln|\boldsymbol{I}_{N_r}+\boldsymbol{S}|.$$

Function χ is convex and monotonic in the sense that

$$\chi(\boldsymbol{S}_1)\le\chi(\boldsymbol{S}_2)\ \ \forall\ \ \boldsymbol{S}_2\succeq\boldsymbol{S}_1\succeq 0.$$

Proof: It is obvious that function χ is convex because $\langle\boldsymbol{S}\rangle$ is linear and $-\ln|\boldsymbol{I}_{N_r}+\boldsymbol{S}|$ is convex. Note that

$$\frac{d}{d\boldsymbol{S}}\chi(\boldsymbol{S}) = \boldsymbol{I}_{N_r} - (\boldsymbol{I}_{N_r}+\boldsymbol{S})^{-1} \succeq \boldsymbol{I}_{N_r} - (\boldsymbol{I}_{N_r})^{-1} = 0,\ \forall\ \boldsymbol{S}\succeq 0.$$

Thus, by the average value theorem

$$\chi(S_2)-\chi(S_1) = \langle\frac{d}{d\boldsymbol{S}}\chi(S^*), S_2-S_1\rangle = \langle\boldsymbol{I}_{N_r}-(\boldsymbol{I}_{N_r}+S^*)^{-1}, S_2-S_1\rangle \ge 0,\ \ \forall\ \ S_2\succeq S_1\succeq 0,$$

where $S^* = \lambda S_1 + (1-\lambda)S_2$ for some $\lambda \in [0,1]$. □

Although functions $g_{i,j}(\boldsymbol{V},\boldsymbol{Y})$ and $f_{i,j}(\boldsymbol{V},\boldsymbol{Y})$ $\forall (i,j) \in \mathcal{I} \times \mathcal{J}$ are convex, the optimization programs are still untractable with existing convex program solvers [80].

Lemma 6. (Convex function and self-concordant variational representation) Function

$$\Psi(\boldsymbol{V}) := \langle \Omega(\boldsymbol{V}) \rangle - \ln |\boldsymbol{I}_{N_r} + \Omega(\boldsymbol{V})|$$

is convex in matrix variable $\boldsymbol{V}$ for convex function $\Omega(\boldsymbol{V})$ with the following variational representation

$$\Psi(\boldsymbol{V}) = \min_{\Omega(\boldsymbol{V}) \preceq \boldsymbol{T}} \left[\langle \boldsymbol{T} \rangle - \ln |\boldsymbol{I}_{N_r} + \boldsymbol{T}| \right]. \tag{5.18}$$

Proof: Note that $\Psi(\boldsymbol{V}) = \chi(\Omega(\boldsymbol{V}))$. Using Lemma 5, whenever $\lambda \in [0,1]$, it is true that

$$\begin{aligned}
\Psi(\lambda \boldsymbol{V}^1 + (1-\lambda)\boldsymbol{V}^2) &= \chi(\Omega(\lambda \boldsymbol{V}^1 + (1-\lambda)\boldsymbol{V}^2)) \\
&\leq \chi(\lambda \Omega(\boldsymbol{V}^1) + (1-\lambda)\Omega(\boldsymbol{V}^2))) \\
&\leq \lambda \chi(\Omega(\boldsymbol{V}^1)) + (1-\lambda)\chi(\Omega(\boldsymbol{V}^2)) \\
&= \lambda \Psi(\boldsymbol{V}^1) + (1-\lambda)\Psi(\boldsymbol{V}^2),
\end{aligned}$$

which shows the convexity of Ψ.

Next, the representation (5.18) follows from Lemma 5. □

Therefore, we are in a position to develop a self-concordant variational representation of (5.12).

Lemma 7. Introduce matrix variables $\boldsymbol{T} := [\boldsymbol{T}_{ij} \in \mathbb{C}^{d \times d}]_{(i,j) \in \mathcal{I} \times \mathcal{J}}$ satisfying

$$\boldsymbol{V}_{i,j}^H H_{i,i,j}^H (\boldsymbol{Y}_{i,j} + \sigma^2 \boldsymbol{I}_{N_r})^{-1} H_{i,i,j} \boldsymbol{V}_{i,j} \preceq \boldsymbol{T}_{i,j}, \ \forall (i,j) \in \mathcal{I} \times \mathcal{J}, \tag{5.19}$$

which can be re-expressed by the following LMIs using Schur Complement,

$$\begin{bmatrix} \boldsymbol{T}_{i,j} & \boldsymbol{V}_{i,j}^H H_{i,i,j}^H \\ H_{i,i,j} \boldsymbol{V}_{i,j} & \boldsymbol{Y}_{i,j} + \sigma \boldsymbol{I}_{N_r} \end{bmatrix} \succeq 0, \forall (i,j) \in \mathcal{I} \times \mathcal{J}. \tag{5.20}$$

The program (5.15) is equivalent to the following:

$$-\min_{\boldsymbol{Y},\boldsymbol{T},\boldsymbol{V}\in\mathcal{V}_B\cap\mathcal{V}_C}\left[F(\boldsymbol{T})-G(\boldsymbol{V},\boldsymbol{Y})\right]\ :\ (5.14),(5.20), \tag{5.21}$$

where $F(\boldsymbol{T}) := F^{\mathsf{S}}(\boldsymbol{T}) \vee F^{\mathsf{M}}(\boldsymbol{T})$ with convex functions

$$\begin{aligned} F^{\mathsf{S}}(\boldsymbol{T}) &= \sum_{(m,n)\in\mathcal{I}\times\mathcal{J}}\left[\mathsf{trace}(\boldsymbol{T}_{m,n})-\log\det(\boldsymbol{I}_d+\boldsymbol{T}_{m,n})\right] \\ F^{\mathsf{M}}(\boldsymbol{T}) &= \max_{(i,j)\in\mathcal{I}\times\mathcal{J}}\Big[\sum_{(m,n)\in\mathcal{I}\times\mathcal{J}}\mathsf{trace}(\boldsymbol{T}_{m,n})-\log\det(\boldsymbol{I}_d+\boldsymbol{T}_{i,j})\Big], \end{aligned} \tag{5.22}$$

and

$$G(\boldsymbol{V},\boldsymbol{Y}) = \sum_{(m,n)\in\mathcal{I}\times\mathcal{J}} g_{m,n}(\boldsymbol{V},\boldsymbol{Y}). \tag{5.23}$$

Proof: The proof follows from the proofs for Lemma 4, Lemma 5 and Lemma 6. □

It is apparent that (5.21) belongs to the canonical d.c. programming (2.5) defined in Chapter 2. In particular, (5.21) is (2.5) with $\boldsymbol{z} \to (\boldsymbol{V},\boldsymbol{Y},\boldsymbol{T})$, $f(\boldsymbol{z}) \to F(\boldsymbol{T})$ which is a convex, and $g(\boldsymbol{z}) \to G(\boldsymbol{V},\boldsymbol{Y})$ which is convex and smooth. The convex set $\mathcal{K}$ is defined by constraints (5.11) (i.e. $\mathcal{V}_B\cap\mathcal{V}_C$), (5.14), and (5.20).

Therefore, (5.21) can be solved by κ-th d.c. iteration program (2.6). The gradient of function $G(\boldsymbol{V},\boldsymbol{Y})$ at (V^{κ},Y^{κ}) for implementing $(\kappa+1)$th-DCI (2.6) can be easily calculated as

$$\begin{aligned} &\langle\nabla G(V^{(\kappa)},Y^{(\kappa)}),(\boldsymbol{V},\boldsymbol{Y})-(V^{(\kappa)},Y^{(\kappa)})\rangle \\ =&\sum_{i,j}\Big\{2.\mathsf{Re}\big[\langle V_{i,j}^{\kappa H}H_{i,i,j}^{H}(Y_{i,j}^{\kappa}+\sigma^2\boldsymbol{I})^{-1}H_{i,i,j}(\boldsymbol{V}_{i,j}-V_{i,j}^{\kappa})\rangle\big] \\ &-\langle V_{i,j}^{\kappa H}H_{i,i,j}^{H}(Y_{i,j}^{\kappa}+\sigma^2\boldsymbol{I})^{-1}(\boldsymbol{Y}_{i,j}-Y_{i,j}^{\kappa})(Y_{i,j}^{\kappa}+\sigma^2\boldsymbol{I})^{-1}H_{i,i,j}V_{i,j}^{\kappa}\rangle\Big\}. \end{aligned}$$

Remark. The precoding matrix design problem turns to beamforming vectors design ($\boldsymbol{w} := [\boldsymbol{w}_{i,j}\in\mathbb{C}^{N_t\times d}]_{(i,j)\in\mathcal{I}\times\mathcal{J}}, d=1$) problem for MISO networks. Now, we will briefly analyze the beamforming design problems in the MISO networks. First, consider the following power minimization problems subject to SINR constraints

$$\min_{\boldsymbol{w}} \quad p(\boldsymbol{w}), \tag{5.24a}$$

$$\text{s.t.} \quad \frac{|\langle \boldsymbol{w}_{i,j}, H^H_{i,i,j}\rangle|^2}{\sum_{(n,k)\in\mathcal{I}\times\mathcal{J}\setminus(i,j)} |\langle \boldsymbol{w}_{n,k}, H^H_{n,i,j}\rangle|^2} \geq \gamma_{i,j}, \tag{5.24b}$$

where $\gamma_{i,j}$ is the target SINR for MT-(i,j), $p(\boldsymbol{w}) = p^t(\boldsymbol{w}) \vee p^i(\boldsymbol{w})$ with total transmit power function defined as

$$p^t(\boldsymbol{w}) := \sum_{(i,j)\in\mathcal{I}\times\mathcal{J}} ||\boldsymbol{w}_{i,j}||^2,$$

and the maximal individual power function defined as

$$p^i(\boldsymbol{w}) := \max_{(i,j)\in\mathcal{I}\times\mathcal{J}} ||\boldsymbol{w}_{i,j}||^2.$$

Other power functions may also be considered.

Introduce matrix variables $\boldsymbol{W}_{i,j} := \boldsymbol{w}_{i,j}\boldsymbol{w}^H_{i,j}, \forall(i,j) \in \mathcal{I}\times\mathcal{J}$ and define $\boldsymbol{W} := [\boldsymbol{W}_{i,j}]_{(i,j)\in\mathcal{I}\times\mathcal{J}}$. It is true that

$$\begin{aligned} p^t(\boldsymbol{w}) &= p^t(\boldsymbol{W}) := \sum_{(i,j)\in\mathcal{I}\times\mathcal{J}} \langle \boldsymbol{W}_{i,j}\rangle, \\ p^i(\boldsymbol{w}) &= p^i(\boldsymbol{W}) := \max_{(i,j)\in\mathcal{I}\times\mathcal{J}} \langle \boldsymbol{W}_{i,j}\rangle. \end{aligned}$$

Thus, the problem (5.24) is equivalent to the following program

$$\min_{\boldsymbol{W}} \quad p(\boldsymbol{W}), \tag{5.25a}$$

$$\text{s.t.} \quad \frac{\langle \boldsymbol{W}_{i,j}, H^H_{i,i,j}H_{i,i,j}\rangle}{\sum_{(n,k)\in\mathcal{I}\times\mathcal{J}\setminus(i,j)} \langle \boldsymbol{W}_{n,k}, H^H_{n,i,j}H_{n,i,j}\rangle} \geq \gamma_{i,j}, \tag{5.25b}$$

$$\boldsymbol{W}_{i,j} \in \mathcal{S}^{N_t}_+, \text{Rank}(\boldsymbol{W}_{i,j}) = 1, \ \forall(i,j) \in \mathcal{I}\times\mathcal{J}. \tag{5.25c}$$

Intuitively, the rank-one constraints (5.25c) render program (5.25) a very hard rank-constrained program. However, as proved by [13, 155], the relaxed program (5.25a-5.25b) will always output rank-one solutions. Thus, problems (5.24) can be equivalently solved by solving the relaxed program (5.25a-5.25b) which is a SDP. Moreover, it is worth pointing out that problems (5.24) can also be solved directly in beamforming vectors since they can be expressed as SOCP programs [149]. Based on these important observations, we can see that the minimal rate optimization problem (5.12) with $\boldsymbol{V}_{i,j} \to \boldsymbol{w}_{i,j}$, $\forall(i,j) \in \mathcal{I} \times \mathcal{J}$ and $\varphi(\boldsymbol{V}) \to \varphi^{\mathsf{M}}(\boldsymbol{w})$ subject to various power and cognitive constraints is in fact a quasi-convex program. Therefore, the minimal rate maximization subject to power constraints can be converted into the following program

$$\max_{\boldsymbol{t},\boldsymbol{W}} \quad \boldsymbol{t}, \tag{5.26a}$$

$$\text{s.t.} \quad \frac{\langle \boldsymbol{W}_{i,j}, H_{i,i,j}^H H_{i,i,j} \rangle}{\sum_{(n,k)\in\mathcal{I}\times\mathcal{J}\setminus(i,j)} \langle \boldsymbol{W}_{n,k}, H_{n,i,j}^H H_{n,i,j} \rangle} \geq \boldsymbol{t}, \tag{5.26b}$$

$$\boldsymbol{W} \in \mathcal{W}_B \cap \mathcal{W}_C \cap \mathcal{S}_+^{N_t}. \tag{5.26c}$$

Obviously, (5.26) can be solved by a bisection procedure in the variable $\boldsymbol{t}$.

Nevertheless, the sum rate maximization problem (5.12) with $\boldsymbol{V}_{i,j} \to \boldsymbol{w}_{i,j}$, $\forall(i,j) \in \mathcal{I} \times \mathcal{J}$ and $\varphi(\boldsymbol{V}) \to \varphi^{\mathsf{S}}(\boldsymbol{w})$ for MISO netowrk still remains non-convex and thus very challenging. So far, in [11], the authors have proposed global optimal algorithms which are prohibitively computationally demanding. The authors in [57] proposed WMMSE-based algorithms which is relatively well-performing. Cyclic optimization methods have been proposed in [163]. In addition, gradient projection-based algorithms or game theory-based algorithms have also been reviewed in [153] but none perform really well. In [10], we particularly analyzed this challenging sum rate optimization problem, and proposed tailored DCI-based algorithm to address it. The algorithm was shown to outperform its counterparts with relatively low computational demands.

5.5 Numerical Results

In this section, Monte Carlo simulation is presented to evaluate covariance and precoding performance of multi-cell multi-user MIMO networks. As illustrated in Figure 5.1, each network realization consists of $N = 3$ base-stations each serving $K = 2$ mobile terminals which are randomly located within their respective hexagonal cells. The distance between any two BSs is fixed at 1.4 km. Each BS is equipped with $N_t = 4$ transmit antennas while each MT with $N_t = 2$ receive antennas. There is one 2-antenna PU randomly located within any of the 3 cells. For each random network realization, the BS-to-MT ($H_{n,i,j}$) and the BS-to-PU ($H_{0,i,1}$) channels are generated based on the relative distance (denoted as D km) between any transmit antenna and receive antenna. More specifically, the channel is generated based on the typical parameters [9, 13, 75] as listed in Table 5.1. The tolerance $\epsilon = 10^{-5}$ is set in all simulations.

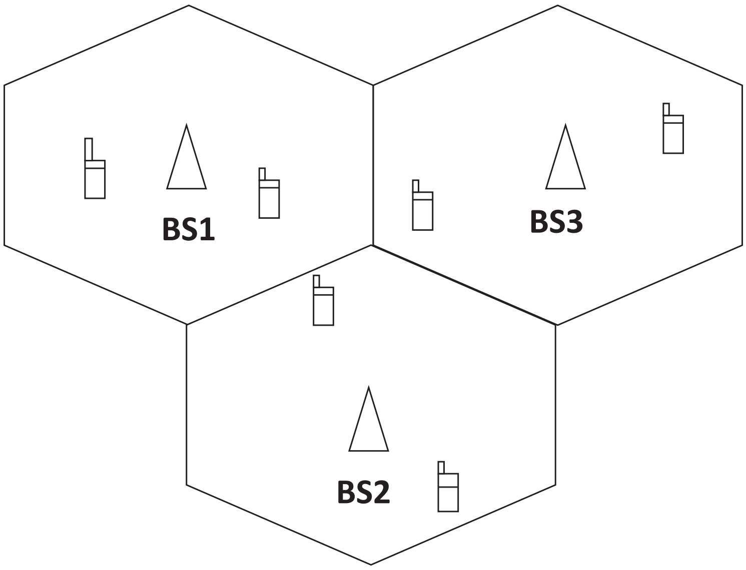

FIGURE 5.1: Illustration of networks $(M, N, N_t, N_r) = (3, 2, 4, 2)$.

TABLE 5.1: Standard channel parameters

Noise PSD	-162 dBm/Hz
Path-loss model	$128.1 + 37.6 \log_{10}(d)$
Log-normal shadowing	8 dB
Antenna gain	15 dBi
Bandwidth	10^7 Hz
Rayleigh fading	Yes

As we have analyzed previously, the design in covariance matrices and the design in precoding matrices are two extremely related problems from an optimization perspective. For a network with N_t-antenna BSs and N_r-antenna MTs (assuming $N_r \leq N_t$), the relevance between the two depends on the number of columns of precoding matrices (d), i.e., the number of multiplexed symbols. The covariance design naturally serves as a rank-relaxed problem for the precoding matrix design problem if it is true that $d < N_t$. Conversely, any precoding problem is equivalent to the covariance problem if additional rank equality constraints $\text{Rank}(Q_{i,j}) = d$ are imposed on the covariance matrix variables. Moreover, the two are equivalent if $d = N_t$ in the sense that they always share the same optimal performance. In the case of beamforming ($d = 1$), the covariance matrix design is only equivalent to the beamforming (precoding with $d = 1$) design if the covariance matrices are forced to be rank-one. On the other hand, it is realized the optimal covariance matrices are not necessarily always full-rank. As shown in Figure 5.2 and Figure 5.3, the vast majority of the DCI covariance matrix solutions for both the sum rate and the minimal rate optimization problems are found not full-rank. In fact, over 90% of the covariance matrices are ranked no greater than 2. This means, in most of cases, the optimal rate performance by covariance matrices could very likely be attained by precoding matrices assuming $d = 2$ simultaneous data streams. This observation coincides with the basic fact that the actual number of simultaneous data streams should be no greater than $\min\{N_t, N_r\} = 2$ due to the limited dimensions offered by receive antennas. Otherwise, inter-symbol interference would occur.

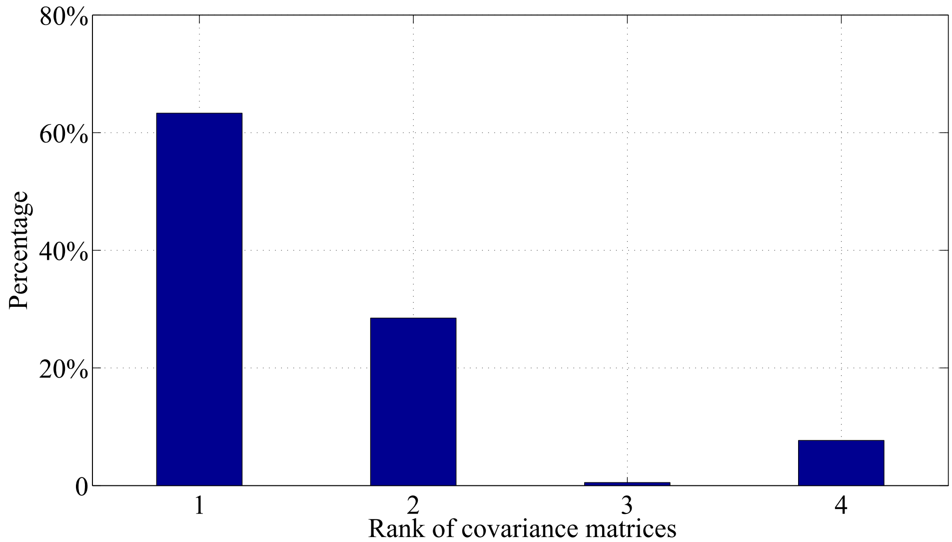

FIGURE 5.2: Min. rate: rank distribution of covariance matrices $(M, N, N_t, N_r) = (3, 2, 4, 2)$

Next, the rate performance of the proposed DCI algorithms is tested under various scenarios. In Figure 5.4 and Figure 5.5, the impacts of cognitive constraints on the minimal and sum rate performance are revealed, respectively. Subject to a tight cognitive constraint ($P_O = -110$ dBm),

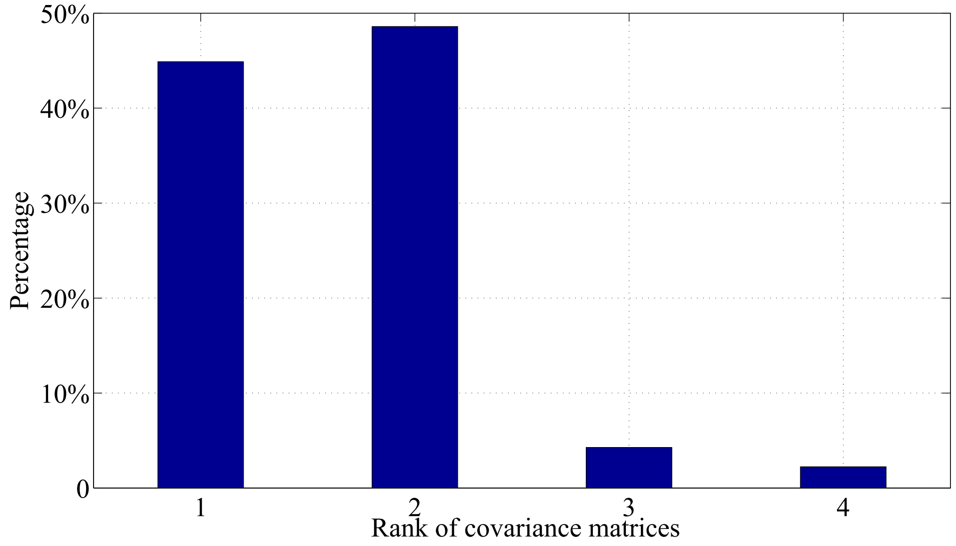

FIGURE 5.3: Sum rate: rank distribution of covariance matrices $(M, N, N_t, N_r) = (3, 2, 4, 2)$

the rates achieved by covariance or beamforming ($d = 1$) experience significant degradation as compared to that without any cognitive constraints ($P_O = +\infty$). Obviously, the achievable rate performance is compromised for satisfying the tight cognitive constraints. Meanwhile, the performance of covariance design constantly outperforms that of the beamforming design. Expectedly, however, the gap is relatively insignificant because most of covariance matrices are ranked no greater than 2. To demonstrate the effectiveness and efficiency of the proposed

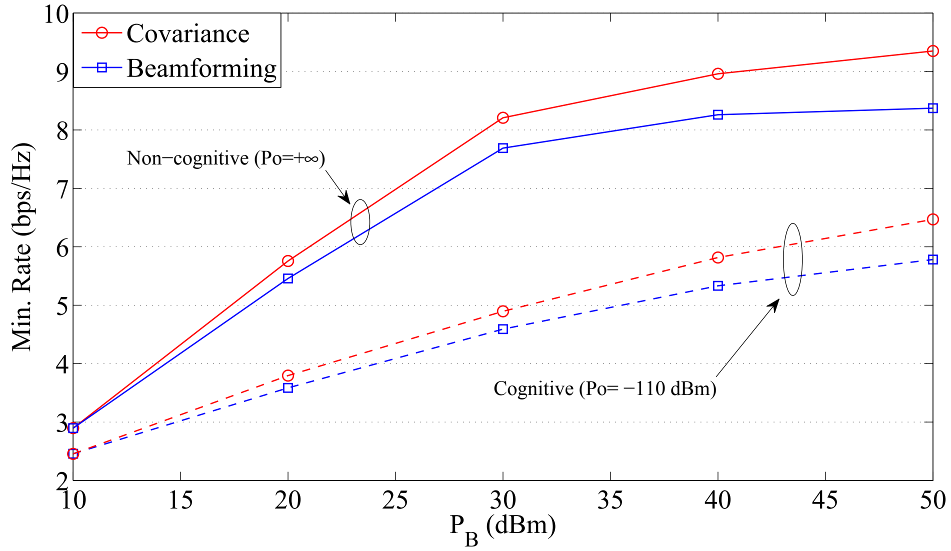

FIGURE 5.4: BS power limit vs. Min. rates $(M, N, N_t, N_r, d) = (3, 2, 4, 2, 1)$. $P_O = -110$ dBm for coginitive constraints.

algorithm in various scenarios, we also present numerous simulation results and convergence

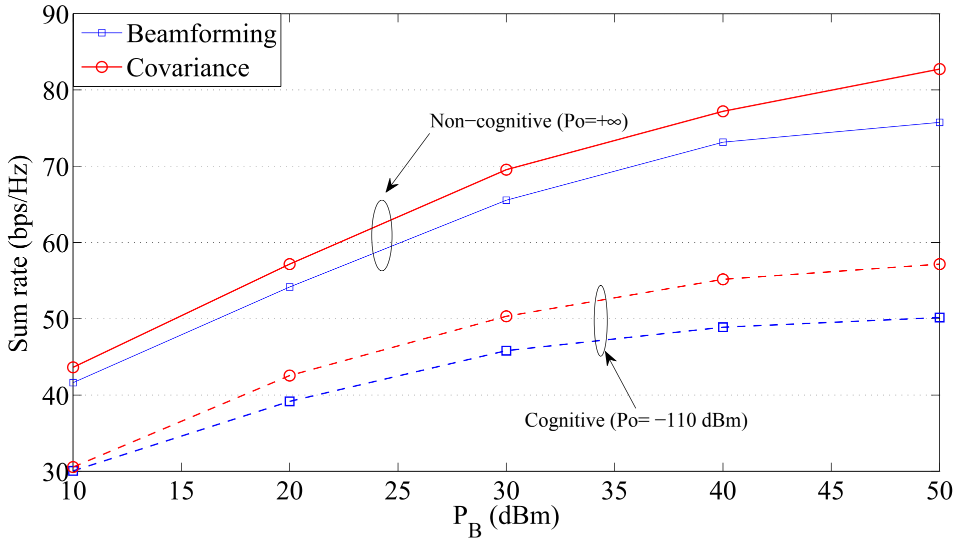

FIGURE 5.5: BS power limit vs. sum rates $(M, N, N_t, N_r, d) = (3, 2, 4, 2, 1)$. $P_O = -110$ dBm for coginitive constraints.

behaviors of the algorithms in the following Chapter 6, Appendix C& D and the published papers [10, 58, 64].

5.6 Conclusions

In this chapter, the optimized design of transmit covariance and precoding matrices is considered for the multi-cell multi-user MIMO downlink systems. The sum rate and minimal rate maximization problems subject to realistic power and cognitive constraints are formulated as very challenging non-convex problems. By exploiting the explicity d.c. structure of the non-convex objective functions, these problems are converted into canonical d.c. optimization programs. We then apply the proposed DCI algorithms to address these problems. The simulation results confirm the effectiveness and efficiency of the proposed algorithm. We show how the addition of cognitive constraints could negatively shrink the achievable information rates. More importantly, the relevance between covariance matrix optimization and precoding matrix optimization is analyzed.

The wireless signal model adopted in this chapter assumes that all interference is noise so it is best minimized. However, no matter how optimally the interference is minimized, treating it as noise results in a wastage of the scarce resources such as energy and bandwidth. Consequently, the rate capacity of certain channels may not be achievable. In the next chapter, we shall introduce the Han-Kobayashi coding scheme which enables some interference to be partially decoded. More importantly, we will further the idea to MIMO channels. As will be analyzed, the signal model studied in this chapter is a special case of the new model. Therefore, the studies presented in this chapter serve as the cornerstone for the following research.

Chapter 6

Successive Interference Mitigation in Multiuser MIMO Interference Channels

6.1 Introduction

Coordinated transmission and interference alignment (see e.g. [149–152]) have been shown to be useful in combating signal interferences. In Chapter 5, we have studied the design of coordinated transmission for cellular MIMO downlink networks with respect to covariance and precoding matrix variables. However, it is based on the fact that interference is treated as noise which is not necessarily capacity-achieving. Even in the simplest scenario of two-user single-input single output (SISO) interference channels (ICs), the full rate capacity may not be reached if the interference is simply treated as noise [59, 60]. In fact the capacity is achieved only in the very weak (low) ICs (see [166] and references therein). For the strong ICs, interference must be decoded in order to achieve capacity [167].

Most of research studies have focused on the achievable rate region characterisation of weak or mixed ICs [7, 59, 168–171] (see definition therein). The Han-Kobayashi (H-K) strategy [7, 59] achieves the largest inner bound while various rate region outer bounds were also reported in [7, 167, 170, 171]. The H-K strategy combines the private and common messages for jointly decoding, which enables each user to decode not only its own common and private messages, but also the common message from the other unintended user. However, the capacity-achieving power allocation to private and common messages in the simplest case of two-user SISO ICs is not exactly known. The closed-form power allocation in [7] to roughly keep the private message received by the unintended receiver at the noise level reaches one-bit rate region. The obtained rates are not necessarily capacity-achieving in terms of the sum rate or the (worst) minimal user's rate. A new equivalent reformulation in the power space was only given recently in [63], for which an efficient iterative algorithm for jointly optimising the private and common message power splits has been developed. This algorithm is capable of achieving the global optimality within a few iterations.

Considering multiple antennas equipped at the transmitters and/or receivers, other research studies have generalized the aforementioned results of two-user SISO ICs to two-user multiple-input multiple-output (MIMO) ICs. In particular, references [6, 61] extend the SISO one-bit region to MIMO N_r-bit region (N_r is the number of receive antennas) or constant-gap region. Reference [166] characterizes the low interference regime so that conventionally treating interference as noise suffices to achieve the sum capacity. Reference [172] establishes the capacity region for very strong and aligned strong ICs.

Reference [9] goes beyond the two-user ICs by considering an arbitrary multi-user MISO IC, where both the common and private messages are beamformed at the base stations and they are sequentially decoded at the receiving ends. Each user must decode the messages commonly decodable by another assigned out-of-cell user and then decodes its private message. Unlike two-user ICs with the unique user pairing choice, one needs to select paired users for commonly decodable messages to improve the IC capacity. This requirement perhaps constitutes one of the most intractable computational problems. Following a given pairing protocol, the problem of common and private rates splitting with supporting beamforming design is still quite challenging.

As the rate region is very complicated and disconnected with no available characterisation, the problem is approached in [9] by an intensive ad hoc search at grinding points of the common and private rate spaces, although the posed optimality of the worst user's rate is still not granted. This check at grinding points is also not suitable for sum-rate maximisation, which is a more popular metric for ICs.

The present research is also concerned with a MIMO interference network (MIMO IC as a special case). Following a pre-pairing procedure of the MIMO users, the covariance matrices of private and common messages in a multi-user MIMO interference network under the base station (BS) power constraints are designed to maximize the sum rate or the worst user's rate. As the achievable rate region is too complicated for any constructive characterisation, any optimization over it would likely be mathematically intractable. Instead, we show that this intractable optimization over the uncharacterisable rate region can be bypassed and the problem can be reformulated as non-smooth function optimization over a simple convex set. Furthermore, these non-smooth functions are shown to be d.c. (difference of two concave functions/sets) [16][1] so their optimization can be solved by very efficient d.c. iterations (DCI) of d.c. programming (see e.g. [56, 92, 137, 164, 165] for developments of DCIs and their successful applications). As a path-following procedure, the theoretical convergence of DCIs to optimal solutions can be easily proved, while intensive simulations results for diversified problems show that they converge in a small number of iterations. The research contribution is two-fold:

- Developing an efficient d.c. optimization framework for sum rate and minimal user's rate maximisation over the disconnected region of the multi-user split private and common rates in MIMO ICs;
- Numerically showing the benefit of the rate split in mitigating multi-user interferences. As a byproduct, the tightness degree of the existing inner and outer bound regions is also numerically analysed.

[1] Conventionally, d.c. stands for a difference of two convex functions [16], which is equivalent to a difference of two concave functions as we deal with in this chapter. The term "d.c." is still used for simplicity of presentation.

The rest of the chapter is as follows. Section 6.2 gives problem formulations and discusses the challenges in finding their solutions. Section 6.3 and Section 6.4 propose new solution methods for covariance matrix and beamforming vector optimization problems, respectively. Section 6.5 provides simulation results, and Section 6.5 concludes the chapter, while some necessary formulas for calculations and numerical solutions can be found in Appendix. B.

6.2 Problem Formulations and Challenges

Consider downlink transmission in a multi-cell multiuser cellular network consisting of N cells. Each cell has one base-station (BS) equipped with $N_t \geq 1$ antennas to serve its K mobile users, each of which is equipped with $N_r \geq 1$ antennas. Define $\mathcal{I} := \{1, 2, \dots, N\}$ and $\mathcal{J} := \{1, 2, \dots, K\}$.

The data of user j in the ith cell (referred to as user (i,j)) consists of a private message $x^{\mathsf{p}}_{i,j} \in \mathbb{C}^{N_t}$ and a common message $x^{\mathsf{c}}_{i,j} \in \mathbb{C}^{N_t}$. The pairing operator $a(\hat{\imath}, \hat{\jmath}) = (i,j)$ with $i \neq \hat{\imath}$ means that user (i,j) is also assigned to decode the common message $x^{\mathsf{c}}_{\hat{\imath},\hat{\jmath}}$ of user $(\hat{\imath}, \hat{\jmath})$. Therefore the common message $x^{\mathsf{c}}_{\hat{\imath},\hat{\jmath}}$ is decodable by the both users $(\hat{\imath}, \hat{\jmath})$ and (i,j). On the other hand, user (i,j) also decodes its own private message $x^{\mathsf{p}}_{i,j}$, and its own common message $x^{\mathsf{c}}_{i,j}$ if pairing $a(i,j) = (\tilde{\imath}, \tilde{\jmath})$ for some $\tilde{\imath} \neq i$. However, $x^{\mathsf{c}}_{i,j} = 0$ for $a(i,j) = \emptyset$, which means that user (i,j) sends only the private message $x^{\mathsf{p}}_{i,j}$. For each (i,j), there are at most one pairing $a(i,j) = (\tilde{\imath}, \tilde{\jmath})$ and one pairing $a(\hat{\imath}, \hat{\jmath}) = (i,j)$. Accordingly, $|a|$ is the cardinality of set $\{(i,j) \in \mathcal{I} \times \mathcal{J} \ : \ a(i,j) \neq \emptyset\}$, i.e., the number of user pairs selected for decoding the common message. In what follows, we denote by $\mathcal{A}$ the set of such assignment operator a and $\mathcal{A}_{\mathcal{L}} \subset \mathcal{A}$ is the set of a with $|a| \leq \mathcal{L}$.

The multiple output $y_{i,j} \in \mathbb{C}^{N_r}$ at user (i,j) is the following combination of intra-cell and inter-cell signals and noise:

$$y_{i,j} = \sum_{k \in \mathcal{J}} \sqrt{\delta_{i,j}} h_{i,i,j} (x^p_{i,k} + x^c_{i,k}) + \sum_{m \in \mathcal{I} \setminus \{i\}} \sum_{k \in \mathcal{J}} \sqrt{\eta_{m,i,j}} h_{m,i,j} (x^p_{m,k} + x^c_{m,k}) + n_{i,j}. \tag{6.1}$$

In (6.1), $n_{i,j} \in \mathbb{C}^{N_r}$ and its entries are independent and identically distributed (i.i.d.) noise samples with zero-mean and variance σ^2. The matrix $h_{m,i,j} \in \mathbb{C}^{N_r \times N_t}$ represents the normalized MIMO channel from BS m to user (i,j). The quantity $\delta_{i,j}$ defines the strength of the direct channel $h_{i,i,j}$, whereas $\eta_{m,i,j}$ $(m \neq i)$ indicates the strength of the interfering channel $h_{m,i,j}$. For convenience, define $H_{i,i,j} := \sqrt{\delta_{i,i,j}} h_{i,i,j}$ and $H_{m,i,j} = \sqrt{\eta_{m,i,j}} h_{m,i,j}$ for $m \neq i$.

For simplicity, the following BS power constraints are considered, although other power constraints can be easily incorporated:

$$\mathcal{W}_B = \{\boldsymbol{Q} := [\boldsymbol{Q}^{\mathsf{p}}_{i,j} \quad \boldsymbol{Q}^{\mathsf{c}}_{i,j}]_{(i,j)\in\mathcal{I}\times\mathcal{J}} \ : \ \boldsymbol{Q}^{\mathsf{p}}_{i,j} \succeq 0, \boldsymbol{Q}^{\mathsf{c}}_{i,j} \succeq 0, \sum_{j\in\mathcal{J}} \mathsf{trace}(\boldsymbol{Q}^{\mathsf{p}}_{i,j} + \boldsymbol{Q}^{\mathsf{c}}_{i,j}) \leq P_B, i \in \mathcal{I}\}, \quad (6.2)$$

where $\boldsymbol{Q}^{\mathsf{p}}_{i,j} \in \mathbb{C}^{N_t \times N_t}$ and $\boldsymbol{Q}^{\mathsf{c}}_{i,j} \in \mathbb{C}^{N_t \times N_t}$ are the covariance matrices of messages $x^{\mathsf{p}}_{i,j}$ and $x^{\mathsf{c}}_{i,j}$, respectively. The channel can thus be fully parameterized by the set of $(\delta, \eta, P_B/\sigma^2)$, where δ is the set of all $\delta_{i,j}$ and η is the set of all $\eta_{m,i,j}$.

The $N_r \times N_r$ covariance matrix of the received interference signal at user (i,j) is given as

$$\mathcal{M}_{i,j}(\boldsymbol{Q}) := \sum_{(n,k)\in\mathcal{I}\times\mathcal{J}} H_{n,i,j}(\boldsymbol{Q}^{\mathsf{p}}_{n,k} + \boldsymbol{Q}^{\mathsf{c}}_{n,k}) H^H_{n,i,j},$$

As in [9], each user (i,j) successively decodes in the following order.

- The user (i,j) decodes its own common message $x^{\mathsf{c}}_{i,j}$ with the achievable rate:

$$r^{\mathsf{c}}_{i,j}(\boldsymbol{Q}) = \log\left|\boldsymbol{I}_{N_r} + H_{i,i,j}\boldsymbol{Q}^{\mathsf{c}}_{i,j}H^H_{i,i,j}(\mathcal{M}^{\mathsf{c}}_{i,j}(\boldsymbol{Q}) + \sigma^2\boldsymbol{I}_{N_r})^{-1}\right|,$$

  where $\mathcal{M}^{\mathsf{c}}_{i,j}(\boldsymbol{Q}) := \mathcal{M}_{i,j}(\boldsymbol{Q}) - H_{i,i,j}\boldsymbol{Q}^{\mathsf{c}}_{i,j}H^H_{i,i,j}$. Accordingly, $r^{\mathsf{c}}_{i,j}(\boldsymbol{Q}) = 0$ if $a(i,j) = \emptyset$.

- If $a(i,j) = (\tilde{i},\tilde{j}) \neq \emptyset$, the common message $x^{\mathsf{c}}_{i,j}$ is also decodable by user $(\tilde{i},\tilde{j})$ with the achievable rate:

$$r^{\mathsf{a}}_{a(i,j)}(\boldsymbol{Q}) = \log\left|\boldsymbol{I}_{N_r} + H_{i,\tilde{i},\tilde{j}}\boldsymbol{Q}^{\mathsf{c}}_{i,j}H^H_{i,\tilde{i},\tilde{j}}(\mathcal{M}^{\mathsf{a}}_{a(i,j)}(\boldsymbol{Q}) + \sigma^2\boldsymbol{I}_{N_r})^{-1}\right|,$$

where $\mathcal{M}^{\mathsf{a}}_{a(i,j)}(\boldsymbol{Q}) := \mathcal{M}^{\mathsf{c}}_{\tilde{i},\tilde{j}}(\boldsymbol{Q}) - H_{i,\tilde{i},\tilde{j}}\boldsymbol{Q}^{\mathsf{c}}_{i,j}H^{H}_{i,\tilde{i},\tilde{j}}$.

- The user (i,j) decodes its own private message $x^{\mathsf{p}}_{i,j}$ lastly, with the achievable rate

$$r^{\mathsf{p}}_{i,j}(\boldsymbol{Q}) = \log|\boldsymbol{I}_{N_r} + H_{i,i,j}\boldsymbol{Q}^{\mathsf{p}}_{i,j}H^{H}_{i,i,j}(\mathcal{M}^{\mathsf{p}}_{i,j}(\boldsymbol{Q}) + \sigma^2\boldsymbol{I}_{N_r})^{-1}|,$$

  for $\mathcal{M}^{\mathsf{p}}_{i,j}(\boldsymbol{Q}) := \mathcal{M}^{\mathsf{a}}_{i,j}(\boldsymbol{Q}) - H_{i,i,j}\boldsymbol{Q}^{\mathsf{p}}_{i,j}H^{H}_{i,i,j}$.

The achievable rate region under this successive decoding is thus given as

$$\mathcal{R}(\boldsymbol{Q}) := \left\{[\boldsymbol{\nu}^{\mathsf{p}}_{i,j} + \boldsymbol{\nu}^{\mathsf{c}}_{i,j}]_{(i,j)\in\mathcal{I}\times\mathcal{J}} : \boldsymbol{\nu}^{\mathsf{p}}_{i,j} \leq r^{\mathsf{p}}_{i,j}(\boldsymbol{Q}), \boldsymbol{\nu}^{\mathsf{c}}_{i,j} \leq r^{\mathsf{c}}_{i,j}(\boldsymbol{Q}), \boldsymbol{\nu}^{\mathsf{c}}_{i,j} \leq r^{\mathsf{a}}_{a(i,j)}(\boldsymbol{Q})\right\} \subset R^{N\times K}. \tag{6.3}$$

Let $\boldsymbol{\nu} := [\boldsymbol{\nu}_{i,j}]_{(i,j)\in\mathcal{I}\times\mathcal{J}}$. The problem of joint rate splitting and pairing to maximize the sum rate under the BS power constraints is stated as

$$\max_{a\in\mathcal{A}}\max_{\boldsymbol{Q},\boldsymbol{\nu}} \sum_{(i,j)\in\mathcal{I}\times\mathcal{J}} \boldsymbol{\nu}_{i,j} \ : \ \boldsymbol{Q}\in\mathcal{W}_B,\ \boldsymbol{\nu}\in\mathcal{R}(\boldsymbol{Q}). \tag{6.4}$$

On the other hand, the minimal rate maximisation problem is

$$\max_{a\in\mathcal{A}}\max_{\boldsymbol{Q},\boldsymbol{\nu}} \min_{(i,j)\in\mathcal{I}\times\mathcal{J}} \boldsymbol{\nu}_{i,j} \ : \ \boldsymbol{Q}\in\mathcal{W}_B,\ \boldsymbol{\nu}\in\mathcal{R}(\boldsymbol{Q}). \tag{6.5}$$

Both (6.4) and (6.5) are extremely intractable mixed-combinatorial optimization problems, for which the optimal solutions cannot be easily found, except by exhaustive search that is impractical even for the simplest case.

Before introducing our methods to solve (6.4) and (6.5), it is worthwhile to discuss a simpler problem for MISO ICs (when $N_r = L = 1$). Such a problem has been considered in [9], in which each user is equipped with a single antenna. The private message $s^{\mathsf{p}}_{i,j}\in\mathbb{C}$ and common message $s^{\mathsf{c}}_{i,j}\in\mathbb{C}$ are beamformed by vectors $\boldsymbol{w}^{\mathsf{c}}_{i,j}\in\mathbb{C}^{N_t}$ and $\boldsymbol{w}^{\mathsf{c}}_{i,j}\in\mathbb{C}^{N_t}$, respectively. The private and common messages to be transmitted become $x^{\mathsf{p}}_{i,j} = \boldsymbol{w}^{\mathsf{p}}_{i,j}s^{\mathsf{p}}_{i,j}$ and $x^{\mathsf{c}}_{i,j} = \boldsymbol{w}^{\mathsf{c}}_{i,j}s_{i,j}$. The single output is a simplified version of the multiple output equation in (6.1), which is

$$y_{i,j} = \sum_{k\in\mathcal{J}} \sqrt{\delta_{i,j}} h_{i,i,j}(\boldsymbol{w}^{\mathsf{p}}_{i,k} s^{\mathsf{p}}_{i,k} + \boldsymbol{w}^{\mathsf{c}}_{m,k} s^{\mathsf{c}}_{m,k}) + \sum_{m\in\mathcal{I}\setminus\{i\}} \sum_{k\in\mathcal{J}} \sqrt{\eta_{m,i,j}} h_{m,i,j}(\boldsymbol{w}^{\mathsf{p}}_{m,k} s^{\mathsf{p}}_{m,k} + \boldsymbol{w}^{\mathsf{c}}_{m,k} s^{\mathsf{c}}_{m,k}) + n_{i,j}. \tag{6.6}$$

The above leads to (6.5) with additional rank-one constraints:

$$\text{rank}(\boldsymbol{Q}^{\mathsf{p}}_{i,j}) = \text{rank}(\boldsymbol{Q}^{\mathsf{c}}_{i,j}) = 1, (i,j) \in \mathcal{I} \times \mathcal{J}, \tag{6.7}$$

where

$$0 \preceq \boldsymbol{Q}^{\mathsf{p}}_{i,j} = \boldsymbol{w}^{\mathsf{p}}_{i,j}(\boldsymbol{w}^{\mathsf{p}}_{i,j})^H,\ 0 \preceq \boldsymbol{Q}^{\mathsf{c}}_{i,j} = \boldsymbol{w}^{\mathsf{c}}_{i,j}(\boldsymbol{w}^{\mathsf{c}}_{i,j})^H. \tag{6.8}$$

Let $\tilde{H}_{i,i,j} := H_{i,i,j} H^H_{i,i,j}$. The problem (6.5) with additional rank-one constraints (6.7) becomes

$$\max_{a\in\mathcal{A}} \max_{\boldsymbol{Q},\boldsymbol{\nu}^{\mathsf{c}},\boldsymbol{\nu}^{\mathsf{p}}} \min_{(i,j)\in\mathcal{I}\times\mathcal{J}} [\boldsymbol{\nu}^{\mathsf{p}}_{i,j} + \boldsymbol{\nu}^{\mathsf{c}}_{i,j}] \quad \text{s.t.} \quad (6.2), (6.7), \tag{6.9a}$$

$$\langle \boldsymbol{Q}^{\mathsf{c}}_{i,j}, \tilde{H}_{i,i,j} \rangle \geq (2^{\boldsymbol{\nu}^{\mathsf{c}}_{i,j}} - 1)\mathcal{M}^{\mathsf{c}}_{i,j}(\boldsymbol{Q}), \tag{6.9b}$$

$$\langle \boldsymbol{Q}^{\mathsf{c}}_{i,j}, \tilde{H}_{i,\tilde{i},\tilde{j}} \rangle \geq (2^{\boldsymbol{\nu}^{\mathsf{c}}_{i,j}} - 1)\mathcal{M}^{\mathsf{a}}_{a(i,j)}(\boldsymbol{Q}) \quad \text{for} \quad a(i,j) = (\tilde{i},\tilde{j}), \tag{6.9c}$$

$$\langle \boldsymbol{Q}^{\mathsf{p}}_{i,j}, \tilde{H}_{i,i,j} \rangle \geq (2^{\boldsymbol{\nu}^{\mathsf{p}}_{i,j}} - 1)\mathcal{M}^{\mathsf{p}}_{i,j}(\boldsymbol{Q}) \quad \text{for} \quad a^{-1}(i,j) = (\hat{i},\hat{j}). \tag{6.9d}$$

It is pointed out that the specific case $a(i,j) = \emptyset\ \forall (i,j) \in \mathcal{I} \times \mathcal{J}$ is the conventional maximin rate coordinated beamforming:

$$\max_{\boldsymbol{Q}^{\mathsf{p}}=[\boldsymbol{Q}^{\mathsf{p}}]_{(i,j)\in\mathcal{I}\times\mathcal{J}},\boldsymbol{\lambda}} \boldsymbol{\lambda} \tag{6.10a}$$

$$\text{s.t.} \quad \sum_{(i,j)\in\mathcal{I}\times\mathcal{J}} \langle \boldsymbol{Q}^{\mathsf{p}}_{i,j} \rangle \leq P_T, \tag{6.10b}$$

$$\langle \boldsymbol{Q}^{\mathsf{p}}_{i,j}, \tilde{H}_{i,i,j} \rangle \geq (2^{\boldsymbol{\lambda}} - 1)(\Phi_{i,j}(\boldsymbol{Q}^{\mathsf{p}}) + \sigma^2) \tag{6.10c}$$

$$\text{rank}(\boldsymbol{Q}^{\mathsf{p}}_{i,j}) = 1, \tag{6.10d}$$

where $\Phi_{i,j}(\boldsymbol{Q}^{\mathsf{p}}) := \sum_{(n,k)\in\mathcal{I}\times\mathcal{J}\setminus(i,j)} \langle \boldsymbol{Q}^{\mathsf{p}}_{n,k}, \tilde{H}_{n,i,j} \rangle, (i,j) \in \mathcal{I} \times \mathcal{J}$, which is nonconvex due to the rank-one constraint (6.10d).

Reference [9] solves (6.10b)-(6.10c) by bisection in $\boldsymbol{\lambda}$, i.e., a sequence of SDP relaxed program (6.10b)-(6.10c) in $\boldsymbol{Q}^{\mathsf{p}}$ with fixed $\boldsymbol{\lambda}$ is solved to find the optimal value λ^{p} of (6.10b)-(6.10c), at which there is rank-one solution $\boldsymbol{Q}^{\mathsf{p}}_{i,j}$. Based on the obtained solution of (6.10), $\mathcal{L}$ user-pairs are selected for candidates in common-private message split. In fact, steps 3–5 of Algorithm 2 in [9] are to check the feasibility of (6.9) at grinding points of $\min_{(i,j)\in\mathcal{I}\times\mathcal{J}} \boldsymbol{\nu}^{\mathsf{p}}_{i,j} > \lambda^{\mathsf{p}}$ and $[\boldsymbol{\nu}^{\mathsf{p}}_{i,j}, \boldsymbol{\nu}^{\mathsf{c}}_{i,j}]_{(i,j)\in\mathcal{I}\times\mathcal{J}}$. It is obvious from (6.9) that each feasibility problem in $\boldsymbol{Q}$ is a nonconvex rank-one constrained problem, which is solved in [9] again by SDP relaxation and randomisation.[2] Such an approach and procedure are not suitable for the sum rate optimization problem (6.4) in MISO networks, nor can they be extended to solve the minimal rate maximisation problem (6.5) in MIMO networks.

6.3 A New Efficient Covariance Solution

Problem (6.4)/(6.5) as it stands is not mathematically tractable. Therefore, it is important to simplify it by predetermining $a \in \mathcal{A}_{\mathcal{L}}$. We will extend the idea of [9] to predetermine $a \in \mathcal{A}_{\mathcal{L}}$ in (6.5) as follows. The conventional coordinated sum rate and covariance maximin rate optimizations correspond to the case $x^{\mathsf{c}}_{i,j} \equiv 0, (i,j) \in \mathcal{I}\times\mathcal{J}$, under which (6.4)/(6.5) becomes

$$\max_{\boldsymbol{Q}^{\mathsf{p}}\in\mathcal{W}^{\mathsf{p}}_{B}} \varphi(\rho(\boldsymbol{Q}^{\mathsf{p}})), \tag{6.11}$$

where $\varphi(\rho) = \varphi^{\mathsf{S}}(\rho) \vee \varphi^{\mathsf{M}}(\rho)$ with $\rho = [\rho_{i,j}]_{(i,j)\in\mathcal{I}\times\mathcal{J}}$, and

$$\varphi^{\mathsf{S}}(\rho) := \sum_{(i,j)\in\mathcal{I}\times\mathcal{J}} \rho_{i,j}, \ \varphi^{\mathsf{M}}(\rho) := \min_{(i,j)\in\mathcal{I}\times\mathcal{J}} \rho_{i,j},$$

[2] The reader is also referred to [14] for efficiency analysis of such a SDP relaxation approach.

while $\rho(\boldsymbol{Q}^{\mathsf{p}}) := [\rho_{i,j}(\boldsymbol{Q}^{\mathsf{p}})]_{(i,j)\in\mathcal{I}\times\mathcal{J}}$ with

$$\rho_{i,j}(\boldsymbol{Q}^{\mathsf{p}}) := \log|\boldsymbol{I}_{N_r} + H_{i,i,j}\boldsymbol{Q}^{\mathsf{p}}_{i,j}H^H_{i,i,j}(\Phi_{i,j}(\boldsymbol{Q}^{\mathsf{p}}) + \sigma^2\boldsymbol{I}_{N_r})^{-1}|,$$
$$\Phi_{i,j}(\boldsymbol{Q}^{\mathsf{p}}) := \sum_{(n,k)\in\mathcal{I}\times\mathcal{J}\setminus(i,j)} H_{n,i,j}\boldsymbol{Q}^{\mathsf{p}}_{n,k}H^H_{n,i,j},$$
$$\mathcal{W}^{\mathsf{p}}_B = \{[\boldsymbol{Q}^{\mathsf{p}}_{i,j}]_{(i,j)\in\mathcal{I}\times\mathcal{J}} \ : \ \boldsymbol{Q}^{\mathsf{p}}_{i,j}\succeq 0, \textstyle\sum_{j\in\mathcal{J}}\mathsf{trace}(\boldsymbol{Q}^{\mathsf{p}}_{i,j}) \le P_B, i\in\mathcal{I}\}.$$

In essence, common messages are introduced in (6.4)/(6.5) to improve the multiuser rate capacity of the coordinated transmissions (6.11).

Suppose $Q^{\mathsf{p}(0)}$ is the optimal solution of (6.11). Define the received interference-plus-noise covariance for user (i,j) by

$$T_{i,j} = \sum_{(n,k)\in\mathcal{I}\times\mathcal{J}\setminus(i,j)} H_{n,i,j}Q^{\mathsf{p}(0)}_{n,k}H^H_{n,i,j} + \sigma^2\boldsymbol{I}_{N_r} \tag{6.12}$$

and the interference-to-noise covariance (INC) by

$$\mathrm{INC}_{(\hat{i},\hat{j})\to(i,j)} = H_{\hat{i},i,j}Q^{\mathsf{p}(0)}_{\hat{i},\hat{j}}H^H_{\hat{i},i,j}(T_{ij} - H_{\hat{i},i,j}Q^{\mathsf{p}(0)}_{\hat{i},\hat{j}}H_{\hat{i},i,j})^{-1} \in \mathbb{C}^{N_r\times N_r} \tag{6.13}$$

The relative strength of interference $\mathrm{INR}_{(\hat{i},\hat{j})\to(i,j)}$ is gauged by $\mathrm{DINC}_{(\hat{i},\hat{j})\to(i,j)} = |\mathrm{INC}_{(\hat{i},\hat{j})\to(i,j)}|$. Then, similar to [9], $(N-1)NK^2$ such DINC values, each representing a potential pairing option, are sorted and trimmed to create an effective list in the decreasing value order such that each $(\hat{i},\hat{j})$ (each (i,j), resp.) appears at most once in $(\hat{i},\hat{j})\to(i,j)$. Then, $\mathcal{L}$ pairs with the highest DINC values are pre-selected for the commonly messaging corresponding to pairing map $a\in\mathcal{A}_{\mathcal{L}}$.

Having chosen pairing map $a\in\mathcal{A}_{\mathcal{L}}$, we now consider the following covariance matrix design problem for the sum rate problem (6.4) and the maximin rate problem (6.5) under the pairing a:

$$\max_{\boldsymbol{Q},\boldsymbol{\nu}} \ \varphi(\boldsymbol{\nu}) \ : \ \boldsymbol{Q}\in\mathcal{W}_B, \ \boldsymbol{\nu}\in\mathcal{R}(\boldsymbol{Q}). \tag{6.14}$$

The objective function $\varphi(\boldsymbol{\nu})$ in (6.14) is obviously concave so (6.14) is concave function maximisation over nonconvex constraints. The difficulty of (6.14) lies on the nonconvexity of set

$\mathcal{R}(\boldsymbol{Q})$ for each fixed $\boldsymbol{Q}$, which is uncharacterisable. Apparently, optimization over $\mathcal{R}(\boldsymbol{Q})$ is computationally intractable. We now provide a novel approach to reformulate (6.14) as function maximisation in $\boldsymbol{Q}$ only over simple convex set $\mathcal{W}_B$ defined by (6.2). To this end, define the map

$$r(\boldsymbol{Q}) := [r_{i,j}(\boldsymbol{Q})]_{(i,j)\in\mathcal{I}\times\mathcal{J}} = [r^{\mathsf{p}}_{i,j}(\boldsymbol{Q}) + \min\{r^{\mathsf{c}}_{i,j}(\boldsymbol{Q}), r^{a}_{a(i,j)}(\boldsymbol{Q})\}]_{(i,j)\in\mathcal{I}\times\mathcal{J}}. \tag{6.15}$$

Theorem 4. *Problem (6.14) in variables* $(\boldsymbol{Q}, \boldsymbol{\nu})$ *is equivalent to the following problem in variable* $\boldsymbol{Q}$ *only*

$$\max_{\boldsymbol{Q}} \ \varphi(r(\boldsymbol{Q})) \ : \ \boldsymbol{Q} \in \mathcal{W}_B. \tag{6.16}$$

The equivalence is in the sense that the two problems share the same optimal value and optimal solution $\boldsymbol{Q}$.

Proof: Each feasible $\boldsymbol{Q}$ of (6.16) will result $[\nu^{\mathsf{p}}_{i,j}]_{(i,j)\in\mathcal{I}\times J} = [r^{\mathsf{p}}_{i,j}(\boldsymbol{Q}]_{(i,j)\in\mathcal{I}\times\mathcal{J}}$ and $[\nu^{\mathsf{c}}]_{(i,j)\in\mathcal{I}\times\mathcal{J}} = [\min\{r^{\mathsf{c}}_{i,j}(\boldsymbol{Q}), r^{a}_{a(i,j)}(\boldsymbol{Q})\}]_{(i,j)\in\mathcal{I}\times\mathcal{J}}$ such that $[\boldsymbol{\nu}^{\mathsf{p}}_{i,j}+\boldsymbol{\nu}^{\mathsf{c}}_{i,j}]_{(i,j)\in\mathcal{I}\times\mathcal{J}} \in \mathcal{R}(\boldsymbol{Q})$, i.e., $(\boldsymbol{Q}, [\boldsymbol{\nu}^{\mathsf{p}}_{i,j}+\boldsymbol{\nu}^{\mathsf{c}}_{i,j}]_{(i,j)\in\mathcal{I}\times\mathcal{J}})$ is feasible to (6.14). Therefore, max (6.16) $\leq$ max (6.14). Now, suppose $(\boldsymbol{Q}, \boldsymbol{\nu})$ is feasible to (6.14). Then $\boldsymbol{\nu} \in \mathcal{R}(\boldsymbol{Q})$ so there are $\boldsymbol{\nu}^{\mathsf{p}}_{i,j} \leq r^{\mathsf{p}}_{i,j}(\boldsymbol{Q})$ and $\boldsymbol{\nu}^{\mathsf{c}}_{i,j} \leq r^{\mathsf{c}}_{i,j}(\boldsymbol{Q})$, $\boldsymbol{\nu}^{\mathsf{c}}_{i,j} \leq r^{\mathsf{a}}_{a(i,j)}(\boldsymbol{Q})$ such that $\boldsymbol{\nu}_{i,j} = \boldsymbol{\nu}^{\mathsf{p}}_{i,j} + \boldsymbol{\nu}^{\mathsf{c}}_{i,j}$. It follows that $\boldsymbol{\nu}_{i,j} \leq r_{i,j}(\boldsymbol{Q})$ so $\varphi(\boldsymbol{\nu}) \leq \varphi(r(\boldsymbol{Q}))$ and max (6.14) $\leq$ max (6.16) yielding max (6.16) $=$ max (6.14). □

One can see that (6.16) is convex constrained optimization with minimal number of variables involved. As the next step, we explore the partial concavities of the objective function $\varphi(r(\boldsymbol{Q})$ that are useful for maximisation purpose. First, each of the rate functions $r^{\mathsf{p}}_{i,j}(\boldsymbol{Q})$, $r^{\mathsf{c}}_{i,j}(\boldsymbol{Q})$ and $r^{\mathsf{a}}_{a(i,j)}(\boldsymbol{Q})$ is a difference of two concave (d.c.) functions:

$$\begin{aligned}
r^{\mathsf{p}}_{i,j}(\boldsymbol{Q}) &= g^{\mathsf{p}}_{i,j}(\boldsymbol{Q}) - f^{\mathsf{p}}_{i,j}(\boldsymbol{Q}),\\
r^{\mathsf{c}}_{i,j}(\boldsymbol{Q}) &= g^{\mathsf{c}}_{i,j}(\boldsymbol{Q}) - f^{\mathsf{c}}_{i,j}(\boldsymbol{Q}),\\
r^{\mathsf{a}}_{a(i,j)}(\boldsymbol{Q}) &= g^{\mathsf{a}}_{a(i,j)}(\boldsymbol{Q}) - f^{\mathsf{a}}_{a(i,j)}(\boldsymbol{Q}),
\end{aligned}$$

with concave functions [116, p. 405]

$$\begin{aligned}
g^{\mathsf{p}}_{i,j}(\boldsymbol{Q}) &= \log|\mathcal{M}^{\mathsf{p}}_{i,j}(\boldsymbol{Q}) + H_{i,i,j}\boldsymbol{Q}^{\mathsf{p}}_{i,j}H^{H}_{i,i,j} + \sigma^2 I_{N_r}|,\\
f^{\mathsf{p}}_{i,j}(\boldsymbol{Q}) &= \log|\mathcal{M}^{\mathsf{p}}_{i,j}(\boldsymbol{Q}) + \sigma^2 I_{N_r}|,\\
g^{\mathsf{c}}_{i,j}(\boldsymbol{Q}) &= \log|\mathcal{M}^{\mathsf{c}}_{i,j}(\boldsymbol{Q}) + H_{i,i,j}\boldsymbol{Q}^{\mathsf{c}}_{i,j}H^{H}_{i,i,j} + \sigma^2 I_{N_r}|,\\
f^{\mathsf{c}}_{i,j}(\boldsymbol{Q}) &= \log|\mathcal{M}^{\mathsf{c}}_{i,j}(\boldsymbol{Q}) + \sigma^2 I_{N_r}|,\\
g^{\mathsf{a}}_{a(i,j)}(\boldsymbol{Q}) &= \log|\mathcal{M}^{\mathsf{a}}_{a(i,j)}(\boldsymbol{Q}) + H_{i,\tilde{i},\tilde{j}}\boldsymbol{Q}^{\mathsf{c}}_{i,j}H^{H}_{i,\tilde{i},\tilde{j}} + \sigma^2 I_{N_r}|,\\
f^{\mathsf{a}}_{a(i,j)}(\boldsymbol{Q}) &= \log|\mathcal{M}^{\mathsf{a}}_{a(i,j)}(\boldsymbol{Q}) + \sigma^2 I_{N_r}|.
\end{aligned}$$

Next, one has the following sequential d.c. representations [16]:

- $\min\{r^{\mathsf{c}}_{i,j}(\boldsymbol{Q}), r^{\mathsf{a}}_{a(i,j)}(\boldsymbol{Q})\} = g^{\mathsf{ca}}_{i,j}(\boldsymbol{Q}) - f^{\mathsf{ca}}_{i,j}(\boldsymbol{Q})$, where the functions

$$\begin{aligned}
g^{\mathsf{ca}}_{i,j}(\boldsymbol{Q}) &:= \min\{g^{\mathsf{c}}_{i,j}(\boldsymbol{Q}) + f^{\mathsf{a}}_{a(i,j)}(\boldsymbol{Q}), g^{\mathsf{a}}_{a(i,j)}(\boldsymbol{Q}) + f^{\mathsf{c}}_{i,j}(\boldsymbol{Q})\},\\
f^{\mathsf{ca}}_{i,j}(\boldsymbol{Q}) &:= f^{\mathsf{c}}_{i,j}(\boldsymbol{Q}) + f^{\mathsf{a}}_{a(i,j)}(\boldsymbol{Q})
\end{aligned}$$

  are concave as they are minimum and sum of concave functions.

- $r_{i,j}(\boldsymbol{Q}) = g_{i,j}(\boldsymbol{Q}) - f_{i,j}(\boldsymbol{Q})$, with concave functions

$$g_{i,j}(\boldsymbol{Q}) := g^{\mathsf{p}}_{i,j}(\boldsymbol{Q}) + g^{\mathsf{ca}}_{i,j}(\boldsymbol{Q}),$$
$$f_{i,j}(\boldsymbol{Q}) := f^{\mathsf{p}}_{i,j}(\boldsymbol{Q}) + f^{\mathsf{ca}}_{i,j}(\boldsymbol{Q}).$$

- $\varphi^{\mathsf{S}}(\boldsymbol{Q}) = \sum_{(i,j)\in\mathcal{I}\times\mathcal{J}} r_{i,j}(\boldsymbol{Q}) = g^{\mathsf{S}}(\boldsymbol{Q}) - f(\boldsymbol{Q})$, with concave functions

$$g^{\mathsf{S}}(\boldsymbol{Q}) := \textstyle\sum_{(i,j)\in\mathcal{I}\times\mathcal{J}} g_{i,j}(\boldsymbol{Q}),$$
$$f(\boldsymbol{Q}) := \sum_{(i,j)\in\mathcal{I}\times\mathcal{J}} f_{i,j}(\boldsymbol{Q})$$

- $\varphi^{\mathsf{M}}(\boldsymbol{Q}) = \min_{(i,j)\in\mathcal{I}\times\mathcal{J}} r_{i,j}(\boldsymbol{Q}) = g^{\mathsf{M}}(\boldsymbol{Q}) - f(\boldsymbol{Q})$, where function

$$g^{\mathsf{M}}(\boldsymbol{Q}) = \min_{(i,j)\in\mathcal{I}\times\mathcal{J}} [g_{i,j}(\boldsymbol{Q}) + \sum_{(n,k)\in\mathcal{I}\times\mathcal{J}\setminus(i,j)} f_{n,k}(\boldsymbol{Q})]$$

is concave as it is a minimum of concave functions [16].

Using the above facts, we obtain the following result:

Theorem 5. *For $g(\boldsymbol{Q}) = g^{\mathsf{S}}(\boldsymbol{Q}) \vee g^{\mathsf{M}}(\boldsymbol{Q})$, problem (6.14) is the following convex constrained d.c. function maximisation:*

$$\max_{\boldsymbol{Q}} \ [g(\boldsymbol{Q}) - f(\boldsymbol{Q})] : \ \boldsymbol{Q} \in \mathcal{W}_B. \tag{6.17}$$

Analogously, the conventional coordinated optimization problem (6.11) is represented by the following convex constrained d.c. function maximisation:

$$\max_{\boldsymbol{Q}} [g^{\mathsf{P}}(\boldsymbol{Q}^{\mathsf{P}}) - f^{\mathsf{P}}(\boldsymbol{Q}^{\mathsf{P}})] : \ \boldsymbol{Q} \in \mathcal{W}_B, \tag{6.18}$$

with concave functions $f^{\mathsf{P}}(\boldsymbol{Q}^{\mathsf{P}}) = \sum_{(i,j)\in\mathcal{I}\times\mathcal{J}} \log|\Phi_{i,j}(\boldsymbol{Q}^{\mathsf{P}}) + \sigma^2 \boldsymbol{I}_{N_r}|$ and

$$\begin{aligned} g^{\mathsf{P}}(\boldsymbol{Q}) \ &= \sum_{(i,j)\in\mathcal{I}\times\mathcal{J}} \log|H_{i,i,j}\boldsymbol{Q}^{\mathsf{P}}_{i,j}H^H_{i,i,j} + \Phi_{i,j}(\boldsymbol{Q}^{\mathsf{P}}) + \sigma^2 \boldsymbol{I}_{N_r}| \\ &\vee \min_{(i,j)\in\mathcal{I}\times\mathcal{J}} [\log|H_{i,i,j}\boldsymbol{Q}^{\mathsf{P}}_{i,j}H^H_{i,i,j} + \Phi_{i,j}(\boldsymbol{Q}^{\mathsf{P}}) + \sigma^2 \boldsymbol{I}_{N_r}| \\ &+ \sum_{(n,k)\in\mathcal{I}\times\mathcal{J}\setminus(i,j)} \log|\Phi_{n,k}(\boldsymbol{Q}^{\mathsf{P}}) + \sigma^2 \boldsymbol{I}_{N_r}|]. \end{aligned}$$

Clearly, (6.17) belongs to the canonical d.c. programming (5.7) as we analyzed in Section 5.3 of Chapter 5. In particular, it is pointed out that (6.17) is (5.7) with $\boldsymbol{z} \to \boldsymbol{Q}$, $G(\boldsymbol{z}) \to g(\boldsymbol{Q})$ and $F(\boldsymbol{z}) \to f(\boldsymbol{Q})$, while (6.18) is (5.7) with $\boldsymbol{z} \to \boldsymbol{Q}^{\mathsf{P}}$, $G(\boldsymbol{z}) \to g^{\mathsf{P}}(\boldsymbol{Q}^{\mathsf{P}})$ and $F(\boldsymbol{z}) \to f^{\mathsf{P}}(\boldsymbol{Q})^{\mathsf{P}}$. Therefore both (6.17) and (6.18) are solved by the DCI described before. The gradients $\langle \nabla f(Q^{(\kappa)}), \boldsymbol{Q} - Q^{(\kappa)} \rangle$ or $\langle \nabla f^{\mathsf{P}}(Q^{\mathsf{P}(\kappa)}), \boldsymbol{Q}^{\mathsf{P}} - Q^{\mathsf{P}(\kappa)} \rangle$ in implementing $(\kappa + 1)$th-DCI (5.8) can be easily calculated based on Equation (B.1) given in Appendix B.

Finally, our approach toward finding the solution of (6.4)/(6.5) is as follows.

- Use DCIs to find optimized solution $Q^{\mathsf{P}(0)}$ of the coordinated covariance matrix problem (6.11)/(6.18);

- Use $Q^{\mathsf{p}(0)}$ to determine the pairing strategy $a \in \mathcal{A}_{\mathcal{L}}$;
- Use DCIs to find optimized solution Q of (6.14)/(6.17).

6.4 A New Beamforming Solution for MISO Application

Now consider the beamforming problem (6.9). The main disadvantage of the formulation in (6.9) is that the dimension of variable $\boldsymbol{Q}$ is very large and there are also difficult rank-one constraints (6.7). As such, we shall focus on a direct formulation involving the original beamforming variable $\boldsymbol{w}$ and without rank-one constraints (6.7). The BS power constraint (6.2) in terms of $\boldsymbol{w}$ is

$$\widetilde{\mathcal{W}}_B = \{\boldsymbol{w} := [\boldsymbol{w}^{\mathsf{p}}_{i,j} \quad \boldsymbol{w}^{\mathsf{c}}_{i,j}]_{(i,j)\in\mathcal{I}\times\mathcal{J}} \ : \ \sum_{j\in\mathcal{J}}(||\boldsymbol{w}^{\mathsf{p}}_{i,j}||^2 + ||\boldsymbol{w}^{\mathsf{c}}_{i,j}||^2) \leq P_B, i \in \mathcal{I}\}. \tag{6.19}$$

The pairing $a \in \mathcal{A}_{\mathcal{L}}$ is chosen according to the previous section, which is based on the solution of coordinated beamforming:

$$\max_{\boldsymbol{w}^{\mathsf{p}}=[\boldsymbol{w}^{\mathsf{p}}_{i,j}]_{(i,j)\in\mathcal{I}\times\mathcal{J}}\in\widetilde{\mathcal{W}}^{\mathsf{p}}_B} \varphi(\tilde{\rho}(\boldsymbol{w}^{\mathsf{p}})), \tag{6.20}$$

where $\tilde{\rho}(\boldsymbol{w}^{\mathsf{p}}) = [\tilde{\rho}_{i,j}(\boldsymbol{w}^{\mathsf{p}})]_{(i,j)\in\mathcal{I}\times\mathcal{J}}$ with

$$\begin{aligned}
\tilde{\rho}_{i,j}(\boldsymbol{w}^{\mathsf{p}}) &:= \log(1 + |\langle \boldsymbol{Q}^{\mathsf{p}}_{i,j}, H_{i,i,j}\rangle|^2/(\tilde{\Phi}_{i,j}(\boldsymbol{w}^{\mathsf{p}}) + \sigma^2)),\\
\tilde{\Phi}_{i,j}(\boldsymbol{w}^{\mathsf{p}}) &:= \sum_{(n,k)\in\mathcal{I}\times\mathcal{J}\setminus(i,j)} |\langle \boldsymbol{w}^{\mathsf{p}}_{n,k}, H_{n,i,j}\rangle|^2,\\
\widetilde{\mathcal{W}}^{\mathsf{p}}_B &= \{[\boldsymbol{w}^{\mathsf{p}}_{i,j}]_{(i,j)\in\mathcal{I}\times\mathcal{J}} \ : \ \textstyle\sum_{j\in\mathcal{J}} |\boldsymbol{w}^{\mathsf{p}}_{i,j}|^2 \leq P_B, i \in \mathcal{I}\}.
\end{aligned}$$

Under the selected pairing map a, it follows from Theorem 4 that the max sum rate and maximin rate problems can be formulated as

$$\max_{\boldsymbol{w}} \ \varphi(\tilde{r}(\boldsymbol{w})) \ : \ \boldsymbol{w} \in \widetilde{\mathcal{W}}_B, \tag{6.21}$$

where $\tilde{r}(\boldsymbol{w}) =: [\tilde{r}_{i,j}(\boldsymbol{w})]_{(i,j)\in\mathcal{I}\times\mathcal{J}}$ and $\tilde{r}_{i,j}(\boldsymbol{w})$ are the following highly-nonlinear functions:

$$\tilde{r}_{i,j}(\boldsymbol{w}) := \tilde{r}^{\mathsf{p}}_{i,j}(\boldsymbol{w}) + \min\{\tilde{r}^{\mathsf{c}}_{i,j}(\boldsymbol{w}), \tilde{r}^{\mathsf{a}}_{a(i,j)}(\boldsymbol{w})\}. \tag{6.22}$$

Define $\boldsymbol{W} := [\boldsymbol{w}^{\mathsf{p}}_{i,j}(\boldsymbol{w}^{\mathsf{p}}_{i,j})^H \quad \boldsymbol{w}^{\mathsf{c}}_{i,j}(\boldsymbol{w}^{\mathsf{c}}_{i,j})^H]_{(i,j)\in\mathcal{I}\times\mathcal{J}}$, and

$$\begin{aligned}
\tilde{r}^{\mathsf{p}}_{i,j}(\boldsymbol{w}) &= r^{\mathsf{p}}_{i,j}(\boldsymbol{W}),\\
\tilde{r}^{\mathsf{c}}_{i,j}(\boldsymbol{w}) &= r^{\mathsf{c}}_{i,j}(\boldsymbol{W}),\\
\tilde{r}^{\mathsf{a}}_{a(i,j)}(\boldsymbol{w}) &= r^{\mathsf{a}}_{a(i,j)}(\boldsymbol{W}).
\end{aligned}$$

Also define the following convex quadratic functions in $\boldsymbol{w}$:

$$\begin{aligned}
\widetilde{\mathcal{M}}^{\mathsf{c}}_{i,j}(\boldsymbol{w}) &= \mathcal{M}^{\mathsf{c}}_{i,j}(\boldsymbol{W}),\\
\widetilde{\mathcal{M}}^{\mathsf{a}}_{a(i,j)}(\boldsymbol{w}) &= \mathcal{M}^{\mathsf{a}}_{a(i,j)}(\boldsymbol{W}),\\
\widetilde{\mathcal{M}}^{\mathsf{p}}_{i,j}(\boldsymbol{w}) &= \mathcal{M}^{\mathsf{p}}_{i,j}(\boldsymbol{W}).
\end{aligned}$$

For the above highly-nonlinear optimization problems, it is very important to classify convex and nonconvex variables [16]. The following result shall be used later to clarify all complex terms $\widetilde{\mathcal{M}}^{\mathsf{c}}_{i,j}(\boldsymbol{w})$, $\widetilde{\mathcal{M}}^{\mathsf{a}}_{a(i,j)}(\boldsymbol{w})$ and $\widetilde{\mathcal{M}}^{\mathsf{p}}_{i,j}(\boldsymbol{w})$.

Theorem 6. *Introduce variables* $\boldsymbol{y}_{i,j} := [\boldsymbol{y}^{\mathsf{c}}_{i,j}, \boldsymbol{y}^{\mathsf{a}}_{a(i,j)}, \boldsymbol{y}^{\mathsf{p}}_{i,j}]_{(i,j)\in\mathcal{I}\times\mathcal{J}}$ *and* $\boldsymbol{y} = [\boldsymbol{y}_{i,j}]_{(i,j)\in\mathcal{I}\times\mathcal{J}}$, *which satisfy the convex inequality constraints:*

$$\begin{aligned}
\widetilde{\mathcal{M}}^{\mathsf{c}}_{i,j}(\boldsymbol{w}) &\le \boldsymbol{y}^{\mathsf{c}}_{i,j},\\
\widetilde{\mathcal{M}}^{\mathsf{a}}_{a(i,j)}(\boldsymbol{w}) &\le \boldsymbol{y}^{\mathsf{a}}_{a(i,j)},\\
\widetilde{\mathcal{M}}^{\mathsf{p}}_{i,j}(\boldsymbol{w}) &\le \boldsymbol{y}^{\mathsf{p}}_{i,j}, (i,j)\in\mathcal{I}\times\mathcal{J},
\end{aligned} \tag{6.23}$$

First define the following concave functions:

$$\begin{aligned}
\tilde{g}^{\mathsf{c}}_{i,j}(\boldsymbol{w}^{\mathsf{c}}_{i,j}, \boldsymbol{y}^{\mathsf{c}}_{i,j}) &= \log(1 + \tfrac{|\langle \boldsymbol{w}^{\mathsf{c}}_{i,j}, H_{i,i,j}\rangle|^2}{\boldsymbol{y}^{\mathsf{c}}_{i,j}+\sigma^2}) - \log(e)\tfrac{|\langle \boldsymbol{w}^{\mathsf{c}}_{i,j}, H_{i,i,j}\rangle|^2}{\boldsymbol{y}^{\mathsf{c}}_{i,j}+\sigma^2},\\
\tilde{f}^{\mathsf{c}}_{i,j}(\boldsymbol{w}^{\mathsf{c}}_{i,j}, \boldsymbol{y}^{\mathsf{c}}_{i,j}) &= -\log(e)\tfrac{|\langle \boldsymbol{w}^{\mathsf{c}}_{i,j}, H_{i,i,j}\rangle|^2}{\boldsymbol{y}^{\mathsf{c}}_{i,j}+\sigma^2},
\end{aligned}$$

$$\tilde{g}^{\mathsf{a}}_{i,j}(\boldsymbol{V}^{\mathsf{c}}_{i,j}, \boldsymbol{Y}^{\mathsf{a}}_{a(i,j)}) = \log(1 + \frac{|\langle \boldsymbol{w}^{\mathsf{c}}_{i,j}, H_{i,a(i,j)}\rangle|^2}{\boldsymbol{y}^{\mathsf{a}}_{a(i,j)} + \sigma^2}) - \frac{|\langle \boldsymbol{w}^{\mathsf{c}}_{i,j}, H_{i,a(i,j)}\rangle|^2}{\boldsymbol{y}^{\mathsf{a}}_{a(i,j)} + \sigma^2},$$

$$\tilde{f}^{\mathsf{a}}_{i,j}(\boldsymbol{w}^{\mathsf{c}}_{i,j}, \boldsymbol{y}^{\mathsf{a}}_{a(i,j)}) = -\log(e)\frac{|\langle \boldsymbol{w}^{\mathsf{c}}_{i,j}, H_{i,a(i,j)}\rangle|^2}{\boldsymbol{y}^{\mathsf{a}}_{a(i,j)} + \sigma^2},$$

$$\tilde{g}^{\mathsf{p}}_{i,j}(\boldsymbol{w}^{\mathsf{p}}_{i,j}, \boldsymbol{y}^{\mathsf{p}}_{i,j}) = \log(1 + \frac{|\langle \boldsymbol{w}^{\mathsf{p}}_{i,j}, H_{i,i,j}\rangle|^2}{\boldsymbol{y}^{\mathsf{p}}_{i,j} + \sigma^2}) - \log(e)\frac{|\langle \boldsymbol{w}^{\mathsf{p}}_{i,j}, H_{i,i,j}\rangle|^2}{\boldsymbol{y}^{\mathsf{p}}_{i,j} + \sigma^2},$$

$$\tilde{f}^{\mathsf{p}}_{i,j}(\boldsymbol{w}^{\mathsf{p}}_{i,j}, \boldsymbol{y}^{\mathsf{p}}_{i,j}) = -\log(e)\frac{|\langle \boldsymbol{w}^{\mathsf{p}}_{i,j}, H_{i,i,j}\rangle|^2}{\boldsymbol{y}^{\mathsf{p}}_{i,j} + \sigma^2}.$$

Then problem (6.21) is equivalent to the following convex constrained problem:

$$\max_{\boldsymbol{w},\boldsymbol{y}} \varphi(h(\boldsymbol{w}, \boldsymbol{y})) \ : \ \boldsymbol{w} \in \widetilde{\mathcal{W}}_B, (6.23) \tag{6.24}$$

where $h(\boldsymbol{w}, \boldsymbol{y}) = [h_{i,j}(\boldsymbol{w}, \boldsymbol{y})]_{(i,j)\in\mathcal{I}\times\mathcal{J}}$, *and*

$$\begin{aligned}
h_{i,j}(\boldsymbol{w}, \boldsymbol{y}) &:= \tilde{\varphi}^{\mathsf{p}}_{i,j}(\boldsymbol{w}^{\mathsf{p}}_{i,j}, \boldsymbol{y}^{\mathsf{p}}_{i,j}) + \min\{\tilde{\varphi}^{\mathsf{c}}_{i,j}(\boldsymbol{w}^{\mathsf{c}}_{i,j}, \boldsymbol{y}^{\mathsf{c}}_{i,j}), \tilde{\varphi}^{\mathsf{a}}_{a(i,j)}(\boldsymbol{w}^{\mathsf{c}}_{i,j}, \boldsymbol{y}^{\mathsf{a}}_{a(i,j)})\},\\
\tilde{\varphi}^{\mathsf{c}}_{i,j}(\boldsymbol{w}^{\mathsf{c}}_{i,j}, \boldsymbol{y}^{\mathsf{c}}_{i,j}) &:= \log(1 + \frac{|\langle \boldsymbol{w}^{\mathsf{c}}_{i,j}, H_{i,i,j}\rangle|^2}{\boldsymbol{y}^{\mathsf{c}}_{i,j} + \sigma^2})\\
&= \tilde{g}^{\mathsf{c}}_{i,j}(\boldsymbol{w}, \boldsymbol{y}^{\mathsf{c}}_{i,j}) - \tilde{f}^{\mathsf{c}}_{i,j}(\boldsymbol{w}, \boldsymbol{y}^{\mathsf{c}}_{i,j}),\\
\tilde{\varphi}^{\mathsf{a}}_{a(i,j)}(\boldsymbol{w}^{\mathsf{c}}_{i,j}, \boldsymbol{y}^{\mathsf{a}}_{a(i,j)}) &:= \log(1 + \frac{|\langle \boldsymbol{w}^{\mathsf{c}}_{i,j}, H_{i,a(i,j)}\rangle|^2}{\boldsymbol{y}^{\mathsf{a}}_{a(i,j)} + \sigma^2})\\
&= \tilde{g}^{\mathsf{a}}_{i,j}(\boldsymbol{w}, \boldsymbol{y}^{\mathsf{a}}_{a(i,j)}) - \tilde{f}^{\mathsf{a}}_{i,j}(\boldsymbol{w}, \boldsymbol{y}^{\mathsf{a}}_{a(i,j)}),\\
\tilde{\varphi}^{\mathsf{p}}_{i,j}(\boldsymbol{w}^{\mathsf{p}}_{i,j}, \boldsymbol{y}^{\mathsf{c}}_{i,j}) &:= \log(1 + \frac{|\langle \boldsymbol{w}^{\mathsf{p}}_{i,j}, H_{i,i,j}\rangle|^2}{\boldsymbol{y}^{\mathsf{p}}_{i,j} + \sigma^2})\\
&= \tilde{g}^{\mathsf{p}}_{i,j}(\boldsymbol{w}, \boldsymbol{y}^{\mathsf{p}}_{i,j}) - \tilde{f}^{\mathsf{p}}_{i,j}(\boldsymbol{w}, \boldsymbol{y}^{\mathsf{p}}_{i,j}).
\end{aligned} \tag{6.25}$$

Proof: The proof of the equivalence between (6.21) and (6.24) is similar to the proof of Theorem 4. The concavity of the concerned functions follow from [10, Lemma 1]. □

Next, one has the following sequential d.c. representations:

- $\min\{\tilde{\varphi}^{\mathsf{c}}_{i,j}(\boldsymbol{w}^{\mathsf{c}}_{i,j},\boldsymbol{y}^{\mathsf{c}}_{i,j}),\tilde{\varphi}^{\mathsf{a}}_{a(i,j)}(\boldsymbol{w}^{\mathsf{c}}_{i,j},\boldsymbol{y}^{\mathsf{a}}_{a(i,j)})\} = \tilde{g}^{\mathsf{ca}}_{i,j}(\boldsymbol{w}^{\mathsf{c}}_{i,j},\boldsymbol{y}^{\mathsf{c}}_{i,j},\boldsymbol{y}^{\mathsf{a}}_{a(i,j)}) - \tilde{f}^{\mathsf{ca}}_{i,j}(\boldsymbol{w}^{\mathsf{c}}_{i,j},\boldsymbol{y}^{\mathsf{c}}_{i,j},\boldsymbol{y}^{\mathsf{a}}_{a(i,j)})$ for

$$\begin{aligned}
\tilde{g}^{\mathsf{ca}}_{i,j}(\boldsymbol{w}^{\mathsf{c}}_{i,j},\boldsymbol{y}^{\mathsf{c}}_{i,j},\boldsymbol{y}^{\mathsf{a}}_{a(i,j)}) &:= \min\{\tilde{g}^{\mathsf{c}}_{i,j}(\boldsymbol{w}^{\mathsf{c}}_{i,j},\boldsymbol{y}^{\mathsf{c}}_{i,j}) + \tilde{f}^{\mathsf{a}}_{i,j}(\boldsymbol{w}^{\mathsf{c}}_{i,j},\boldsymbol{y}^{\mathsf{a}}_{a(i,j)}), \tilde{g}^{\mathsf{a}}_{i,j}(\boldsymbol{w},\boldsymbol{y}^{\mathsf{a}}_{a(i,j)}) + \tilde{f}^{\mathsf{c}}_{i,j}(\boldsymbol{w},\boldsymbol{y}^{\mathsf{c}}_{i,j})\},\\
\tilde{f}^{\mathsf{ca}}_{i,j}(\boldsymbol{w}^{\mathsf{c}}_{i,j},\boldsymbol{y}^{\mathsf{c}}_{i,j},\boldsymbol{y}^{\mathsf{a}}_{a(i,j)}) &:= \tilde{f}^{\mathsf{c}}_{i,j}(\boldsymbol{w},\boldsymbol{y}^{\mathsf{c}}_{i,j}) + \tilde{f}^{\mathsf{a}}_{i,j}(\boldsymbol{w},\boldsymbol{y}^{\mathsf{a}}_{a(i,j)}).
\end{aligned}$$

- $\tilde{\varphi}_{i,j}(\boldsymbol{w}_{i,j},\boldsymbol{y}_{i,j}) = \tilde{f}_{i,j}(\boldsymbol{w},\boldsymbol{y}) - \tilde{g}_{i,j}(\boldsymbol{w},\boldsymbol{y})$ for

$$\begin{aligned}
g_{i,j}(\boldsymbol{w},\boldsymbol{y}) &:= \tilde{g}^{\mathsf{p}}_{i,j}(\boldsymbol{w}^{\mathsf{p}}_{i,j},\boldsymbol{y}^{\mathsf{p}}_{i,j}) + \tilde{g}^{\mathsf{ca}}_{i,j}(\boldsymbol{w}^{\mathsf{c}}_{i,j},\boldsymbol{y}^{\mathsf{c}}_{i,j},\boldsymbol{y}^{\mathsf{a}}_{a(i,j)}),\\
\tilde{f}_{i,j}(\boldsymbol{w},\boldsymbol{y}) &:= \tilde{f}^{\mathsf{p}}_{i,j}(\boldsymbol{w}^{\mathsf{p}}_{i,j},\boldsymbol{y}^{\mathsf{p}}_{i,j}) + \tilde{f}^{\mathsf{ca}}_{i,j}(\boldsymbol{w}^{\mathsf{c}}_{i,j},\boldsymbol{y}^{\mathsf{c}}_{i,j},\boldsymbol{y}^{\mathsf{a}}_{a(i,j)}),
\end{aligned}$$

- $\min_{(i,j)\in\mathcal{I}\times\mathcal{J}}\tilde{\varphi}_{i,j}(\boldsymbol{w}_{i,j},\boldsymbol{y}_{i,j}) = \tilde{g}^{\mathsf{M}}(\boldsymbol{w},\boldsymbol{y}) - \tilde{f}(\boldsymbol{w},\boldsymbol{y})$ for

$$\begin{aligned}
\tilde{g}^{\mathsf{M}}(\boldsymbol{w},\boldsymbol{y}) &:= \min_{(i,j)\in\mathcal{I}\times\mathcal{J}}\left[\tilde{g}_{i,j}(\boldsymbol{w},\boldsymbol{y}) + \sum_{(n,k)\in\mathcal{I}\times\mathcal{J}\setminus(i,j)}\tilde{f}_{n,k}(\boldsymbol{w},\boldsymbol{y}))\right]\\
&= \min_{(i,j)\in\mathcal{I}\times\mathcal{J}}\left\{\tilde{g}^{\mathsf{p}}_{i,j}(\boldsymbol{w}^{\mathsf{p}}_{i,j},\boldsymbol{y}^{\mathsf{p}}_{i,j}) + \min\left\{\tilde{g}^{\mathsf{c}}_{i,j}(\boldsymbol{w}^{\mathsf{c}}_{i,j},\boldsymbol{y}^{\mathsf{c}}_{i,j}) + \tilde{f}^{\mathsf{a}}_{i,j}(\boldsymbol{w}^{\mathsf{c}}_{i,j},\boldsymbol{y}^{\mathsf{a}}_{a(i,j)}),\right.\right.\\
&\quad \left.\tilde{g}^{\mathsf{a}}_{i,j}(\boldsymbol{w}^{\mathsf{c}}_{i,j},\boldsymbol{y}^{\mathsf{a}}_{a(i,j)}) + \tilde{f}^{\mathsf{c}}_{i,j}(\boldsymbol{w}^{\mathsf{c}}_{i,j},\boldsymbol{y}^{\mathsf{c}}_{i,j})\right\}\\
&\quad \left. + \sum_{(n,k)\in\mathcal{I}\times\mathcal{J}\setminus(i,j)}(\tilde{f}^{\mathsf{c}}_{n,k}(\boldsymbol{w}^{\mathsf{c}}_{n,k},\boldsymbol{y}^{\mathsf{c}}_{n,k}) + \tilde{f}^{\mathsf{a}}_{n,k}(\boldsymbol{w}^{\mathsf{c}}_{n,k},\boldsymbol{y}^{\mathsf{a}}_{a(n,k)}) + \tilde{f}^{\mathsf{p}}_{n,k}(\boldsymbol{w}^{\mathsf{p}}_{n,k},\boldsymbol{y}^{\mathsf{p}}_{n,k}))\right\}\\
\tilde{f}(\boldsymbol{w},\boldsymbol{y}) &:= \sum_{(i,j)\in\mathcal{I}\times\mathcal{J}}\left[\tilde{f}^{\mathsf{c}}_{i,j}(\boldsymbol{w}^{\mathsf{c}}_{i,j},\boldsymbol{y}^{\mathsf{c}}_{i,j}) + \tilde{f}^{\mathsf{a}}_{i,j}(\boldsymbol{w}^{\mathsf{c}}_{i,j},\boldsymbol{y}^{\mathsf{a}}_{a(i,j)}) + \tilde{f}^{\mathsf{p}}_{i,j}(\boldsymbol{w}^{\mathsf{p}}_{i,j},\boldsymbol{y}^{\mathsf{p}}_{i,j})\right].
\end{aligned}$$

- $\sum_{(i,j)\in\mathcal{I}\times\mathcal{J}}\tilde{\varphi}_{i,j}(\boldsymbol{w}_{i,j},\boldsymbol{y}_{i,j}) = \tilde{g}^{\mathsf{S}}(\boldsymbol{w},\boldsymbol{y}) - \tilde{f}(\boldsymbol{w},\boldsymbol{y})$ for

$$\tilde{g}^{\mathsf{S}}(\boldsymbol{w},\boldsymbol{y}) = \sum_{(i,j)\in\mathcal{I}\times\mathcal{J}}\left[\tilde{g}^{\mathsf{p}}_{i,j}(\boldsymbol{w}^{\mathsf{p}}_{i,j},\boldsymbol{y}^{\mathsf{p}}_{i,j}) + \tilde{g}^{\mathsf{ca}}_{i,j}(\boldsymbol{w}^{\mathsf{c}}_{i,j},\boldsymbol{y}^{\mathsf{c}}_{i,j},\boldsymbol{y}^{\mathsf{a}}_{a(i,j)})\right].$$

Based on the above sequential d.c. representations we obtain the following result.

Theorem 7. For $\tilde{g}(\boldsymbol{w},\boldsymbol{y}) = \tilde{g}^{\mathsf{S}}(\boldsymbol{w},\boldsymbol{y}) \vee \tilde{g}^{\mathsf{M}}(\boldsymbol{w},\boldsymbol{y})$*, problem (6.21) is the following semi-definite constrained d.c. function maximisation*

$$\max_{\boldsymbol{w},\boldsymbol{y}}\ [\tilde{g}(\boldsymbol{w},\boldsymbol{y}) - \tilde{f}(\boldsymbol{w},\boldsymbol{y})]\ :\ \boldsymbol{w}\in\widetilde{\mathcal{W}}_B, (6.23), \tag{6.26}$$

where function $\tilde{f}(\boldsymbol{w},\boldsymbol{y})$ is concave and smooth while function $\tilde{g}(\boldsymbol{w},\boldsymbol{y})$ is concave but non-smooth.

Program (6.26) is in the form of (5.7) with $\boldsymbol{z} \to (\boldsymbol{w},\boldsymbol{y})$, $\mathcal{D} \to \{(\boldsymbol{w},\boldsymbol{y}) \ : \ \boldsymbol{w} \in \widetilde{\mathcal{W}}_B, (6.23)\}$, $G(\boldsymbol{z}) \to \tilde{g}(\boldsymbol{w},\boldsymbol{y})$ and $F(\boldsymbol{z}) \to \tilde{f}(\boldsymbol{w},\boldsymbol{y})$. Accordingly, initialized from a feasible solution $(w^{(0)}, y^{(0)})$ of (6.26), κ-iteration (5.8) for $\kappa = 1, 2, \ldots,$ generates a feasible solution $(w^{(\kappa+1)}, y^{(\kappa+1)})$ by solving the convex program

$$\max_{\boldsymbol{w},\boldsymbol{y}} \ [\tilde{g}(\boldsymbol{w},\boldsymbol{y}) - \tilde{f}(w^{(\kappa)}, y^{(\kappa)}) - \langle \nabla \tilde{f}(w^{(\kappa)}, y^{(\kappa)}), (\boldsymbol{w},\boldsymbol{y}) - (w^{(\kappa)}, y^{(\kappa)} \rangle] \ : \ \boldsymbol{w} \in \widetilde{\mathcal{W}}_B, (6.23). \quad (6.27)$$

The gradient $\langle \nabla \tilde{f}(w^{(\kappa)}, y^{(\kappa)}), (\boldsymbol{w},\boldsymbol{y}) - (w^{(\kappa)}, y^{(\kappa)}) \rangle$ can be easily calculated from Equation (B.2) in Appendix B.

Although (6.27) is a convex program, it is still not easily solved by existing convex solvers. Thus, for computationally-efficient implementation of (6.27) by existing convex solvers, we next introduce slack variables $\boldsymbol{t}_{i,j} := (\boldsymbol{t}^{\mathsf{c}}_{i,j}, \boldsymbol{t}^{\mathsf{a}}_{a(i,j)}, \boldsymbol{t}^{\mathsf{p}}_{i,j})$, $\boldsymbol{t} := [\boldsymbol{t}_{i,j}]_{(i,j)\in\mathcal{I}\times\mathcal{J}}$. These variables satisfy the following semi-definite constraints

$$\begin{array}{rcl} \frac{|\langle \boldsymbol{w}^{\mathsf{c}}_{i,j}, H_{i,i,j} \rangle|^2}{\boldsymbol{y}^{\mathsf{c}}_{i,j} + \sigma^2} & \leq & \boldsymbol{t}^{\mathsf{c}}_{i,j}, \\ \frac{|\langle \boldsymbol{w}^{\mathsf{c}}_{i,j}, H_{i,a(i,j)} \rangle|^2}{\boldsymbol{y}^{\mathsf{a}}_{a(i,j)} + \sigma^2} & \leq & \boldsymbol{t}^{\mathsf{a}}_{a(i,j)}, \\ \frac{|\langle \boldsymbol{w}^{\mathsf{p}}_{i,j}, H_{i,i,j} \rangle|^2}{\boldsymbol{y}^{\mathsf{p}}_{i,j} + \sigma^2} & \leq & \boldsymbol{t}^{\mathsf{p}}_{i,j}, (i,j) \in \mathcal{I} \times \mathcal{J} \end{array} \quad (6.28)$$

and the self-concordant functions:

$$\begin{array}{rcl} \tilde{g}^{\mathsf{cc}}_{i,j}(\boldsymbol{t}^{\mathsf{c}}_{i,j}, \boldsymbol{y}^{\mathsf{c}}_{i,j}) & = & \log(1 + \boldsymbol{t}^{\mathsf{c}}_{i,j}) - \log(e)\boldsymbol{t}^{\mathsf{c}}_{i,j}, \\ \tilde{f}^{\mathsf{cc}}_{i,j}(\boldsymbol{t}^{\mathsf{c}}_{i,j}, \boldsymbol{y}^{\mathsf{c}}_{i,j}) & = & -\log(e)\boldsymbol{t}^{\mathsf{c}}_{i,j}, \\ \tilde{g}^{ac}_{i,j}(\boldsymbol{t}^{\mathsf{a}}_{i,a(i,j)}, \boldsymbol{y}^{\mathsf{a}}_{a(i,j)}) & = & \log(1 + \boldsymbol{t}^{\mathsf{a}}_{a(i,j)}) - \log(e)\boldsymbol{t}^{\mathsf{a}}_{a(i,j)}, \\ \tilde{f}^{ac}_{i,j}(\boldsymbol{t}^{\mathsf{a}}_{i,a(i,j)}, \boldsymbol{y}^{\mathsf{a}}_{a(i,j)}) & = & -\log(e)\boldsymbol{t}^{\mathsf{a}}_{a(i,j)}, \\ \tilde{g}^{\mathsf{pc}}_{i,j}(\boldsymbol{t}^{\mathsf{p}}_{i,j}, \boldsymbol{y}^{\mathsf{p}}_{i,j}) & = & \log(1 + \boldsymbol{t}^{\mathsf{p}}_{i,j}) - \log(e)\boldsymbol{t}^{\mathsf{p}}_{i,j}, \\ \tilde{f}^{\mathsf{pc}}_{i,j}(\boldsymbol{t}^{\mathsf{p}}_{i,j}, \boldsymbol{y}^{\mathsf{p}}_{i,j}) & = & -\log(e)\boldsymbol{t}^{\mathsf{p}}_{i,j}. \end{array}$$

Accordingly,

$$\begin{aligned}\tilde{g}^{\mathsf{c}}(\boldsymbol{t},\boldsymbol{y}) \quad := \quad & \min_{(i,j)\in\mathcal{I}\times\mathcal{J}}\Big\{\tilde{g}^{\mathsf{pc}}_{i,j}(\boldsymbol{t}^{\mathsf{p}}_{i,j},\boldsymbol{y}^{\mathsf{p}}_{i,j}) + \min\Big\{\tilde{g}^{\mathsf{cc}}_{i,j}(\boldsymbol{t}^{\mathsf{c}}_{i,j},\boldsymbol{y}^{\mathsf{c}}_{i,j}) + \tilde{f}^{ac}_{i,j}(\boldsymbol{t}^{\mathsf{a}}_{a(i,j)},\boldsymbol{y}^{\mathsf{a}}_{a(i,j)}),\\ & \tilde{g}^{ac}_{i,j}(\boldsymbol{t}^{\mathsf{a}}_{a(i,j)},\boldsymbol{y}^{\mathsf{a}}_{a(i,j)}) + \tilde{f}^{\mathsf{cc}}_{i,j}(\boldsymbol{t}^{\mathsf{c}}_{i,j},\boldsymbol{y}^{\mathsf{c}}_{i,j})\Big\}\\ & + \sum_{(n,k)\in\mathcal{I}\times\mathcal{J}\setminus(i,j)}\Big(\tilde{f}^{\mathsf{cc}}_{n,k}(\boldsymbol{t}^{\mathsf{c}}_{n,k},\boldsymbol{y}^{\mathsf{c}}_{\tilde{i},\tilde{j}}) + \tilde{f}^{ac}_{n,k}(\boldsymbol{t}^{\mathsf{a}}_{a(n,k)},\boldsymbol{y}^{\mathsf{a}}_{a(\tilde{i},\tilde{j})}) + \tilde{f}^{\mathsf{pc}}_{n,k}(\boldsymbol{t}^{\mathsf{p}}_{\tilde{i},\tilde{j}},\boldsymbol{y}^{\mathsf{p}}_{n,k})\Big)\Big\}.\end{aligned}$$

The convex program (6.27) is equivalent to the following convex computationally-tractable program:

$$\max_{\boldsymbol{w},\boldsymbol{t},\boldsymbol{y}}\Big[\tilde{g}^{\mathsf{c}}(\boldsymbol{t},\boldsymbol{y}) - \tilde{f}(w^{(\kappa)},y^{(\kappa)}) - \langle\nabla f(w^{(\kappa)},y^{(\kappa)}),(\boldsymbol{w},\boldsymbol{y}) - (w^{(\kappa)},y^{(\kappa)})\rangle\Big] \;:\; \boldsymbol{w}\in\widetilde{\mathcal{W}}_B, (6.23), (6.28). \tag{6.29}$$

Likewise, (6.20) can be equivalently converted into the canonical d.c. (difference of concave functions) program (5.7) with $\boldsymbol{z}\to(\boldsymbol{w}^{\mathsf{p}},\boldsymbol{y}^{\mathsf{p}})$, $\mathcal{D}\to\{(\boldsymbol{w}^{\mathsf{p}},\boldsymbol{y}^{\mathsf{p}}) \;:\; \boldsymbol{w}^{\mathsf{p}}\in\widetilde{\mathcal{W}}^{\mathsf{p}}_B, \tilde{\Phi}_{i,j}(\boldsymbol{w}^{\mathsf{p}})\le\boldsymbol{y}^{\mathsf{p}}_{i,j}, (i,j)\in\mathcal{I}\times\mathcal{J}\}$ and

$$\begin{aligned}F(\boldsymbol{z}) \quad &\to \quad \tilde{f}^{\mathsf{p}}(\boldsymbol{w}^{\mathsf{p}},\boldsymbol{y}^{\mathsf{p}}) := \sum_{(i,j)\in\mathcal{I}\times\mathcal{J}}\tilde{f}^{\mathsf{p}}_{i,j}(\boldsymbol{w}^{\mathsf{p}}_{i,j},\boldsymbol{y}^{\mathsf{p}}_{i,j}),\\ G(\boldsymbol{z}) \quad &\to \quad \tilde{g}^{\mathsf{pS}}(\boldsymbol{w}^{\mathsf{p}},\boldsymbol{y}^{\mathsf{p}}) := \sum_{(i,j)\in\mathcal{I}\times\mathcal{J}}\tilde{g}^{\mathsf{p}}_{i,j}(\boldsymbol{w}^{\mathsf{p}}_{i,j},\boldsymbol{y}^{\mathsf{p}}_{i,j})\\ &\vee \quad \tilde{g}^{\mathsf{pM}}(\boldsymbol{w}^{\mathsf{p}},\boldsymbol{y}^{\mathsf{p}}) := \min_{(i,j)\in\mathcal{I}\times\mathcal{J}}\Big[\tilde{g}^{\mathsf{p}}_{i,j}(\boldsymbol{w}^{\mathsf{p}},\boldsymbol{y}^{\mathsf{p}}) + \sum_{(n,k)\in\mathcal{I}\times\mathcal{J}\setminus(i,j)}\tilde{f}^{\mathsf{p}}_{n,k}(\boldsymbol{w}^{\mathsf{p}},\boldsymbol{y}^{\mathsf{p}}))\Big].\end{aligned}$$

Therefore it can also be solved by the DCIs described before. The gradient $\langle\nabla\tilde{f}^{\mathsf{p}}(w^{\mathsf{p}(\kappa)},y^{\mathsf{p}(\kappa)}),(\boldsymbol{w}^{\mathsf{p}},\boldsymbol{y}^{\mathsf{p}}) - (w^{\mathsf{p}(\kappa)},y^{\mathsf{p}(\kappa)})\rangle$ can also be easily calculated as Equation (B.2) in Appendix. B.

In summary, our approach toward finding the solution of (6.9) is as follows.

- Use DCIs to find optimized solution $w^{\mathsf{p}(0)}$ of the coordinated covariance matrix problem (6.20);
- Use $w^{\mathsf{p}(0)}$ to determine the pairing strategy $a_{\mathcal{L}}$;

- Use DCIs to find optimized solution w of (6.21)/(6.26).

6.5 Simulation Results

Except for the two deterministic simulation cases presented in subsection 6.5.1.1, all other Monte-Carlo simulation results are obtained by averaging over 200 random channel realisations. For the new common and private message splitting scheme (which shall be referred to in this section as the "new scheme"), the number of common user pairs is made equal to the total number of users ($\mathcal{L} = NK$). When $\mathcal{L} = 2$, there is only one pairing $a \in \mathcal{A}_2$. Otherwise, the pairing map $a \in \mathcal{A}_{NL}$ is then predetermined according to the procedure described at the beginning of Section 6.3 to form problems (6.14) and (6.21). Naturally, the conventional private-only message scheme, i.e., the conventional coordinate precoding/beamforming by (6.11) and (6.20) is referred to as "conventional scheme" with no message splitting. The computational tolerance in DCIs is set as $\epsilon = 10^{-5}$.

6.5.1 Covariance splitting

In this part, the SNR P_B/σ^2 is set to 30 dB, unless otherwise indicated. The initial feasible solutions for DCI are generated as follows:

- For $a(i,j) = (\hat{i},\hat{j}) \neq \emptyset$,

$$\begin{aligned} Q_{i,j}^{\mathsf{p}(0)} &= \beta\Big[\tfrac{\sigma^2 P_B}{KN_t}(I_{N_t} + H_{i,\hat{i},\hat{j}}^H H_{i,\hat{i},\hat{j}})^{-1} + Z\Big], \\ Q_{i,j}^{\mathsf{c}(0)} &= \beta\Big[\tfrac{P_B}{KN_t}(I_{N_t} - \sigma^2(I_{N_t} + H_{i,\hat{i},\hat{j}}^H H_{i,\hat{i},\hat{j}})^{-1}) + Z\Big], \end{aligned} \tag{6.30}$$

  where random matrix $Z \in \mathcal{S}_+^{N_t}$ and real factor $\beta \in (0,1)$ are added to avoid trapped local optimal solutions. The entries of Z are i.i.d. standard uniform random variables, while β ensures that the initial solution takes 10% of the available power. This setting keeps user (i,j)'s private message received by user $(\hat{i},\hat{j})$ below the noise level [6, 7, 59].

- For $a(i,j) = \emptyset$, user (i,j)'s private covariance matrix is

$$\boldsymbol{Q}_{i,j}^{\mathsf{p}(0)} = \arg \min_{\boldsymbol{Q}_{i,j}^{p} \in \mathcal{S}_{+}^{N_t}} \sum_{(n,k)\in\mathcal{I}\times\mathcal{J}\setminus(i,j)} \langle H_{i,n,k} \boldsymbol{Q}_{i,j}^{p} H_{i,n,k} \rangle : \langle \boldsymbol{Q}_{i,j}^{p} \rangle \geq \beta P_B / K. \tag{6.31}$$

This ensures that user (i,j) maintains its private message transmission at a certain power level while causing the minimal interference to other unintended receivers.

6.5.1.1 MIMO H-K network [6, Example 1] (Two examples)

There are two transmitters, each of them is equipped with $N_t = 2$ antennas. The first receiver has 3 antennas and the second receiver has 2 antennas. The BS power budget is normalized to $P_B = 1$ and the noise power is also normalized to $\sigma^2 = 1$. The channel strengths are given by $(\delta_{1,1}, \delta_{2,1}) = (20, 20)$ dB and $(\eta_{1,2}, \eta_{2,1}) = (8, 12)$ dB, respectively. The channel matrices are as given in [6, p. 4789]. In Fig. 6.1, the inner bounds are plotted by solving the linear inequalities [6, (52a)-(52i)] and the outer bounds by [6, (11)-(17)] (which are also shown in [6, Fig. 6b]). The joint decoding rates of obtained from successive decoding is calculated according to [9, (3)-(9)]. Numerical results are provided in Table 6.1 with the obtained solutions given by (B.3)-(B.5) in Appendix. B. The so-called $\mathcal{HK}^{(s1)}$ splitting scheme in [6] performs best among all schemes in [6] in terms of the sum rate, but it even does not perform better than the conventional scheme (with no message splitting). In terms of the minimal rate, the advantage of the new scheme is marginal. Therefore, splitting message is not beneficial in this specific example. The rates obtained by solving the optimal sum-rate and minimal rate problems are well outside the inner bound region. To see the benefit of the new scheme over the conventional one, we increase

TABLE 6.1: Rate performance for [6, Example 1].

		Sum rate (in bps/Hz)			Minimal rate (in bps/Hz)		
		private rates	common rates	sum rate	private rates	common rates	minimal rate
Conv. scheme	-	$(9.3409, 6.5278)$	-	15.8687	$(7.6581, 7.6581)$	-	7.6581
New scheme	Joint	same as above			$(6.0933, 5.9680)$	$(1.6464, 1.7717)$	7.7397
	Succ.	same as joint rates					
[6]	Joint	$(10.4210, 0.676)$	$(0, 3.3623)$	14.4593	$(3.8006, 1.8307)$	$(2.9388, 4.9087)$	6.7394
	Succ.	$(11.8524, 0.7030)$	$(0, 1.9039)$	14.4593	$(5.5637, 1.8432)$	$(2.9262, 3.1456)$	4.9888

the interfering channel strength $\eta_{2,1}$ from 12 dB to 19 dB, but keeping all other parameters

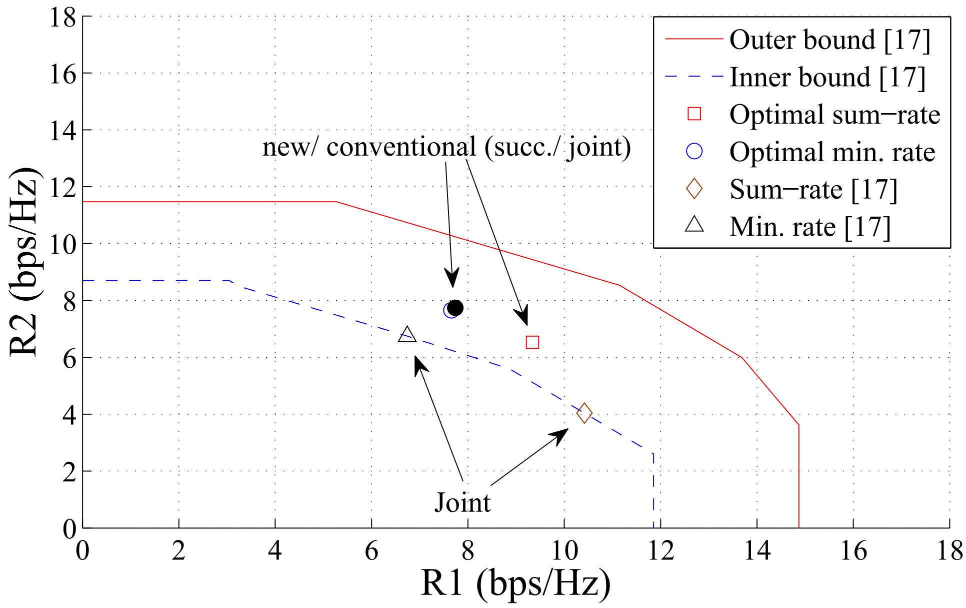

FIGURE 6.1: Rate region and achievable rates for [6, Example 1].

unchanged. The achievable rates are provided in Table 6.2 with the obtained solutions given by (B.6)-(B.9) in Appendix. B. The new scheme clearly enlarges the rate region when compared to that of the conventional scheme. The joint and successive decoding rates of the optimal solutions are almost the same, but the minimal rate obtained as in [6] drops significantly when changing from joint decoding to successive decoding.

TABLE 6.2: Rate performance for the modified example in subsection 6.5.1.1

		Sum rate (in bps/Hz)			Minimal rate (in bps/Hz)		
		private rates	common rates	sum rate	private rates	common rates	minimal rate
Conv. scheme	-	$(9.0907, 6.6317)$	-	15.7224	$(7.6407, 7.6407)$	-	7.6407
New scheme	Joint	$(9.1105, 0)$	$(2.8398, 5.8573)$	17.8076	$(6.4958, 3.5853)$	$(1.4584, 4.3689)$	7.9542
	Succ.	$(9.2143, 0)$	$(2.8398, 5.7535)$	17.8076	same as joint rates		
[6]	Joint	$(11.3856, 0.1608)$	$(0, 4.9788)$	16.5252	$(5.2993, 0.5518)$	$(2.1952, 6.9427)$	7.4945
	Succ.	$(11.8214, 0.1607)$	$(0, 4.5431)$	16.5252	$(5.5368, 0.5517)$	$(3.7025, 5.4355)$	5.9872

6.5.1.2 MIMO H-K network ($N = 2, K = 1, N_t = 4, N_r = 2$)

Next, the statistical performance of MIMO H-K networks is illustrated. To clarify the mechanism of the new scheme, following [7, 158], the direct channel gains are fixed at $(\delta_{1,1}, \delta_{2,1}) = (10\text{dB}, 20\text{dB})$, while the interfering channel gains $\eta_{1,2,1} = \eta_{2,1,1}$ are increased from -5dB to 20dB. This is depicted in Fig. 6.3. These gain values are set to represent one or multiple channel effects

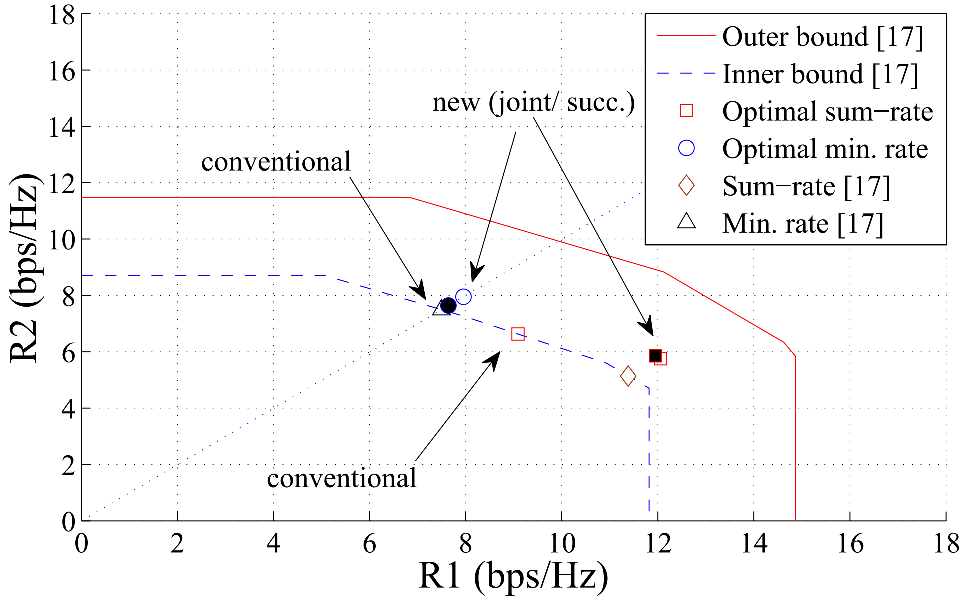

FIGURE 6.2: Rate region and achievable rates for the modified example in subsection 6.5.1.1

such as path loss which mainly depend on the specific environment and relative transmitter/receiver positions. The simulation scenarios thus vary from weak MIMO IC to mixed MIMO IC. Fig. 6.6 and Fig. 6.7 show the sum rates and the minimal rates versus the interfering channel gains, respectively. Under the conventional scheme, the interference is simply treated as noise so its achievable rates drop dramatically. In contrast, the benefit of decoded common messages in the new scheme actually amplifies as the interfering gains increase. The corresponding sum rates and minimal rates are seen improved in the presence of stronger interference.

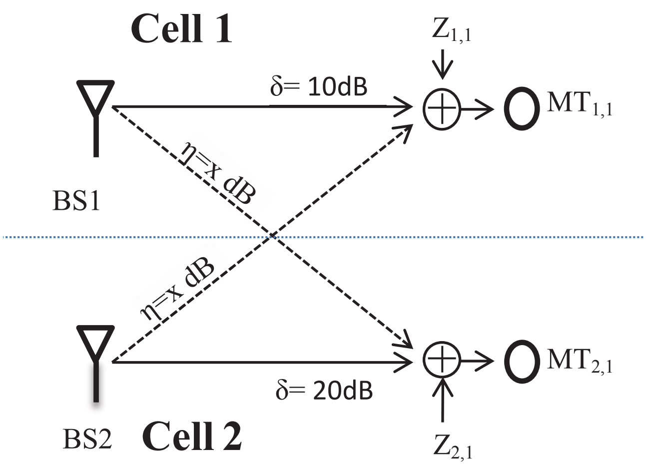

FIGURE 6.3: Network configuration I: $N = 2, K = 1, N_t = 4, N_r = 2$.

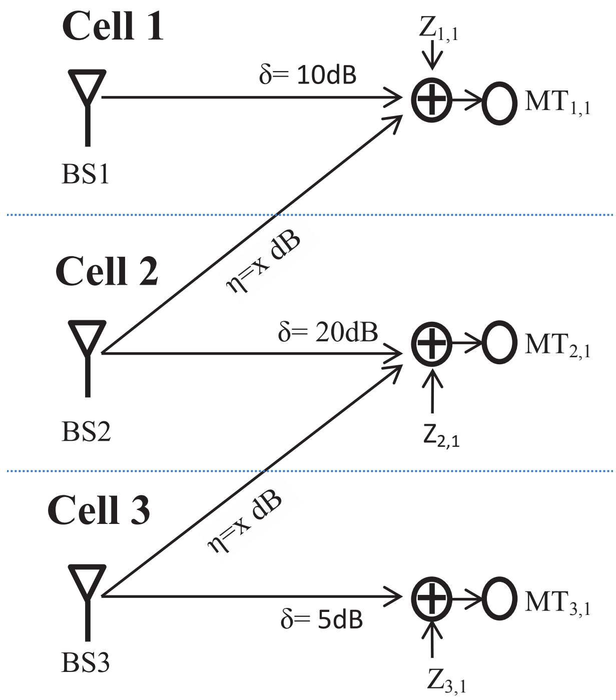

FIGURE 6.4: Network configuration II: $N = 3, K = 1, N_t = 4, N_r = 2$.

6.5.1.3 Three-user MIMO IC ($N = 3, K = 1, N_t = 4, N_r = 2$)

Fig. 6.4 depicts a 3-BS network where each BS serves only one user. As shown in Fig. 6.4, the interfering channels $\eta_{1,2,1} = \eta_{1,3,1} = \eta_{2,3,1} = \eta_{3,1,1}$ are virtually disabled by setting them to a very low value of -50dB, while the direct channel gains $(\delta_{1,1,1}, \delta_{2,2,1}, \delta_{3,3,1})$ are fixed at $(10\text{dB}, 20\text{dB}, 5\text{dB})$. The interfering channel gains $\eta_{2,1,1} = \eta_{3,2,1}$ are increased from -10 dB to 30 dB for testing different scenarios of interference strength. Under this setting, user 1 and user 2 suffer increasingly from inter-cell interference. The rate capacity of the conventional scheme shrinks as Fig. 6.8 and Fig. 6.9 show. In contrast, the new scheme is not only immune from any significant rate deterioration, but also improve the rate gains slightly. Again, the benefit of decoded common messages emerges as the level of interference increases.

6.5.1.4 Four-user MIMO IC ($N = 2, K = 2, N_t = 4, N_r = 2$)

As shown in Fig. 6.5, the direct channel gains $\delta_{1,1,1} = \delta_{2,2,1}$ and $\delta_{1,1,2} = \delta_{2,2,2}$ are, respectively, fixed at 10dB and 15dB, and the interfering channels $\eta_{2,1,1} = \eta_{2,1,2}$ are disabled by setting them

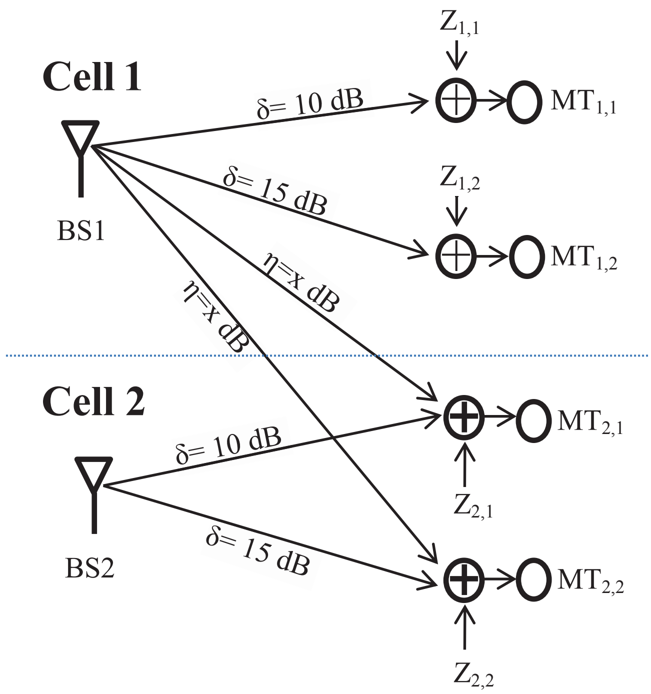

FIGURE 6.5: Network configuration III: $N = 2, K = 2, N_t = 4, N_r = 2$.

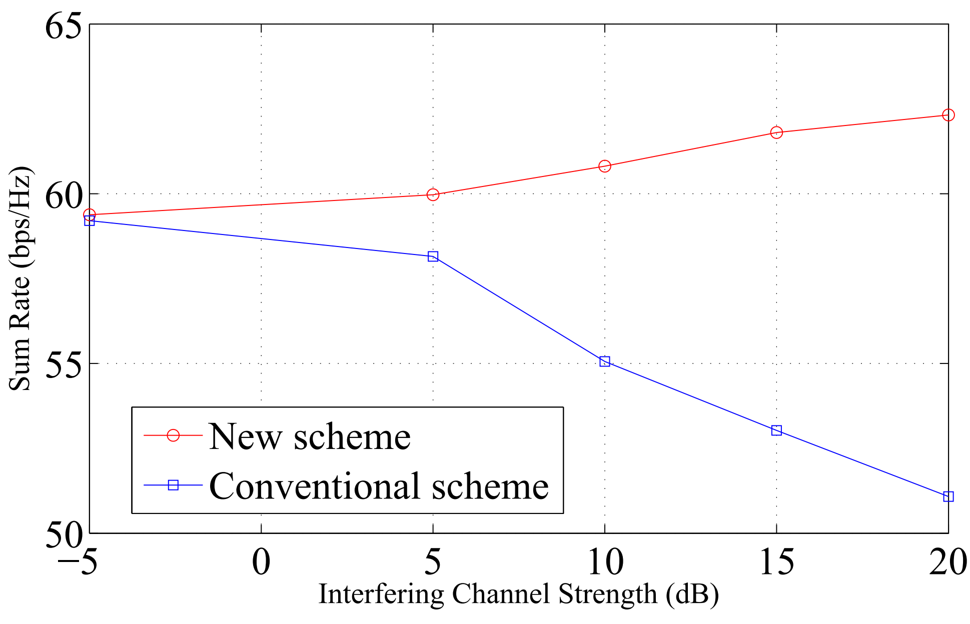

FIGURE 6.6: Sum rate vs. interfering channel strength $\eta_{2,1,1} = \eta_{1,2,1}$.

to −50dB. The interfering channel gains $\eta_{1,2,1} = \eta_{1,2,2}$ are increased from −10dB to 50dB. The new scheme is able to moderate the rate deterioration as inter-cell interference increases.

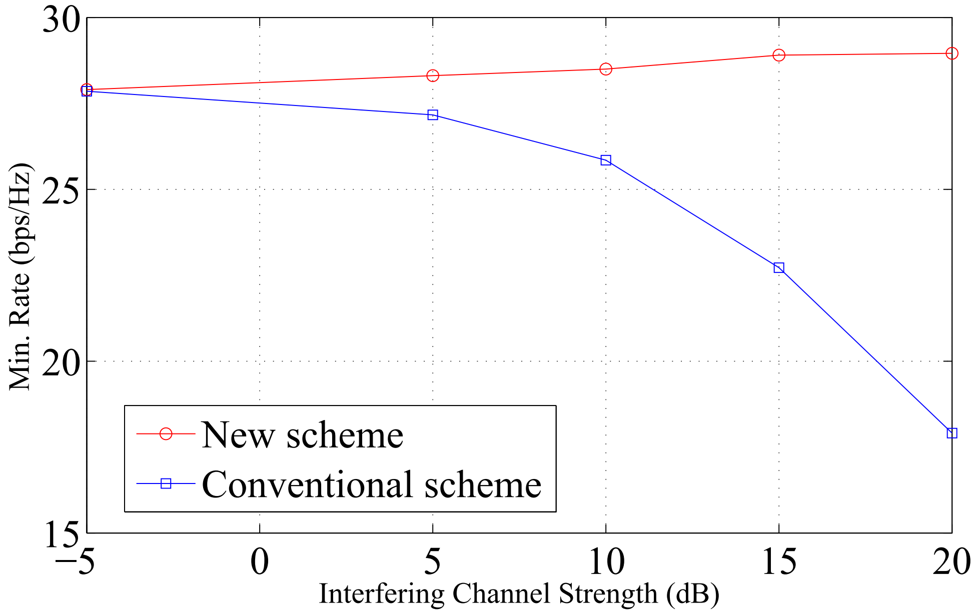

FIGURE 6.7: Minimal rate vs. interfering channel strength $\eta_{2,1,1} = \eta_{1,2,1}$.

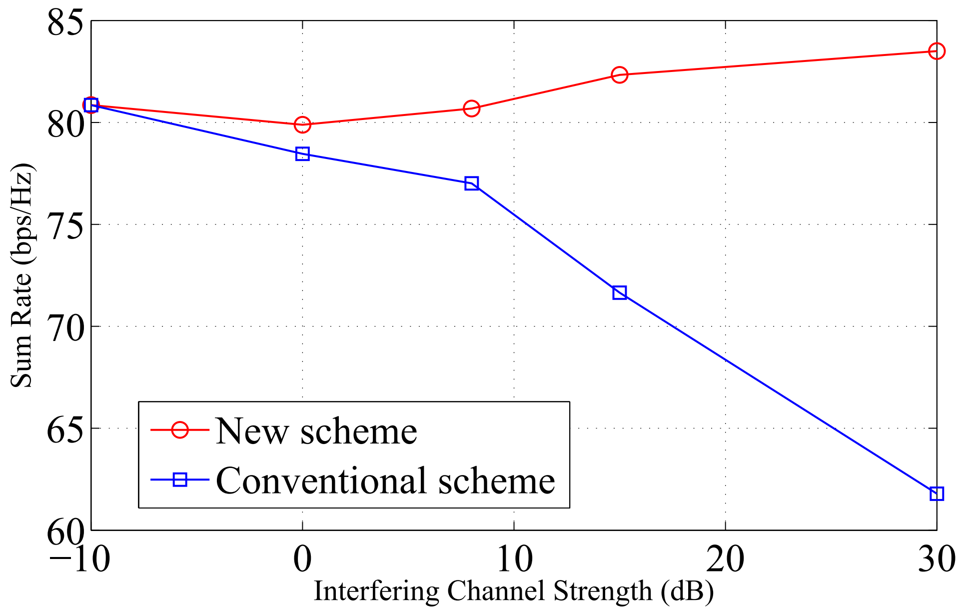

FIGURE 6.8: Sum rate vs. interfering channel strength $\eta_{2,1,1} = \eta_{3,2,1}$.

6.5.1.5 Computational experience

The first column block in Table 6.3 provides the number of d.c. iterations for all the MIMO networks investigated in this section. A typical convergence behavior for sum rate optimization ($N = 2, K = 2, N_t = 4, N_r = 2$) is given in Fig. 6.12, which is also a typical pattern for

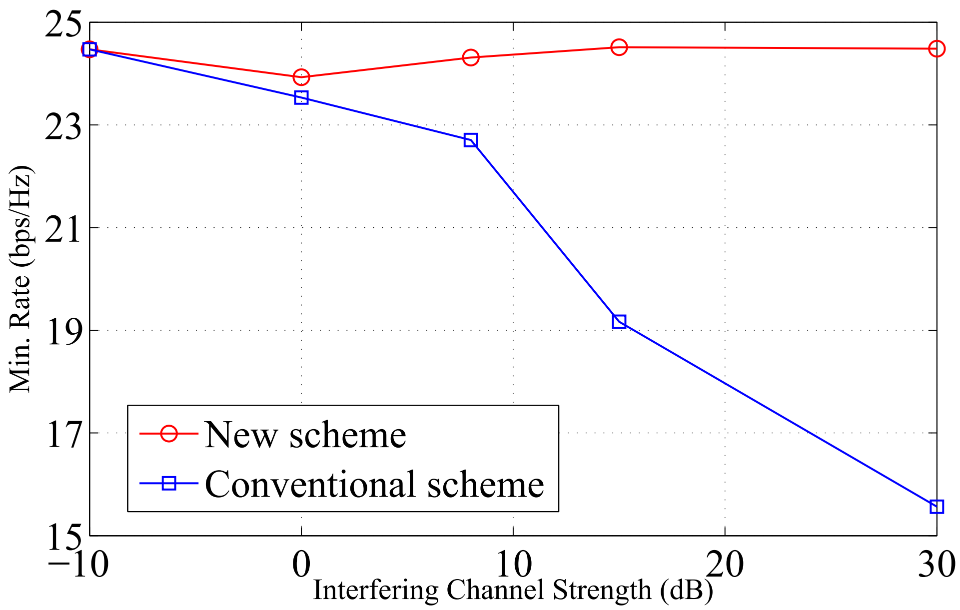

FIGURE 6.9: Minimal rate vs. interfering channel strength $\eta_{2,1,1} = \eta_{3,2,1}$).

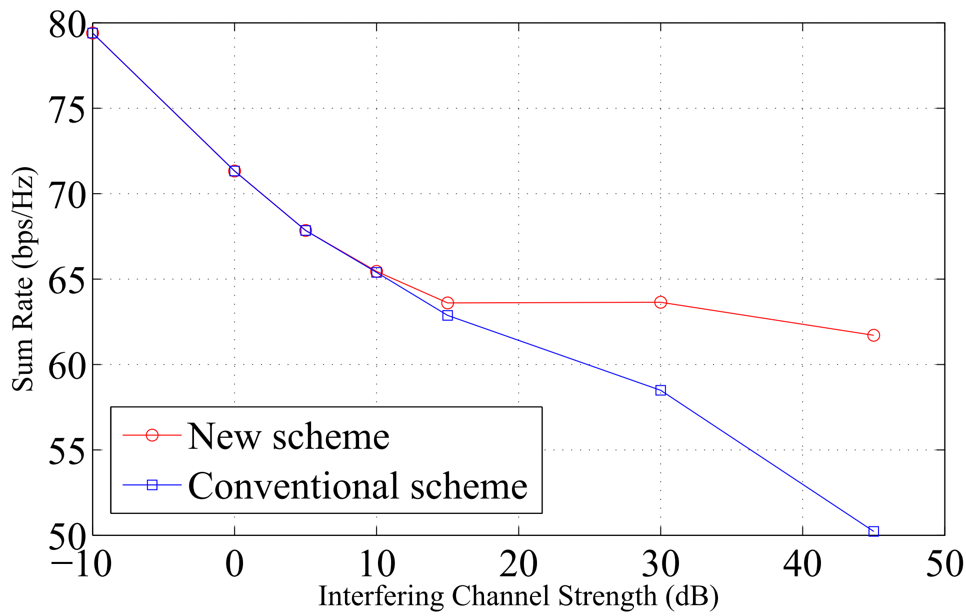

FIGURE 6.10: Sum rate vs. interfering channel strength $\eta_{1,2,1} = \eta_{1,2,2}$.

the minimal rate problem. Due to the complexity of the problem, DCI may experience a few slow-progressing stages but its solutions are always guaranteed to be iteratively improved.

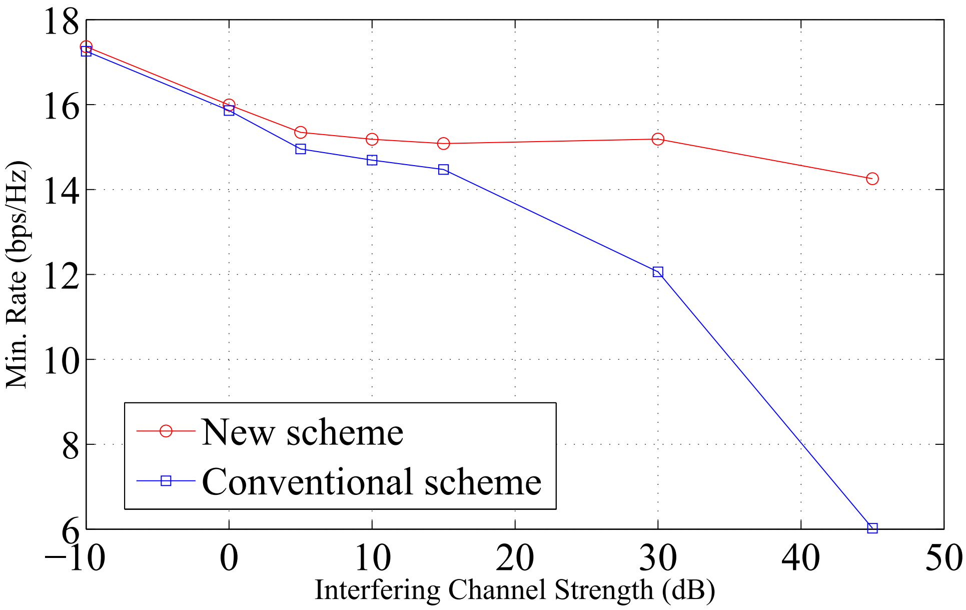

FIGURE 6.11: Minimal rate vs. interfering channel strength $\eta_{1,2,1} = \eta_{1,2,2}$.

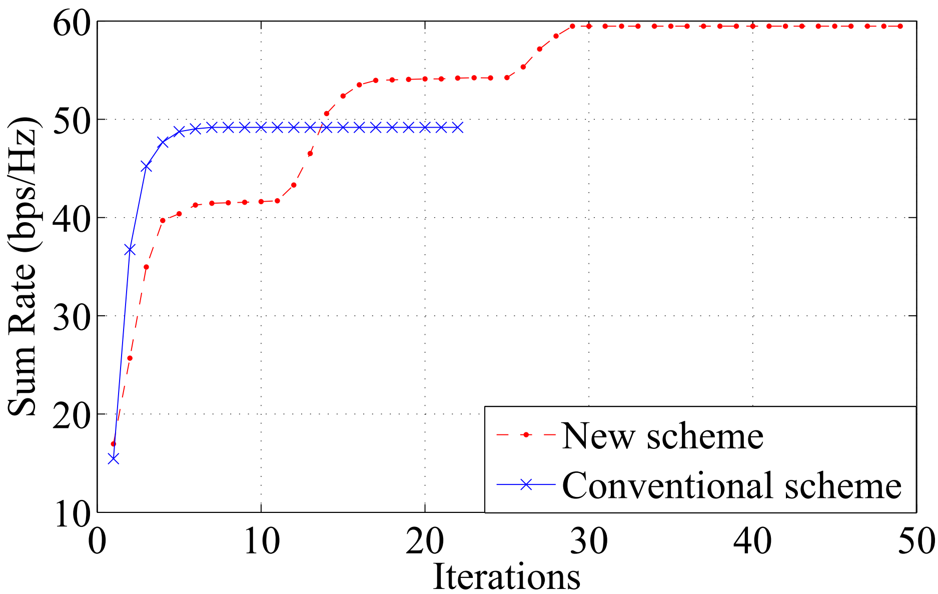

FIGURE 6.12: A typical DCI convergence pattern.

6.5.2 Beamforming splitting

Suppose $Q_{i,j}^{\mathsf{p}(0)}$ and $Q_{i,j}^{\mathsf{c}(0)}$ are the covariance matrix solution obtained by (6.30)-(6.31) with maximum eigenvalues $\lambda_{i,j}^{\mathsf{p}(0)}$ and $\lambda_{i,j}^{\mathsf{c}(0)}$) and corresponding eigenvectors ($v_{i,j}^{\mathsf{p}(0)}$ and $v_{i,j}^{\mathsf{c}(0)}$). Then the initial feasible solutions for implementing DCI are taken by $w^{\mathsf{p}(0)} = \sqrt{\lambda^{\mathsf{p}(0)}}v^{\mathsf{p}(0)}$ and $w^{\mathsf{c}(0)} = \sqrt{\lambda^{\mathsf{c}(0)}}v^{\mathsf{c}(0)}$.

6.5.2.1 Four-user MISO IC: $N = 2, K = 2, N_t = 4, N_r = 1$

The direct channel gains are all fixed at 5dB. The interfering channel gains $\eta_{1,2,1} = \eta_{1,2,2}$ vary from 0dB to 30dB while all other interfering channels are virtually removed by setting their gains to -50 dB. The SNR (P_B/σ^2) is set at 20dB. Fig. 6.13 and Fig. 6.14 depict the sum rate and minimal rate, respectively. The conventional scheme fails to maintain both sum rate and the worst user's rate because interference becomes dominating. On the contrary, the new scheme is able to maintain and even improve the rate metrics due to partially decoded interference by means of common messages.

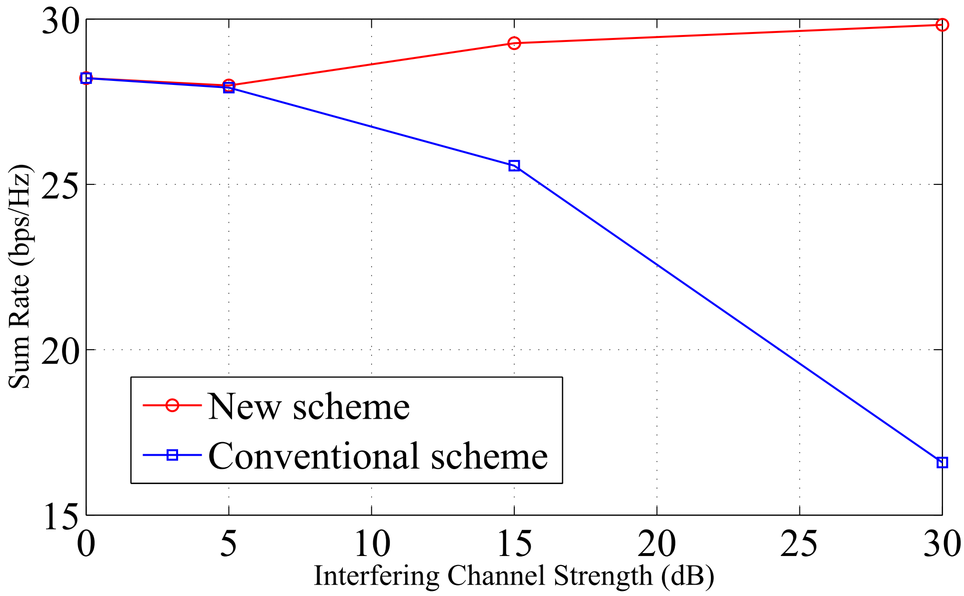

FIGURE 6.13: Sum rate vs. interfering channel strength $\eta_{1,2,1} = \eta_{1,2,2}$.

6.5.2.2 9-user MISO IC $(N = 3, K = 3, N_t = 4, N_r = 1)$

Consider a more practical three-cell network with three users per cell. The BSs are 1.4km apart from each other. The users are uniformly distributed within their respective cells. All channel assumptions are adopted from [9]. Although $a \in \mathcal{A}_9$ is predetermined, it should be emphasized that $a(i,j) \neq \emptyset$ does not mean that $\boldsymbol{Q}^{\mathsf{p}}_{i,j} \neq 0$ at the optimality of (6.14), so the actual number of active common message user pairs still varies from 0 to 9. Our investigation indicates that not

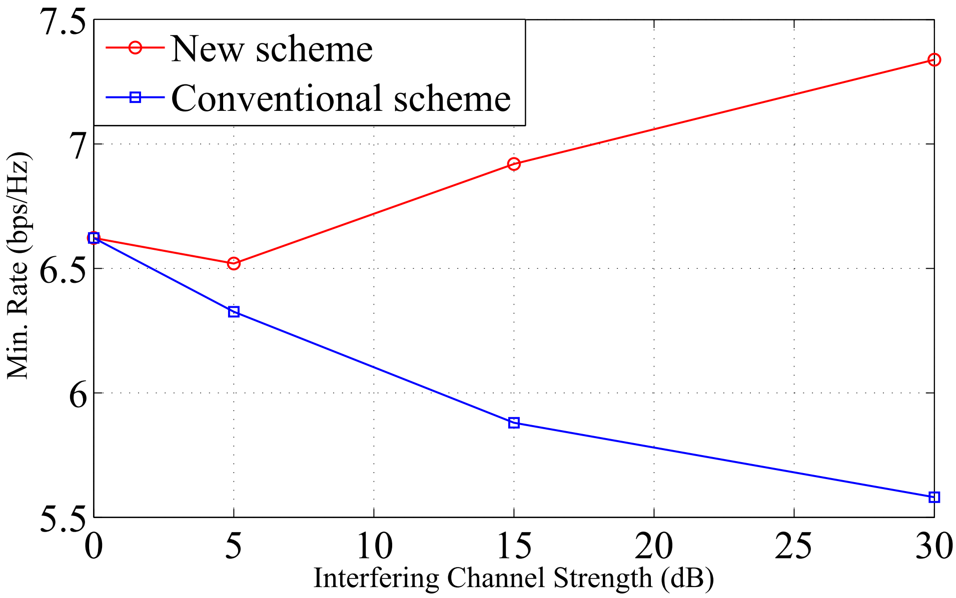

FIGURE 6.14: Minimal rate vs. interfering channel strength $\eta_{1,2,1} = \eta_{1,2,2}$.

more than 5 common user pairs are actually selected. Due to uniform user distribution and path fading/ shadowing effects, the data $(\eta, \delta, \frac{P_B}{\sigma^2})$ represents quite a complicated and unpredictable interference situation. It has been reported that the conventional scheme could achieve rate capacity for certain channel realizations [166]. We call a channel realisation "effective" if the rate achieved by the new scheme outperforms that by the conventional scheme by more than 1%. Otherwise, it is said to be "ineffective". Fig. 6.15 and Fig. 6.16 show the worst user's rates and sum rates versus BS power budgets, respectively. With $P_B = 30$dBm, effective channels account for 21.00% and 22.50% for the two problems, respectively. With the power budget increased to $P_B = 70$dBm, the numbers grow to 66.75% and 78.25%, accordingly. Clearly, the new scheme is more effective for higher-SNR regimes.

6.5.2.3 Computational experience

The second column block in Table 6.3 provides the numbers of DCIs (6.29) for all the MISO networks considered in this section. The numbers of SOCPs for solving the minimal rate maximisation for the MISO case are also included. The typical convergence behavior of DCI for beamforming design is similar to that presented in Fig. 6.12. Table 6.4 provides the number of SDP needed for feasibility check by the algorithm of Reference [9]. It is also noted that the performance of the algorithm in [9] strongly depends on the order of pairs picked for private message decoding.

6.6 Conclusions

This chapter studied the optimized transmission strategies for interference mitigation in multi-cell multi-user MIMO networks. The ability of splitting user massages into private and common messages to expand the achievable rate region has been well understood, but its optimization has never been adequately addressed. As an important contribution to addressing this issue, this research formulated the optimal rate split problem as a non-smooth d.c. objective function minimisation subject to convex constraints in the reduced space of the designed covariance matrix variables only. Then tailored DCI algorithms were provided which guarantee rate improvement after each iteration. In the presence of mild-to-strong interferences, comprehensive simulation results demonstrated significant rate gains obtained by the new message-splitting scheme for MIMO/MISO ICs. The results also showed that DCIs outperform the other existing methods and converge within a relatively low number of iterations.

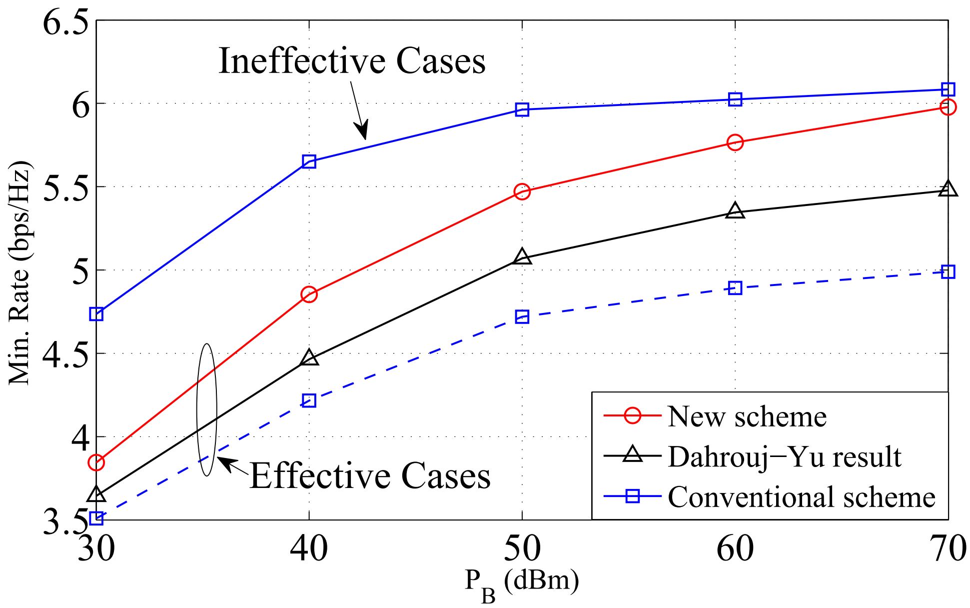

FIGURE 6.15: Power vs. minimal rate: beamforming design.

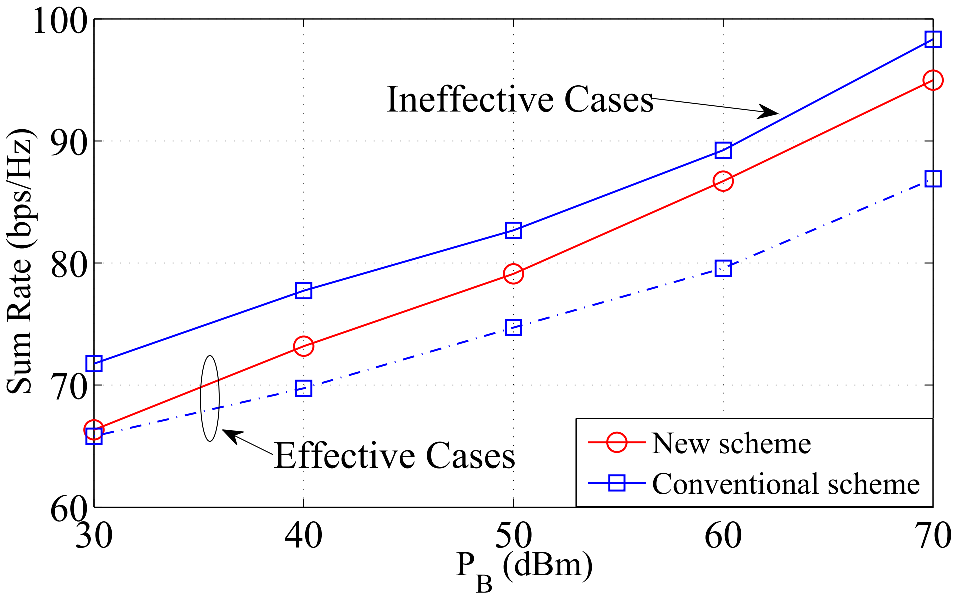

FIGURE 6.16: Power vs. sum rate: beamforming design.

TABLE 6.3: Average number of total d.c. iterations.

	MIMO IC			MISO IC	
	two-user	three-user	four-user	four-user	nine-user
Conventional Sum-Rate	11.53	14.26	16.28	10.89	16.49
New Sum-Rate	19.34	24.62	36.82	17.35	35.24
Conventional Min-Rate	12.92	17.76	19.02	12.04	18.12
New Min-Rate	22.01	27.17	44.29	20.13	38.12
Conventional Min-Rate by bisection	-	-	-	20.06	18.45

TABLE 6.4: Algorithmic statistics: total number of SDP calls by the procedure in [9].

Designed Number of Common User Pairs ($\mathcal{L}$)								
1	2	3	4	5	6	7	8	9
250.5	270.1	319.2	326.2	340.9	340.2	342.4	342.2	342.2

Chapter 7

Conclusion

In this chapter, a review of the main contributions of this dissertation shall be outlined. In general, the works in this dissertation address several challenging optimization designs with respect to continuous and/or binary link variables which represent cross-layer controllable resources of wireless systems. The main contributions of this thesis are three-fold:

- We observed that the binary link constraints are equivalent to the difference of two convex sets. Therefore, the non-tractable binary constraints can be converted to d.c. constraints in various forms. Based on this observation, the seemingly hard binary constraints are converted into more tractable forms.

- We proposed effective d.c. decompositions for the concerned non-convex objective functions and we proved the convexity of all member functions.

- Through the proof of strong Lagrangian duality, we showed that, the d.c. optimization of d.c. function over d.c., and/or convex and/or affine sets can be equivalently converted into a canonical d.c. optimization form where a d.c. function is optimized over convex and/or affine sets only. We further develop various locally optimal DCI algorithms which perform effectively with affordable computational complexity.

In Chapter 1, a brief introduction to the concerned works and an overview of interesting problems in the related fields was given.

In Chapter 2, we outlined some basic knowledge in wireless communications and optimization theory. In particular, a generic d.c. optimization framework was proposed for frequent exploitation in the following chapters.

In Chapter 3, a sensor network for spectrum sensing was studied. In achieving accurate sensing while prolonging the overall battery life of the entire sensor network, the least correlated group of sensors is to be selected. This design task embracing various correlation measure functions was unified in a Bregman matrix deviation-based framework. Despite the non-smoothness of the problem, we showed that it can be universally fit into the d.c. optimization framework and solved efficiently by the proposed DCI algorithm. Accompanying simulation results clearly showed the benefits of sensor selections and the effectiveness of the proposed algorithm.

In Chapter 4, we studied a relay-assisted multi-user wireless network. The relays were each assigned with binary link variables as well as beamforming variables. In both of orthogonal transmission and non-orthogonal transmission scenarios, the relays could be activated/deactivated for achieving optimal SNR or SINR fairness performance, respectively. This setting of self-organizing network enabled flexibility of the relay array and could reduce consumption power and communication overheads. We managed to represent the binary link variables in the form of d.c. constraints and proved the SNR and SINR functions are also explicit d.c. functions. We then proved that these general d.c. programs can be converted into a canonical d.c. program in the form of d.c. objective function over convex and/or affine sets. Therefore, efficient optimization procedures were proposed to jointly optimize the binary link variables and the beamforming variables under the d.c. optimization framework. The extensive simulation results demonstrated the viability of the novel relay selection scheme, as well as the efficiency of the proposed procedure.

In Chapter 5 & 6, we started by studying the optimized covariance and precoding matrix design in the conventional transmission scheme which treats interference as noise. The sum rate and minimal rate maximization problems were proved to be d.c. programs which could be handled effectively by the d.c. optimization techniques. Later, the focus of research was shifted to a novel transmission scheme which is based on the Han-Kobayashi message splitting [59] and successive decoding [9]. Inspired by the Han-Kobayashi scheme [7, 59] which was devised for the simplest 2-user SISO ICs, we split some users' messages into common and private messages for general MIMO interference networks which include MIMO IC as a special case. A brand-new non-smooth reformulation of the combined rate for each user was firstly proposed which is instrumental for all later developments. Pairing optimization is solved by a proposed heuristic algorithm separately due to the great difficulty of joint optimization in this case. Then, the hidden d.c. structure of the rate functions was revealed so the problems were subsequently converted into d.c. programs. In a similar fashion, path-following algorithms were proposed for these optimization tasks under the d.c. optimization framework which perform exceptionally well in finding optimized solutions. Through extensive simulation results, we showed the obvious benefits of this message-splitting scheme for some scenarios. As expected, its advantage over the conventional scheme generally relies on the strength of interferences. Therefore, this new scheme is particularly necessary for medium-/ strong-interference channels for which the conventional scheme is obviously unable to achieve rate capacity.

We noted that the original works by Han-Kobayashi [59] was done in the 2-user SISO interference channel which is a special case of MIMO and largely remains a puzzle today. Therefore, in Appendix C, we dedicated to this case and placed our achieved rate pairs for some deterministic channels in the rate region. By comparing them with the known inner bound, outer bounds and rate pairs achieved by other splitting methods, we were able to see the benefit of the proposed algorithm for more optimized and flexible power splits.

We also realized that, the conventional private message-only scheme which treats interference merely as interference, is also a special case of the new message-splitting scheme when all common messages are zero. Therefore, in addition to Chapter 5, we presented detailed studies in covariance design of cognitive MISO downlink networks in Appendix D. It was shown that the rate functions can also be interpreted as the difference of concave functions. Therefore, in the framework of d.c. programming, we were able to show a variant method based on concave programming for the considered cases. Compared to the generic d.c. programming based on convex functions, this change leads to easier iterative programs which pave the way to computationally-inexpensive closed-form solutions in some particular cases.

Appendix A

Proof for Proposition. 2

Suppose $\varphi(\mu)$ and (z^μ, x^μ) are the optimal value and optimal solution of the convex constrained program (2.17), so

$$\sup_{\mu\geq 0}\varphi(\mu) = \sup_{\mu\geq 0}\min_{(\boldsymbol{z},\boldsymbol{x})\in\mathcal{D}}\mathcal{L}(\boldsymbol{z},\boldsymbol{x},\mu) \leq \min_{(\boldsymbol{z},\boldsymbol{x})\in\mathcal{D}}\max_{\mu\geq 0}\mathcal{L}(\boldsymbol{z},\boldsymbol{x},\mu) = \min\ (2.15). \tag{A.1}$$

Note that $\sum_{n=1}^{N}\boldsymbol{x}_n - \sum_{n=1}^{N}\boldsymbol{x}_n^2 \geq 0\ \forall(\boldsymbol{z},\boldsymbol{x}) \in \mathcal{D}$ so function $\mathcal{L}(\boldsymbol{z},\boldsymbol{x},\mu)$ is increasing in μ for $(\boldsymbol{z},\boldsymbol{x}) \in \mathcal{D}$. This means $\varphi(\mu)$ is increasing in μ and bounded by the optimal value of program (2.15). If $\sum_{n=1}^{N}x_n^{\mu_0} - \sum_{n=1}^{N}(x_n^{\mu_0})^2 = 0$ for some $0 \leq \mu_0 < +\infty$ then (z^{μ_0}, x^{μ_0}) is feasible to (2.15), so

$$\varphi(\mu_0) = \mathcal{L}(z^{\mu_0}, x^{\mu_0}, \mu_0) = f(z^{\mu_0}) - g(z^{\mu_0}) \geq \min\ (2.15)$$

which together with (A.1) imply (2.16) and moreover $\varphi(\mu_0) = \sup_{\mu\geq 0}\varphi(\mu)$ as well as

$$\varphi(\mu) = f(z^{\mu_0}) - g(z^{\mu_0}) = \min\ (2.15) \quad \forall\ \mu \geq \mu_0, \tag{A.2}$$

proving the second statement of the Proposition.

Now, suppose that $\sum_{n=1}^{N}x_n^{(\mu)} - \sum_{n=1}^{N}(x_n^{(\mu)})^2 > 0$ for all $\mu > 0$. The sequence $\{(z^\mu, x^\mu)\}$ is bounded and by taking a subsequence if necessary one can assume $(z^\mu, x^{(\mu)}) \to (z^\infty, x^{(\infty)}) \in \mathcal{D}$ with

$\sum_{n=1}^{N} x_n^{(\infty)} - \sum_{n=1}^{N} (x_n^{(\infty)})^2 = 0$, because otherwise $\varphi(\mu) = f(z^{(\mu)}) - g(z^{(\mu)}) + \mu(\sum_{n=1}^{N} x_n^{(\mu)} - \sum_{n=1}^{N} (x_n^{(\mu)})^2) \to +\infty$, a contradiction. This means (z^{∞}, x^{∞}) is feasible to (2.15) and

$$\sup_{\mu \geq 0} \varphi(\mu) = f(z^{\infty}, x^{\infty}) - g(z^{\infty}, x^{\infty}) \geq \min \text{ (2.15)},$$

which together with (A.1) yield (2.16). Furthermore, if the supremum of the righ hand side of (2.16) attains at μ_0 then the second statement of the Proposition also follows by noticing that $f(z^{\infty}, x^{\infty}) - g(z^{\infty}, x^{\infty}) = \varphi(\mu_0)$ so (z^{∞}, x^{∞}) is the optimal solution of (2.17).

Appendix B

Gradients & Numerical Solutions

B.1 Gradient formula 1

For function $\Theta(\boldsymbol{Q}) = \log(\sum_{(i,j)\in\mathcal{I}\times\mathcal{J}} H_{i,j}\boldsymbol{Q}_{i,j}H_{i,j}^H + \delta^2\boldsymbol{I}_{N_r})$, the gradient is

$$\langle\nabla\Theta(Q^{(\kappa)}), \boldsymbol{Q} - Q^{(\kappa)}\rangle = \mathsf{trace}\{(\sum_{(i,j)\in\mathcal{I}\times\mathcal{J}} H_{i,j}Q_{i,j}^{(\kappa)}H_{i,j}^H + \delta^2\boldsymbol{I}_{N_r})^{-1}\sum_{(i,j)\in\mathcal{I}\times\mathcal{J}} H_{i,j}(\boldsymbol{Q}_{i,j} - Q_{i,j}^{(\kappa)})H_{i,j}^H\} \tag{B.1}$$

B.2 Gradient formula 2

For function $\theta(\boldsymbol{w}, \boldsymbol{y}) = |\langle\boldsymbol{w}, H\rangle|^2/(\boldsymbol{y} + \sigma^2)$, the gradient is

$$\langle\nabla\theta(w^{(\kappa)}, y^{(\kappa)}), (\boldsymbol{w}, \boldsymbol{y}) - (w^{(\kappa)}, y^{(\kappa)})\rangle = 2\mathsf{Re}\{\frac{\langle w^{(\kappa)}, H\rangle}{y^{(\kappa)} + \sigma^2}\langle\boldsymbol{w} - w^{(\kappa)}, H\rangle\} - \frac{|\langle w^{(\kappa)}, H\rangle|^2}{(y^{(\kappa)} + \sigma^2)^2}(\boldsymbol{y} - y^{(\kappa)}). \tag{B.2}$$

B.3 Numerical solutions

B.3.1 Solutions for [6, Example 1] in subsection 6.5.1.1

- For sum rate optimisation under the conventional scheme:

$$Q^p_{1,1} = \left[\begin{smallmatrix} 0.7909 & -0.0507+0.1009i \\ -0.0507-0.1009i & 0.2091 \end{smallmatrix}\right],\ Q^p_{2,1} = \left[\begin{smallmatrix} 0.7018 & 0.0040+0.4575i \\ 0.0040-0.4575i & 0.2982 \end{smallmatrix}\right]. \tag{B.3}$$

- For sum rate optimisation under the new scheme: It is the same as above with $Q^c = \mathbf{0}$.
- For minimal rate optimisation under the conventional scheme:

$$Q^p_{1,1} = \left[\begin{smallmatrix} 0.6508 & -0.2651+0.3962i \\ -0.2651-0.3962i & 0.3492 \end{smallmatrix}\right],\ Q^p_{2,1} = \left[\begin{smallmatrix} 0.6177 & -0.1103+0.4733i \\ -0.1103-0.4733i & 0.3823 \end{smallmatrix}\right]. \tag{B.4}$$

- For minimal rate optimisation under the new scheme:

$$\begin{aligned} Q^p_{1,1} &= \left[\begin{smallmatrix} 0.2057 & -0.0839+0.1738i \\ -0.0839-0.1738i & 0.1811 \end{smallmatrix}\right],\ Q^p_{2,1} = \left[\begin{smallmatrix} 0.1608 & -0.0117+0.1397i \\ -0.0117-0.1397i & 0.1222 \end{smallmatrix}\right], \\ Q^c_{1,1} &= \left[\begin{smallmatrix} 0.6099 & -0.0409-0.0194i \\ -0.0409+0.0194i & 0.0034 \end{smallmatrix}\right],\ Q^c_{2,1} = \left[\begin{smallmatrix} 0.4621 & -0.1206+0.2705 \\ -0.1206-0.2705i & 0.2550 \end{smallmatrix}\right]. \end{aligned} \tag{B.5}$$

B.3.2 Solutions for the modified example in subsection 6.5.1.1

- For sum rate optimisation under the conventional scheme:

$$Q^p_{1,1} = \left[\begin{smallmatrix} 0.8274 & -0.0401+0.1202i \\ -0.0401-0.1202i & 0.1726 \end{smallmatrix}\right],\ Q^p_{2,1} = \left[\begin{smallmatrix} 0.6809 & -0.0137+0.4659i \\ -0.0137-0.4659i & 0.3191 \end{smallmatrix}\right]. \tag{B.6}$$

- For sum rate optimisation under the new scheme:

$$\begin{aligned} Q^p_{1,1} &= \left[\begin{smallmatrix} 0.1189 & -0.0913+0.0451i \\ -0.0913-0.0451i & 0.2392 \end{smallmatrix}\right],\ Q^p_{2,1} = \mathbf{0}, \\ Q^c_{1,1} &= \left[\begin{smallmatrix} 0.5886 & 0.1326-0.1173i \\ 0.1326+0.1173i & 0.0532 \end{smallmatrix}\right],\ Q^c_{2,1} = \left[\begin{smallmatrix} 0.6015 & 0.0134+0.1352i \\ 0.0134-0.1352i & 0.3985 \end{smallmatrix}\right]. \end{aligned} \tag{B.7}$$

- For minimal rate optimisation under the conventional scheme:

$$Q^p_{1,1} = \left[\begin{smallmatrix} 0.6101 & -0.2737+0.4037i \\ -0.2737-0.4037i & 0.3899 \end{smallmatrix}\right],\ Q^p_{2,1} = \left[\begin{smallmatrix} 0.5724 & -0.2297+0.4382 \\ -0.2297-0.4382 & 0.4276 \end{smallmatrix}\right]. \tag{B.8}$$

- For minimal rate optimisation under the new scheme:

$$
\begin{aligned}
&Q^p_{1,1} = \begin{bmatrix} 0.2135 & -0.1285+0.1420i \\ -0.1285-0.1420i & 0.1718 \end{bmatrix},\ Q^p_{2,1} = \begin{bmatrix} 0.0153 & -0.0380+0.0045i \\ -0.0380-0.0045i & 0.0958 \end{bmatrix},\\
&Q^c_{1,1} = \begin{bmatrix} 0.6129 & -0.0285-0.0159i \\ -0.0285+0.0159 & 0.0017 \end{bmatrix},\ Q^c_{2,1} = \begin{bmatrix} 0.6392 & 0.0484+0.3008i \\ 0.0484-0.3008i & 0.2497 \end{bmatrix}.
\end{aligned}
\tag{B.9}
$$

Appendix C

Optimized Power Splits for Han-Kobayashi Interference Mitigation

C.1 Introduction

Two-user interference channels (ICs) have been a central research topic for over five decades but their capacity region has not been fully characterized. In fact, the capacity region is known only for extremal cases such as zero IC, strong or very strong IC and strong one-sided IC (see e.g. [7] and references therein). It is still unknown for weak or moderate and mixed IC.

The best capacity region for weak or mixed IC is due to Han and Kobayashi (HK) scheme [59], where each sender splits its message into a private message and a common message. The private message is decoded by the intended receiver while the common message is decoded by both receivers. The characterisation of this HK capacity region is very complex. In this context, power split for private and common messages is crucial but its optimal solution is still unsolvable. For weak ICs, the known suboptimal split is to keep power of interference by private message at the level of power noise for the unintended receiver [7]. It achieves rates within 1 bps/Hz of capacity outer bound. Since then, various outer bounds have also been developed [7, 61, 173]. A more general form of outer bound and sum-rate capacity for weak IC was given in [171]. There is also another outer bound for the weak and mixed IC [170]. To the authors's best knowledge, the optimized power split has been considered only very recently in [9] for multi-user ICs. To avoid the complicated joint decoding of common and private messages, [9] employed successive decoding with a sub-optimal heuristic method to maximize the worst user's combined rate. It was shown there that the less complex successive decoding matches the rates by joint decoding in most cases. However, their power split scheme is not efficient and not suitable for sum rate optimisation.

In this research, we adopt successive decoding and consider the two mentioned problems of sum rate maximisation and maximin combined rate optimisation in a unified d.c. (difference of convex functions) optimisation framework [16]. Unlike previous studies, the problem model and formulation are suitable for all categories of ICs. A tailored iterative algorithm (DCI) improves the solution at each iteration. The optimality of the algorithm is seen by plotting its obtained rates in the rate region along with the known inner and outer bounds and the private-only rate region. The results also suggest when making interference decodable (common message) is beneficial and when it should simply be treated as noise.

The research is organized as follows. Section C.2 is devoted to the problem formulation and the proposed solution. Section C.3 presents simulation results for different types of ICs and Monte Carlo tests. Section C.4 concludes the research.

C.2 Problem Statement

Consider a two-user Gaussian interference channel where two single-antenna transmitters transmit to their respective receivers,

$$\begin{aligned} y_1 &= \sqrt{\delta_{1,1}}h_{1,1}x_1 + \sqrt{\eta_{2,1}}h_{2,1}x_2 + z_1, \\ y_2 &= \sqrt{\eta_{2,1}}h_{2,1}x_1 + \sqrt{\delta_{2,2}}h_{2,2}x_2 + z_2, \end{aligned} \tag{C.1}$$

where x_i and y_i are the transmit and receive signals. z_i is noise at receiver i which is independent and identically distributed (i.i.d.) with zero-mean and unit-variance σ^2. $E[|x_i|^2] = 1$. $h_{i,j} \in \mathbb{C}$ is the normalized channel from transmitter i to receiver j.

Assuming unit power and unit variance of noise, $\delta_{i,i}$ represents the signal-to-noise ratio for user i (SNR_i) and $\eta_{i,j}$ ($i \neq j$) is the interference-to-noise ratio for user j (INR_j) due to interference from user i. Let $\tilde{h}_{i,i} := \sqrt{\delta_{i,i}}h_{i,i}$ for $i = 1, 2$, and $\tilde{h}_{i,j} = \sqrt{\eta_{i,j}}h_{i,j}$ for $i \neq j$. The channel is thus fully parameterized by the set of $(SNR_i,\, INR_j)$.

Following the superposition coding and joint decoding in HK, each user i splits its message into a private message x_i^p and a common message x_i^c (i.e., $x_i = x_i^p + x_i^c$). The private message of each transmitter is decoded by its dedicated receiver, while its common message can be decoded by both receivers. Let the power allocated to user i's private message be $\boldsymbol{p}_i^p = E(|x_i^p|^2)$ and its corresponding rate be $\tilde{R}_i^p$. Similarly, let the power allocated to its common message be $\boldsymbol{p}_i^c = E(|x_i^c|^2)$ and the corresponding rate be $\tilde{R}_i^c$. The normalized power constraint is

$$\boldsymbol{p}_i^p + \boldsymbol{p}_i^c \leq 1, i = 1, 2. \tag{C.2}$$

Under joint decoding, a pair of achievable rates $(\tilde{R}^p, \tilde{R}^c)$ must satisfy the following system of inequalities for $i = 1, 2$, $j \neq i$ and $S_i = |\tilde{h}_{j,i}|^2\boldsymbol{p}_j^p + \sigma^2$ [9]: $|\tilde{h}_{i,i}|^2\boldsymbol{p}_i^p \leq (2^{\tilde{R}_i^p} - 1)S_i$, $|\tilde{h}_{i,i}|^2\boldsymbol{p}_i^c \leq (2^{\tilde{R}_i^c} - 1)S_i$, $|\tilde{h}_{j,i}|^2\boldsymbol{p}_j^c \leq (2^{\tilde{R}_j^c} - 1)S_i$, $|\tilde{h}_{i,i}|^2\boldsymbol{p}_i^p + |\tilde{h}_{i,i}|^2\boldsymbol{p}_i^c \leq (2^{\tilde{R}_i^p + \tilde{R}_i^c} - 1)S_i$, $|\tilde{h}_{i,i}|^2\boldsymbol{p}_i^p + |\tilde{h}_{j,i}|^2\boldsymbol{p}_j^c \leq (2^{\tilde{R}_i^p + \tilde{R}_j^c} - 1)S_i$, $|\tilde{h}_{i,i}|^2\boldsymbol{p}_i^c + |\tilde{h}_{j,i}|^2\boldsymbol{p}_j^c \leq (2^{\tilde{R}_i^c + \tilde{R}_j^c} - 1)S_i$, $|\tilde{h}_{i,i}|^2\boldsymbol{p}_i^p + \tilde{h}_{i,i}|^2\boldsymbol{p}_i^c + |\tilde{h}_{j,i}|^2\boldsymbol{p}_j^c \leq (2^{\tilde{R}_i^p + \tilde{R}_i^c + \tilde{R}_j^c} - 1)S_i$. To avoid the prohibitive complexity posed by joint decoding, [9] used successive decoding which is able to retain the achievable rates by joint decoding but with great simplicity. Therefore, a natural design objective is to find the optimal private-to-common message power split for each user so that the network's sum rate or minimum rate is maximized.

Let $\boldsymbol{p} := (\boldsymbol{p}^c, \boldsymbol{p}^p)^T$ be the design power split vectors where $\boldsymbol{p}^c := (\boldsymbol{p}_1^c, \boldsymbol{p}_2^c)$ and $\boldsymbol{p}^p := (\boldsymbol{p}_1^p, \boldsymbol{p}_2^p)$. The power of the received signal plus interference for user-i is

$$\boldsymbol{M}_i(\boldsymbol{p}) = \sum_{n=1}^{2} |\tilde{h}_{n,i}|^2(\boldsymbol{p}_n^p + \boldsymbol{p}_n^c).$$

Following the successive decoding order, user i decodes its own common message with rate $R_i^c(\boldsymbol{p}) = \log_2(1 + |\tilde{h}_{i,i}|^2 \boldsymbol{p}_i^c/(\boldsymbol{M}_i^c + \sigma^2))$; user i's common message is decoded by user $j \neq i$ with rate $R_i^a(\boldsymbol{p}) = \log_2(1 + |\tilde{h}_{i,j}|^2 \boldsymbol{p}_i^c/(\boldsymbol{M}_j^a + \sigma^2))$; user i decodes its own private message with rate $R_i^p(\boldsymbol{p}) = \log_2(1 + |\tilde{h}_{i,i}|^2 \boldsymbol{p}_i^p/(\boldsymbol{M}_i^p + \sigma^2))$. Here $\boldsymbol{M}_i^c = \boldsymbol{M}_i - |\tilde{h}_{i,i}|^2 \boldsymbol{p}_i^c$, $\boldsymbol{M}_j^a = \boldsymbol{M}_j^c - |\tilde{h}_{i,j}|^2 \boldsymbol{p}_i^c$ and $\boldsymbol{M}_i^p = \boldsymbol{M}_i^a - |\tilde{h}_{i,i}|^2 \boldsymbol{p}_i^p, j \neq i$. The achievable rate region under this successive decoding order is thus

$$\begin{aligned} \boldsymbol{R}(\boldsymbol{p}) \quad := \quad & \{\{\boldsymbol{R}_i^p + \boldsymbol{R}_i^c\}_{i=1:2} : \boldsymbol{R}_i^p \leq R_i^p(\boldsymbol{p}), \\ & \boldsymbol{R}_i^c \leq R_i^c(\boldsymbol{p}), \boldsymbol{R}_i^c \leq R_i^a(\boldsymbol{p})\} \end{aligned}$$

The crucial step is to represent the achievable rate of user i by nonsmooth function [62]

$$R_i(\boldsymbol{p}) = R_i^p(\boldsymbol{p}) + \min\{R_i^c(\boldsymbol{p}), R_i^a(\boldsymbol{p})\}.$$

For the overall system performance, the following sum rate optimization problem is studied

$$\max_{\boldsymbol{p}} \ R_1(\boldsymbol{p}) + R_1(\boldsymbol{p}) \quad \text{s.t.} \quad (C.2). \tag{C.3}$$

For the fairness of the achievable rates among users, the following maximin rate problem is addressed

$$\max_{\boldsymbol{p}} \min\{R_1(\boldsymbol{p}), R_2(\boldsymbol{p})\} \quad \text{s.t.} \quad (C.2). \tag{C.4}$$

Even with successive decoding, the above problems are still highly nonconvex and very complicated and thus pose great challenges to optimisation. Below, Theorem 8 reveals that each of the rate functions can be decomposed into a d.c. function and Theorem 9 indicates that both of the problems can be unified in a d.c. optimisation framework and properly addressed by the proposed DCI algorithm [56, 92]

Theorem 8. [56] Each of functions $R_i^c(\boldsymbol{p}), R_i^a(\boldsymbol{p})$ and $R_i^p(\boldsymbol{p})$ is a d.c. function: $R_i^c(\boldsymbol{p}) = \log_2(e)(f_i^c(\boldsymbol{p}) - g_i^c(\boldsymbol{p}))$, $R_i^a(\boldsymbol{p}) = \log_2(e)(f_i^a(\boldsymbol{p}) - g_i^a(\boldsymbol{p}))$, $R_i^p(\boldsymbol{p}) = \log_2(e)(f_i^p(\boldsymbol{p}) - g_i^p(\boldsymbol{p}))$, with convex functions $f_i^c(\boldsymbol{p}) = -\ln(\sigma^2 + \boldsymbol{M}_i^c(\boldsymbol{p}))$, $g_i^c(\boldsymbol{p}) = -\ln(\sigma^2 + \boldsymbol{M}_i(\boldsymbol{p}))$, $f_i^a(\boldsymbol{p}) = -\ln(\sigma^2 + \boldsymbol{M}_j^a(\boldsymbol{p}))$, $g_i^a(\boldsymbol{p}) = -\ln(\sigma^2 + \boldsymbol{M}_j^a(\boldsymbol{p}) + |\tilde{h}_{i,j}|^2 \boldsymbol{p}_i^c)$, $f_i^p(\boldsymbol{p}) = -\ln(\sigma^2 + \boldsymbol{M}_i^p(\boldsymbol{p}))$, $g_i^p(\boldsymbol{p}) = -\ln(\sigma^2 + \boldsymbol{M}_i^p(\boldsymbol{p}) + |\tilde{h}_{i,i}|^2 \boldsymbol{p}_i^p)$.

Now, using the following sequential d.c. representations [16]

- $\frac{1}{\log_2(e)}\min\{R_i^c(\boldsymbol{p}), R_i^a(\boldsymbol{p})\} = f_i^{ca}(\boldsymbol{p}) - g_i^{ca}(\boldsymbol{p})$ with $f_i^{ca}(\boldsymbol{p}) := f_i^c(\boldsymbol{p}) + f_i^a(\boldsymbol{p})$, $g_i^{ca}(\boldsymbol{p}) := \max\{g_i^c(\boldsymbol{p}) + f_i^a(\boldsymbol{p}), g_i^a(\boldsymbol{p}) + f_i^c(\boldsymbol{p})\}$.
- $\frac{1}{\log_2(e)}R_i(\boldsymbol{p}) := f_i(\boldsymbol{p}) - g_i(\boldsymbol{p})$ with $f_i(\boldsymbol{p}) := f_i^p(\boldsymbol{p}) + f_i^{ca}(\boldsymbol{p})$, $g_i(\boldsymbol{p}) := g_i^p(\boldsymbol{p}) + g^{ca}(\boldsymbol{p})$.
- $\dfrac{1}{\log_2(e)}\min_{i=1,2} R_i(\boldsymbol{p}) = F(\boldsymbol{p}) - G^{\max}(\boldsymbol{p})$ with $F(\boldsymbol{p}) := f_1(\boldsymbol{p}) + f_2(\boldsymbol{p})$, $G^{\max}(\boldsymbol{p}) := \max_{i=1,2}[g_i(\boldsymbol{p}) + f_{3-i}(\boldsymbol{p})]$
- $\dfrac{1}{\log_2(e)}\sum_{i=1,2} R_i(\boldsymbol{p}) = F(\boldsymbol{p}) - G^{\sum}(\boldsymbol{p})$ with $G^{\sum}(\boldsymbol{p}) := g_1(\boldsymbol{p}) + g_2(\boldsymbol{p})$.

we come up with the following

Theorem 9. Let $G(\boldsymbol{p}) \in \{G^{\max}(\boldsymbol{p}), G^{\sum}(\boldsymbol{p})\}$, problem (C.3) or (C.4) is the following convex constrained d.c. function minimisation

$$\min_{\boldsymbol{p}} \, [G(\boldsymbol{p}) - F(\boldsymbol{p})] : (C.2). \tag{C.5}$$

Proof: See proof in [62]. □

Initialized from a feasible solution $\boldsymbol{p}^{(0)}$ satisfying (C.2), κ-th iteration for $\kappa = 1, 2, \cdots$ generates a feasible solution $p^{(\kappa)}$ by solving the convex program

$$\min_{\boldsymbol{p}}[G(\boldsymbol{p}) - \langle \nabla F(p^{(\kappa-1)}), \boldsymbol{p} - p^{(\kappa-1)}\rangle] \; : \; (C.2), \tag{C.6}$$

where $\nabla F(p^{(\kappa-1)}), \boldsymbol{p} - p^{(\kappa-1)}\rangle = -\sum_{i=1}^{2}\langle \nabla f_i^c(p^{(\kappa)}) + \nabla f_i^a(p^{(\kappa)}) + \nabla f_i^p(p^{(\kappa)}), \boldsymbol{p} - p^{(\kappa)}\rangle$.

Proposition 3. [56, 92] The above d.c. iterations (DCI) generate a sequence of improved feasible solutions $\{p^{(\kappa)}\}$ to (C.3) or (C.4), which converge to an optimal solution $\bar{p}$. Consequently, it terminates after finitely many iterations under the stopping criterion $\Omega(p^{(\kappa)}) - \Omega(p^{(\kappa-1)}) \leq \epsilon \, \Omega(p^{(\kappa)})$ for $\Omega(p) \in \{\min_{i=1,2} R_i(p), \sum_{i=1}^{2} R_i(p)\}$.

Proof: See proof in [56]. □

C.3 Simulation Results

Three case studies of the weak or mixed IC followed by Monte Carlo simulation are presented. The tolerance $\epsilon = 10^{-5}$ is set in all simulations. In all the figures, the legends "Inner", "Outer ETW", and "Outer SKC" refer to the inner/ outer bounds developed by [7] and [171], respectively. The performance of the proposed algorithm is found not sensitive to particular initialized solutions. Like [7], $\mathsf{HK}(\alpha, \beta)$ refers to power split $|\tilde{h}_{1,2}|^2 p_1^p/\sigma^2 = \alpha$ and $|\tilde{h}_{2,1}|^2 p_2^p/\sigma^2 = \beta$.

C.3.1 Weak interference channel

C.3.1.1 Case 1 [7, (60)] ($SNR_1 = 38.799$, $SNR_2 = 46.108$, $INR_1 = 37.861$, $INR_2 = 13.089$ (dB))

The inner bound is found by solving the system of inequalities [7, (61)], and the outer bounds by [7, (36)] and [171, (1-3)], respectively.

Using successive decoding, the proposed DCI converges to $\mathsf{HK}(0.0290, 2.3085)$ and $\mathsf{HK}(0.6906, 1.8096)$ in 11 and 15 iterations for sum rate (C.3) and maximin rate (C.4), respectively. Obviously, the rate performance of successive decoding is always bounded by joint decoding. However, we have found that these successive decoding rates and joint decoding rates are not different under the optimal $\mathsf{HK}(0.0290, 2.3085)$ and $\mathsf{HK}(0.6906, 1.8096)$, but they are different under the suboptimal $\mathsf{HK}(1, 1)$ by [7]. Compared to the conventional private only messaging, $\mathsf{HK}(0.0290, 2.3085)$ improves the sum rate by 4.75% to 16.0443 bps/Hz, while $\mathsf{HK}(0.6906, 1.8096)$ improves the minimal rate by 35.88% to 7.6384 bps/Hz. The total fairness among user rates only results in a 4.78% sum rate loss. Both optimal $\mathsf{HK}(0.0290, 2.3085)$ and $\mathsf{HK}(0.6906, 1.8096)$ are very close to their respective theoretical upper bounds. Additional exhaustive search through all power splitting ratios ($p_1^c \in [0, 1], p_2^c \in [0, 1]$) also verifies the optimality of DCI for this case. It is noted such a method requires very fine searching (at least 10^5 sampling points on each ratio parameter) that takes much longer computation time than the proposed algorithm.

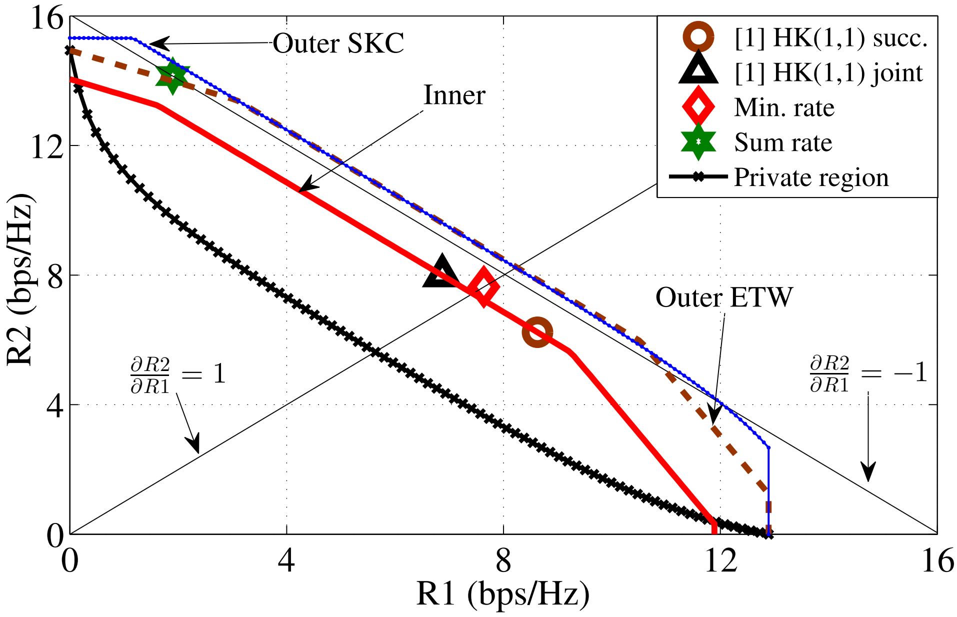

FIGURE C.1: Weak interference channel rate region: case 1.

C.3.1.2 Case 2 [7, (64)] ($SNR_1 = 19.841$, $SNR_2 = 17.037$, $INR_1 = -1.843$, $INR_2 = 11.879$ (dB))

The inner bound is found by solving [7, (66), p.5550], and the outer bounds by [7, (36)] and [171, (1-3)], respectively.

Different from the above case, the convex private-only rate region in Fig. C.2 indicates that the channel is more noise-limited than interference-limited. The private-only rate region mostly overlaps with the 1-bit region (the region between the inner and ETW outer bound) due to weaker interference links. The squeezed tight transitional region makes any rate improvement unlikely.

Again, the suboptimal split $\mathsf{HK}(1, INR_1)$ by [7] results in different joint rates and successive rates. The optimal $\mathsf{HK}(2.8029, 0.6543)$ for the maximin rate by DCI in 5 iterations improves the minimal rate slightly from 3.7021 bps/Hz of the private-only messaging to 3.8370 bps/Hz. It lies in a very close neighborhood of the theoretical outer bound. However, there is no improvement in terms of sum rate. Again, exhaustive search proves the optimality of the solutions found by

DCI for both problems. It is important to realize that common message may not always improve certain rate performance such as sum rate.

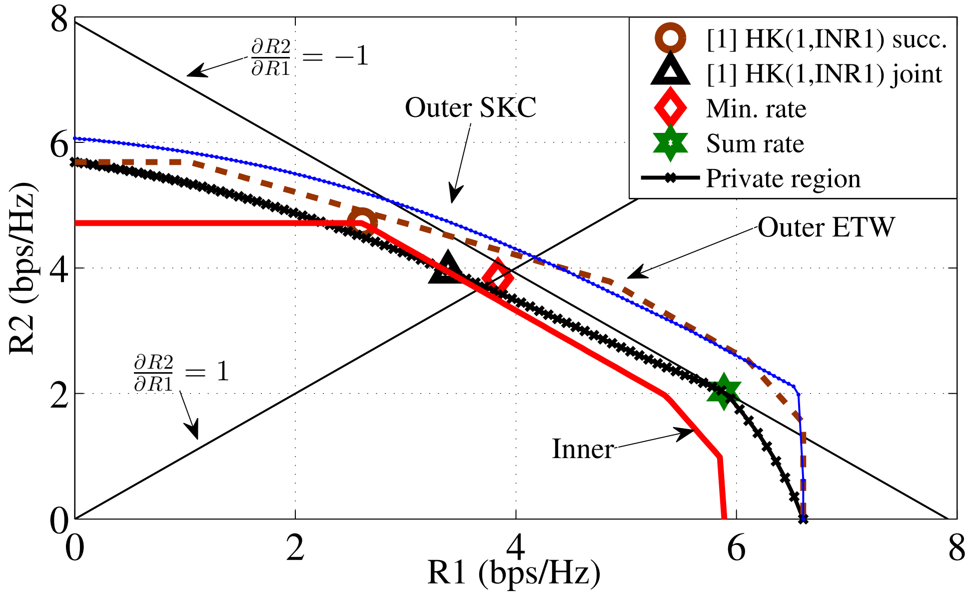

FIGURE C.2: Weak interference channel rate region: case 2.

C.3.2 Mixed interference channel [7, (70)] ($SNR_1 = 20$, $SNR_2 = 10$, $INR_1 = 15$, $INR_2 = 5$ (dB))

The inner bound and outer bounds are found by solving the system of inequalities [7, (70)], and [7, (36),(48)], respectively.

From Fig. C.3, we can see the channel is interference-limited (concave). Its optimal sum rate occurs when user 2 is disabled, and its optimal minimal rate is achieved with a substantial 46.2% sum rate loss. The suboptimal $\mathsf{HK}(1, 0)$ by [7] results in user rates (R_1, R_2) lying on the overlapping section $\partial R_2/\partial R_1 = -1$ of the outer bound and the inner bound so it is actually the optimal solution for sum rate optimisation. Similarly, the joint rates and successive rates based on $\mathsf{HK}(0.3846, 0)$ by DCI also lie on the outmost section of the outer bound $\partial R_2/\partial R_1 = -1$. This means both splits output the optimal sum rate of 7.0512 bps/Hz, which is about 6.0% better than that by the private-only messaging. Remarkably, the DCI stops in 5 iterations for the sum rate optimisation and the user rates by joint decoding and successive decoding are different even when their sum rates remain the same. For the maximin rate problem, DCI locates a solution $\mathsf{HK}(0.1295, 0)$ in 4 iterations, improving the minimal rate by more than 50% to 2.8495 bps/Hz, which is very close to its upper bound.

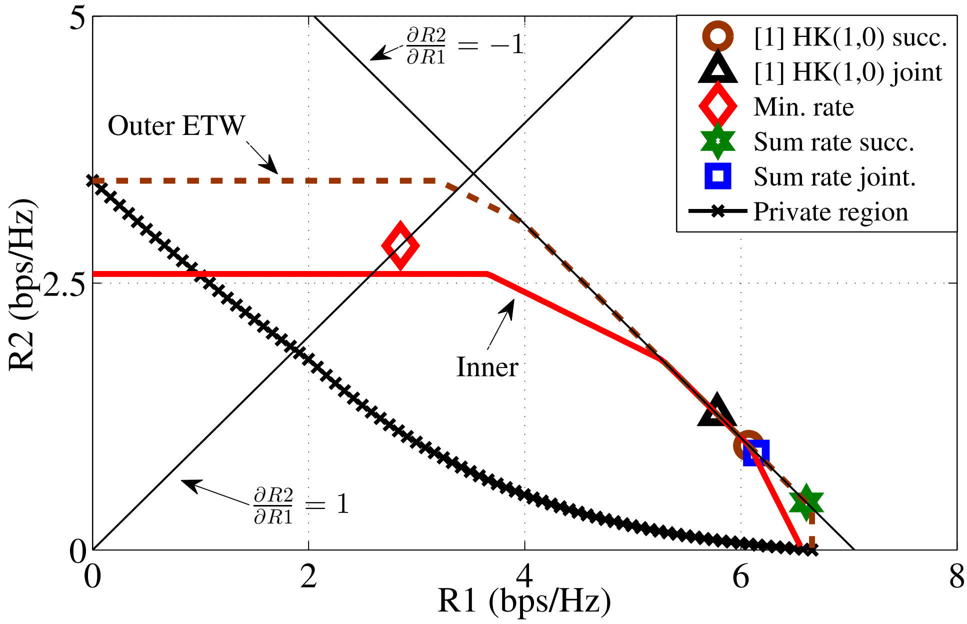

FIGURE C.3: Mixed interference channel rate region

C.3.3 Monte Carlo simulation

The two transmitters are placed 1.4 km apart forming two hexagonal cells and the receivers are uniformly distributed within their respective cells. Same simulation assumptions on fading channel and antenna gains are adopted from [9]. From the above case-2 and case-3, we have realized that common message may not always lead to rate gains for certain types of channels, especially noise-limited channels for which the private-only scheme may already be able to achieve the minimal rate or sum rate capacity. Therefore, we define a channel as 'effective' if the rate performance of common message scheme outperforms that of the private-only scheme by at least 1%. Otherwise, it is defined as an 'ineffective' channel.

It is seen from Fig. C.4 and Fig. C.5 that the benefits of common message increases as the available power grows, especially for the minimal rate performance. The private-only messaging performance for effective channels is worse than that for ineffective channels because the former generally suffer more from interference (interference-limited) than the latter. For the more interference-limited channels (effective), the HK scheme takes advantage of decoded interference and thus effectively improves rate performance in general. For the more noise-limited channels (ineffective), such cooperation is not beneficial due to ignorable interference. In fact, private-only scheme alone tends to achieve the rate capacity for these channels.

C.4 Conclusion

In this research, we study the optimized power split of common and private messages under the Han-Kobayashi scheme for interference channels. By using successive decoding and recasting the resulted problems into much more tractable formulations of d.c. programming, we have developed an efficient iterative algorithm. In the presented cases, the algorithm was able to locate almost optimal solutions. Monte Carlo simulation results also proved its effectiveness.

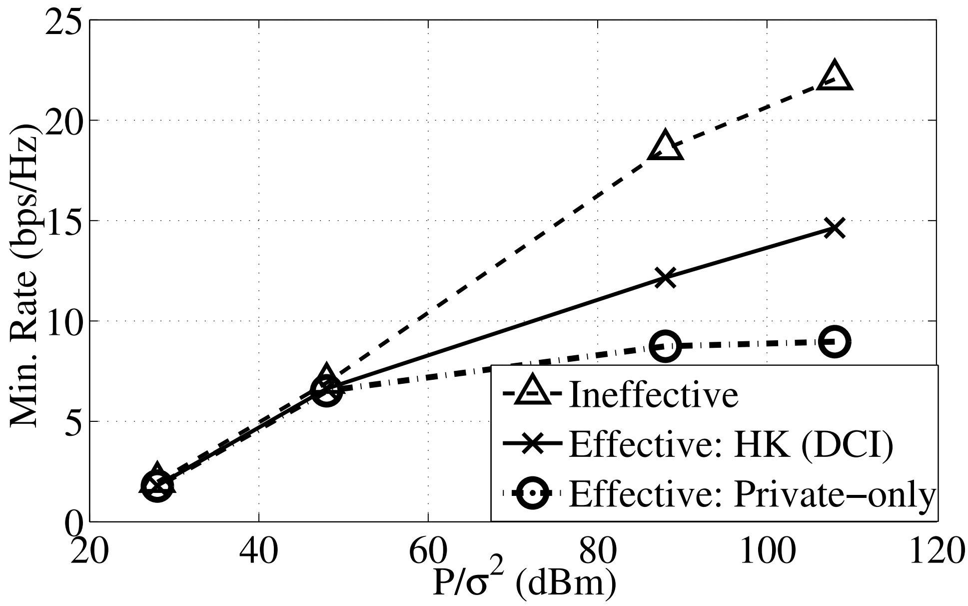

FIGURE C.4: Min. rate performance vs. P/σ^2

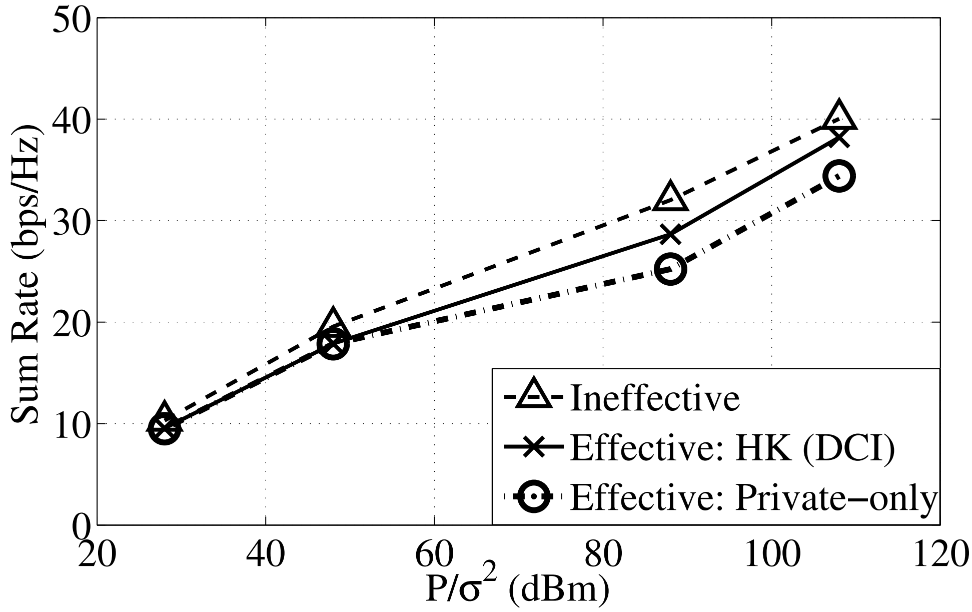

FIGURE C.5: Sum rate performance vs. P/σ^2

Appendix D

Maximization of Sum Rate in Cognitive Multi-cell Wireless Networks with QoS Constraints

D.1 Introduction

In a cellular communication network, coordinated transmission among the base stations (BSs) plays a crucial role in alleviating inter-cell interference, leading to improvement of the network's capacity. This research is concerned with a MISO communication scenario that applies to the downlink of such a communication network. In particular, the BSs are equipped with multiple antennas, whereas each mobile terminal (MT) is equipped with a single antenna. Transmission is over flat-fading channels with perfect CSI available at the BSs (or a central processing unit connected to all BSs). The BSs jointly determine the optimal transmit covariance matrices to maximize the weighted sum rate subject to different QoS constraints.

Several specific cases of such sum-rate maximisation problems were studied in [174, 175] from the viewpoint of game theory, while Reference [176] employs uplink-downlink duality to develop an iterative algorithm based on geometric programming. Reference [11] applies the monotonic optimization framework [138, 157] to locate the global optimal solutions. All these mentioned references were concerned with noncognitive networks under some particular power constraints, in which all MTs are PUs with no requirement for their individual QoS. It should be emphasized that the individual QoSs in terms of the rate thresholds are absolutely necessary to prevent the user discrimination inherent in sum-rate maximization, which usually assigns most of the sum rate to a few users only and thus practically disable the service for other users.

In cognitive networks, where MTs become secondary users (SUs), the BS transmit powers must satisfy additional ”cognitive” constraints so the existing algorithms, which are appropriate for some particular power constraints of non-cognitive networks, are no longer suitable. Similarly, while the procedure of alternating optimization developed in [177, Table 1] is computationally inexpensive, it is specifically developed for a single-cell network under individual user power constraints. but again it is purposely only for a single cell network under individual user power constraints. If only a simple convex constraint is added, the method proposed in [177] looses its tractability and is not suitable for cognitive multi-cell networks. In fact, the method of alternating optimisation was extended to the uplink transmission of a non-cognitive multi-cell network in [178] but it suffers from the same drawback, namely it does not work if simple convex constraints are added. The alternating optimization approach is simply not suitable for the class of optimisation problems considered in this research.

The remaining of this research is organized as follows. Section D.2 introduces the optimization problem and a useful reformulation based on concave programming is presented. Then, a simple Frank-and-Wolfe type (FW) algorithm is applied to find the solutions. Simulation results in Section D.3 show that the FW algorithm converges in a modest number of iterations. The advantages of the FW algorithm are its simple implementation, fast convergence and good performance under various constraints. Section D.4 concludes the research.

D.2 Problem Formulation and Iterative FW

Consider a multicell cellular network consisting of N BSs. Each BS is equipped with N_t transmit antennas and exclusively serves K MTs within its cell in downlink transmission. Let $x_{i,j}$ be the signal vector intended for the jth MT in the ith cell (which shall be referred to as user (i,j)) and $\boldsymbol{W}_{i,j} \in \mathcal{S}_+^{N_t}$ be its covariance matrix. Accordingly, $\boldsymbol{W} := [\boldsymbol{W}_{i,j}]_{i=1:N,j=1:K} \in \mathbb{C}^{(N_tN)\times(KN_t)}$ is the collection of all covariance matrices. By defining the index sets $\mathcal{I} = \{1 : N\}$ and $\mathcal{J} = \{1 : K\}$, the received signal $z_{i,j}$ at user (i,j) is the following combination of intra-cell signals, inter-cell interferences plus noise:

$$z_{i,j} = h_{i,i,j}^H x_{i,j} + \sum_{(m,k)\in\mathcal{I}\times\mathcal{J}\setminus(i,j)} h_{m,i,j}^H x_{m,k} + n_{i,j}.$$

In the above expression, $h_{m,i,j}^H \in \mathbb{C}^{1\times N_t}$ is the channel vector from the BS in the mth cell to user (i,j), whereas the additive white noise component $n_{i,j}$ is modeled as zero-mean circularly-symmetric complex Gaussian random variable with variance σ^2.

The achievable information rate (in nats) at the user (i,j) is

$$\varphi_{i,j}(\boldsymbol{W}) := \ln(1 + h_{i,i,j}^H \boldsymbol{W}_{i,j} h_{i,i,j}/(\Phi_{i,j}(\boldsymbol{W}) + \sigma^2)),$$

where $\Phi_{i,j}(\boldsymbol{W}) := \sum_{(m,k)\in\mathcal{I}\times\mathcal{J}\setminus(i,j)} h_{m,i,j}^H \boldsymbol{W}_{m,k} h_{m,i,j}$. Given the rate thresholds $\gamma_{i,j} > 0, (i,j) \in \mathcal{I}\times\mathcal{J}$, the QoS constraints $\varphi_{i,j}(\boldsymbol{W}) \geq \gamma_{i,j}$ are the following convex set

$$\mathcal{W}_{qos} = \{\boldsymbol{W} : h_{i,i,j}^H \boldsymbol{W}_{i,j} h_{i,i,j} \geq (2^{\gamma_{i,j}} - 1)(\Phi_{i,j}(\boldsymbol{W}) + \sigma^2), (i,j) \in \mathcal{I}\times\mathcal{J}\}. \tag{D.1}$$

Meanwhile, other relevant and practical constraints considered

$$\mathcal{W}_B = \{\boldsymbol{W} \ : \ \psi_B(\boldsymbol{W}) := \max_{i\in\mathcal{I}} \sum_{j\in\mathcal{J}} \langle \boldsymbol{W}_{i,j} \rangle \leq P_B\}, \tag{D.2}$$

$$\mathcal{W}_C = \{\boldsymbol{W} : \max_{r=1:R} \sum_{(i,j)\in\mathcal{I}\times\mathcal{J}} h_{0,i,r}^H \boldsymbol{W}_{i,j} h_{0,i,r} \leq P_0\}. \tag{D.3}$$

The constraint in (D.2) sets the BS transmit power limit [1], while the constraint in (D.3) applies for a cognitive network in which users (i, j) are secondary users (SUs) and share the spectrum with R primary users (PUs)[14, 179]. Here, $h_{0,i,r}$ is the channel vector from ith BS to PU r, and P_0 sets a tolerance level toward the secondary interference.

In this research, we are concerned with the following program of sum rate maximisation

$$\max_{\boldsymbol{W}} \sum_{i=1}^{N}\sum_{j=1}^{K} \varphi_{i,j}(\boldsymbol{W}) \ : \ \boldsymbol{W} \in \mathcal{W} := \mathcal{W}_{qos} \cap \mathcal{W}_B \cap \mathcal{S}_+^{N_t}. \tag{D.4}$$

As briefly mentioned in the Introduction, without the QoS constraint (D.1), the sum rate maximisation (D.4) tends to discriminate many users by allocating most of sum rates to a few users only. The issue can be overcome by weighted sum rate maximization but there is no systematic way for weight assignments.

It is obvious that

$$\varphi_{i,j}(\boldsymbol{W}) = f_{i,j}(\boldsymbol{W}) - g_{i,j}(\boldsymbol{W}),$$

with

$$\begin{aligned} f_{i,j}(\boldsymbol{W}) &:= \ln(\Psi_{i,j}(\boldsymbol{W}) + \sigma^2) \\ \Psi_{i,j}(\boldsymbol{W}) &:= h_{i,i,j}^H \boldsymbol{W}_{i,l} h_{i,i,j} + \Phi_{i,j}(\boldsymbol{W}) = \textstyle\sum_{(m,k)\in\mathcal{I}\times\mathcal{J}} h_{m,i,j}^H \boldsymbol{W}_{m,k} h_{m,i,j} \end{aligned}$$

and

$$g_{i,j}(\boldsymbol{W}) := \ln(\Phi_{i,j}(\boldsymbol{W}) + \sigma^2)$$

are concave functions in $\boldsymbol{W}$ [116, p. 465]. Each function $\varphi_{i,j}(\boldsymbol{W})$ thus is a d.c. function [16]. Therefore, (D.4) is a d.c. program [16]. Similar to [56], the DCI algorithm can generate a sequence of improved solutions $\{W^{(\kappa)}\}$, which converge to an optimized solution of (D.4) in a finite number of iterations [62]. Extensive simulations done in [62] have shown that DCI converges fairly quickly. However, its iterations are max det maximisation, which, although convex, are not easily implemented. We now develop an alternative procedure, which involves only convex

[1] The antenna transmit power limit $\mathcal{W}_A := \{\boldsymbol{W} : \ \psi_A(\boldsymbol{W}) := \max_{(i,\ell)\in\{1:N\}\times\{1:N_t\}} \sum_{j=1}^{K} \boldsymbol{W}_{i,j}(\ell,\ell) \le P_A\}$ can be also easily incorporated

quadratic iterations and thus is easily implementable.

It is immediate to see that $\varphi_{i,j}(\boldsymbol{W}) = -\psi_{i,j}(\boldsymbol{W})$ where $\psi_{i,j}(\boldsymbol{W}) = \ln(1-h^H_{i,i,j}\boldsymbol{W}_{i,j}h_{i,i,j}/(\Psi_{i,j}(\boldsymbol{W})+\sigma^2))$, so (D.4) is equivalent to

$$\min_{\boldsymbol{W}} \ \psi(\boldsymbol{W}) := \sum_{(i,j)\in\mathcal{I}\times\mathcal{J}} \psi_{i,j}(\boldsymbol{W}) \ : \ \boldsymbol{W}\in\mathcal{W} \tag{D.5}$$

in the sense that they share the same optimal solution with the sign-opposite optimal values. Our main result is the following theorem.

Theorem 10. Program (D.5) is equivalent to

$$\min_{\boldsymbol{W},\boldsymbol{V}=[\boldsymbol{V}_{i,j}]_{(i,j)\in\mathcal{I}\times\mathcal{J}}} \gamma(\boldsymbol{V},\boldsymbol{W}) := \sum_{(i,j)\in\mathcal{I}\times\mathcal{J}} \gamma_{i,j}(\boldsymbol{V}_{i,j},\boldsymbol{W}) : \tag{D.6a}$$

$$\boldsymbol{W}\in\mathcal{W}, \boldsymbol{V}_{i,j}\boldsymbol{V}_{i,j}^H \preceq \boldsymbol{W}_{i,j}, (i,j)\in\mathcal{I}\times\mathcal{J}, \tag{D.6b}$$

which is a concave program because functions $\gamma_{i,j}(\boldsymbol{V}_{i,j},\boldsymbol{W}) := \ln(1-h^H_{i,i,j}\boldsymbol{V}_{i,j}\boldsymbol{V}^H_{i,j}h_{i,i,j}/(\Psi_{i,j}(\boldsymbol{W})+\sigma^2))$ are concave in their variables $(\boldsymbol{V}_{i,j},\boldsymbol{W})$ while constraint (D.6b) is convex.

Lemma 8. Function and $\tau_{i,j}(\boldsymbol{V}_{i,j},\boldsymbol{W}) := h^H_{i,i,j}\boldsymbol{V}_{i,j}\boldsymbol{V}^H_{i,j}h_{i,i,j}/(\Psi_{i,j}(\boldsymbol{W})+\sigma^2)$ is convex in $\boldsymbol{V}\in\mathbb{C}^{N_t\times N_t}$ and $\boldsymbol{W}=[\boldsymbol{W}_{i,j}]_{(i,j)\in\mathcal{I}\times\mathcal{J}}$ with $\boldsymbol{W}_{i,j}\succeq 0$.

Proof: By [137, Th. 2], function $\chi(\boldsymbol{t},\boldsymbol{y}) := |\boldsymbol{t}|^2/(\boldsymbol{y}^2+\sigma^2)$ is convex in $(\boldsymbol{t},\boldsymbol{y})\in\mathbb{C}\times\mathbb{R}_+$, i.e. for all $(t_\ell,y_\ell)\in\mathbb{C}\times\mathbb{R}_+$, $\ell=1,2$ and $\alpha\in[0,1]$,

$$\chi(\alpha(t_1,y_1)+(1-\alpha)(t_2,y_2)) \le \alpha\chi(t_1,y_1)+(1-\alpha)\chi(t_2,y_2).$$

Therefore, for every $(V^{(\ell)}_{i,j},W^{(\ell)})$, setting $t_\ell=(V^{(\ell)}_{i,j})^Hh_{i,i,j}$, $y_\ell=\Psi_{i,j}(W^{(\ell)})$, $\ell=1,2$, gives

$$\begin{aligned}\tau_{i,j}(\alpha(V^{(1)}_{i,j},W^{(1)})+(1-\alpha)(V^{(2)}_{i,j},W^{(2)})) &= \chi(\alpha(t_1,y_1)+(1-\alpha)(t_2,y_2))\\ &\le \alpha\chi(t_1,y_1)+(1-\alpha)\chi(t_2,y_2)\\ &= \alpha\tau_{i,j}(V^{(1)}_{i,j},W^{(1)})+(1-\alpha)\tau_{i,j}(V^{(2)}_{i,j},W^{(2)}),\end{aligned}$$

showing the convexity of $\tau_{i,j}(\boldsymbol{V}_{i,j}, \boldsymbol{W})$. □

Proof of Theorem 10. Each $\boldsymbol{W} = [\boldsymbol{W}_{i,j}]_{(i,j)\in\mathcal{I}\times\mathcal{J}}$ feasible to (D.4) can be factorized as $\boldsymbol{W}_{i,j} = \boldsymbol{V}_{i,j}\boldsymbol{V}_{i,j}^H$ with $(\boldsymbol{W}, \boldsymbol{V})$ feasible to (D.6) and $\psi(\boldsymbol{W}) = \gamma(\boldsymbol{V}, \boldsymbol{W})$. Therefore, min $(D.4) \geq$ min $(D.6)$. On the other hand, under constraint $\boldsymbol{V}_{i,j}\boldsymbol{V}_{i,j}^H \preceq \boldsymbol{W}_{i,j}$ in (D.6), it is true that $h_{i,i,j}^H\boldsymbol{V}_{i,j}\boldsymbol{V}_{i,j}^H h_{i,i,j}/\Psi_{i,j}(\boldsymbol{W}) \leq h_{i,i,j}^H\boldsymbol{W}_{i,j}h_{i,i,j}/\Psi_{i,j}(\boldsymbol{W})$, so $\gamma_{i,j}(\boldsymbol{V}_{i,j}, \boldsymbol{W}) \geq \psi_{i,j}(\boldsymbol{W})$ yielding $\gamma(\boldsymbol{V}, \boldsymbol{W}) \geq \psi(\boldsymbol{W})$ for all $(\boldsymbol{V}, \boldsymbol{W})$ feasible to (D.6). Since each $(\boldsymbol{V}, \boldsymbol{W})$ feasible to (D.6) results in $\boldsymbol{W}$ feasible to (D.4), the later comparison between the objectives of (D.4) and (D.6) means min $(D.6) \geq$ min $(D.4)$, proving min $(D.6) =$ min $(D.4)$.

It remains to show that each function $\psi_{i,j}(\boldsymbol{V}_{i,j}, \boldsymbol{W})$ is concave, or $-\psi_{i,j}(\boldsymbol{V}_{i,j}, \boldsymbol{W})$ is convex, which is written as the composition $-\ln(1 - \tau_{i,j}(\boldsymbol{V}_{i,j}, \boldsymbol{W}))$. Function $-\ln(1 - \tau_{i,j})$ is convex and increasing in $0 < \tau_{i,j} < 1$ while $\tau_{i,j}(\boldsymbol{V}_{i,j}, \boldsymbol{W})$ is convex in $(\boldsymbol{V}_{i,j}, \boldsymbol{W})$ according to the above Lemma 8, so the composition $-\ln(1 - \tau_{i,j}(\boldsymbol{V}_{i,j}, \boldsymbol{W}))$ is convex by [16, Prop. 2.8]. □

For the above concave program (D.6), initialized from feasible solution $W^{(0)} \in \mathcal{W}$ and $V^{(0)}$ with $W_{i,j}^{(0)} = V_{i,j}^{(0)}(V_{i,j}^{(0)})^H$, the well known FW algorithm [88, 89] generates the iterative solution $(W^{(\kappa+1)}, V^{(\kappa+1)})$ for $\kappa = 0, 1, \ldots$ by solving the convex program

$$\min_{(\boldsymbol{W},\boldsymbol{V})} \langle \nabla\gamma(V^{(\kappa)}, W^{(\kappa)}), (\boldsymbol{V}, \boldsymbol{W})\rangle : \ (D.6b). \tag{D.7}$$

The reader is referred to [88, 89] for the convergence of such sequence $\{(W^{(\kappa)}, V^{(\kappa)})\}$ to an optimized solution. The FW algorithm is thus terminated in finitely many iterations by the stop criterion $|\gamma(V^{(\kappa)}, W^{(\kappa)}) - \gamma(V^{(\kappa+1)}, W^{(\kappa+1)})|/|\gamma(V^{(\kappa)}, W^{(\kappa)})| \leq \epsilon$ for some tolerance level ϵ. Due to the concavity of the objective function, the line search involved in the conventional FW algorithm is bypassed because each convex program (D.7) provides a majorant minimization for the concave program (D.6). In fact, $\{(W^{(\kappa)}, V^{(\kappa)}\}$ is a sequence of improved solution, i.e. $\gamma(V^{(\kappa+1)}, W^{(\kappa+1)}) < \gamma(V^{(\kappa)}, W^{(\kappa)})$ for all $\kappa = 0, 1, \cdots$.

It is straightforward to calculate the linear objective function in (D.7):

$$\begin{aligned}\sum_{(i,j)\in\mathcal{I}\times\mathcal{J}} \langle \nabla\gamma_{i,j}(V_{i,j}^{(\kappa)}, W^{(\kappa)}), (\boldsymbol{V}_{i,j}, \boldsymbol{W})\rangle &= \sum_{(i,j)\in\mathcal{I}\times\mathcal{J}} [-2a_{i,j}^{(\kappa)}\Re\{h_{i,i,j}^H \boldsymbol{V}_{i,j}(V_{i,j}^{(\kappa)})^H h_{i,i,j}\} \\ &+ (a_{i,j}^{(\kappa)} - b_{i,j}^{(\kappa)}) \sum_{(m,k)\in\mathcal{I}\times\mathcal{J}} h_{m,i,j}^H \boldsymbol{W}_{m,k} h_{m,i,j}]\end{aligned} \quad (D.8)$$

with $0 < b_{i,j}^{(\kappa)} := 1/(\Psi_{i,j}(W^{(\kappa)}) + \sigma^2) < a_{i,j}^{(\kappa)} := 1/(\Psi_{i,j}(W^{(\kappa)}) + \sigma^2 - h_{i,i,j}^H V_{i,j}^{(\kappa)}(V_{i,j}^{(\kappa)})^H h_{i,i,j})$.

Remark. Since $a_{i,j}^{(\kappa)} - b_{i,j}^{(\kappa)} > 0$ in (D.8), in view of constraints $\boldsymbol{V}_{m,k}\boldsymbol{V}_{m,k}^H \preceq \boldsymbol{W}_{m,k}$ in (D.6b), it can be shown that $\boldsymbol{W}_{m,k}$ can be equivalently replaced by $\boldsymbol{V}_{m,k}\boldsymbol{V}_{m,k}^H$, $(m,k) \in \mathcal{I}\times\mathcal{J}$ in (D.8), i.e the linear objective function in $(\boldsymbol{V}, \boldsymbol{W})$ in (D.7) can be equivalently transformed to a convex quadratic function $F^{(\kappa)}(\boldsymbol{V})$ in $\boldsymbol{V}$ only. Also the constrained sets $\mathcal{W}_B$ and $\mathcal{W}_C$ in (D.2) and (D.3) on $\boldsymbol{W}$ correspond to the following convex constrained sets Ω_B and Ω_C on $\boldsymbol{V}$. Thus, without the QoS constraints (D.1), FW iteration (D.7) is the convex quadratic $\min_{\boldsymbol{V}\in\Omega_B\cap\Omega_C} F^{(\kappa)}(\boldsymbol{V})$ in $\boldsymbol{V}$ only. Without the cognitive constraints $\boldsymbol{V} \in \Omega_C$, the iteration $\min_{pmbV\in\Omega_B} F^{(\kappa)}(\boldsymbol{V})$ admits the closed-form optimal solution and thus is very computationally inexpensive. However, the QoS constraint in (D.1), which is convex in $\boldsymbol{W}$, corresponds to (non-convex) indefinite quadratic constrained one in $\boldsymbol{V}$, so it is not recommended to make such substitutions in (D.7).

$$\Omega_B = \{\boldsymbol{V} \ : \ \max_{i\in\mathcal{I}} \sum_{j\in\mathcal{J}} \langle \boldsymbol{V}_{i,j}\boldsymbol{V}_{i,j}^H\rangle \le P_B\}, \quad (D.9)$$

$$\Omega_C = \{\boldsymbol{V} : \max_{r=1:R} \sum_{(i,j)\in\mathcal{I}\times\mathcal{J}} h_{0,i,r}^H \boldsymbol{V}_{i,j}\boldsymbol{V}_{i,j}^H h_{0,i,r} \le P_0\}, \quad (D.10)$$

D.3 Simulation Results

We consider different cases with $N = 7$ BSs (cells) and $K = 2$ users (MTs) per cell. The cells are hexagon-shaped with one in the center and six surrounding. The adjacent BS-to-BS distance is 1.4 km, and MTs are uniformly distributed within each hexagonal cell. A typical 3GPP signal model [75] is adopted, in which the channel gain for each transmission link consists of three parts: (i) distance-dependent path loss component $L = 128.1 + 37.6\log_{10}(D)$, where D is the transmission distance in km; (ii) 8 dB log-normal shadowing component; and (iii) Rayleigh-fading component. The noise power spectral density and bandwidth is set to be −162 dBm/Hz and 10^7 Hz, respectively. Antenna gain is 15 dBi. For simplicity, all the required rates in (D.1) are equal to γ. The tolerance $\epsilon = 10^{-5}$ is set in all simulations. In all the figures, the legend "Grad. Proj." refers to the performance of the gradient projection method in [153].

Fig. D.1 illustrates unfair rate distribution caused by ignoring QoS rate constraints (D.1). In more than 90% of channel realizations, there are at least 2 disabled users (whose rate is less than 0.1% of the sum rate). Fig. D.2 shows the sum rate performance versus BS power constraints

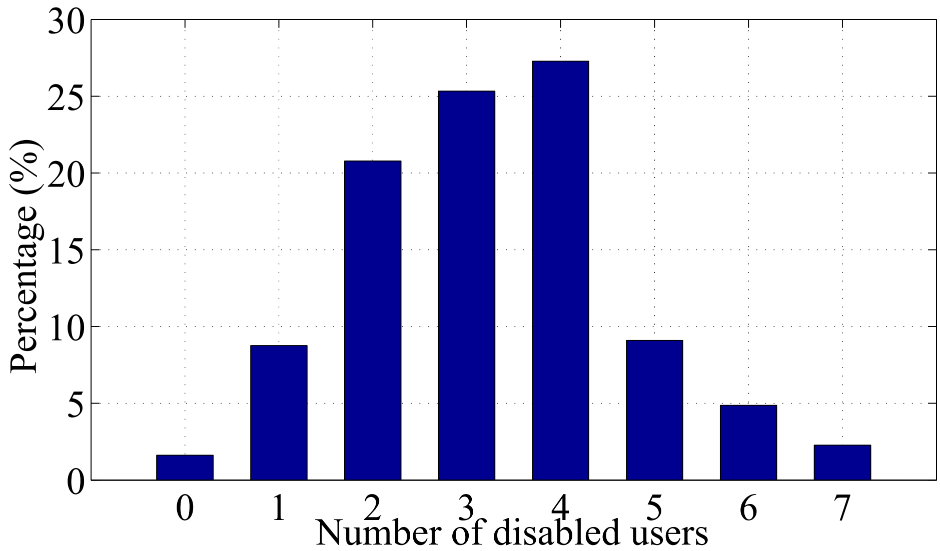

FIGURE D.1: Percentage vs. number of disabled users: $P_B = 30$ dBm, $P_o = -90$ dBm

under different QoS rate constraints. To set appropriate QoS constraints, we denote the maximin rate by R_{mm} as the optimal value of the problem $\max_{\boldsymbol{W}} \min_{(i,j)\in\mathcal{I}\times\mathcal{J}} \psi_{i,j}(\boldsymbol{W}) : \boldsymbol{W} \in \mathcal{W}_B \cap \mathcal{W}_C$, which is easily solved by a bisection procedure. The sum rate maximization problem is only feasible when the required rate $\gamma \in [0, R_{mm}]$. The ratio of $\frac{\gamma}{R_{mm}} \in [0, 1]$ represents the tightness degree of the QoS rate constraints. It can be seen that with very high QoS setting ($\frac{\gamma}{R_{mm}} = 0.95$), the sum rate performance degrades significantly.

Next, we study the impact of different QoS and cognitive constraints on the sum rate performance under fixed BS power constraints. It is observed from Fig. D.3 that the tight cognitive power constraints with $P_o = -110$ dBm in (D.3) leads to a sharp decrease of the sum rates. However,

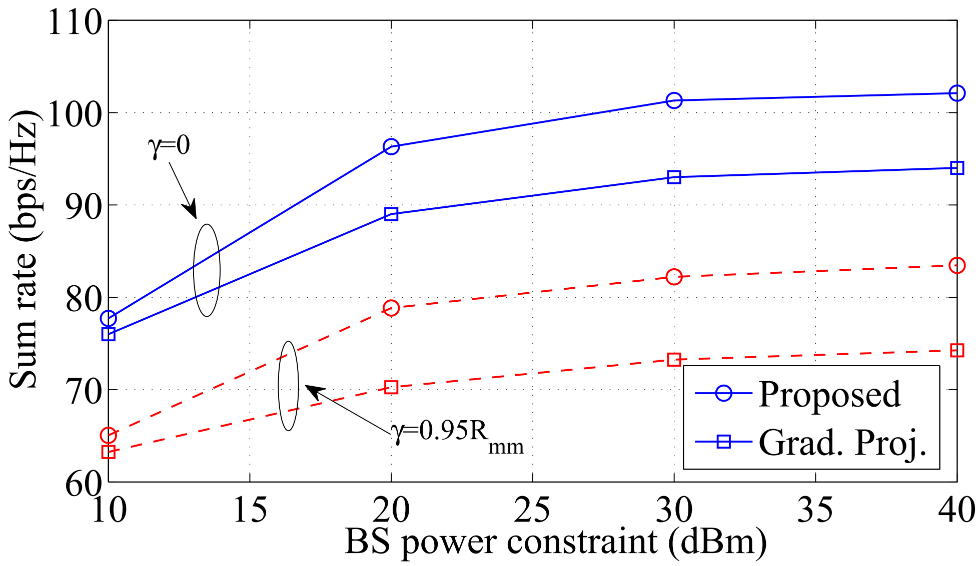

FIGURE D.2: Sum rate vs. BS power constraint: $P_o = -90$ dBm

with $P_o = -90$ dBm in (D.3), the sum rates drop by only about 10% even when all users achieve 85% of the maximin rate R_{mm}. The sum rates and QoS thus can be flexibly traded off.

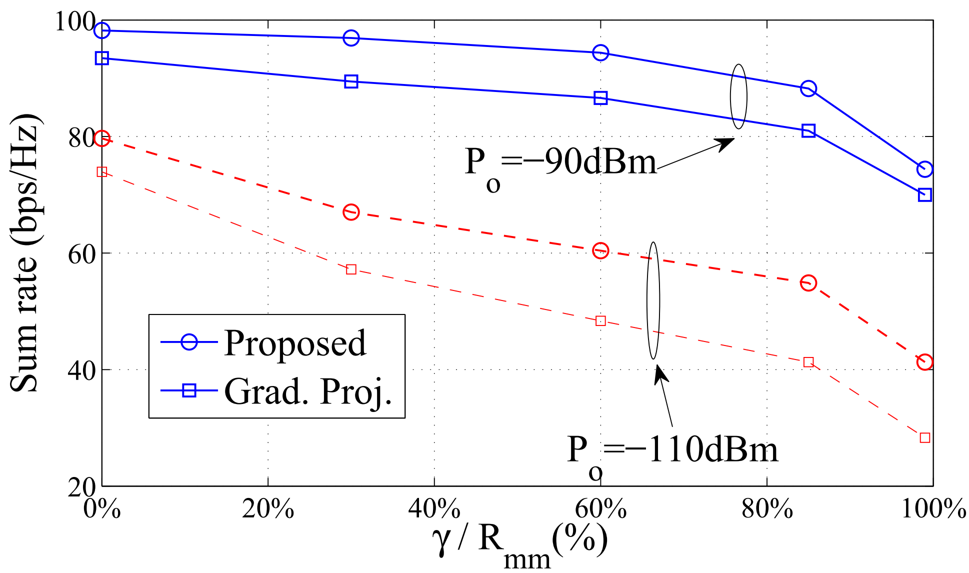

FIGURE D.3: Sum rate vs. required minimum rate: $P_B = 30$ dBm

Further, Fig. D.4 shows how the sum rate performance increases in degree of freedom expressed by the number of antennas employed at the BSs. Moreover, the gap between the two sum rate curves (with QoS and without QoS constraints) is reduced gradually. The feasible rate capacity region also grows effectively.

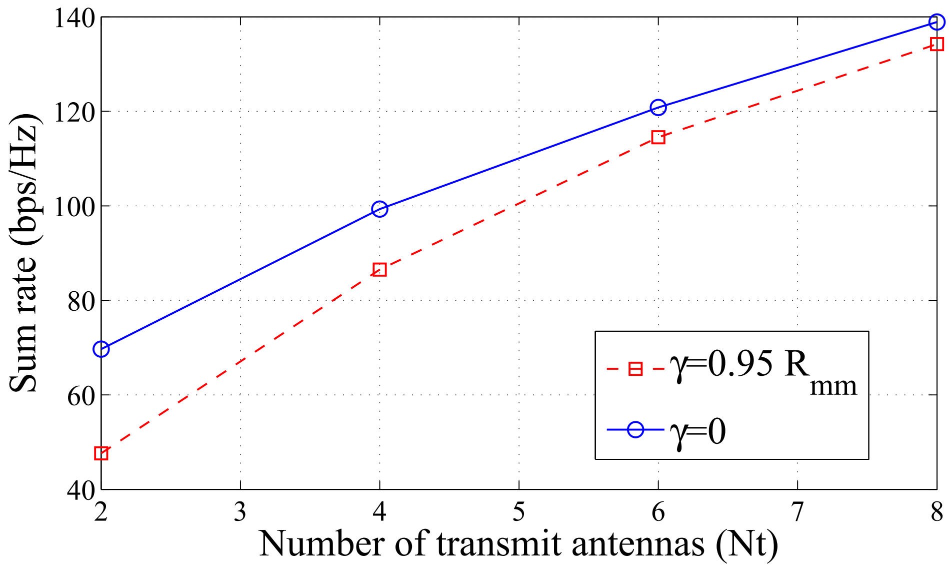

FIGURE D.4: Sum rate vs. number of transmit antennas: $P_B = 30$ dBm, $P_o = -90$ dBm

Finally, Table. D.1 provides the average number of iterations required by the proposed FW algorithm and the gradient projection method [153] with the same stopping criterion. Both algorithms are very computationally inexpensive because they all involve a small number of simple convex programs. Fig. D.5 shows one typical example of the convergence behaviours of the two algorithms initialized from the same feasible solution. It is observed that FW algorithm converges to the same optimal solution independently on initial feasible solutions $(V^{(0)}, W^{(0)})$.

TABLE D.1: Algorithmic statistics: number of iterations and total CPU time. $N, K, P_B, P_o = (7, 2, 30 \text{ dBm}, -90\text{dBm})$.

N_t		2	4	6	8
Proposed	Iter. #	35.41	36.29	38.13	38.24
	CPU time	96.60	118.30	227.25	365.95
Grad. Proj.	Iter. #	25.52	25.24	26.24	25.64
	CPU time	50.57	55.53	78.24	133.41

D.4 Conclusions

This research has presented efficient d.c. iterations for obtaining the optimal coordinated transmission strategies for the downlink in cognitive multi-cell wireless networks. Results have shown

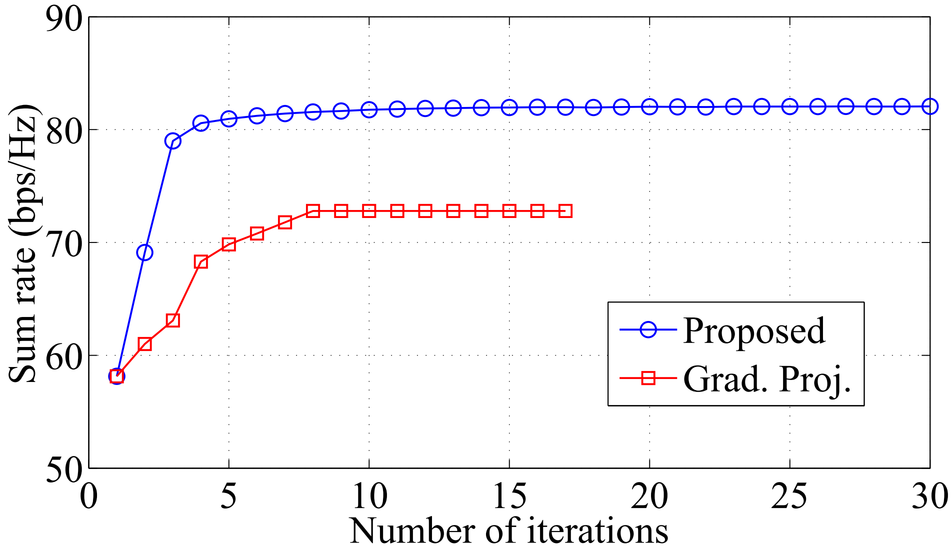

FIGURE D.5: Convergence behaviour example: $P_B = 30$ dBm, $P_o = -90$ dBm, $\gamma = 0.95R_{mm}$

that our proposed method exhibits quick convergence with low computational load but nevertheless still performs as well as the global optimisation algorithms of prohibitively high complexity.

Bibliography

[1] Q. Spencer, C. Peel, A. Swindlehurst, and M. Haardt, "An introduction to the multi-user mimo downlink," *IEEE Communications Magazine*, vol. 42, pp. 60–67, Oct. 2004.

[2] D. Tse and P. Viswanath, *Fundamentals of Wireless Communications.* New York, NY, USA: Cambridge University Press, 2005.

[3] L. Wolsey and G. Nemhauser, *Integer and Combinatorial Optimization.* Wiley Series in Discrete Mathematics and Optimization, Wiley, 1999.

[4] L. Huang, S. Kumar, and C.-C. Kuo, "Adaptive resource allocation for multimedia qos management in wireless networks," *IEEE Trans. Vehicular Technology*, vol. 53, pp. 547–558, Mar. 2004.

[5] D. Gesbert, S. Hanly, H. Huang, S. S. Shitz, O. Simeone, and W. Yu, "Multi-cell MIMO cooperative networks: A new look at interference," *IEEE Journal on Selected Areas in Communications*, vol. 28, pp. 1380 –1408, Dec. 2010.

[6] S. Karmakar and M. K. Varanasi, "The capacity region of the MIMO interference channel and its reciprocity to within a constant gap," *IEEE Trans. Information Theory*, vol. 59, pp. 4781–4797, Aug. 2013.

[7] R. H. Etkin, D. Tse, and H. Wang, "Gaussian interference channel capacity to within one bit," *IEEE Trans. Information Theory*, vol. 54, pp. 5534 –5562, Dec. 2008.

[8] A. Goldsmith, *Wireless Communications.* New York, NY, USA: Cambridge University Press, 2005.

[9] H. Dahrouj and W. Yu, "Multicell interference mitigation with joint beamforming and common message decoding," *IEEE Trans. Communications*, vol. 59, pp. 2264 –2273, Aug. 2011.

[10] E. Che and H. D. Tuan, "Sum-rate based coordinated beamforming in multicell multi-antenna wireless networks," *IEEE Communications Letters*, vol. 18, pp. 1019–1022, Jun. 2014.

[11] W. Utschick and J. Brehmer, "Monotonic optimization framework for coordinated beamforming in multicell networks," *IEEE Trans. Signal Processing*, vol. 60, pp. 1899 –1909, Apr. 2012.

[12] E. Che, H. Tuan, and H. Nguyen, "Joint optimization of cooperative beamforming and relay assignment in multi-user wireless relay networks," *IEEE Trans. Wireless Communications*, Accepted, 2014.

[13] H. Dahrouj and W. Yu, "Coordinated beamforming for the multicell multi-antenna wireless system," *IEEE Trans. Wireless Communications*, vol. 9, pp. 1748 –1759, May 2010.

[14] A. H. Phan, H. D. Tuan, H. H. Kha, and D. T. Ngo, "Non-smooth optimization for efficient beamforming in cognitive radio multicast transmission," *IEEE Trans. Signal Processing*, 2012.

[15] K. Sohrabi, J. Gao, V. Ailawadhi, and G. J. Pottie, "Protocols for self-organization of a wireless sensor network," *IEEE Personal Commun.*, vol. 7, no. 5, pp. 16–27, 2000.

[16] H. Tuy, *Convex Analysis and Global Optimization.* Kluwer Academic, 1998.

[17] R. Horst and H. Tuy, *Global Optimization: Deterministic Approaches.* Springer, 1996.

[18] "Spectrum policy task force report. technical report 02-135," *Federal Communications Commission*, Nov. 2002.

[19] S. Haykin, "Cognitive radio: brain-empowered wireless communications," *IEEE Journal on Selected Areas in Comm.*, vol. 23, pp. 201–220, Feb. 2005.

[20] J. Mitola and J. Maguire, G.Q., "Cognitive radio: making software radios more personal," *IEEE Personal Communications*, vol. 6, pp. 13–18, Aug. 1999.

[21] S. Mishra, A. Sahai, and R. Brodersen, "Cooperative sensing among cognitive radios," in *IEEE Inter. Conf. on Communication (ICC)*, pp. 1658–1663, June 2006.

[22] S. Joshi and S. Boyd, "Sensor selection via convex optimization," *IEEE Trans. Signal Processing*, vol. 57, pp. 451–462, Feb 2009.

[23] M. Lazaro, M. Sanchez-Fernandez, and A. Artes-Rodriguez, "Optimal sensor selection in binary heterogeneous sensor networks," *IEEE Trans. Signal Processing*, vol. 57, pp. 1577–1587, Apr. 2009.

[24] X. R. Wang, E. Aboutanios, M. Trinkle, and M. Amin, "Reconfigurable adaptive array beamforming by antenna selection," *IEEE Trans. Signal Processing*, vol. 62, pp. 2385–2396, May. 2014.

[25] L. Zhang, Y.-C. Liang, and Y. Xin, "Joint beamforming and power allocation for multiple access channels in cognitive radio networks," *IEEE Journal on Selected Areas in Comm.*, vol. 26, pp. 38–51, Jan. 2008.

[26] J.-H. Noh and S.-J. Oh, "Cognitive radio channel with cooperative multi-antenna secondary systems," *IEEE Journal on Selected Areas in Comm.*, vol. 32, pp. 539–549, Mar. 2014.

[27] A. Behbahani, R. Merched, and A. Eltawil, "Optimizations of a mimo relay network," *IEEE Trans. Signal Processing*, vol. 56, pp. 5062–5073, Oct. 2008.

[28] U. Rashid, H. Tuan, H. Kha, and H. Nguyen, "Joint optimization of source precoding and relay beamforming in wireless mimo relay networks," *IEEE Trans. Communications,*, vol. 62, pp. 488–499, Feb. 2014.

[29] R. Pabst et al, "Relay-based deployment concepts for wireless and mobile broadband radio," *IEEE Communication Magazine*, vol. 42, pp. 80–89, Sep. 2004.

[30] Y. Liu, R. Hoshyar, X. Yang, and R. Tafazolli, "Integrated radio resource allocation for multihop cellular networks with fixed relay stations," *IEEE J. on Selected Areas in Communications*, vol. 24, pp. 2137–2146, Nov. 2006.

[31] L. Le and E. Hossain, "Multihop cellular networks: potential gains, research challenges, and a resource allocation framework," *IEEE Communication Magazine*, vol. 45, pp. 66–73, Sep. 2007.

[32] Y. Jing and H. Jafarkhani, "Single and multiple relay selection schemes and their achievable diversity orders," *IEEE Trans. Wireless Communications*, vol. 8, pp. 1414–1423, Mar. 2009.

[33] Y. Zhao, R. S. Adve, and T. J. Lim, "Improving amplyfy-and-forward relay networks: optimal power allocation versus selection," *IEEE Trans. Wireless Communications*, vol. 6, pp. 3114–3123, Aug. 2007.

[34] M. Ju, H.-K. Song, and I.-M. Kim, "Joint relay-and-antenna selection in multi-antenna relay networks," *IEEE Trans. Communications*, vol. 58, pp. 3417–3422, Dec. 2010.

[35] Y. Li, Q. Yin, W. Su, and H.-M. Wang, "On the design of relay selection strategies in regenerative cooperative networks with outdated CSI," *IEEE Trans. Wireless Communications*, vol. 10, pp. 3086–3097, Sep. 2011.

[36] A. Ikhlef, D. S. Michalopoulos, and R. Schober, "Max-max relay selection for relays with buffers," *IEEE Trans. Wireless Communications*, vol. 11, pp. 1124–1135, Mar. 2012.

[37] D. S. Michalopoulos, H. A. Suraweera, G. K. Karagiannidis, and R. Schober, "Amplify-and-foward relay selection with outdated channel estimates," *IEEE Trans. Communications*, vol. 60, pp. 1278–1290, May. 2012.

[38] S. S. Soliman and N. C. Beaulieu, "Exact analysis of dual-hop AF maximum end-to-end SNR relay selection," *IEEE Trans. Communications*, vol. 60, pp. 2135–2145, Aug. 2012.

[39] J. Laneman, D. Tse, and G. Wornel, "Cooperative diversity in wireless networks: effcient protocols and outage behavior," *IEEE Trans. Information Theory*, vol. 50, pp. 3062–3080, Dec. 2004.

[40] X. Deng and A. M. Haimovich, "Power allocation for cooperative relaying in wireless network," *IEEE Communication Letters*, vol. 9, pp. 994–996, Nov. 2005.

[41] Y. Liang and V. Veeravalli, "Gaussian orthogonal relay channel: optimal resourse allocation and capacity," *IEEE Trans. Information Theory*, vol. 51, pp. 3284–3289, Sep. 2005.

[42] A. H. Madsen and J. Zhang, "Capacity bounds and power allocation for cooperative strategies in Gaussian relay networks," *IEEE Trans. Information theory*, vol. 51, pp. 2020–2040, June 2005.

[43] Y. Jing and H. Jafarkhani, "Network beamforming using relays with perfect channel information," *IEEE Trans. Information Theory*, vol. 55, pp. 2499–2511, Jun. 2009.

[44] V. I. Morgenshtern and H. Bolcskei, "Crystallization in large wireless networks," *IEEE Trans. Information Theory*, vol. 53, pp. 3319–3349, Oct. 2007.

[45] D. H. N. Nguyen, H. H. Nguyen, and H. D. Tuan, "Distributed beamforming in relay-assisted multiuser communications," in *Proc. of IEEE International Conference on Communications (ICC), Dresden, Germany*, Jun. 2009.

[46] S. Fazeli-Dehkordy, S. Shahbazpanahi, and S. Fazor, "Multiple peer-to-peer communications using a network of relays," *IEEE Trans. Signal Processing*, vol. 57, pp. 3053–3062, Aug 2009.

[47] L. Dong, A. P. Petropulu, and H. V. Poor, "Weighted cross-layer cooperative beamforming for wireless networks," *IEEE Trans. Signal Processing*, vol. 57, pp. 3240–3252, Aug. 2009.

[48] A. Phan, H. D. Tuan, H. H. Kha, and H. H. Nguyen, "Nonsmooth optimization-based beamforming in multiuser wireless relay networks," in *Proc. of 4th International Conference on Signal Processing and Communication Systems (ICSPCS), Gold Coast, Australia*, Dec. 2010.

[49] A. H. Phan, H. D. Tuan, and H. H. Kha, "Space-time beamforming for multiuser wireless relay networks," in *Proc. of International Conference on Acoustics, Speech and Signal Processing(ICASSP), Prague, Czech*, May. 2011.

[50] A. H. Phan, H. D. Tuan, and H. H. Kha, "Optimized solutions for beamforming problems in amplify-and-forward wireless relay networks," in *Proc. of Global Communication Conference (Globecom), Houston, TX, USA*, Dec. 2011.

[51] E. Koyuncu and H. Jafarkhani, "Distributed beamforming in wireless multiuser relay-interference networks with quantized feedback," *IEEE Trans. Information Theory*, vol. 58, pp. 4538–3576, Jul. 2012.

[52] M. Karakayali, G. Foschini, and R. Valenzuela, "Network coordination for spectrally efficient communications in cellular systems," *IEEE Trans. Wireless Communications*, vol. 13, pp. 56 –61, Aug. 2006.

[53] A. Sibile, C. Oestges, and A. Zanella, eds., *MIMO From Theory to Implementation*. Academic Press, 2011.

[54] G. J. Foschini, "Layered space-time architecture for wireless communication in a fading environment when using multi-element antennas," *Bell Labs Technical Journal*, vol. 1, no. 2, pp. 41–59, 1996.

[55] L. Zheng and D. Tse, "Diversity and multiplexing: a fundamental tradeoff in multiple-antenna channels," *IEEE Trans. Information Theory,*, vol. 49, pp. 1073–1096, May. 2003.

[56] H. H. Kha, H. D. Tuan, and H. H. Nguyen, "Fast global optimal power allocation in wireless networks by local d.c. programming," *IEEE Trans. Wireless Communications*, vol. 11, pp. 510–515, Feb. 2012.

[57] Q. J. Shi, M. Razaviyayn, Z. Q. Luo, and C. He, "An iteratively weighted MMSE approach to distributed sum-utility maximization for a MIMO interfering broadcast channel," *IEEE Trans. Signal Processing*, vol. 59, pp. 4331–4340, Sep. 2011.

[58] H. Tam, E. Che, and H. Tuan, "Optimized linear precoder in mimo interference channel using d.c. programming," in *International Conference on Signal Processing and Communication Systems (ICSPCS),*, pp. 1–5, Dec. 2013.

[59] T. Han and K. Kobayashi, "A new achievable rate region for the interference channel," *IEEE Trans. Information Theory*, vol. 27, pp. 49–60, Jan. 1981.

[60] A. B. Carleial, "A case where interference does not reduce capacity," *IEEE Trans. Information Theory*, vol. 21, pp. 569–570, Sep. 1975.

[61] E. Telatar and D. Tse, "Bounds on the capacity region of a class of interference channels," in *IEEE Intl. Symp. on Information Theory (ISIT)*, pp. 2871–2874, Jun. 2007.

[62] E. Che and H. D. Tuan, "Interference mitigation by jointly splitting rates and beamforming for multi-cell multi-user networks," in *Intl. Symp. Communications and Inf. Technologies (ISCIT)*, pp. 41–45, Sep. 2013.

[63] E. Che, H. D. Tuan, and H. H. M. Tam, "Optimised power splits for Han-Kobayashi interference mitigation," *(Submitted).*

[64] E. Che and H. Tuan, "Optimized coordinated precoding in multicell mimo wireless systems," in *Intl. Symp. Comm. and Inf. Tech. (ISCIT),*, pp. 188–191, Sep. 2013.

[65] B. Sklar, "Rayleigh rading channels in mobile digital communication systems .i. characterization," *IEEE Comm. Magazine*, vol. 35, pp. 90–100, Jul. 1997.

[66] T. S. Rappaport, *Wireless Communications: Principles and Practice.* Upper Saddle River, NJ. Prentice-Hall, 1996.

[67] T. Okumura, E. Ohmori, and K. Fukuda, "Field strength and its variability in vhf and uhf land mobile service," *Review Electrical Communication Laboratory*, vol. 16, pp. 825–873, Sept.-Oct. 1968.

[68] C. Anderson, T. Rappaport, K. Bae, A. Verstak, N. Tamakrishnan, W. Trantor, C. Shaffer, and L. T. Waton, "In-building wideband multipath characteristics at 2.5 and 60 ghz," *Proceedings: IEEE Vehicular Technology Conference*, pp. 24–28, Sep. 2002.

[69] A. Hrovat, G. Kandus, and T. Javornik, "A survey of radio propagation modeling for tunnels," *IEEE Communications Surveys Tutorials*, vol. 16, pp. 658–669, Feb. 2014.

[70] M. Kim, Y. Konishi, Y. Chang, and J. Takada, "Large scale parameters and double-directional characterization of indoor wideband radio multipath channels at 11 ghz," *IEEE Trans. Antennas and Propagation,*, vol. 62, pp. 430–441, Jan. 2014.

[71] K. Ghanem, "Effect of channel correlation and path loss on average channel capacity of body-to-body systems," *IEEE Trans. Antennas and Propagation,*, vol. 61, pp. 6260–6265, Dec. 2013.

[72] N. Seifi, *Base Station Coordination in Multicell MIMO Networks.* PhD thesis, Chalmers University of Technology, 2012.

[73] N. Nakagami, "The m-distribution, a general formula for intensity distribution of rapid fading," *Statistical Methods in Radio Wave Propagation*, 1960.

[74] T. M. Cover and J. A. Thomas, *Elements of Information Theory.* John Wiley and Sons, Inc, 1991.

[75] "3GPP TR 36.913, requirements for further advancements for evolved universal terrestrial radio access (LTE-advanced)," Mar. 2009.

[76] P. Stoica, Y. Jiang, and J. Li, "On mimo channel capacity: an intuitive discussion," *IEEE Signal Processing Magazine*, vol. 22, pp. 83–84, May. 2005.

[77] I. E. Telatar, "Capaity of multi-antenna gaussian channels," *European Trans. Telecommunications*, pp. 585 –595, Dec. 1999.

[78] G. B. Dantzig, A. Orden, and P. Wolfe, "The generalized simplex method for minimizing a linear form under linear inequality restraints.," *Pacific Journal of Mathematics*, vol. 5, no. 2, pp. 183 – 195, 1955.

[79] E. A. Jorswieck and E. G. Larsson, "Monotonic optimization framework for the two-user MISO interference channel," *IEEE Trans. Communications*, vol. 58, pp. 2159–2168, Jul. 2010.

[80] S. Boyd and L. Vandenberghe, *Convex Optimization.* Cambridge University Press, 2004.

[81] Y. Nesterov and A. Nemirovkii, "Interior-point polynomial algorithms in convex programming.," *Society for Industry and Applied Mathematics*, 1994.

[82] F. Alizadeh and D. Goldfarb, "Second-order cone programming," *Mathematical programming*, vol. 95, no. 1, pp. 3 – 51, 2003.

[83] H. Tuy, "Robust solution of nonconvex global optimization problems," *J. of Global Optimization*, vol. 32, pp. 307–323, Feb. 2005.

[84] H. Tuy and N. T. Hoai-Phuong, "A robust algorithm for quadratic optimization under quadratic constraints," *J. of Global Optimization*, vol. 37, pp. 557–596, Apr. 2007.

[85] H. Tuy, "A new minimax theorem with applications," *J. of Global Optimization*, vol. 50, no. 3, pp. 371–378, 2011.

[86] H. A. Le-Thi and T. Pham-Dinh, "DC optimization algorithms for solving the trust region subproblem," *SIAM J. on Optimization*, vol. 8, pp. 476–505, Apr. 1998.

[87] A. H. Phan, H. D. Tuan, H. H. Kha, and H. H. Nguyen, "Beamforming optimization in multi-user Amplify-and-Forward wireless relay networks," *IEEE Trans. Wireless Communications,*, vol. 11, pp. 1510 –1520, Apr. 2012.

[88] P. Apkarian and H. D. Tuan, "Robust control via concave optimization: local and global algorithms," *IEEE Trans. Automatic Control*, vol. 45, pp. 299–305, Feb. 2000.

[89] P. Apkarian and H. D. Tuan, "Concave programming in control theory," *J. of Global Optimization*, vol. 15, pp. 243–270, Apr. 1999.

[90] T. Pham-Dinh, N. Nguyen-Canh, and H. A. Le-Thi, "An efficient combined DCA and B&B using DC/SDP relaxation for globally solving binary quadratic programs," *J. of Global Optimization*, vol. 48, pp. 595–632, 2010.

[91] H. Konno, P. T. Thach, and H. Tuy, *Optimization on low rank nonconvex structure*. Kluwer Academic, 1997.

[92] H. D. Tuan, P. Apkarian, S. Hosoe, and H. Tuy, "D.C. optimization approach to robust controls: the feasibility problems," *International J. of Control*, vol. 73, pp. 89–104, Feb. 2000.

[93] J. C. Dunn, "Rates of convergence for conditional gradients algroritms," *SIAM J. on Control and Optimization*, vol. 17, pp. 187–121, Jan. 1979.

[94] G. L. Nemhauser and L. A. Wolsey, *Integer and combinatorial optimization*, vol. 18. Wiley New York, 1988.

[95] H. Tuy, "$\mathcal{D}(\mathcal{C})$-optimization and robust global optimization," *J. of Global Optimization*, vol. 47, pp. 485–501, Apr. 2010.

[96] H. Tuy and H. D. Tuan, "Generalized S-lemma and strong duality in nonconvex quadratic programming," *J. of Global Optimization*, 2012.

[97] V. Gupta, T. Chung, B. Hassibi, and R. Murray, "On stochastic sensor selection algorithm with application in sensor scheduling and sensor coverage," *Automatica*, vol. 42, pp. 251–260, Feb. 2006.

[98] H. Rowaihy, S. Eswaran, M. Johnson, D. Verma, A. Bar-Noy, T. Brown, and T. L. Porta, "A survey of sensor selection schmes in wireless sensor networks," in *Proc. SPIE*, 2007.

[99] S. Haykin, "Cognitive radio: brain-empowered wireless communication," *IEEE J. of Selected Areas in Communications*, vol. 23, pp. 201–220, Feb. 2005.

[100] R. Broderson, A. Wolisz, D. Cabric, and S. Mishra, "White paper: CORVUS a cognitive radio approach for usage of virtual unlicensed spectrum," *Technical Report*, 2004.

[101] "FCC report of the use of the spectrum efficiency working group," tech. rep., 2002.

[102] T. Erpek, M. Lofquist, and K. Patton, "Spectrum occupancy measurements: loring commence centre," *Limestone, Maine, September 18-20, shared Spectrum Company Report*, 2007.

[103] B. Romano, "Fcc adopts rule changes for smart radio," *Federal Communications Commission, Press Release*, 2005.

[104] A. Ghasemi and E. Sousa, "Collaborative spectrum sensing for opportunistic access in fading environments," in *IEEE Intl. Symp. on New Frontiers in Dynamic Spectrum Access Networks*, pp. 131 –136, Nov. 2005.

[105] Y. Selen, H. Tullberg, and J. Kronander, "Sensor selection for cooperative spectrum sensing," in *3rd IEEE Symposium on New Frontiers in Dynamic Spectrum Access Networks*, pp. 1 –11, Oct. 2008.

[106] H. D. Tuan, T. T. Son, H. Tuy, and H. H. Nguyen, "Optimum multi-user detection by nonsmooth optimization," in *Proc. of IEEE International Conference on Acoustics, Speech and Signal Processing (ICASSP), Prague*, May. 2011.

[107] G. N. Karystinos and D. A. Pados, "The maximum squared correlation, total asymptotic effciency, and sum capacity of minimum total-squared-correlation binary signature sets," *IEEE Trans. Information Theory*, vol. 51, pp. 348–355, Jan 2005.

[108] L. Bregman, "The relaxation method of finding the common point of convex sets and its application to the solution of problems in convex programming," *USSR Compt. Mathematics and Mathematical Physics*, vol. 7, pp. 200–217, 1967.

[109] I. S. Dhillon and J. A. Tropp, "Matrix nearness problems with bregman divergence," *SIAM J. on Matrix Analysis and Applications*, vol. 29, pp. 112011–46, Aug. 2007.

[110] B. Kulis, M. A. Sustik, and I. S. Dhillon, "Low-rank kernel learning with Bregman matrix divergence," *J. of Machine Learning Research*, vol. 10, pp. 341–376, Apr. 2009.

[111] E. Larsson and M. Skoglund, "Cognitive radio in a frequency-planned environment: some basic limits," *IEEE Trans. Wireless Communications*, vol. 7, pp. 4800 –4806, Dec. 2008.

[112] J. D. Parsons, *The mobile radio propagation channel.* John Wiley & Sons, 2000.

[113] M. Gudmundson, "Correlation model for shadow fading in mobile radio systems," *Electronics Letters*, vol. 27, pp. 2145 –2146, Nov. 1991.

[114] B. Scholkopf and A. J. Smola, *Learning with kernels.* MIT Press, Cambridge, MA, 2002.

[115] R. Schneider, *Convex bodies: The Brunn-Minkowski theory.* Cambridge University Press, Cambridege, 1993.

[116] R. Horn and C. Johnson, *Matrix analysis.* Cambridge University Press, 1985.

[117] H. D. Tuan, D. H. Pham, B. Vo, and T. Q. Nguyen, "Entropy of general Gaussian distributions and MIMO channel capacity maximizing precoder and decoder," in *Proc. IEEE Int. Conf. on Acoustics, Speech, and Signal Processing (ICASSP 2007).*

[118] D. Parsavan and M. K. Varanasi, "RMS bandwidtch constrained signature waverforms that maximize the total capacity of PAM-synchornous CDMA channels," *IEEE Trans. Communications*, vol. 44, pp. 65–75, Jan. 1996.

[119] D.-T. Pham, "Joint approximate diagonaliztion of positive definite hermitian matrices," *SIAM J. Matrix Anal. Appl.*, vol. 22, pp. 1136–1152, Aug. 2001.

[120] M. A. Nielsen and I. L. Chuang, *Quantum computation and quantum information.* Cambridge University Press, 2000.

[121] K. Tsuda and S. Noble, "Learning kernels from biological networks by maximizing entropy," *Bioinformatics*, vol. 20, pp. 326–333, Mar. 2004.

[122] P. Apkarian and H. D. Tuan, "A sequential SDP/Gauss-Newton algorithm for rank-constrained LMI problems," in *Proc. of the 38-th Conference on Decision and Control (CDC), Phoenix, Arizona*, pp. 2238–2245, Dec. 1999.

[123] P. Apkarian, D. Noll, and H. D. Tuan, "Fixed-order h_∞ control design via a partially augmented Lagrangian method," *International Journal of Robust and Nonlinear Control*, vol. 12, pp. 1137–1148, Dec. 2003.

[124] P. Apkarian, D. Noll, J. B. Thevenet, and H. D. Tuan, "A spectral quadratic-SDP method with applications to fixed-order H_2 and H_∞ synthesis," *European Journal of Control*, vol. 10, pp. 527–538, Dec. 2004.

[125] D. Noll, M. Torki, and P. Apkarian, "Partially augmented Lagrangian method for matrix inequality constraints," *SIAM J. of Optimization*, vol. 15, pp. 161–184, Jan. 2004.

[126] P. Apkarian, D. Noll, and A. Rondepierre, "Mixed H_2/H_∞ control via nonsmooth optimization," *SIAM J. Control Optimz.*, vol. 47, pp. 1516–1546, Mar. 2008.

[127] J. F. Sturm, "Using sedumi 1.02, a matlab toolbox for optimization over symmetric cones," *Optim. Methods Softw.*, vol. 11-12, pp. 625–653, 1999.

[128] V. Fedorov, *Theory of optimal experiments.* New York: Academic, 1985.

[129] A. Miler and N.-K. Nguyen, "Algorithm AS 295: a Fedorov exchange algorithm for D-optimal design," *J. of Royal Satitistical Society Serie C (Appl. Statist.)*, vol. 43, no. 4, pp. 669–677, 1994.

[130] I. Ahmed, A. Nasari, D. S. Michalopoulos, R. Schober, and R. K. Mallik, "Relay subset selection and fair power allocation for best and partial relay selection in generic noise and interference," *IEEE Trans. Wireless Communications*, vol. 11, pp. 1828–1939, May. 2012.

[131] B. Wang, Z. Han, and K. J. R. Liu, "Distributed relay selection and power control for multi-user cooperative communication networks using Stackelberg game," *IEEE Trans. Mobile Computing*, vol. 8, pp. 975–990, Jul. 2009.

[132] K. T. Phan, D. H. N. Nguyen, and T. Le-Ngoc, "Joint power allocation and relay selection in cooperative networks," in *Proc. of IEEE Global Telecommunications Conference (GLOBECOM), Honolulu, Hawaii, USA*, Dec. 2009.

[133] G. Zheng, Y. Zhang, C. Li, and K.-K. Wong, "A stochastic optimization approach for joint relay assignment and power allocation in orthogonal amplify-and-forward cooperative wireless networks," *IEEE Trans. Wireless Communications*, vol. 12, pp. 4091–4099, Dec. 2011.

[134] S. Mallick, M. R. Rashid, and V. K. Bhargava, "Joint relay selection and power allocation for decode-and-forward cellular relay ntewrok with imperfect CSI," in *Proc. of IEEE Globecom*, 2011.

[135] H. Fang, X. Lin, and T. M. Lok, "Power allocation for multiuser cooperative communication netwroks under relay selection degree bound," *To appear in IEEE Trans. Vehicle Technology.*

[136] U. Rashid, H. D. Tuan, and H. H. Nguyen, "Relay beamforming in multi-user wireless relay networks based on throughput maximin optimization," *IEEE Trans. Communications*, vol. 61, p. 1739–1749, 2013.

[137] H. H. Kha, H. D. Tuan, H. H. Nguyen, and T. T. Pham, "Optimization of cooperative beamforming for SC-FDMA multi-user multi-relay networks by tractable D.C. programming," *IEEE Trans. Signal Processing*, vol. 61, pp. 467–479, Jan. 2013.

[138] H. Tuy, M. Minoux, and N. T. H. Phuong, "Discrete monotonic optimization with application to a discrete location problem," *SIAM Journal on Optimization*, vol. 17, no. 1, pp. 78–97, 2006.

[139] H. D. Tuan, T. T. Son, H. Tuy, and P. T. Khoa, "Monotonic optimization based decoding for linear codes," *J. of Global Optimization*, 2011.

[140] S. A. Jafar, *Interference alignment: a new look at signal dimensions in a communication network*. Now Publisher Inc, 2011.

[141] N. Tran, H. Nguyen, H. Tuan, and D. Dodds, "Training designs for amplify-and-forward relaying with spatially correlated antennas," *IEEE Trans. Vehicular Technology*, vol. 61, pp. 2864–2870, Jul. 2012.

[142] M. Arti, R. Bose, M. Bhatnagar, and A. Hjorungnes, "Relay strategies for high rate space-time code in cooperative mimo networks," in *Intl. Symp. on Wireless Commun. Sys. (ISWCS)*, 2007.

[143] M. R. Bhatnagar, M. K. Arti, A. H. R. Bose, and L. Song, "A time efficient multi-user relay strategy for cooperative mimo networks," in *Intl. Symp. on Wireless Personal Multimedia Communications (WPMC)*, 2007.

[144] M. R. Bhatnagar, M. K. Arti, A. Hjorungnes, and L. Song, "Multi-user relaying of high-rate space-time code in cooperative networks," *Wireless Personal Communications*, vol. 54, pp. 69–81, 2010.

[145] P. Gahinet, A. Nemirovski, A. J. Laub, and M. Chilali, *LMI Control Toolbox User's Guide*. The Mathworks Partner Series, 1995.

[146] M. Chen, S. Serbetli, and A. Yener, "Distributed power allocation strategies for parallel relay networks," *IEEE Trans. Wireless Communications*, vol. 7, pp. 552 –561, Feb. 2008.

[147] A. Wyner, "Shannon-theoretic approach to a gaussian cellular multiple-access channel," *IEEE Trans. Information Theory*, vol. 40, no. 6, pp. 1713–1727, 1994.

[148] K. Wang, X. Wang, W. Xu, and X. Zhang, "Coordinated linear precoding in downlink multicell mimo-ofdma networks," *IEEE Trans. Signal Processing*, vol. 60, no. 8, pp. 4264–4277, 2012.

[149] A. Wiesel, Y. C. Eldar, and S. Shamai, "Linear precoding via conic optimization for fixed mimo receivers," *IEEE Trans. Signal Processing*, vol. 54, pp. 161 – 176, Jan. 2006.

[150] L. Venturino, N. Prasad, and X. Wang, "Coordinated linear beamforming in downlink multi-cell wireless networks," *IEEE Trans. Wireless Communications*, vol. 9, pp. 1451 –1461, Apr. 2010.

[151] M. Maddah-Ali, A. Motahari, and A. Khandani, "Communication over mimo x channels: Interference alignment, decomposition, and performance analysis," *IEEE Trans. Information Theory*, vol. 54, pp. 3457–3470, Aug. 2008.

[152] V. Cadambe and S. Jafar, "Interference alignment and degrees of freedom of the k -user interference channel," *IEEE Trans. Information Theory*, vol. 54, pp. 3425–3441, Aug. 2008.

[153] S. G. Ye and R. S. Blum, "Optimized signaling for MIMO interference systems with feedback," *IEEE Trans. Signal Processing*, vol. 51, pp. 2839 – 2848, Nov. 2003.

[154] Y. Rong, Y. Hua, A. Swami, and A. L. Swindlehurst, "Space-time power schedule for distributed mimo links without instantaneous channel state information at the transmitting nodes," *IEEE Trans. Signal Processing,*, vol. 56, no. 2, pp. 686–701, 2008.

[155] Y. Wang, W. Feng, S. Zhou, Y. Li, and J. Wang, "Corrections to the proof in 'coordinated beamforming for the multicell multi-antenna wireless system'," *IEEE Trans. Wireless Communications*, vol. 10, pp. 4366 –4367, Dec. 2011.

[156] E. Björnson, G. Zheng, M. Bengtsson, and B. Ottersten, "Roobsut monotonic optimization framework for multicell MISO systems," *IEEE Trans. Signal Processing*, vol. 60, pp. 2508–2522, May. 2012.

[157] H. Tuy, "Monotonic optimization: Problems and solution approaches," *SIAM Journal on Optimization*, vol. 11, no. 2, pp. 463–494, 2000.

[158] R. Blum, "Mimo capacity with interference," *IEEE Journal on Selected Areas in Communications*, vol. 21, pp. 793–801, Jun. 2003.

[159] S. Christensen, R. Agarwal, E. Carvalho, and J. Cioffi, "Weighted sum-rate maximization using weighted mmse for mimo-bc beamforming design," *IEEE Trans. Wireless Communications*, vol. 7, pp. 4792–4799, Dec. 2008.

[160] S. Serbetli and A. Yener, "Mmse transmitter design for correlated mimo systems with imperfect channel estimates: power allocation trade-offs," *IEEE Trans. Wireless Communications*, vol. 5, no. 8, pp. 2295–2304, 2006.

[161] M. Ding and S. Blostein, "Mimo minimum total mse transceiver design with imperfect csi at both ends," *IEEE Trans. Signal Processing*, vol. 57, no. 3, pp. 1141–1150, 2009.

[162] H. Tam, H. Tuan, and E. Che, "Coordinated downlink beamforming in multicell wireless network," in *Intl. Conf. on Commu. and Electr. (ICCE),*, Accepted, 2014.

[163] Y. F. Liu, Y. H. Dai, and Z. Q. Luo, "Coordinated beamforming for MISO interference channel: Complexity analysis and efficient algorithms," *IEEE Trans. Signal Processing*, vol. 59, pp. 1142 –1157, Mar. 2011.

[164] A. H. Phan, H. D. Tuan, H. H. Kha, and H. H. Nguyen, "Iterative D.C. optimization of precoding in wireless mimo relaying," *IEEE Trans. Wireless Communications*, vol. 11, pp. 1617–1627, Apr. 2013.

[165] H. H. Kha, H. D. Tuan, and H. H. Nguyen, "Joint optimization of source power allocation and cooperative beamforming for SC-FDMA multi-user multi-relay networks," *IEEE Trans. Communications*, vol. 61, pp. 2248–2259, Jun. 2013.

[166] V. Annapureddy and V. Veeravalli, "Sum capacity of mimo interference channels in the low interference regime," *IEEE Trans. Information Theory*, vol. 57, pp. 2565–2581, May. 2011.

[167] H. Sato, "The capacity of the gaussian interference channel under strong interference (corresp.)," *IEEE Trans. Information Theory*, vol. 27, pp. 786–788, Nov. 1981.

[168] I. Sason, "On achievable rate regions for the gaussian interference channel," in *Proceedings. International Symposium on Information Theory (ISIT)*, p. 1, Jun. 2004.

[169] D. Tuninetti, "Gaussian fading interference channels: Power control," in *Asilomar Conference on Signals, Systems and Computers*, pp. 701 –706, Oct. 2008.

[170] A. S. Motahari and A. K. Khandani, "Capacity bounds for the Gaussian interference channel," *IEEE Trans. Information Theory*, vol. 55, pp. 620 –643, Feb. 2009.

[171] X. Shang, G. Kramer, and B. Chen, "A new outer bound and the noisy-interference sum-rate capacity for gaussian interference channels," *IEEE Trans. Information Theory*, vol. 55, pp. 689–699, Feb. 2009.

[172] X. Shang, B. Chen, G. Kramer, and H. Poor, "Capacity regions and sum-rate capacities of vector Gaussian interference channels," *IEEE Trans. Information Theory*, vol. 56, pp. 5030–5044, Oct. 2010.

[173] G. Kramer, "Outer bounds on the capacity of gaussian interference channels," *IEEE Trans. Information Theory*, vol. 50, pp. 581–586, Mar. 2004.

[174] E. Larsson and E. Jorswieck, "Competition versus cooperation on the miso interference channel," *IEEE Journal on Selected Areas in Communications*, vol. 26, pp. 1059–1069, Sep. 2008.

[175] E. Jorswieck and E. Larsson, "The MISO interference channel from a game-theoric perpective: A combination of selfishness and altruism achieve pareto optimality," in *Proc. Intel. Conf. Acoustics, Speech and Signal Processing (ICASSP), Las Vegas*, Apr. 2008.

[176] S. He, Y. Huang, L. Yang, A. Nallanathan, and P. Liu, "A multi-cell beamforming design by uplink-downlink max-min SINR duality," *IEEE Trans. Wireless Communications*, vol. 11, pp. 2858–2867, Aug. 2012.

[177] S. J. Kim and G. B. Giannakis, "Optimal resource allocation for MIMO ad hoc cognitive radio networks," *IEEE Trans. Information Theory*, vol. 57, pp. 3117–3151, May. 2011.

[178] D. H. N. Nguyen and T. Le-Ngoc, "Sum-rate maximization in the multicell MIMO multiple-access channel with interference coordination," *IEEE Trans. Wireless Communications*, vol. 13, pp. 36–48, Jan. 2014.

[179] A. H. Phan, H. D. Tuan, and H. H. Kha, "D.C. iterations for SINR maximum multicasting in cognitive radio," in *Proc. 6th Int. Conf. on Signal Processing and Coomunication Systems (ICSPCS)*, pp. 1–5, 2012.